Chapter 2
Analytic Regularization Methods

Abstract The chapter is devoted to analytic regularization method, which main advantage is the ability to reduce equivalently in the mathematical sense the ill-conditioned problems to the well-conditioned ones.

In spite of it almost half a century history, the method seems to be not very well known in the West scientific community. It has been developed in Kharkov scientific school due to constant concern and inspiration of V.P. Shestopalov. Here we outline the key issues of the method and focus our attention at most recent results.

2.1 General Description and Classification of the Analytic Regularization Methods: History, Provenance, and Survey

The growth in qualitative analysis of boundary value problems in mathematical physics is among most pronounced trends in today's mathematics. Various practical needs have spurred the development of numerical techniques for solving problems of this kind. Yet a vast gap exists between the practical engineering and the experimental physics on one side and the capabilities of today's numerical techniques on the other. In radio physics, the same situation is found.

Among other factors, purely psychological reasons stand behind this gap. After the solvability of the boundary value problem has been proved and other qualitative characteristics of the problem operator have been revealed, mathematicians are often just bored with the further numerical solution of the problem. The background of engineers is, as a rule, not in mathematics. And if they make themselves employ numerical methods for solving boundary value mathematical physical problems and even take up the invention of new methods, they are simply not aware of the genuinely mathematical nature of the encountered numerical difficulties, even though the diffraction problem to solve is seemingly elementary, and therefore cannot cope with them.

For the past decades, the situation has been changing for the better due to a series of brilliant works [55, 56] (see also the references used there) spelling out why the

Y.K. Sirenko, S. Ström (eds.), *Modern Theory of Gratings*, Springer Series in Optical Sciences 153, DOI 10.1007/978-1-4419-1200-8_2,

innocent use of the method of moments or others fail to give a physically valid solutions.

In today's radio-physical community, a practice has spread that a numerical technique is not evaluated by criteria of its intrinsic features but via comparisons of the computation results with a full-scale experiment, as if geometrical theorems were proved by geodesic surveys. It is thought that the things should be quite the reverse. And if the physical adequacy of the employed mathematical model is certain, it is the numerical simulation results that must serve a standard for experiment accuracy estimations. In actual practice, however, one can see that the numerical solution techniques are so insecure that the authors and users of the methods prefer the measured results to the theoretical predictions and take the former as being accurate.

Another popular way of numerical method verification relies upon a comparison of computing results with analogous data owing to another author's technique. But if the techniques have the same-nature intrinsic instability, their numerical results, close or not, will be wrong. In particular, it is safe to say that every technique (the method of moments and others) based on the direct discretization of an integral equation of the first kind produces false solutions. Equations of this nature arising in some diffraction problems will be exemplified below.

A technique that works well for solving boundary value problems in diffraction theory and yet is little known in the West is the analytic regularization method [10, 11, 16, 17, 21, 22, 45, 48, 57–68] which, as we strongly believe, has capacity to bridge the above-mentioned gap between the qualitative and the quantitative means of boundary value problem analysis in radio physics. In cases, first of all for two-dimensional and axially symmetric problems, this method can satisfactorily solve by far the majority of engineering problems today. The conversion of the initial boundary value problem to the second-kind equation in the space l_2 is a characteristic feature of the method guaranteeing computational stability with any desired accuracy of the solution.

To be more specific, address the integral equation of the form

$$[D+S]\,z=f;z=z(\theta);f=f(\theta);\theta\in[-\pi;\pi],$$

where

$$[Dz]\ (\theta)=\frac{1}{2\pi}\int\limits_{-\pi}^{\pi}\left[1-2\ln\left|2\sin\frac{\theta-\tau}{2}\right|\right]z(\tau)\ d\tau;\theta\in[-\pi;\pi],$$

$$[Sz]\ (\theta)=\frac{1}{2\pi}\int\limits_{-\pi}^{\pi}K(\theta,\tau)\,z(\tau)\,d\tau;\theta\in[-\pi;\pi].$$

Here, $z=z(\theta),\theta\in[-\pi;\pi]$ is the unknown function, the right-hand side $f=f(\theta)$, $\theta\in[-\pi;\pi]$ is given, and the $K(\theta,\tau)$, $\theta,\ \tau\in[-\pi;\pi]$, is the kernel. The

kernel $K(\theta,\tau)$ is assumed to be smoother than the function $\ln\left|2\sin\left((\theta-\tau)/2\right)\right|$, say, suppose that it is continuously differentiable with respect to θ and τ.

This equation models essential features of the integral equations appearing in simplest two-dimensional diffraction problems.

We start with the problem formulation for this equation in the space $\mathbf{L}_2[-\pi,\pi]$, assuming that $z,\ f \in \mathbf{L}_2[-\pi;\pi]$. Let the solution $z_0 = z_0(\theta)$ to this equation exist for the right-hand side $f_0(\theta)$ given. Consider the family of functions $e_N(\tau) = N^{1/2}\exp(iN\tau)$, $N = 1,2,3$. Obviously the functions $z_N = z_0 + e_N$ will be solutions to the equations

$$[D+S]\,z_N = f_N; \quad f_N = f_0 + \tilde{e}_N + e_N^S, \quad \tilde{e}_N = De_N, \quad e_N^S = Se_N.$$

In the $\mathbf{L}_2([-\pi;\pi]\times[-\pi;\pi])$, the kernel of the operator D can be written in the form of its Fourier series

$$1-2\ln\left|2\sin\frac{\theta-\tau}{2}\right| = \sum_{n=-\infty}^{\infty}\frac{e^{in(\theta-\tau)}}{\tau_n^2}; \qquad \theta,\tau\in[-\pi;\pi], \quad \tau_n = \max\left(1,|n|^{1/2}\right).$$

Therefore $\tilde{e}_N(\theta) = N^{-1/2}\exp(iN\theta)$. The continuous differentiability of the kernel $K(\theta,\tau)$ lends $e_N^S = O\left(N^{-1}\right)$. Thus, $\|f_N - f_0\| \to 0, N\to\infty$ but $\|z_N - z_0\| \to \infty, N\to\infty$.

So, even if there is an infinitely small error in the right-hand side, the solution of the considered integral equation can be affected to an infinitely large extent. And, similarly, an infinitesimal in the $\mathbf{L}_2$ metric error in the $K(\theta,\tau)$ kernel calculation can infinitely affect the solution $z = z(\theta)$. Notice that the described instability of the solution toward $f(\theta)$ and $K(\theta,\tau)$ is not related to a particular solution technique but to the nature of the equation itself.

From a functional analysis standpoint, the discussed instability is easily explained. That the kernel of the integral operator $D + S$ is square integrable and entails the operator $D + S$ being compact in $\mathbf{L}_2[-\pi,\pi]$. Hence the equation $[D + S]s = f$ is ill conditioned (ill posed or incorrect, according to A.N. Tikhonov).

The problem with the numerical solution of the considered equation consists in the following. Whatever the algorithm, the numerical solution of this integral equation is subject to rounding-off errors caused by a finite-length mantissa of the arithmetic processor. These errors can be considered random, and the equivalent disturbances δf and δK belong to $\mathbf{L}_2$, but we cannot think of them as smooth anymore. Hence, beginning with a certain size of the system, the errors of this sort can fully destroy the solution (as it was already seen), and they really do it, which is confirmed by numerical experiment.

The solution practice of the considered integral equation consists in putting it through one or another discretization scheme and reducing it to the linear algebraic equation of a finite size. The condition number of the system tends to infinity as the system size grows, and so does a level of the solution error, which is proportional to the condition number. Thus, beginning with some critical size of the system, the numerical solution not only does not improve as a number of the equations

increases but, on the contrary, the error grows fast, ending up with a full collapse. This suggests that there exists an optimum size of the algebraic system with the solution accuracy at its best (actually not very good). Unfortunately this critical size is usually unknown.

In the theory of incorrect problems [69], the correctness set of the operator A:$\mathbf{H}\to\mathbf{H}$ is the pair $\mathbf{H}_1$ $\mathbf{H}_2$ of sets or spaces on which the operator A:$\mathbf{H}_1\to\mathbf{H}_2$ is bounded and has a bounded inverse operator. As a rule, $\mathbf{H}_1$ and $\mathbf{H}_2$ are built, respectively, as an extension and a contraction of $\mathbf{H}$, with $\mathbf{H}_2 \subseteq \mathbf{H} \subseteq \mathbf{H}_1$. At the same time, a choice of $\mathbf{H}$ and, consequently, $\mathbf{H}_1$ and $\mathbf{H}_2$ is not unique and dictated by the problem's physical sense.

Consider a Sobolev space $\mathbf{H}^s[-\pi;\pi]$ as a space of (generalized) functions $\varphi(\theta)$, $\theta\in[-\pi;\pi]$, with the norm $\|\varphi\|_{\mathbf{H}^s} = \left\{ \sum\limits_{n=-\infty}^{\infty} \tau^{4s} (\varphi_n)^2 \right\}^{1/2}$, where $\{\varphi_n\}_{n=-\infty}^{\infty}$ are the Fourier coefficients of the function $\varphi(\theta)$. One easily sees that the operator D realizes the isometric isomorphism of the spaces $\mathbf{H}^s$ and $\mathbf{H}^{s+1}$ for any real s according to the rule

$$\psi = D\varphi; \quad \varphi(\theta) = \sum_{n=-\infty}^{\infty} \varphi_n e^{in\theta}, \quad \psi(\theta) = \sum_{n=-\infty}^{\infty} \tau_n^{-2} \varphi_n e^{in\theta}, \quad \|\psi\|_{\mathbf{H}^{s+1}} = \|\varphi\|_{\mathbf{H}^s}.$$

Hence the operator D:$\mathbf{H}^s\to\mathbf{H}^{s+1}$ has its bounded inverse D^{-1}:$\mathbf{H}^{s+1}\to\mathbf{H}^s$ and

$$\varphi = D^{-1}\psi; \ \psi(\theta) = \sum_{n=-\infty}^{\infty} \psi_n e^{in\theta}, \ \varphi(\theta) = \sum_{n=-\infty}^{\infty} \tau_n^{2} \psi_n e^{in\theta}, \ \|\psi\|_{\mathbf{H}^{s+1}} = \|\varphi\|_{\mathbf{H}^s}.$$

Correspondingly, the pair $\mathbf{H}^s$, $\mathbf{H}^{s+1}$ is the correctness set of the operator D.

For diffraction problems, picking $s = -1/2$ is most natural. Hence, the problem of solving the integral equation is formulated as

$$[D + S]z = f; \quad z \in \mathbf{H}^{-1/2}[-\pi;\pi], \quad f \in \mathbf{H}^{1/2}[-\pi;\pi].$$

It should be mentioned that Sobolev's spaces are very convenient for the theoretical analysis of the problem. However, for practical computational purposes, the sets $\mathbf{H}_1 = \mathbf{H}^{-1/2}[-\pi;\pi] \cap \mathbf{C}^{0,\alpha}[-\pi;\pi]$ and $\mathbf{H}_2 = \mathbf{H}^{1/2}[-\pi;\pi] \cap \mathbf{C}^{1,\alpha}[-\pi;\pi]$ are far more suitable. Moreover, taking $\mathbf{H}_2$ in the form $\mathbf{H}^{1/2} \cap \mathbf{C}^{m,\alpha}$ with an arbitrary m=2,3,... and even $H_2 = \mathbf{H}^{1/2} \cap \mathbf{C}^{\infty}$ is still better (here the standard notation $\mathbf{C}^{m,\alpha}$ is used to indicate the class of m-times continuously differentiable functions whose mth derivative satisfies the Hölder condition with index α, see [9]). The designation $\mathbf{H}^{1/2} \cap \mathbf{C}^{m,\alpha}$ means that the space $\mathbf{C}^{m,\alpha}$ is considered with the metric of the space $\mathbf{H}^{1/2}$ ($\mathbf{C}^{m,\alpha}$ is not complete in this metric). Two factors stand behind the choice $\mathbf{H}_2 = \mathbf{H}^{1/2} \cap \mathbf{C}^{\infty}$. First, the more is m, the more effective can be the algorithm of the integral equation solution. Second, in all practical diffraction problems, the function f is governed by the incident field, which, being a solution of Helmholtz or Maxwell's equations, is infinitely differentiable (and even real analytic) in the spatial variables.

From the indicated structure of the operator D it follows that the numerical solution of the considered integral equation cannot in principle be stable on only one of the $\mathbf{H}$ spaces. The immunity of the solution to input data errors requires a pair of the spaces (or linear manifolds) $\mathbf{H}_1$ and $\mathbf{H}_2$ forming the correctness set of the considered equation operator. Broadly speaking, the latter means that the linear manifold $\mathbf{H}_2$ consists of all the derivatives of the functions from $\mathbf{H}_1$, and the norms of $\mathbf{H}_1$ and $\mathbf{H}_2$ are matching each other as shown above.

Returning to our instability example, it should be noticed that e_N does not increase in the $\mathbf{H}_1$ metric and $\tilde{e}_N$ does not decrease in the $\mathbf{H}_2$ metric. To be specific, $\|e_N\|_{\mathbf{H}^{-1/2}} = \|\tilde{e}_N\|_{\mathbf{H}^{1/2}} \equiv 1$. As a consequence, the described instability example collapsed in the new problem formulation.

It is needless to say that the discussed change in the problem formulation leaves the actual process of the computation of the solution unaffected. Therefore the next step, which is the analytic regularization, has to transform the considered integral equation in such a way that the input data inserted into the computer be a stable system of equations of the second kind in the space l_2 of square-summable sequences. It is in the space l_2 where the system stability is important. As it was already seen and it will be shown still further, the theoretical stability in any other space or a pair of spaces other than the l_2 inevitably leads to the numerical instability.

Having finished with the stability analysis of the previous simplest integral equation, consider the situation from a more general point of view.

Lots of publications are devoted to the numerical solution of boundary value problems in the stationary diffraction theory. In great many of them, the approximate solution depends on the reduction of the initial boundary value problem to the finite linear algebraic system of the kind

$$A_N x^N = b^N$$

with the matrix operator A_N of size N. This system, directly or indirectly, is the truncation result of the corresponding infinite system of the first kind in the form

$$Ax = b$$

or, which is the same, is the result of the algebraization of some functional (for one, integral) equation of the first kind. To decide whether this finite-dimensional system solution is worth solving at all, it is reasonable to answer the following two questions:

- Does the solution x^N of this system tend to the solution x^∞ of the initial infinite system?
- Will (or not) the "numerical catastrophe" $\left\|x^N - \bar{x}^N\right\| \Big/ \left\|x^N\right\| > 1$ come with N growing, where $\bar{x}^N$ is the approximate solution of the $A_N x = b^N$ system computed of necessity of a finite mantissa which carries only a finite m_c number of binary digit?

Clearly the second question is reasonable to consider only if the first question is answered positively, implying that $x^N \to x^\infty$ in a relevant metric coordinated with the metric of the functional space where the initial boundary value problem solution is sought. In its turn, in view of the applied aspect of the study, this metric has to be coordinated with the physical nature of the phenomenon modeled by the boundary value problem.

It is known [70] that in the general case, the first question is answered negatively. Broadly speaking, in any metric, a solution $\bar{x}^N$ of the system of the first kind does not tend to x^∞ as N grows. For boundary value diffraction problems, this situation is typical (see [56]).

Nevertheless let us assume that by virtue of some specific properties of the operator A this convergence somehow takes place, and, what is more, it does so in a desired metric. The standard definition (see [70, 71]) of condition number ν_N of the operator A_N is

$$\nu_N = \|A_N\|_2 \times \left\|A_N^{-1}\right\|_2,$$

where the operator norm $\|...\|_2$ is produced by the Euclidean metric of vectors of some N-dimensional space. Systems of the first kind are characterized by that $\|A_N\|_2 \to \infty$ or $\left\|A_N^{-1}\right\|_2 \to \infty$ as $N \to \infty$. That is, the operator A or A^{-1} is unbounded in the operator norm produced by the vector norm of the space l_2. Correspondingly $\nu_N \to \infty$ as $N \to \infty$.

It has been verified [71] that a number of right binary digits in components of the solution $\bar{x}^N$ does not exceed the value

$$m_r = m_c - \log_2 \nu_N,$$

where m_r is the number of right digits of the maximum-module component of the vector $\bar{x}^N$. Correspondingly, a relative error of components smaller in module is far larger. And if these components decrease fast, only a few of the first of them can carry right significant digits, the rest cannot be computed at all.

Thus, if $m_r \le 0$, the solution $\bar{x}^N$ has none of significant digits right. In this case, the discrepancy $\delta^N \equiv A_N \bar{x}^N - b^N$ will be $\left\|\delta^N\right\|_2 \approx N 2^{-m_c} \left\|\bar{x}^N\right\|_2$ in the order of the value, which is evidently quite small. The accurate solution x^N rounded to m_c binary digits shows the same-order discrepancy.

It must be emphasized that a unique practical way to recognize that a "numerical catastrophe" is coming is through a straightforward ν_N and m_r calculation. Various indirect criteria such as energy balance (as δ^N is small, the energy conservation law can be satisfied with a very high accuracy even with $m_r < 0$ and $\bar{x}^N$ having no significant digits right) or stabilization of solution $\bar{x}^N$ with N (after $m_r < 0$ is reached, the $\bar{x}^N$ solutions can be either indifferent to N changes or varying very slowly, in compliance with the arithmetic processor rounding procedures) can, as a rule, only give an illusion of solution correctness of the initial boundary value problem.

Notice that the selection of the norm $\|...\|_2$ in the ν_N definition is not random, and there exist certain arguments behind the A or A^{-1} unboundedness in just the space l_2 operator norm. Though, as known [70], all finite-dimensional space norms are equivalent, their equivalence constants depend on N. And in some valuable sense the computer acts as if it modeled a metric close to the Euclidean metric [71]. That is, in the limit $N\to\infty$, it simulates the metric of the l_2. That is why the existence and the boundedness of the operators A and A^{-1} on the relevant pairs of spaces, mathematical justifications of the $\bar{x}^N$ convergence to $\bar{x}^\infty$ in the metrics of these spaces and such like are of no concern to the actual computation process: the computer interprets the algebraic system as if it were given on the l_2, demonstrating every delight of the "numerical catastrophe" as $\nu_N\to\infty$.

It is known that the "numerical catastrophe" can be delayed to large N by a proper choice of the basis in the method of moments, calling on special quadratic formulas, enhancing the arithmetic accuracy and such like. Yet these impediments cannot cancel characteristic features of equations of the first kind. Sooner or later the "numerical catastrophe" comes, excluding any possibility to solve the initial boundary value problem with an accuracy desired and cutting down possible intervals of variation of problem parameters.

It is a lack of understanding of the indicated difficulties and, first of all, the ignorance of the arithmetic routine of a particular machine (including such a bore as its specific rounding-off scheme), underestimating the difficulties preventing a stable numerical realization of many theoretically correct – in precision arithmetic – computational algorithms that seem to accompany a great body of publications inventing more and more methods intended for the numerical solution of boundary value problems in diffraction theory. And frequently the authors do not even mention the condition numbers of the algebraic schemes they use.

Let us turn to an alternative situation. Suppose that the original boundary value problem is equivalently reduced to the infinite system of algebraic equations of the form $Ax = b$; $x, b\in l_2$. The operator A takes the form $A=E + H$, where operator H is compact on the l_2 and E is the identity operator. A reasonably formulated boundary value problem has, as a rule, a unique solution, whence, by virtue of the indicated equivalence, it follows that the operator $A^{-1} = (E + H)^{-1}$ bounded on the l_2 space exists with a correct determination of the value

$$\nu_\infty = \|E + H\|_2 \times \left\|(E + H)^{-1}\right\|_2 < \infty.$$

As in the procedure above, consider the truncated systems

$$(E + H_N)\, x^N = b^N,$$

and in view of the compactness of H, the sequence of the finite-dimensional operators H_N can be chosen as

$$\|H - H_N\|_2 \to 0; \qquad N \to \infty.$$

It readily follows that the condition numbers ν_N tend to ν_∞: $\nu_N = \|E + H_N\|_2 \times \left\|(E + H_N)^{-1}\right\|_2 \to \nu_\infty$ as $N \to \infty$, and, hence, ν_N are uniformly bounded for any N large enough. In all practical situations of our knowledge that arise in the solution of a wide class of diffraction problems, the value ν_N varies within several tens or at most hundreds of units. Hence $\nu_N \ll 2^{m_c}$ for most modern computers.

So, compared to equations of the first kind, the second-kind equations have none of the indicated principal disadvantages preventing their effective solution. In particular, $x^N \to x^\infty$ and $\left\|\tilde{x}^N - x^N\right\| / \left\|x^N\right\| \to \nu_\infty 2^{-m_c+1}$ as $N \to \infty$ (see [70, 71]). The value $\nu_\infty 2^{-m_c+1}$ is so small that practically any accuracy can be achieved when N is large enough. The iterative refinement procedure [70] allows $\left\|\tilde{x}^N - x^N\right\|_2 / \left\|x^N\right\|_2 \approx 2^{-m_c}$ for any $\nu_\infty < 2^{m_c}$.

Thus, the equivalent conversion of the boundary value problem to an equation of the second kind in the l_2 can guarantee effective solution algorithms for this problem.

The techniques reducing the original boundary value problem to second-kind equations are built around the regularization of the problem operator. In functional analysis terms, this idea is well known and simple enough [72]. Let the linear operator $A:\mathbf{M}_1 \to \mathbf{M}_2$ be defined on a pair of functional (say, Banach) spaces $\mathbf{M}_1$ and $\mathbf{M}_2$. Additionally on some known space $\mathbf{M}$, the pair $L:\mathbf{M}_2 \to \mathbf{M}$ and $R:\mathbf{M} \to \mathbf{M}_1$ of bounded linear operators is given such that the inverse bounded operators L^{-1} and R^{-1} exist. It is evident that $LAR:\mathbf{M} \to \mathbf{M}$. If the relationship $LAR = E + H$ holds, with the operator H compact on $\mathbf{M}$, the pair L, R is referred to as a two-sided regularizer of the operator A.

This definition can be evidently extended to the case when the operators L, A, and R are only given on dense sets of the corresponding spaces. Then by $LAR = E + H$ is meant an operator obtained by the closure of the initial LAR.

When $\mathbf{M} = \mathbf{M}_1$ and $R = E$, the operator L is called a left-sided regularizer, and when $\mathbf{M} = \mathbf{M}_2$ and $L = E$, the operator R is a right-sided regularizer.

Take up the functional equation of the first kind $Ax = b$; $x \in \mathbf{M}_1$, $b \in \mathbf{M}_2$. Since the operator R^{-1} is bounded, any element $x \in \mathbf{M}_1$ is available in the form $x = Ry$ for some $y = R^{-1}x \in \mathbf{M}$. The usage of this representation yields $ARy = b$. Acting by the operator L on the left-hand side of this equation gives $LARy = Lb$. And in so far as the pair L, R is a two-sided regularizer of the operator A, we come up with the equation

$$(E + H)\, y = Lb; \qquad y, Lb \in \mathbf{M}$$

in the new unknown, y. With y constructed, the former unknown is expressed in the form $x = Ry$.

By the regularizer definition given right above, the equations $Ax = b$ and $(E + H)y = Lb$ are equivalent in the sense of the one-to-one correspondence existing between their solutions due to the operator R. At the same time, the second of these two is a second-kind equation.

Furthermore, let $\mathbf{M}$ be a Hilbert space. Having chosen a suitable basis there, we can match the Fourier coefficients in the left- and right-hand sides of the equation $(E + H)y = Lb$. By virtue of the well-known isomorphism of all Hilbert spaces, the

obtained equation is a second-kind equation belonging to the space l_2 and taking the form $\left(E+\tilde{H}\right)\tilde{y}=\tilde{b}$, where $\tilde{y},\ \tilde{b}\in l_2$ and $\tilde{H}\colon\ l_2\to l_2$ is a compact operator with necessity.

Thus, the analytic regularization method can be understood as a set of analytic transfoms coming up with a two-sided closed-form regularizer L, R in order for the first-kind equation $Ax=b$ to be analytically transformed to the equivalent second-kind equation $\left(E+\tilde{H}\right)\tilde{y}=\tilde{b};\tilde{y},\ \tilde{b}\in l_2$ with the operator $\tilde{H}$ compact in l_2. Of course, this is only an abstract sketch of the analytic regularization method. It does not answer the question how the procedure should be built for one or other boundary value diffraction problem, including specifications of functional spaces where the operator A should be defined (the boundary value problem formulation) in correspondence with a particular physical problem under modeling. The construction of the operators L and R in closed form is not in a priori evidence all the more. Therefore, any extension of the analytic regularization method to a further class of problems is an intellectual challenge.

Notwithstanding all gained experience, we cannot offer a readymade recipe but information about building blocks composing the analytic regularization method. They are

- reduction of the initial boundary value problem to the integral or integral differential equation based on a more or less standard technology of Green's functions;
- singularity analysis of the obtained equation kernel, derivation of the so-called singular expansion as a finite sum of the leading singularities of the kernel;
- extraction of the leading singularities from the kernel until the rest becomes sufficiently smooth (the additive decomposition of the integral equation operator);
- conversion of the integral equation to the canonical form whose regularization algorithm is available or is known how to build;
- construction of a proper family of two-sided regularizers and selection of the best one out of them by criteria of computational efficiency.

In so far as the book is mainly concerned with the theory of periodic structures, we have little possibility to enlarge on these principal points of the method providing a successful solution of a great variety of problems. Yet in Section 2.6, we fill in many details about periodic structures. Now let us return to the elementary integral equation whose analysis has already been started.

So, we understand the analytic regularization method as a philosophy of numerical modeling as applied to sophisticated problems in diffraction theory rather than a set of theoretical formulas and technical expedients, even though we stock a whole arsenal of mathematical tools and computational algorithms. It is due to this philosophy that high-efficiency numerical models have been built, coming up with a wide diversity of diffraction problems solvable today. This philosophy directs our efforts to attack increasingly more difficult problems in diffraction theory.

For the reader's convenience, we will continue with the elementary equation taken up earlier, planning to construct one (simplest) of possible families of two-sided regularizers and discuss how the most suitable regularizer of this family should be chosen.

The Fourier series of the operator D kernel (the function $1-2\ln|2\sin(\theta-\tau)/2|$) was previously given. The Fourier series of the functions $K(\theta,\tau)$, $z(\tau)$, and $f(\theta)$ are

$$K(\theta,\tau)=\sum_{s=-\infty}^{\infty}\sum_{n=-\infty}^{\infty}K_{sn}e^{i(s\theta+n\tau)},\ z(\tau)=\sum_{n=-\infty}^{\infty}z_n e^{in\tau},$$

$$f(\theta)=\sum_{n=-\infty}^{\infty}f_n e^{in\theta};\ \theta,\ \tau\in[-\pi;\pi].$$

Substitute the functions involved in the equation $[D+S]z=f$ by their Fourier series, interchange the orders of summation and integration and integrate them term by term on account of the orthogonality property of trigonometric functions (all the operations are legitimate for corresponding classes of functions). Matching the obtained coefficients in the left- and right-hand sides yields the algebraic system

$$\frac{z_s}{\tau_s^2}+\sum_{n=-\infty}^{\infty}K_{s,-n}z_n=f_s;\qquad s=0,\ \pm1,\ \pm2,\ ...$$

in the unknowns $\{z_n\}_{n=-\infty}^{\infty}$. The obtained infinite algebraic system is evidently a first-kind equation since the diagonal matrix $\left\{\delta_s^n\tau_s^{-2}\right\}_{s,n=-\infty}^{\infty}$ (δ_s^n being the Kronecker symbol) produces an operator compact in l_2. The same is clearly true for the matrix operator $\tilde{K}=\left\{K_{s,-n}\right\}_{s,n=-\infty}^{\infty}$.

For the considered equation, the following regularizer scheme seems evident. First, introduce the new unknowns $z_n^{\gamma}=\tau_n^{-\gamma}z_n$, where γ is some parameter to determine. Second, multiply each of the obtained equations of the number $s=0,\pm1,\pm2...$ by the factor $\tau_s^{2-\gamma}$. Finally,

$$z_s^{\gamma}+\sum_{n=-\infty}^{\infty}\left(\tau_s^{2-\gamma}\tau_n^{\gamma}K_{s,-n}\right)z_n=\tau_s^{2-\gamma}f_s;\qquad s=0,\ \pm1,\ \pm2,\ ...$$

The obtained system appears to be $(I+K_{\gamma})z^{\gamma}=f^{\gamma}$, where $z^{\gamma}=\left\{z_n^{\gamma}\right\}_{n=-\infty}^{\infty}$, $f^{\gamma}=\left\{\tau_n^{2-\gamma}f_n\right\}_{n=-\infty}^{\infty}$, and $K_{\gamma}=T^{2-\gamma}\tilde{K}T^{\gamma}$, with T being a diagonal matrix operator of the form $T=\left\{\tau_n\delta_s^n\right\}_{s,n=-\infty}^{\infty}$. Is this system a second-kind equation in l_2? Or, which is the same, is the operator K_{γ} compact in l_2? One easily verifies that the compactness of the operator K_{γ} depends, first, on how fast the coefficients $K_{s,n}$ decrease as $s,n\to\pm\infty$, which, in turn, depends on the smoothness of the kernel

$K(\theta,\tau)$ as a function that is 2π-periodic in both arguments. Second, one should properly choose a parameter γ according to the decrease character of the coefficients $K_{s,n}$ as $s,n\to\pm\infty$.

It is easy to see that the factor $\tau_s^{2-\gamma}\tau_n^{\gamma}$ degrades the decrease of the $K_{s,-n}$ coefficients for any γ. Therefore, it may happen that the operator K_γ is not compact whatever γ we use. This means that the logarithmic singularity removal from the kernel of the operator $D + S$ is inadequate to remedy this. And we have to derive such a leading singularity $K_0(\theta,\tau)$ from the function $K(\theta,\tau)$ that, first, the remainder $K(\theta,\tau)$–$K_0(\theta,\tau)$ will be sufficiently smooth and, second, the kernel $1 - 2\ln\left|2\sin\frac{\theta-\tau}{2}\right| + K_0(\theta,\tau)$ will have a sufficiently simple matrix (diagonal one is the best) of the Fourier coefficients. This expedient is employed for solving the diffraction problem of a corrugated surface in Section 2.6.

Now assume that the kernel $K(\theta,\tau)$ is so smooth as to have $\gamma = \gamma_0$ for which the operator K_γ is compact. Then it can be proved that there is a vicinity $(\gamma_1;\gamma_2)$ that contains γ_0 and provides compactness of the operator K_γ for any $\gamma\in(\gamma_1;\gamma_2)$. Thus, we get a family of regularizers rather than a single one and one of them is providing the fastest convergence of the reduction procedure for the relevant algebraic system.

Let us consider some examples. Let $K(\theta,\tau)$ be a continuous 2π-periodic function of its variables. If there is no more information about it, we cannot say that operator K_γ will be compact in l_2. Accept an extra assumption that the function $K(\theta,\tau)$ is continuously differentiable with respect to τ for any θ. Then the operator compactness will be provided by the choice $\gamma = 2$. In this case, $z_n^{\gamma} = \tau_n^{-2}z_n$. Analogously, if the function $K(\theta,\tau)$ is continuously differentiable with respect to θ (and is not differentiable with respect to τ), the operator K_γ is compact under the choice $\gamma = 0$, with $z_n^{\gamma} = z_n$. Finally, if $K(\theta,\tau)$ is continuously differentiable with respect to θ and τ, then any $\gamma\in[0;2]$ will be good enough to provide the operator K_γ compactness. To choose the best γ out of them, the differential properties of the $K(\theta,\tau)$ function should be studied in greater depth. For most (but not all) diffraction problems reduced to the equation of the concerned type, $\gamma = 1$ is an optimum choice.

At this stage of our explanation, the reader may feel disappointed about the simplicity of the analytic regularization scheme we have constructed (much ado about nothing). If so, we have to remind that, first, a most elementary integral equation was treated, coming up with a simplest-structure regularizer. Second, the disappointment, if any, should become amazement because we have so easily gained in such a vital characteristic as computational algorithm stability.

Concerning the evolution of the analytic regularization idea as applied to boundary value problems in diffraction theory (in particular, electrodynamical theory of gratings) and the relevant techniques for building regularizing operators, the following points are worth noting. The earliest boundary value problems solved substantially in terms of the above-described regularization idea were 2-D coordinate problems of wave diffraction by infinitely thin, perfectly conducting nonclosed screens (see [73–75] and the references used there), where the so-called semi-inversion method used to be employed. This method is a variant of the left-hand-sided regularization discussed here. Here, by coordinate problems we mean

boundary value problems proceeding from the Helmholtz equation and characterized by the fact that the boundary surface (or the contour), where the boundary conditions are applied, coincide with a part of the coordinate surface of one of the such special coordinate systems that the variables of the Helmholtz (or Maxwell's) equation can be separated.

By the partial domain (or sewing, or mode matching) method the coordinate problems are naturally reduced to the functional equations of the kind $Ax = b$, where the operator A depends on the excitation wave frequency and, of course, on other parameters, including the problem geometrical properties. The key point of the semi-inversion method is finding such an operator A_0 that, first, the bounded operator A_0^{-1} exists in a suitable functional space and, second, $A_0^{-1}A = E + H$, where H is a compact operator and E is the identity operator. For grating diffraction problems, one of the most common ways of building the operators A_0 and A_0^{-1} consists in the development of the operator part established by a single element of the grating to be extracted then from the operator A. When the considered diffraction problem for a single element can be solved in explicit form (for an arbitrary excitation field) or reduced to the equation of the second kind, one always arrives at the regularized equation $x + Hx = b$. It is easily understood that the resulting operator equation of the second kind is most suitable when periodic grating components are sufficiently spaced apart [16, 76–78].

One more variant of the semi-inversion method was originally suggested in [79] to solve diffraction problems of plane strip gratings. The key point is the development of the operator A_0 corresponding, conventionally speaking, to the electrostatic problem. In terms of the Riemann–Hilbert problem in theory of analytic functions [80] or using the integral transform method like the fractional integration (differentiation) technique [81], it was succeeded to explicitly construct the operator A_0^{-1} as a left-hand regularizer of the functional equations in the sewing method (some generalizations of this approach are discussed in Sections 2.2, 2.4, and 2.5). In this way, a wide class of diffraction problems for multielement and multilayer gratings, variously arrayed circular cylindrical screens, spherical segments, etc., has been examined (see [16, 18, 45, 74, 82] and references therein). In [22], the semi-inversion method was designed upon the development of the operator A_0 corresponding to the limiting value of one of the parameters of the initial diffraction problem. Thus, for instance, in the case of wave diffraction by jalousie-type gratings, the operator corresponding to the grating of semi-infinite planes was extracted from the sewing method operator. This operator inversion (A_0^{-1}) was due to the Wiener–Hopf method. In general, this variant of the semi-inversion method is based on the inversion of matrix convolution-type equations [17]. The employed mathematical technology is based on Mittag–Leffler's theorem about a meromorphic function representation (some aspects of the approach are given in Section 2.3). The results of this semi-inversion method variant are surveyed in [16–18].

An original variant of the semi-inversion method is suggested in references [83–85], where the wave diffraction is solved for a finite number of strip screens located in the same plane. The method develops from an explicit solution of the

Riemann–Hilbert problem for a finite number of real-axis segments [80], coming up with a single integral Fredholm equation of the second kind (for an arbitrary number of strip screens) with a smooth kernel of quite a simple appearance.

It seems that the most valuable methodological result concerning the semi-inversion method is that the so constructed regularization algorithms covering a wide diversity of model problems are unique in their speed, accuracy, efficiency, and reliability. With no additional expedients, these algorithms are capable of studying physical properties of different types of gratings from the long-wavelength and resonance regions to the really short-wave end of spectrum when the grating period measures several tens of the wavelengths.

It is these capabilities of the semi-inversion method that encouraged a lot of effort going into the further enhancement of the analytic regularization method. At the time when most algorithms for solving coordinate problems had been designed or so, the reasons providing their success were not clear enough. And soon it was discovered that the class of coordinate problems solved in this technology terms was coming to an end. In any event, the difficulties of further progress were enormous. It used to seem that a high computational efficiency of the developed algorithms had much to do with their specialization: each variant of the semi-inversion method used to be tailored for analyzing objects of essentially similar geometry. And, for instance, the solution of the electrostatic part $x_0 = A_0^{-1} b$ owing to the operator A_0^{-1} used to consider a specific character of a particular boundary value problem so comprehensively that the computation of the dynamical addition to the exact solution used to be a simple and effectively solved problem. Hence, the abandonment of narrow specialization had to lead to a severe decrease in efficiency.

With the things commonly adopted at that time, one could hardly expect a principal possibility for equally efficient and, at the same time, rather universal solution techniques for boundary value diffraction problems. Certain intellectual effort has been spared to overcoming this stereotype of thinking, recognition, and analysis of the key reasons providing a high quality of algorithms for coordinate diffraction problems, to elaboration of more general methods considering these reasons. Eventually far more general regularization procedures have come into being for quite an extensive class of boundary value diffraction problems. And the algorithms based on these principles are highly competitive in their computational efficiency with those commonly used for solving coordinate problems.

To this end, the regularization scenario suitable for coordinate problems had to be essentially modified [11]. First of all, it was no more possible to use the sewing (partial domain) method and enjoy the former simplicity of the algorithms as applied to arbitrarily shaped contours associated with the boundary conditions. It was found that the best alternative is the method of boundary integral equations based on familiar Green's functions (see, e.g., [86]). And in this case, both for closed and especially unclosed contours, the original boundary value problem should be reduced to integral equations of the first kind (see Section 2.6) rather than seemingly more convenient equations of the second kind. The next, and maybe the most important, is the idea of closing of the unclosed contour by imbedding it in some smooth closed configuration. This closure largely predetermines a principal

feasibility of a high computational efficiency of the developed algorithms (see [11]). The parametrization of the closed contour and analysis of the kernels of the constructed integral operators for the singular structure (differential properties) allow, via a relevant Fourier transform, reducing these integral equations to special-form dual series equations (some of them are examined in Section 2.2). The regularization of these dual series equations eventually gives the operator equations of the second kind.

A mention should be made that against the coordinate diffraction problems, we generally have to build the two-sided regularizer L and R whose analytic (closed form) derivation is closely related to the structure of kernel singularities of the above-mentioned integral operators and, also, to some properties of the closed contour parametrization. The computational efficiency of the outlined algorithmic scheme largely depends on the realization of the contour-closure procedure, choice of optimum (in a way) parametrization of the closed contour, method of computation of Fourier coefficients of integral operator kernels, summation procedures of slowly converging series for limiting values of the fields and their normal derivatives (i.e., for currents), etc. The mentioned range of ideas was originally applied in [63, 64] to the 2-D diffraction problem of infinitely thin perfectly conducting cylindrical screens. A detailed description of this approach to diffraction theory problems is the subject matter of book [11].

This brief schematic description of the analytic regularization method shows that the development of relevant computational algorithms and their computer realization are not a trivial activity. Therefore, the basic mathematical expedients and approaches will be considered in Sections 2.2, 2.3, 2.4, 2.5 and 2.6.

2.2 The Riemann–Hilbert Problem Method and Its Generalization

This subsection essentially portrays an approach (added on in subsequent sections) to solve boundary value problems of single-periodic gratings and different media interfaces (anisotropic dielectrics, chiral composites, metamaterials, etc.) in wave diffraction and propagation theory. In it, certain generalizations (modifications) are presented in regard to the classical variant of the Riemann–Hilbert problem method [45, 74] to deal with a wide class of dual series equations involving the functions $\exp(in\vartheta)$, $n = 0, \pm 1, \ldots$. It is these dual series equations that appear, e.g., in the electromagnetic wave diffraction by strip gratings located on an anisotropic dielectric interface (see Sections 2.4 and 2.5).

By means of regularization procedures specially designed for the case, all dual series equations considered in this section are equivalently reduced on a relevant l_2 space of quadratically summable sequences to the infinite system of linear algebraic equations of the form $x + Hx = b$, $x, b \in l_2$, with the operator H being compact on l_2. These systems are known to be effectively solved by various numerical methods.

Some of the results in this section (in a little different appearance), their modifications and relationships with corresponding boundary value problems in diffraction theory can be found in [75, 87–92].

2.2.1 Classical Dual Series Equations and the Riemann–Hilbert Problem

In this subsection, according to the major ideas of the references [45, 79], a study is conducted for one type of dual series equations, the simplest ones arising in modeling 2-D coordinate problems of the wave diffraction by systems of nonclosed infinitesimally thin screens, such as, in particular, single-periodic strip gratings [74]. From this point on, by a coordinate diffraction problem is meant a boundary value problem such that the structure interface coincides with a coordinate surface part referring to an orthogonal coordinate system enabling the separation of variables for the Helmholtz (Maxwell's) equation. The separation of variables (partial domain, or sewing method) reduces the coordinate problems to the dual series equations of the form

$$\sum_{n=-\infty}^{\infty} \gamma_n x_n \mathrm{e}^{in\vartheta} = F\left(\mathrm{e}^{i\vartheta}\right);\ |\vartheta| < \vartheta_0, \tag{2.1}$$

$$\sum_{n=-\infty}^{\infty} x_n \mathrm{e}^{in\vartheta} = G\left(\mathrm{e}^{i\vartheta}\right);\ |\vartheta| > \vartheta_0. \tag{2.2}$$

for the unknowns $x = \{x_n\}_{n=-\infty}^{\infty}$. Here, $F(\exp(i\vartheta))$ and $G(\exp(i\vartheta))$ are given functions, $\vartheta \in [-\pi;\pi]$, $\{\gamma_n\}_{n=-\infty}^{\infty}$ is a given sequence of complex numbers, and $\vartheta_0 \in [0;\pi]$ is a parameter.

Assume that the following conditions are satisfied:

- as $|n| \to \infty$, the values γ_n take on the form

$$\gamma_n = |n|\,(1 - \delta_n), \tag{2.3}$$

  where $\delta_n = O\left(n^{-2}\right)$;
- the given right-hand sides $F(\exp(i\vartheta))$ and $G(\exp(i\vartheta))$ are expanded into the Fourier series

$$F\left(\mathrm{e}^{i\vartheta}\right) = \sum_{n=-\infty}^{\infty} f_n \mathrm{e}^{in\vartheta}, \qquad G\left(\mathrm{e}^{i\vartheta}\right) = \sum_{n=-\infty}^{\infty} g_n \mathrm{e}^{in\vartheta}; \tag{2.4}$$

- all the series in (2.1) and (2.2) are the Fourier series of their sums: the series in (2.2) and (2.1) are Fourier series of the functions belonging, respectively, to the $\mathbf{L}_2[-\pi;\pi]$ and $\mathbf{L}_1[-\pi;\pi]$ spaces. The space $\mathbf{L}_p[-\pi;\pi]$, $p = 1,2$, is defined, e.g., in [70] (see also Appendix).

A solution of equations (2.1) and (2.2) will be sought in the infinite-sequence space $l_2(1)$, assuming that the Fourier coefficients of the functions $F(\exp(i\vartheta))$ and $G(\exp(i\vartheta))$ belong to the spaces $l_2(1)$ and $l_2(3)$, respectively. From here on, the infinite-sequence space $l_2(\eta)$ is defined as

$$l_2(\eta) = \left\{ \{x_n\}_{n=-\infty}^{\infty} : \sum_{n=-\infty}^{\infty} |x_n|^2 (1+|n|)^{\eta} < \infty \right\}. \tag{2.5}$$

The infinite series in the left-hand sides of (2.1) and (2.2) converge slowly (below one can see that $x_n = O\left(|n|^{-3/2}\right)$ as $|n| \to \infty$), making the dual series equations of little use for the direct analytic or numerical search of $x = \{x_n\}_{n=-\infty}^{\infty}$.

Let us show that the previous assumptions enable one to equivalently reduce these equations to an infinite system of linear algebraic equations of the second kind in the space $l_2 = l_2(0)$ (one easily finds that $l_2(1) \subset l_2$).

Introduce the new unknowns $y = \{y_n\}_{n=-\infty}^{\infty}$ by the formula

$$y_n = x_n - g_n;\ n = 0,\ \pm 1, \ldots. \tag{2.6}$$

Then equations (2.1) and (2.2) will take the appearance

$$\sum_{n=-\infty}^{\infty} |n|\, y_n e^{in\vartheta} = \sum_{n=-\infty}^{\infty} \psi_n e^{in\vartheta};\ |\vartheta| < \vartheta_0, \tag{2.7}$$

$$\sum_{n=-\infty}^{\infty} y_n e^{in\vartheta} = 0;\ |\vartheta| > \vartheta_0, \tag{2.8}$$

where

$$\psi_n = \begin{cases} f_0 - \gamma_0 (y_0 + g_0); & n = 0 \\ f_n + |n|\, \delta_n y_n + |n| (\delta_n - 1)\, g_n; & n \neq 0 \end{cases}. \tag{2.9}$$

Assume for a while that the function $\psi(\exp(i\vartheta)) = \sum_{n=-\infty}^{\infty} \psi_n \exp(in\vartheta)$ is available and construct a solution to equations (2.7) and (2.8) in explicit form (express y_n via ψ_n).

Differentiating equation (2.8) and taking $z_n = n y_n$ gives

$$\sum_{n \neq 0} z_n e^{in\vartheta} = 0;\ |\vartheta| > \vartheta_0, \tag{2.10}$$

$$\sum_{n \neq 0} z_n \frac{|n|}{n} e^{in\vartheta} = \psi\left(e^{i\vartheta}\right);\ |\vartheta| < \vartheta_0. \tag{2.11}$$

Equations (2.10) and (2.11) will be equivalent to equations (2.7) and (2.8) on the addition of the equality

$$\sum_{n\neq 0} \frac{(-1)^n z_n}{n} = -y_0, \tag{2.12}$$

coming from (2.8) at $\vartheta = \pi$.

Now let us show that the dual series equations (2.10) and (2.11) represent the well-known Riemann–Hilbert problem in the theory of analytic functions [79]. Indeed, according to [80], define the functions

$$X^+(z) = \sum_{n=1}^{\infty} z_n z^n, \quad X^-(z) = -\sum_{n=-\infty}^{-1} z_n z^n, \tag{2.13}$$

analytic, respectively, on inside and outside the circle $|z| \leq 1$.

From (2.10),

$$X^+\left(e^{i\vartheta}\right) - X^-\left(e^{i\vartheta}\right) = 0 \tag{2.14}$$

on the arc $\mathbf{P}_1$ of the unit circle connecting the points $\exp(-i\vartheta_0)$ and $\exp(i\vartheta_0)$ through the point $z = -1$. Hence, the function

$$X(z) = \begin{cases} X^+(z); & |z| < 1 \\ X^-(z); & |z| > 1 \end{cases} \tag{2.15}$$

is analytic in the complex plane with a cut along the arc $\mathbf{P}_2$ complementary to the arc $\mathbf{P}_1$. In view of (2.7), on the complementary arc $\mathbf{P}_2$,

$$X^+\left(e^{i\vartheta}\right) + X^-\left(e^{i\vartheta}\right) = \psi\left(e^{i\vartheta}\right); |\vartheta| < \vartheta_0, \tag{2.16}$$

where $X^+(\exp(i\vartheta))$ and $X^-(\exp(i\vartheta))$ are the function $X(z)$ limiting values, respectively, inside and outside the circle $|z| \leq 1$. Hence, equations (2.10) and (2.11) have been reduced to the problem of the function of the $X(z)$ determination by the sum of its limiting values on the arc $\mathbf{P}_2$. This is the Riemann–Hilbert problem whose simple solution was developed by T. Carleman [93].

The solution to this problem will be sought in the class of functions that have an integrable singularity at the points $z_0^{\pm} = \exp(\pm i\vartheta_0)$ and decrease as $|z| \to \infty$. The sought function $X(z)$ and the function $R(z) = \sqrt{\left(z - z_0^+\right)\left(z - z_0^-\right)}$ are analytic and unique in the complex plane cut along the arc $\mathbf{P}_2$. For $R(z)$, a root branch is chosen such that $R(0) = 1$. From (2.13), $X(z) = X^-(z) = z^{-1}(-z_{-1} + O(1))$ as $|z| \to \infty$. Therefore, the function $X(z)R(z)$ is bounded as $|z| \to \infty$, and upon the Cauchy theorem [94], we have

$$X(z)R(z) = \frac{1}{2\pi i} \oint_{\Gamma} \frac{X(\tau)R(\tau)}{\tau - z} d\tau + C. \tag{2.17}$$

Here, $\mathbf{\Gamma}$ is a sufficiently smooth closed contour to enclose the cut along the arc $\mathbf{P}_2$ and C is some constant proportional to the residue of the function $X(z)R(z)$ at an infinitely distant point $z = \infty$.

Refer to (2.17) and contract the contour $\mathbf{\Gamma}$ toward the arc $\mathbf{P}_2$. Considering (2.16), we obtain

$$X(z)R(z) = \frac{1}{2\pi i}\int\limits_{\mathbf{P}_2} \frac{\psi(\tau)\,\mathbf{R}^+(\tau)}{\tau - z}d\tau + C, \tag{2.18}$$

where $R^+(\tau)$ is the $R(z)$ limiting value on the arc $\mathbf{P}_2$ as $z \to \tau$ from inside of the unit circle.

Formula (2.18) is a solution to the Riemann–Hilbert problem (2.16), and this formula is sufficient to solve equations (2.7) and (2.8). Applying the Sokhotskyi-Plemelj formulas [94] for limiting values of functions represented by the Cauchy-type integrals, from (2.18) it follows that

$$\sum_{n\neq 0} z_n e^{in\vartheta} = K\left(e^{i\vartheta}\right)\left[\frac{1}{\pi i}\int\limits_{\mathbf{P}_2}\frac{\psi(\tau)}{K(\tau)\left(\tau - e^{i\vartheta}\right)}d\tau + 2C\right]. \tag{2.19}$$

on the unit circle $|z| = 1$. Here the integral is understood as the Cauchy principal value, and

$$K\left(e^{i\vartheta}\right) = \begin{cases} \frac{1}{\mathbf{R}^+\left(e^{i\vartheta}\right)}; & |\vartheta| < \vartheta_0 \\ 0; & |\vartheta| > \vartheta_0 \end{cases}. \tag{2.20}$$

Passing to the Fourier coefficients in (2.19) and removing the C constant in view of (2.12), one arrives at

$$y_0 = W_0\psi_0 + \sum_{n\neq 0}\psi_n\frac{V_{n-1}^{-1}}{n}, \tag{2.21}$$

$$y_m = \sum_{n=-\infty}^{+\infty}\psi_n\frac{V_{m-1}^{n-1}}{m} \tag{2.22}$$

with the notations [45, 74]

$$V_n(e^{i\vartheta}) = \frac{1}{\pi i}\int\limits_{\mathbf{P}_2}\frac{\tau^n d\tau}{K(\tau)\left(\tau - e^{i\vartheta}\right)},\ V_m^n = \frac{1}{2\pi}\int\limits_{-\pi}^{\pi} V_n\left(e^{i\vartheta}\right)K\left(e^{i\vartheta}\right)e^{-im\vartheta}d\vartheta \text{ and}$$

$$W_0 = \frac{1}{2\pi}\int\limits_{-\pi}^{\pi}\vartheta K\left(e^{i\vartheta}\right)d\vartheta.$$

The values W_0, V_m^n have been calculated in [45] by making use of the formulas

$$V_{m-1}^{n-1} = \frac{1}{2}\begin{cases} \frac{m}{m-n}\left[P_{m-1}(u)P_n(u) - P_m(u)P_{n-1}(u)\right]; & m \neq n \\ \sum_{s=0}^{n} \rho_{n-s}(u)P_{s-n}(u); & m = n \geq 0 \end{cases}, \qquad (2.23)$$
$$V_{-n-1}^{-n-1} = -V_{n-1}^{n-1}; \quad n \geq 1, W_0 = -\ln\frac{1+u}{2}.$$

Here $u = \cos\vartheta_0$ and $P_n(u)$ are the Legendre polynomials [95], which for negative n indices are defined by the formula

$$P_n(u) = P_{|n|-1}(u).$$

The functions $\rho_n(u)$, $n = 0,1,2,\ldots$, are expressed via the Legendre polynomials (see (2.66) below).

So, assuming that the Fourier coefficients $\{\psi_n\}_{n=-\infty}^{\infty}$ of the function $\psi(\exp(i\vartheta))$ [see (2.11)] are known, we have solved equations (2.10) and (2.11) in explicit form [see (2.21) and (2.22)]. Let us show how on the basis of this solution the infinite system of linear algebraic equations equivalent to equations (2.1) and (2.2.) should be derived. Evidently $\{y_n\}_{n=-\infty}^{\infty}$ and $\{\psi_n\}_{n=-\infty}^{\infty}$ in (2.21) and (2.22) should be substituted by their representations via $\{x_n\}_{n=-\infty}^{\infty}$ and $\{g_n\}_{n=-\infty}^{\infty}$, $\{f_n\}_{n=-\infty}^{\infty}$ [see (2.6) and (2.9)]. After some elementary manipulations,

$$x_m = \sum_{n=-\infty}^{\infty} a_{mn}x_n + b_m;\ m = 0, \pm 1, \ldots, \qquad (2.24)$$

with the matrix elements a_{mn} and the right-hand sides b_m being

$$a_{mn} = \begin{cases} -W_0\gamma_0; & m = n = 0 \\ \frac{|n|}{n}\delta_n V_{n-1}^{-1}; & m = 0, \quad n \neq 0 \\ -\gamma_0\frac{V_{m-1}^{-1}}{m}; & m \neq 0, \quad n = 0 \\ \frac{|n|}{m}\delta_n V_{m-1}^{n-1} & m \neq 0, \quad n \neq 0 \end{cases}, \qquad (2.25)$$

$$b_m = \begin{cases} g_0 + W_0 f_0 + \sum_{n\neq 0} \frac{V_{n-1}^{-1}}{n}(f_n - |n|\, g_n); & m = 0 \\ g_m + \sum_{n=-\infty}^{+\infty} \frac{V_{m-1}^{n-1}}{m}(f_n - |n|\, g_n); & m \neq 0 \end{cases}. \qquad (2.26)$$

Express the system of equations in vector form. For this, introduce the infinite-dimensional matrix $A = \{a_{mn}\}_{m,n=-\infty}^{\infty}$ and the column vectors $x = \{x_n\}_{n=-\infty}^{\infty}$, $b = \{b_m\}_{m=-\infty}^{\infty}$. In these denotations, (2.24) has the form

$$x = Ax + b. \qquad (2.27)$$

Equation (2.27) will be considered on the sequence space l_2. Let us show that the matrix A gives a compact operator on the space l_2, with the column vector $b \in l_2$. To this end, it is sufficient to ensure the convergence of the series $\sum_{m,n=-\infty}^{\infty} |a_{mn}|^2 < \infty$

and $\sum_{m=-\infty}^{\infty} |b_m|^2$. As it is known [95], Legendre polynomials obey the inequality

$$|P_n(u)| < \frac{2}{\sqrt{\pi |n| \left(1-u^2\right)}}; n = \pm 1, \pm 2, \ldots . \tag{2.28}$$

In view of (2.28), expression (2.23) readily gives as $|n|, |m| \to \infty$ the inequalities

$$\left|V_{m-1}^{n-1}\right| < \frac{C_1\sqrt{|m|}}{\sqrt{|n|}\,|m-n|}; m \neq n, \qquad \left|V_{m-1}^{m-1}\right| < C_2, \tag{2.29}$$

where C_1, C_2 are constants independent of m and n.

Now, considering (2.29) and upon the fact that $\delta_n = O(n^{-2})$ [see (2.3)], we obtain

$$|a_{mn}| < \frac{C_3}{\sqrt{|m|}\,|n|^{3/2}\,|m-n|}; \; m \neq n, \; |a_{mm}| < \frac{C_4}{m^2}. \tag{2.30}$$

Here C_3, C_4 are some constants. From (2.30) follows the convergence of the series $\sum_{m,n=-\infty}^{\infty} |a_{mn}|^2 < \infty$. Previously we assumed that the Fourier coefficients of the functions $F(\exp(i\vartheta))$ and $G(\exp(i\vartheta))$ satisfy the conditions $\{f_n\}_{n=-\infty}^{\infty} \in l_2$ (1) and $\{g_n\}_{n=-\infty}^{+\infty} \in l_2$ (3). On this account and in view of (2.23) and (2.29), we have from (2.26) that as $|m| \to \infty$

$$b_m = A_0 \frac{P_{m-1}(u)}{m} + A_1 \frac{P_m(u)}{m} + \frac{\widehat{b}_m}{|m|^{3/2}}, \tag{2.31}$$

where $A_s = \frac{(-1)^s}{2} \sum_{n=-\infty}^{\infty} (f_n - |n|\, g_n)\, P_{n-s}(u)$, $s = 0,1$, and $\widehat{b}_m$ are some values with $\sum_{m=-\infty}^{\infty} \left|\widehat{b}_m\right|^2 < \infty$. Hence the series $\sum_{m=-\infty}^{\infty} |b_m|^2 < \infty$ converges, which is the required result.

From the above discussion, it follows that equation (2.27) is a second-kind equation in the space l_2.

So, the initial dual series equations (2.1) and (2.2) have been reduced to the infinite system of linear algebraic equations of the second kind. These systems guarantee their numerical solution with any desired accuracy. Besides, the established properties of equation system (2.4) suggest the solvability and the uniqueness of the solution using, for instance, the corresponding Fredholm theory for operator equations of the second kind [70]. Furthermore, using (2.24), one arrives at an asymptotical estimation of the unknowns x_m as $|m| \to \infty$, which is identical to asymptotical estimation (2.31). Namely,

$$x_m = B_0 \frac{P_{m-1}(u)}{m} + B_1 \frac{P_m(u)}{m} + \frac{\widehat{x}_m}{|m|^{3/2}}, \tag{2.32}$$

where $B_s = A_s + C_s$, $C_s = 0.5(-1)^s \left[-\gamma_0 x_0 + \sum\limits_{n=-\infty}^{\infty} x_n \delta_n |n| P_{n-s}(u) \right]$, $s = 0,1$, and the values $\widehat{x}_m$ satisfy the condition $\sum\limits_{m=-\infty}^{\infty} \left| \widehat{x}_m \right|^2 < \infty$.

We will not go into details of the demonstration of (2.32) but only mention that the derivation of this asymptotic estimate rests on the explicit expression of V_{m-1}^{n-1} through the Legendre polynomials, inequality (2.28), and representation (2.3) for γ_n. Asymptotic estimates of this kind are found very useful in the summation of the x_m involving series, in particular, the series of the type (2.1) and (2.2). In diffraction theory (electrodynamics), they play the part of currents or charge densities, etc. These series, as seen from (2.1) and (2.2), have a slow rate of convergence so that their summation presents a problem. An evident means of the convergence improvement of these series is recognizing the x_m asymptotic behavior as $|m| \to \infty$ for the explicit summation of the asymptotic terms. The latter is possible in so far as in actual practice, the values γ_m, f_m, g_m usually satisfy stronger conditions than those above.

2.2.2 *Classical Dual Series Equations with "Matrix Perturbation"*

The elementary dual series equations discussed in the previous paragraph allow some generalizations. One such is the dual series equations

$$\sum_{n=-\infty}^{\infty} \left[\gamma_n x_n + (Vx)_n \right] e^{in\vartheta} = F(\vartheta);\ |\vartheta| < \vartheta_0, \tag{2.33}$$

$$\sum_{n=-\infty}^{\infty} \left[x_n + (Ux)_n \right] e^{in\vartheta} = G(\vartheta);\ \vartheta_0 < |\vartheta| \le \pi, \tag{2.34}$$

where $x = \{x_n\}_{n=-\infty}^{\infty}$ is the column vector of the unknowns, $U = \left\{U_{pq}\right\}_{p,q=-\infty}^{\infty}$ and $V = \left\{V_{pq}\right\}_{p,q=-\infty}^{\infty}$ are some given infinite-dimensional matrix operators with matrix elements U_{pq} and V_{pq} decreasing fast enough as $|p|,|q| \to \infty$. $(Ux)_n$ and $(Vx)_n$ are the nth components of the vector columns Ux and Vx, respectively, $F(\vartheta)$ and $G(\vartheta)$ are given functions, and $\vartheta_0 \in (0;\pi)$ is a fixed parameter. Concerning the given sequence γ_n, $n = 0,\pm1,\pm2\ldots$, it is assumed that

$$\gamma_n = |n| \begin{cases} C^+ \left[1 + O\left(n^{-2}\right) \right];\ n \to \infty \\ C^- \left[1 + O\left(n^{-2}\right) \right];\ n \to -\infty \end{cases} \tag{2.35}$$

with $C^{\pm}$ being some n-independent constants. In the general case, $C^+ \neq C^-$.

Below, the problem formulation for some classes of series equations is elaborated to recognize the spaces of the column vector x and the functions $F(\vartheta)$, $G(\vartheta)$, the sense of equations (2.33) and (2.34), and other specific points.

By the commonly accepted terminology, expressions (2.33) and (2.34) are dual series equations involving $\exp(in\vartheta)$ functions. We will call them standard equations when $U = V = 0$. If $U \neq 0$ and (or) $V \neq 0$, then (2.33) and (2.34) are matrix perturbation equations. And, finally, they are equations with diagonal matrix perturbation when U and V represent diagonal matrices.

It is not difficult to see that multiplying (2.33) and (2.34) by $\exp(im\vartheta)$, $m = 0,\pm1,\ldots$, and integrating between $(-\vartheta_0;\vartheta_0)$ and $(-\pi,\vartheta_0)$, $(\vartheta_0;\pi)$, respectively, yields the infinite system of linear algebraic equations, which is a functional equation of the first kind for x, with all notorious disadvantages of the equations of that kind.

Clearly any other straightforward algebraization of equations (2.33) and (2.34) will end up with a similar result, forcing us to invent a proper regularization procedure in an effort to solve equations (2.33) and (2.34). In this section, a regularization procedure of the kind will be developed for equations (2.33) and (2.34) in the case $C^+ = C^-$ [see (2.35)] [75, 92]. The regularization procedure described below is based on the development of a closed-form solution to the standard ($U = V = 0$) dual series equations by means of the Riemann–Hilbert boundary value problem theory [80]. With this knowledge, system (2.33) and (2.34) can be equivalently reduced to an infinite system of linear algebraic equations of the second kind to be effectively numerically solved by truncation.

If $C^+ = C^-$, dual series equations (2.33) and (2.34) appear to be

$$ax_0 + \sum_{n=-\infty}^{\infty} x_n |n| \, \mathrm{e}^{in\vartheta} + \sum_{n=-\infty}^{\infty} \left[\left(\bar{V}x \right)_n - f_n \right] \mathrm{e}^{in\vartheta} = 0; \ |\vartheta| < \vartheta_0, \tag{2.36}$$

$$\sum_{n=-\infty}^{\infty} x_n \mathrm{e}^{in\vartheta} + \sum_{n=-\infty}^{\infty} \left[(Ux)_n - g_n \right] \mathrm{e}^{in\vartheta} = 0; \ |\vartheta| > \vartheta_0, \tag{2.37}$$

where $a = \gamma_0/C^+, f = \{f_n\}_{n=-\infty}^{\infty}$ and $g = \{g_n\}_{n=-\infty}^{\infty}$ are the Fourier coefficients of the functions $(1/C^+)$. $F(t)$ and $G(t)$, respectively. The matrix operator $\bar{V}$ is related to V as

$$\bar{V} = V + D, \tag{2.38}$$

where $D = \left\{ d_p \delta_p^q \right\}_{q,p=-\infty}^{\infty}$ is a diagonal matrix operator, $d_p = \gamma_p / C^+ - |p|$, $p = \pm1,\pm2,\ldots$, $d_0 = 0$ and δ_p^q is the Kronecker delta. From (2.35) it follows that $d_p = O\left(|p|^{-1}\right)$. As to the unknown column vectors x and the coefficients f and g, we assume that

$$x \in l_2(1); \tag{2.39}$$

$$g \in l_2(1), f \in l_2(-1). \tag{2.40}$$

In addition, all the series in (2.36) and (2.37) are assumed to be the Fourier series of their sums. That is, the series in (2.36) and (2.37) are [according to (2.39)] the Fourier series of the relevant functions belonging, respectively, to $\mathbf{L}_1[-\pi;\pi]$ and $\mathbf{L}_2[-\pi;\pi]$. Regarding the matrix operators $\bar{V}$, assume that the operators $T^{-1}\bar{V}T^{-1}$ and TUT^{-1} are compact as long as they act in the l_2 space, where the diagonal operator T is given by the matrix

$$T = \left\{\tau_n \delta_m^n\right\}_{m,n=-\infty}^{\infty};\ \tau_0 = 1, \tau_n = |n|^{1/2},\ n \neq 0. \tag{2.41}$$

Introduce the column vectors ψ,φ by the formulas

$$\varphi = \{\varphi_n\}_{n=-\infty}^{\infty}, \psi = \{\psi_n\}_{n=-\infty}^{\infty}, \tag{2.42}$$

$$\psi_n = (Ux)_n - g_n, \quad \varphi_n = ax_0\delta_0^n + \left(\bar{V}x\right)_n - f_n;\ n = 0, \pm 1, \pm 2,... \tag{2.43}$$

With this notation, equations (2.36) and (2.37) take the form

$$\sum_{n=-\infty}^{\infty} x_n \mathrm{e}^{in\vartheta} + \sum_{n=-\infty}^{\infty} \psi_n \mathrm{e}^{in\vartheta} = 0;\ |\vartheta| > \vartheta_0, \tag{2.44}$$

$$\sum_{n=-\infty}^{\infty} x_n |n| \mathrm{e}^{in\vartheta} + \sum_{n=-\infty}^{\infty} \varphi_n \mathrm{e}^{in\vartheta} = 0;\ |\vartheta| < \vartheta_0. \tag{2.45}$$

Now put aside formulas (2.42) and (2.43), assuming that the column vectors φ,ψ are known. Our immediate task is to construct for (2.44) and (2.45) a closed-form solution that satisfies condition (2.39). We will begin with a formal scheme for the derivation of the solution, ending with a brief mathematical justification (for details, see [11, 92]).

Introduce the new unknowns $y = \{y_n\}_{n=-\infty}^{\infty}$

$$y_0 = x_0 + \psi_0,\ y_n = n\left(x_n + \psi_n\right);\ n = \pm 1, \pm 2,... \tag{2.46}$$

Differentiate (2.44) with respect to ϑ term by term and, making use of (2.46), obtain from (2.44) and (2.45) the following system of equations:

$$\sum_{n\neq 0} y_n \mathrm{e}^{in\vartheta} = 0;\ |\vartheta| > \vartheta_0, \tag{2.47}$$

$$\sum_{n\neq 0} \frac{|n|}{n} y_n \mathrm{e}^{in\vartheta} = \sum_{n=-\infty}^{\infty} \left(|n|\,\psi_n - \varphi_n\right) \mathrm{e}^{in\vartheta};\ |\vartheta| < \vartheta_0, \tag{2.48}$$

$$\sum_{n\neq 0} (-1)^n n^{-1} y_n = -y_0. \tag{2.49}$$

Equation (2.49) comes directly from (2.44) at $\vartheta = \pi$ owing to (2.46). The fact is that the differentiation of (2.44) loses the zeroth Fourier coefficient information. To

avoid this error and guarantee an equivalent passage from (2.44), (2.45) to (2.47), (2.48), equation (2.44) is applied at some ϑ point, $|\vartheta| > \vartheta_0$, e.g., $\vartheta = \pi$. One easily checks that the solution of equations (2.44) and (2.45) does not depend on a particular choice of this point.

According to [92], the dual series equations (2.47), (2.48), and (2.49) can be converted to some Riemann–Hilbert boundary value problem. Indeed, define some two functions of the complex variable z as

$$X^+(z) = \sum_{n=1}^{\infty} y_n z^n, \quad X^-(z) = -\sum_{n=1}^{\infty} y_{-n} z^{-n}. \tag{2.50}$$

The functions $X^+(z)$ and $X^-(z)$ are analytic inside and outside, respectively, the circle $|z| = 1$. Let some arc $\mathbf{P}_2$ on the circle $|z| = 1$ connect the points $\exp(-i\vartheta_0)$ and $\exp(i\vartheta_0)$ through $z = -1$, with arc $\mathbf{P}_1$ complementing $|z| = 1$ to the full circle. With these functions, equations (2.47) and (2.48) take on the appearance ($z = \exp(i\vartheta_0)$)

$$X^+(z) - X^-(z) = 0; z \in P_2, \tag{2.51}$$

$$X^+(z) + X^-(z) = \sum_{n=-\infty}^{\infty} (|n|\,\psi_n - \varphi_n)\, z^n; z \in P_1. \tag{2.52}$$

From (2.51) it follows that the function

$$X(z) = \begin{cases} X^+(z); & |z| < 1 \\ X^-(z); & |z| > 1 \end{cases} \tag{2.53}$$

continues as a function analytic in the complex plane with a cut along $\mathbf{P}_1$ arc and decreases as $|z| \to \infty$ according to (2.50). Namely,

$$X(z) = -y_{-1} z^{-1} + O\left(z^{-2}\right). \tag{2.54}$$

As (2.36) and, consequently, (2.48) are assumed to be the series of their sums on $\mathbf{L}_1[-\pi;\pi]$, the limiting $X(z)$ values on the circle $|z| = 1$ belong to $\mathbf{L}_1[-\pi;\pi]$ as well. In this case, equations (2.47) and (2.48) are equivalent to the problem of the $X(z)$ reconstruction by the sum of its limiting values on arc $\mathbf{P}_1$, where the function $X(z)$ is not analytic. This problem represents an elementary variant of the Riemann–Hilbert boundary value problem (see [80]). Its solution is well known and available in the form (see [80])

$$X(z) = \frac{1}{2\pi i R(z)} \int_{\mathbf{P}_1} \frac{F(\tau) R(\tau)}{\tau - z} d\tau + \frac{y_{-1}}{R(z)}, \tag{2.55}$$

where

$$F(\tau) = \sum_{n=-\infty}^{\infty} (|n|\,\psi_n - \varphi_n)\ \tau^n, \tag{2.56}$$

$$R(z) = \left[\left(z - e^{i\vartheta_0}\right)\left(z - e^{-i\vartheta_0}\right)\right]^{1/2}. \tag{2.57}$$

The function $R(z)$ is analytic in the complex plane cut along arc $\mathbf{P}_1$, the root branch $R(0) = 1$ chosen.

Now let us show how dual series equations (2.47), (2.48), and (2.49) should be solved using (2.55). By virtue of the Sokhotskyi-Plemelj formulas (see [94]), from expression (2.55), it follows that for $|z| = 1$

$$X^+\left(e^{i\vartheta}\right) - X^-\left(e^{i\vartheta}\right) = \frac{K\left(e^{i\vartheta}\right)}{\pi i}\int\limits_{\mathbf{P}_1} \frac{F(\tau)\,\mathbf{R}^+(\tau)}{\tau - e^{i\vartheta}} d\tau + 2y_{-1}K\left(e^{i\vartheta}\right), \tag{2.58}$$

where the integral is regarded as the Cauchy principal value, $R^+(\tau)$ denotes the limiting value of $R(z)$ on the inside of unit-circle arc $\mathbf{P}_1$: at $z = \tau(1–\varepsilon)$ and $\varepsilon \to +0$, and

$$K(\tau) = \begin{cases} \frac{1}{\mathbf{R}^+(\tau)};\ \ \tau \in \mathbf{P}_1 \\ 0;\ \ \tau \in \mathbf{P}_2 \end{cases}. \tag{2.59}$$

Match the Fourier coefficients on both sides of equation (2.58) and on account of (2.56), get the relations

$$y_m = \sum_{n=-\infty}^{\infty} (|n|\,\psi_n - \varphi_n)\ V_m^n + 2y_{-1}R_m;\ m = \pm 1, \pm 2, \ldots, \tag{2.60}$$

$$0 = \sum_{n=-\infty}^{\infty} (|n|\,\psi_n - \varphi_n)\ V_0^n + 2y_{-1}R_0, \tag{2.61}$$

with V_m^n and R_m given below [see (2.63) and (2.64)]. Equations (2.60) and (2.61) should be completed with equation (2.49), which on the substitution of the right-hand side of equation (2.60) for y_m becomes

$$-y_0 = \sum_{n=-\infty}^{\infty} (|n|\,\psi_n - \varphi_n)\, V_\sigma^n + 2y_{-1}R_\sigma. \tag{2.62}$$

The coefficients V_m^n, R_m, V_σ^n, R_σ originally calculated in [45] are expressed via Legendre polynomials $P_n(u)$, (see [95] for their definition $P_0(u) = 1$, $P_1(u) = u, \ldots$)

$$V_m^n = \begin{cases} \frac{m+1}{2(m-n)}\left[P_m(u)P_{n+1}(u) - P_{m+1}(u)P_n(u)\right]; & m \neq n \\ \frac{1}{2}\sum\limits_{p=0}^{m+1} \rho_{m+1-p}(u); & n = m \geq 0 \\ -V_{|m|-2}^{|m|-2}(u); & n = m \leq -2 \\ 0; & n = m = -1 \end{cases}, \tag{2.63}$$

$$\begin{cases} R_m = \frac{1}{2}P_m(u); & m = 0, \pm 1, \pm 2, \ldots \\ P_{-n-1}(u) = P_n(u); & n = 0,1,2,\ldots \\ R_\sigma = -\frac{1}{2}\ln\frac{1+u}{2} \end{cases}, \tag{2.64}$$

$$V_\sigma^n = \begin{cases} \frac{1}{2}\rho_{\bar{n}}(u)\ln\frac{1+u}{2} + \frac{1}{2|n|}\left[P_{|n|}(u) - P_{|n|-1}(u)\right]; & n \neq 0, -1 \\ \frac{u-1}{2}\left(\ln\frac{1+u}{2} + 1\right); & n = -1 \\ \frac{1+u}{2}\ln\frac{1+u}{2}; & n = 0 \end{cases}, \tag{2.65}$$

where $u = \cos\vartheta_0$, $\bar{n} = \begin{cases} n+1; n > 0 \\ -n; \quad n < -1 \end{cases}$, $\rho_0(u) = 1$, $\rho_1(u) = -u$, and

$$\rho_n(u) = P_n(u) - 2uP_{n-2}(u) + P_{n-2}(u); \; n = 2,3,\ldots \tag{2.66}$$

In order to get y_m, $m = 0,\pm 1,\ldots$, in explicit form (recall that φ_n, ψ_n are assumed to be known), one only needs, on account of (2.61), to discard y_{-1} from (2.60) and (2.62). Indeed, substitute the expression

$$y_{-1} = 0.5R_0^{-1}\sum_{n=-\infty}^{\infty}(|n|\psi_n - \varphi_n)\; V_0^n \tag{2.67}$$

obtained from (2.61) into the right-hand sides of (2.60) and (2.62) to obtain

$$\begin{cases} y_m = \sum\limits_{n=-\infty}^{\infty}(|n|\psi_n - \varphi_n)\left(V_m^n - R_0^{-1}R_m V_0^n\right); & m = \pm 1, \pm 2, \ldots \\ y_0 = \sum\limits_{n=-\infty}^{\infty}(|n|\psi_n - \varphi_n)\left(R_0^{-1}R_\sigma V_0^n - V_\sigma^n\right) \end{cases}. \tag{2.68}$$

With formulas (2.63), (2.64), (2.65), and (2.66), it is not difficult to check the identities

$$V_{m-1}^{n-1} = V_m^n - R_0^{-1}R_m V_0^n,\; R_0^{-1}R_\sigma V_0^n - V_\sigma^n = \begin{cases} -\ln\frac{1+u}{2}; & n = 0 \\ n^{-1}V_{n-1}^{-1}; & n \neq 0 \end{cases}. \tag{2.69}$$

Substitute (2.69) into (2.68) and return to the unknowns $\{x_m\}_{m=-\infty}^{\infty}$. Then the solution to equations (2.44) and (2.45) with ψ_n, φ_n known is

$$x_0 = W_0\varphi_0 - \psi_0 + \sum_{n\neq 0}(|n|\psi_n - \varphi_n)\; n^{-1}V_{n-1}^{-1}, \tag{2.70}$$

$$x_m = -\psi_m + \sum_{n=-\infty}^{\infty} (|n|\,\psi_n - \varphi_n)\, m^{-1} V_{m-1}^{n-1}; \quad m = \pm 1, \pm 2, \ldots,$$
$$W_0 = \ln \frac{1+u}{2} \tag{2.71}$$

Thus, formulas (2.70) and (2.71) lend a closed-form solution to the standard dual series equations (2.44) and (2.45). On this basis, we will build an infinite system of linear algebraic equations of the second kind equivalent to the initial dual series equations (2.33) and (2.34) with matrix perturbation. For this, pass from the column vectors x, φ, ψ (see 2.43) assumed to satisfy the conditions [see (2.39) and (2.40)] $x \in l_2(1)$, $\psi \in l_2(1)$, and $\varphi \in l_2(-1)$, to the column vectors

$$\widehat{x} = \left\{\widehat{x}_n\right\}_{n=-\infty}^{\infty} = Tx \in l_2, \qquad \widehat{\psi} = \left\{\widehat{\psi}_n\right\}_{n=-\infty}^{+\infty} = T\psi \in l_2,$$
$$\widehat{\varphi} = \left\{\widehat{\varphi}_n\right\}_{n=-\infty}^{\infty} T^{-1}\varphi \in l_2$$

lying on the l_2 space, the operator T is defined in (2.41).

Relations (2.70) and (2.71) are readily transformed to become

$$\widehat{x}_m = \sum_{n=-\infty}^{\infty} W_{mn}\left(\widehat{\psi}_n - \widehat{\varphi}_n\right) + \sum_{n=-\infty}^{\infty} P_{mn}\,\widehat{\psi}_n - \widehat{\psi}_m \qquad m = 0, \pm 1, \ldots \tag{2.72}$$

with

$$W_{mn} = \begin{cases} -W_0; \ m = n = 0 \\ \frac{\tau_n V_{n-1}^{-1}}{n}; \ n \neq 0, \quad m = 0 \\ \frac{\tau_n \tau_m V_{m-1}^{n-1}}{m}; \ m \neq 0 \end{cases}, P_{mn} = \begin{cases} W_0; \ m = n = 0 \\ -W_{m0}; \ m \neq 0, \quad n = 0 \\ 0; \ n \neq 0 \end{cases}. \tag{2.73}$$

Thus, by virtue of (2.73) with the matrix operators

$$W = \{W_{mn}\}_{m,n=-\infty}^{\infty}, \qquad P = \{P_{mn}\}_{m,n=-\infty}^{\infty}, \tag{2.74}$$

formulas (2.72) become

$$\widehat{x} = W\left(\widehat{\psi} - \widehat{\varphi}\right) + (P - E)\,\widehat{\psi}, \tag{2.75}$$

where E is the identity matrix operator.

Armed with formula (2.75) for solving equations (2.44) and (2.45) with φ, ψ known, proceed to the regularization of equations (2.73) and (2.37) on account of expressions (2.42) and (2.43) relating ψ_n, φ_n and f_n, g_n, x_n. To this end, define the column vectors

$$f = \{f_n\}_{n=-\infty}^{\infty}, \; g = \{g_n\}_{n=-\infty}^{\infty}, \tag{2.76}$$

$$\widehat{f} = \left\{\widehat{f}_n\right\}_{n=-\infty}^{\infty} = T^{-1}f, \quad \widehat{g} = \left\{\widehat{g}_n\right\}_{n=-\infty}^{\infty} = Tg. \tag{2.77}$$

Consequently, formulas (2.43) become

$$\widehat{\psi}_n = \left(\widehat{U}\,\widehat{x}\right)_n - \widehat{g}_n, \;\; \widehat{\varphi}_n = a\delta_0^n \widehat{x}_n + \left(\widehat{V}\,\widehat{x}\right)_n - \widehat{f}_n, \tag{2.78}$$

where $\widehat{U}$ and $\widehat{V}$ are the matrix operators

$$\widehat{U} = TUT^{-1}, \;\; \widehat{V} = T^{-1}\bar{V}T^{-1} \tag{2.79}$$

which are compact, by assumption, on the space l_2. Then relations (2.78) in the vector form are

$$\widehat{\psi} = \widehat{U}\,\widehat{x} - \widehat{g}\,, \;\widehat{\varphi} = a\,\widehat{E}\,\widehat{x} + \widehat{V}\,\widehat{x} - \widehat{f} \tag{2.80}$$

with the matrix operator $\widehat{E}$ defined as $\widehat{E} = \left\{\delta_m^0 \delta_n^0\right\}_{m,n=-\infty}^{\infty}$.

Considering (2.75) and (2.80) as a system of equations for the unknowns $\widehat{x}$, $\widehat{\varphi}$, $\widehat{\psi}$ and removing the unknowns $\widehat{\varphi}$, $\widehat{\psi}$ from (2.75) in view of (2.80), one arrives after some elementary transformations at the equation for $\widehat{x}$

$$(E + H)\,\widehat{x} = \widehat{b}\,, \tag{2.81}$$

with the matrix operator H and the column vector $\widehat{b}$ in the form

$$H = -aP + (E - P)\,\widehat{U} + W\left(\widehat{V} - \widehat{U}\right), \tag{2.82}$$

$$\widehat{b} = (E - P)\,\widehat{g} + W\left(\widehat{f} - \widehat{g}\right). \tag{2.83}$$

Now let us prove that the operator H available from (2.82) is compact on l_2 and, hence, equation (2.81) is a second-kind equation on l_2. In this case, we will assume that the matrix operators $\widehat{U}$, $\widehat{V}$ defined by formulas (2.79) are compact on l_2.

First of all we will show that the operator W is bounded on l_2. Put the column vector $x = \{x_n\}_{n=-\infty}^{\infty} \in l_2$ and prove that the column vector $y = \{y_m\}_{m=-\infty}^{\infty}$ such that $y{=}Wx$ belongs to l_2 for any $x{\in}l_2$. Indeed, in view of (2.73) and (2.63), we have

$$\begin{aligned} y_0 &= \sum_{n\neq 0} W_{0n}x_n = -W_0x_0 + \sum_{n\neq 0} \tau_n n^{-1} V_{n-1}^{-1} x_n = \\ &= -W_0x_0 + \tfrac{1}{2}\sum_{n\neq 0} \tau_n n^{-1}\left[P_{n-1}(u) - P_n(u)\right]x_n. \end{aligned}$$

On account of the inequality [see (2.60)]

$$|P_n(u)| < \frac{2}{\sqrt{\pi |n| \left(1-u^2\right)}}; \; n = \pm 1, \pm 2, \ldots \tag{2.85}$$

together with the Cauchy–Bunyakowsky inequality, the absolute convergence of the series (2.84) is ensured. Next let $m \neq 0$. Then

$$\begin{aligned} y_m = \sum_{n=-\infty}^{\infty} W_{mn} x_n = m^{-1} \tau_m^2 V_{m-1}^{m-1} x_m + \tfrac{P_{m-1}(u)}{2} \tau_m \sum_{m \neq n} \tfrac{\tau_n P_n(u)}{m-n} x_n - \\ - \tfrac{P_m(u)}{2} \tau_m \sum_{m \neq n} \tfrac{\tau_n P_{n-1}(u)}{m-n} x_n; \quad m = \pm 1, \pm 2, \ldots \end{aligned} \tag{2.86}$$

Make use of the fact that the matrix

$$\{\alpha_{mn}\}_{m,n=-\infty}^{\infty}: \; \alpha_{mn} = \begin{cases} 0; & m = n \\ \frac{1}{m-n}; & m \neq n \end{cases}$$

produces the bounded operator (see [70]) on l_2. Considering the estimate (2.85), we obtain from (2.86) that y_m can be written as

$$y_m = m^{-1} \tau_m^2 V_{m-1}^{m-1} x_m + \tau_m P_{m-1}(u) f_m^1 + \tau_m P_m(u) f_m^2, \tag{2.87}$$

where $\left\{f_m{}^j\right\}_{m=-\infty}^{\infty}, j = 1,2$, are some vector columns belonging to l_2. In view of the inequality

$$\left| V_{m-1}^{m-1} \right| < 2; \; m = \pm 1, \pm 2, \ldots$$

it immediately follows that the values y_m, $m = \pm 1, \pm 2, \ldots$, are quadratically summable.

The finite-valuedness of y_0 has been shown, proving, in turn, that the matrix W produces a linear operator defined everywhere on l_2. From the definition of W_{mn} [see (2.73)] it follows that the matrix W is self-adjoint. The previously established facts suggest, according to [70], that the operator W is bounded on l_2.

Now let us prove that the matrix $\{P_{mn}\}_{m,n=-\infty}^{\infty}$ produces a Hilbert–Schmidt operator on l_2. For this purpose, the convergence of $\sum\limits_{m,n} |P_{mn}|^2$ will suffice (see [70]). From (2.73),

$$\sum_{m,n} |P_{mn}|^2 = \sum_{m} \left|P_{m_0}\right|^2 = W_0^2 + \sum_{m \neq 0} m^{-2} \tau_m^2 \left(V_{m-1}^{-1}\right)^2 < W_0^2 + \text{const} \sum_{m \neq 0}^{\infty} m^{-3/2} < \infty.$$

Hence it immediately follows that the operator H defined by formula (2.82) is compact on l_2. Indeed, the operator R is compact as a Hilbert–Schmidt operator. Also, we have already shown that operator W is bounded, while the operators $\widehat{U}$

and $\widehat{V}$ are compact by assumption. Hence, the operator $W\left(\widehat{V}-\widehat{U}\right)$ is compact, too, which is what we set out to prove.

Based on the properties of operators R and W, one finds that, in view of (2.77) and (2.83), the column vectors $\widehat{b}$ and $\widehat{x}$ belong to l_2.

Thus, (2.81) represents an infinite system of linear algebraic equations of the second kind on l_2.

It is not difficult to extend the validity of the analytic regularization procedure designed for dual series equations (2.36) and (2.37) to the coupled system of a finite number of these equations below

$$\begin{cases} a_j x_0^j + \sum\limits_{n=-\infty}^{\infty} |n|\, x_n^j \mathrm{e}^{in\vartheta} + \sum\limits_{p=1}^{M} \sum\limits_{n=-\infty}^{\infty} \left[\left(V^{jp}x^p\right)_n - f_n^j\right] \mathrm{e}^{in\vartheta} = 0; \quad |\vartheta| < \vartheta_j \\ \sum\limits_{n=-\infty}^{\infty} x_n^j \mathrm{e}^{in\vartheta} + \sum\limits_{p=1}^{M} \sum\limits_{n=-\infty}^{\infty} \left[\left(U^{jp}x^p\right)_n - g_n^j\right] \mathrm{e}^{in\vartheta} = 0; \qquad |\vartheta| > \vartheta_j, j = 1,2,...,M \end{cases} \tag{2.88}$$

in the unknowns $x^j = \left\{x_n^j\right\}_{n=-\infty}^{\infty}, j = 1,2,\ldots, M$.

Both the values involved in (2.88) and the requirements imposed on them are the same as for equations (2.36) and (2.37), and therefore we avoid repetition of the details.

The regularization of equations (2.88), in other words, their reduction to an infinite system of linear algebraic equations of the second kind obeys the scheme developed for equations (2.36) and (2.37). First, the vectors

$$\psi^j = \sum_{p=1}^{M} U^{jp}x^p - g^j, \quad \varphi^j = a^j \widehat{E}\, x^j + \sum_{p=1}^{M} V^{jp}x^p - f^j \tag{2.89}$$

are assumed to be known and possessing the properties desired. By analogy with the previous case, equations of (2.44) and (2.45) type are obtained for every $j = 1,2,\ldots, M$. In view of (2.89), they are transformed to the analog of equation (2.81) in the form

$$\widehat{x}^j + \sum_{p=1}^{M} H^{jp}\, \widehat{x}^p = \widehat{b}^{\,j}; \; j = 1,2,...,M, \tag{2.90}$$

where

$$H^{jp} = -a^j P^j + \left(E - P^j\right) \widehat{U}^{jp} + W^j \left(\widehat{V}^{jp} - \widehat{U}^{jp}\right),$$
$$\widehat{b}^j = \left(E - P^j\right) \widehat{g}^j + W^j \left(\widehat{f}^j - \widehat{g}^j\right).$$

In equations (2.90), $\widehat{x}^j$, $\widehat{f}^j$, $\widehat{g}^j$ for all $j = 1,2,\ldots, M$ are expressed, respectively, through x^j, f^j, g^j via (2.76) and (2.77). The operators U^{jp} and V^{jp} are related to

U^{jp} and V^{jp} by formulas (2.79). Finally, the operators P^j, W^j for every $j = 1,2,\ldots,M$ come from formulas (2.63) to (2.66), (2.73), and (2.74), with ϑ_0 substituted by ϑ_j.

By construction, all the vectors in (2.90) belong to the l_2 space. It is easily proved that all the matrix operators involved in (2.90) and considered as operators acting on l_2 are compact. Hence, (2.90) is a system of equations of the second kind.

In closing mention should be made that the two-dimensional problem of electromagnetic (acoustic) wave diffraction by a grating consisting of finite-number elements like nonclosed arbitrarily shaped cylindrical screens is reduced to the systems of equations of (2.88) type [11].

2.2.3 Dual Series Equations with the Nonunit Coefficient of Conjugation

In this paragraph, the dual series equations (2.33) and (2.35) are examined in the case $C^{\pm} \neq C^{-}$ [see (2.35)]. Equations of this nature appear, to give one example, in problems of wave diffraction by a single-periodic perfectly conducting grating located on the interface of a gyrotropic medium (magnetoactive plasma, anisotropic dielectric, ferrite, etc.).

The regularization algorithm of these equations is designed to use the relevant standard equations solved in analytic (explicit) terms by considering the boundary value Riemann–Hilbert problem in theory of analytic functions. Suppose that we are given constants $C^{\pm}$ from (2.35) as complex numbers with the imaginary part other than zero (Im $C^{\pm} \neq 0$). The dual series equations (2.33) and (2.34) then take on the appearance

$$ax_0 + \sum_{n=1}^{\infty} nx_n e^{in\vartheta} - b \sum_{n=-\infty}^{-1} nx_n e^{in\vartheta} + \sum_{n=-\infty}^{\infty} \left[\left(\bar{V}x\right)_n - f_n\right] e^{in\vartheta} = 0;\ |\vartheta| < \vartheta_0, \tag{2.91}$$

$$\sum_{n=-\infty}^{\infty} x_n e^{in\vartheta} + \sum_{n=-\infty}^{\infty} \left[(Ux)_n - g_n\right] e^{in\vartheta} = 0;\ |\vartheta| > \vartheta_0, \tag{2.92}$$

where $a = \gamma_0/C_+$, $b = C_-/C_+$.

Evidently for b=1 ($C^+ = C^-$), these equations coincide with (2.36) and (2.37). Hereafter the parameter b will be called the conjugation coefficient of the dual series equations of the type (2.91) and (2.92). Assume that the imaginary part of the conjugation coefficient does not vanish (Im $b \neq 0$) and the column vectors $x = \{x_n\}_{n=-\infty}^{\infty}$, $f = \{f_n\}_{n=-\infty}^{\infty}$, and $g = \{g_n\}_{n=-\infty}^{\infty}$ are such that

$$x \in l_2(\eta), \tag{2.93}$$

$$g \in l_2(\eta), \qquad f \in l_2(-\eta), \tag{2.94}$$

where $\eta = 1+(\arg b)/\pi, -\pi < \arg b < \pi$, and the space $l_2(\eta)$ is defined in (2.5). The matrix operators $\widehat{T}\,U\,\widehat{T}^{-1}$ and $\widehat{T}^{-1}\bar{V}\,\widehat{T}^{-1}$ are assumed to be compact in the space l_2, the matrix operator $\widehat{T}$ is given by the formula

$$\widehat{T} = \left\{\widehat{\tau}_n \delta_m^n\right\}_{m,\,n=-\infty}^{\infty}; \quad \widehat{\tau}_0 = 1, \quad \widehat{\tau}_n = |n|^{\eta/2}; \, n \neq 0. \tag{2.95}$$

Besides, the matrix operator $\bar{V}$, as opposed to (2.38), is

$$\bar{V} = V + D. \tag{2.96}$$

Here,

$$D = \left\{d_n \delta_m^n\right\}_{m,\,n=-\infty}^{\infty}; \quad d_o = 0, \quad d_n = \begin{cases} \dfrac{\gamma_n}{C^+} - n; & n > 0 \\ \dfrac{\gamma_n}{C^+} + n\dfrac{C^-}{C^+}; & n < 0 \end{cases}.$$

The remaining requirements imposed on the values in (2.91) and (2.92) and, also, the Fourier series convergence are the same as for equations (2.31) and (2.37).

In view of (2.42) and (2.43), transform equations (2.91) and (2.92) to be similar to (2.47), (2.48), and (2.49) as follows:

$$\sum_{n\neq 0} y_n \mathrm{e}^{in\vartheta} = 0; \; |\vartheta| > \vartheta_0, \tag{2.97}$$

$$\sum_{n=1}^{\infty} y_n \mathrm{e}^{in\vartheta} - b \sum_{n=-\infty}^{-1} y_n \mathrm{e}^{in\vartheta} = \sum_{n=-\infty}^{\infty} \left(|n|\,\psi_n \delta_n - \varphi_n\right) \mathrm{e}^{in\vartheta}; \tag{2.98}$$

$$\sum_{n\neq 0} (-1)^n n^{-1} y_n = -y_0, \tag{2.99}$$

where

$$y_n = \delta_n^0 (x_0 + \psi_0) + n\,(x_n + \psi_n)\,, \; \delta_n = \begin{cases} 1; & n \geq 0 \\ b; & n < 0 \end{cases}.$$

Suppose that we are given the column vectors $\psi = \{\psi_n\}_{n=-\infty}^{\infty}$, $\varphi = \{\varphi_n\}_{n=-\infty}^{\infty}$ and check that equations (2.97), (2.98), and (2.99) are uniquely solvable for any value of the conjugation coefficient b, $\mathrm{Im}\, b \neq 0$. For this purpose, one only needs to know if the corresponding homogeneous equations ($\psi_n = \varphi_n = 0$; $n = 0, \pm 1, \ldots$) possess the trivial $y_n{=}0$, $n = 0, \pm 1, \ldots$, solution. Introduce the two functions

$$F_1(\vartheta) = \sum_{n\neq 0} y_n \mathrm{e}^{in\vartheta}, \qquad F_2(\vartheta) = \sum_{n=1}^{\infty} y_n \mathrm{e}^{in\vartheta} - b \sum_{n=-\infty}^{-1} y_n \mathrm{e}^{in\vartheta} \tag{2.100}$$

on the interval $[-\pi;\pi]$. Insofar as for $x = \{x_n\}_{n=-\infty}^{\infty}$, condition (2.93) must hold and the corresponding series in (2.91) and (2.92) are the Fourier series of their sums; functions (2.100) obey the Parseval equation

$$\int_{-\pi}^{\pi} F_1^* F_2 d\vartheta = 2\pi \sum_{n=-\infty}^{\infty} f_{1n}^* f_{2n}, \tag{2.101}$$

where $*$ indicates complex conjugation, f_{1n} and f_{2n} are the Fourier coefficients of the functions $F_1(\vartheta)$ and $F_2(\vartheta)$, respectively. From (2.97), (2.98), and (2.101), $\sum_{n=-\infty}^{\infty} f_{1n}^* f_{2n} = 0$. Therefore,

$$\sum_{n=1}^{\infty} |y_n|^2 - b \sum_{n=-\infty}^{-1} |y_n|^2 = 0. \tag{2.102}$$

After separation of the imaginary part

$$\sum_{n=-\infty}^{-1} |y_n|^2 \mathrm{Im} b = 0.$$

Hence $\sum_{n=-\infty}^{-1} |y_n|^2 = 0$ and $\sum_{n=1}^{\infty} |y_n|^2 = 0$. That is, $y_n = 0$, $n = 0,\pm1,\pm2\ldots$. From (2.99), $y_0 = 0$. And it has been shown that equations (2.97), (2.98), and (2.99) possess only a trivial solution for $\psi_n = \varphi_n = 0$, $n = 0,\pm1,\ldots$.

Now let us build a solution of these equations assuming that the column vectors $\varphi = \{\varphi_n\}_{n=-\infty}^{\infty}$ and $\psi = \{\psi_n\}_{n=-\infty}^{\infty}$ are known. To this end, reduce (2.97), (2.98), and (2.99) to the boundary value Riemann–Hilbert problem. Let $y = \{y_n\}_{n=-\infty}^{\infty}$ be the sought solution. Similar to (2.50) and (2.53), give the function $X(z)$ of a complex variable z by the formula

$$X(z) = \begin{cases} \sum_{n=-1}^{\infty} y_n z^n; |z| < 1 \\ -\sum_{n=-\infty}^{-1} y_n z^n; \quad |z| > 1 \end{cases}. \tag{2.103}$$

As follows from (2.97), this function is analytic on the complex plane with a cut along the unit-circle arc $\mathbf{P}$ connecting the points $\exp(-i\vartheta_0)$ and $\exp(i\vartheta_0)$ through the point $z = 1$. Denote by $X^+(z)$ and $X^-(z)$ the limiting values of $X(z)$ on the arc $\mathbf{P}$, correspondingly, inside and outside the unit circle $|z| \le 1$. Then from (2.98),

$$X^+(z) + bX^-(z) = \sum_{n=-\infty}^{\infty} (|n|\,\psi_n \delta_n - \varphi_n) z^n; z \in P. \tag{2.104}$$

We have arrived at the boundary value Riemann–Hilbert problem: it is needed to construct the $X(z)$ function that is analytic everywhere but on the arc $\mathbf{P}$ and whose limiting values on this arc satisfy condition (2.72). The solution to this problem will be sought in the class of functions having an integrable singularity at the ends of the arc $\mathbf{P}$ and decreasing as $|z|\to\infty$. By the techniques suggested in [80], this problem solution is easily obtained in the form

$$X(z) = G(z)\left[\frac{1}{2\pi i}\int\limits_{\mathbf{P}} \frac{F(\tau)\,d\tau}{G^{+}(\tau)(\tau - z)} + C\right]; z \notin \mathbf{P}, \tag{2.105}$$

where $F(\tau) = \sum\limits_{n=-\infty}^{\infty} (|n|\,\psi_n\delta_n - \varphi_n)\,\tau^n$ and C is an arbitrary constant.

The function $G(z)$ from (2.105) is a solution of the homogeneous boundary value Riemann–Hilbert problem ($\psi_n = \varphi_n = 0$, $n = 0, \pm 1, \ldots$). It belongs to the above-mentioned class of functions and can be expressed in the form

$$G(z) = \left(z - e^{i\vartheta_0}\right)^{-1} \exp\left(\left(\frac{1}{2} - id\right)\int\limits_{P} \frac{d\tau}{\tau - z}\right), \tag{2.106}$$

where $d = \ln b/2\pi$, $\ln b = \ln|b| + i\arg b$, $-\pi < \arg b < \pi$. The function $G^{+}(\tau)$ in (2.105) is the limiting value of the function $G(z)$ on the arc $\mathbf{P}$ inside the circle $|z| \le 1$.

Straightforward calculations show that the $G(z)$ function satisfies the following differential equation:

$$\frac{dG(z)}{dz} = \frac{2d\sin\vartheta_0 + \cos\vartheta_0 - z}{z^2 + 1 - 2z\cos\vartheta_0} G(z); \qquad z \neq e^{\pm i\vartheta_0}, G(0) = -e^{2\vartheta_0 d}. \tag{2.107}$$

On this basis, the $G(z)$ and $G^{-1}(z)$ functions can be expressed as the following series in terms of powers of the variable z:

$$G(z) = \begin{cases} -e^{2\vartheta_0 d}\sum\limits_{n=0}^{\infty} P_n(d,\vartheta_0)\,z^n; & |z| < 1 \\ \sum\limits_{n=0}^{\infty} P_n(d,-\vartheta_0)\,z^{-n-1}; & |z| > 1 \end{cases}, \tag{2.108}$$

$$G^{-1}(z) = \begin{cases} e^{-2\vartheta_0 d}\sum\limits_{n=0}^{\infty} Q_n(d,-\vartheta_0)\,z^n; & |z| < 1 \\ \sum\limits_{n=0}^{\infty} Q_n(d,\vartheta_0)\,z^{-n+1}; & |z| > 1 \end{cases}. \tag{2.109}$$

Here the function $P_n(d,\vartheta_0)$ satisfies the recurrence formulas

$$\begin{aligned} &P_0(d,\vartheta_0)=1, \qquad P_1(d,\vartheta_0)=\cos\vartheta_0+2d\sin\vartheta_0,\\ &nP_n(d,\vartheta_0)=[(2n-1)\cos\vartheta_0+2d\sin\vartheta_0]P_{n-1}(d,\vartheta_0)-\\ &\quad-(n-1)P_{n-2}(d,\vartheta_0);\quad n=2,3,... \end{aligned} \tag{2.110}$$

and the functions $Q_n(d,\vartheta_0)$ are expressed via $P_n(d,\vartheta_0)$ as follows:

$$\begin{aligned} &Q_0(d,\vartheta_0)=1, Q_1(d,\vartheta_0)=-\cos\vartheta_0+2d\sin\vartheta_0,\\ &Q_n(d,\vartheta_0)=P_n(d,\vartheta_0)-2\cos\vartheta_0 P_{n-1}(d,\vartheta_0)+P_{n-2}(d,\vartheta_0);\\ &n=2,3,... \end{aligned} \tag{2.111}$$

Remark. For the conjugation coefficient $b=1$, it is easy to see that the functions $P_n(d,\vartheta_0)$ coincide with the Legendre polynomials and, furthermore, the function $G(z)$ is no different from the function $R^{-1}(z)$ [see (2.55), (2.56), and (2.57)].

For the next step toward the solution of equations (2.97), (2.98), and (2.99), take the Sokhotskyi-Plemelj formulas [94] for the Cauchy-type integral. The application of these formulas to (2.105) finally gives

$$\sum_{n\neq 0} y_n e^{in\vartheta}=\frac{b-1}{b}\widehat{F}\left(e^{i\vartheta}\right)+\widehat{G}\left(e^{i\vartheta}\right)\left[\frac{1}{2\pi i}\int\limits_{\mathbf{P}}\frac{F(\tau)\,d\tau}{G^{+}(\tau)\left(\tau-e^{i\vartheta}\right)}+C\right];-\pi\le t\le\pi, \tag{2.112}$$

where

$$\widehat{G}\left(e^{i\vartheta}\right)=G^{+}\left(e^{i\vartheta}\right)-G^{-}\left(e^{i\vartheta}\right);\ \widehat{F}\left(e^{i\vartheta}\right)=\begin{cases}0; & |\vartheta|>\vartheta_0\\ F\left(e^{i\vartheta}\right); & |\vartheta|<\vartheta_0\end{cases}\ \text{and}$$
$$G^{-}\left(e^{i\vartheta}\right)=\lim_{\xi\to+0}G\left(e^{i\vartheta}(1+\xi)\right).$$

Calculate the singular integral in (2.112) (say, by using the Cauchy residue theorem [94] and expanding the functions $G(z)$ and $G^{-1}(z)$ from (2.108) and (2.109) into power series) and match the Fourier coefficients to have

$$y_0=\widehat{W}_0\varphi_0+\sum_{n\neq 0}n^{-1}\widehat{V}_{n-1}^{-1}(d,\vartheta_0)(|n|\psi_n\delta_n-\varphi_n), \tag{2.113}$$

$$y_m=\sum_{n=-\infty}^{\infty}\widehat{V}_{m-1}^{n-1}(d,\vartheta_0)(|n|\psi_n\delta_n-\varphi_n);m=\pm1,\pm2,... \tag{2.114}$$

The values $\widehat{W}_0$ and $\widehat{V}_{m-1}^{n-1}(d,\vartheta_0)$ are expressed via the functions $P_n(d,\vartheta_0)$ and $Q_n(d,\vartheta_0)$ by the formulas below. If $m=n$,

$$\widehat{V}_{m-1}^{m-1}(d,\vartheta_0)=\left(1+\mathrm{e}^{2\pi d}\right)^{-1}\begin{cases}0;m=0\\ \sum\limits_{n=0}^{m}Q_{m-n}(d,\vartheta_0)\,P_{n-m}(d,-\vartheta_0);m\geq 1\\ -\sum\limits_{n=0}^{|m|}Q_{|m|-n}(d,-\vartheta_0)\,P_{n+m}(d,\vartheta_0);\ m\leq -1\end{cases}. \tag{2.115}$$

If $m\neq n$,

$$\widehat{V}_{m-1}^{n-1}(d,\vartheta_0)=\left(1+\mathrm{e}^{2\pi d}\right)^{-1}\times \\ \times\begin{cases}\dfrac{\mathrm{e}^{2d\vartheta_0}m}{m-n}[P_{m-1}(d,\vartheta_0)\,P_n(d,\vartheta_0)-P_m(d,\vartheta_0)\,P_{n-1}(d,\vartheta_0)];n\neq 0\\ \mathrm{e}^{2d\vartheta_0}P_{m-1}(d,\vartheta_0)-P_m(d,\vartheta_0);n=0\end{cases}, \tag{2.116}$$

$$\widehat{W}_0=\left(1+\mathrm{e}^{2\pi d}\right)^{-1}\sum_{n=1}^{\infty}\tfrac{(-1)^n}{n}[\mathrm{e}^{2d\vartheta_0}P_{n-1}(d,\vartheta_0)+\mathrm{e}^{-2d\vartheta_0}P_{n-1}(d,-\vartheta_0)+ \\ +P_n(d,-\vartheta_0)+P_n(d,\vartheta_0)]. \tag{2.117}$$

By definition, for the $P_n(d,\vartheta_0)$ functions with negative n indices, we have

$$P_n(d,\vartheta_0)=\mathrm{e}^{-2d\vartheta_0}P_{|n|-1}(d,-\vartheta_0);n=-1,-2,... \tag{2.118}$$

So, formulas (2.113), (2.114), and (2.115), (2.116), (2.117), and (2.118) give a closed-form solution to equations (2.97), (2.98), and (2.99). This solution makes it possible to reduce the initial equations (2.91) and (2.98) to an infinite system of linear algebraic equations of the second kind.

Indeed, pass to the unknowns $x=\{x_n\}_{n=-\infty}^{\infty}$ in (2.113) and (2.114) and introduce the new column vectors $\widehat{x}=\left\{\widehat{x}_n\right\}_{n=-\infty}^{\infty}$, $\widehat{\psi}=\left\{\widehat{\psi}_n\right\}_{n=-\infty}^{\infty}$, $\widehat{\varphi}=\left\{\widehat{\varphi}_n\right\}_{n=-\infty}^{\infty}$ according to the formulas

$$\widehat{x}=\widehat{T}x,\quad \widehat{\psi}=\widehat{T}\psi,\quad \widehat{\varphi}=\widehat{T}^{-1}\varphi. \tag{2.119}$$

Let us remind that the operator $\widehat{T}$ is defined in (2.95). Then (2.113) and (2.114) can be expressed in the vector form

$$\widehat{x}=\widehat{W}\left(\widehat{D}\,\widehat{\psi}-\widehat{\varphi}\right)+\left(\widehat{P}-E\right)\widehat{\psi}. \tag{2.120}$$

The matrix operators $\widehat{W},\widehat{D},\widehat{P}$ are defined as $\widehat{W} = \left\{\widehat{W}_{mn}\right\}_{m,n=-\infty}^{\infty}$, $\widehat{P} = \left\{\widehat{P}_{mn}\right\}_{m,n=-\infty}^{\infty}$, $\widehat{D} = \left\{\delta_n\delta_n^m\right\}_{m,n=-\infty}^{\infty}$, with

$$\widehat{W}_{mn} = \begin{cases} -\widehat{W}_0; & m=n=0 \\ \dfrac{\widehat{\tau}_n\,\widehat{V}_{n-1}^{-1}(d,\vartheta_0)}{n}; & n\neq 0, \quad m=0 \\ \dfrac{\widehat{\tau}_n\,\widehat{\tau}_m\,\widehat{V}_{m-1}^{n-1}(d,\vartheta_0)}{m}; & m\neq 0 \end{cases}, \quad \widehat{P}_{mn} = \begin{cases} \widehat{W}_0; & m=n=0 \\ -\widehat{W}_{m0}; & m\neq 0, \quad n=0 \\ 0; & n\neq 0 \end{cases},$$

and

$$\delta_n = \begin{cases} 1; & n\geq 0 \\ b; & n<0 \end{cases}, \quad \widehat{\tau}_n = \begin{cases} 1; & n=0 \\ |n|^{\eta/2}; & n>0 \end{cases}, \quad \eta = 1+\frac{\arg b}{\pi}.$$

In view of (2.80), exclude $\widehat{\varphi}$ and $\widehat{\psi}$ from (2.120) to obtain the following equation for the unknown column vectors $\widehat{x}$:

$$\left(E+\widehat{H}\right)\widehat{x} = \widehat{b}\,, \tag{2.121}$$

where

$$\widehat{H} = -a\,\widehat{P} + \left(E-\widehat{P}\right)\widehat{U} + \widehat{W}\left(\widehat{V}-\widehat{D}\,\widehat{U}\right), \quad \widehat{b} = \left(E-\widehat{P}\right)\widehat{g} + \widehat{W}\left(\widehat{f}-\widehat{D}\,\widehat{g}\right).$$

The compactness of the matrix operator $\widehat{H}$ in the space l_2 is shown using the asymptotic estimates of the functions $P_n(d,\vartheta_0)$ at a large index $|n|\to\infty$, the same as it was done in the case when the conjugation coefficient is $b=1$, saving us from having to go into the details. A mention should be only made that the asymptotic estimates of the $P_n(d,\vartheta_0)$ function can be obtained by the method of generating functions [94]. For $n\to+\infty$,

$$P_n(d,\vartheta_0) = \left[\Gamma\left(\frac{1}{2}+id\right)\right]^{-1}\left(1-\mathrm{e}^{i2\vartheta_0}\right)^{-1/2+id}\mathrm{e}^{-in\vartheta_0}n^{-1/2+id}\left(1+O\left(\frac{1}{n}\right)\right), \tag{2.122}$$

where $d=(\ln b)/2\pi$ and $\Gamma(\ldots)$ is the gamma function. The asymptotical estimation for $n\to-\infty$ comes directly from (2.118). It is easily checked that for $b=1$, formula (2.122) agrees with the Legendre polynomial asymptotical estimation $P_n(\cos\vartheta_0)$.

Thus, it has been demonstrated that the dual series equations (2.91) and (2.92) are reduced to an infinite system of linear algebraic equations of the second kind of the type (2.121). In the subsequent sections, this fact will be used for designing numerical algorithms to solve the problem of plane electromagnetic wave diffraction by perfectly conducting strip gratings located on the interface of a magnetoactive plasma-type medium.

2.2.4 The System of Dual Series Equations and Riemann–Hilbert Vector Problem

So far, we have dealt with such dual series equations whose regularization algorithm is effectively constructed using the explicit solution of the conjugation (Riemann–Hilbert) problem in theory of analytic functions. However, in diffraction problems of single-periodic gratings one often faces systems of dual equations whose nature differs from what was discussed in Sections 2.2.1, 2.2.2, and 2.2.3. Generally, they can be written in the form

$$\sum_{n=-\infty}^{\infty} x_n \mathrm{e}^{in\vartheta} = 0;\ |\vartheta| < \vartheta_0, \tag{2.123}$$

$$\sum_{n=-\infty}^{\infty} |n|\,(bx_n + y_n)\,\mathrm{e}^{in\vartheta} + \sum_{n=-\infty}^{\infty} \left[\left(V^{11}x\right)_n + \left(V^{12}y\right)_n - f_{1n}\right]\mathrm{e}^{in\vartheta} = 0;\ |\vartheta| < \vartheta_0, \tag{2.124}$$

$$\sum_{n=-\infty}^{\infty} y_n \mathrm{e}^{in\vartheta} = 0;\ |\vartheta| > \vartheta_0, \tag{2.125}$$

$$\sum_{n=-\infty}^{\infty} |n|\,(ay_n + x_n)\,\mathrm{e}^{in\vartheta} + \sum_{n=-\infty}^{\infty} \left[\left(V^{21}x\right)_n + \left(V^{22}y\right)_n - f_{2n}\right]\mathrm{e}^{in\vartheta} = 0;\ |\vartheta| > \vartheta_0. \tag{2.126}$$

Here, $x = \{x_n\}_{n=-\infty}^{\infty}$, $y = \{y_n\}_{n=-\infty}^{\infty}$ are the unknown column vectors, $V^{pq} = \left\{V_{mn}^{pq}\right\}_{m,n=-\infty}^{\infty}$, $p,q = 1,2$, are the given infinite-dimensional matrix operators, $(V^{pq}x)$ $(V^{pq}y)$ are the nth components of the column vectors $(V^{pq}x)_n$ and $(V^{pq}y)_n$, respectively, $f_1 = \{f_{1n}\}_{n=-\infty}^{\infty}$ and $f_2 = \{f_{2n}\}_{n=-\infty}^{\infty}$ are some given column vectors, $\vartheta_0 \in (0;\pi)$, and a and b are, in general, some complex numbers.

The assumptions about the Fourier series convergence in (2.123), (2.124), (2.125), and (2.126) are identical to those in Section 2.2.2. The matrix operators V^{pq}, $p,q = 1,2$, meet the condition that the operators $T^{-1}V^{pq}T^{-1}$ are compact in the space l_2, with operator T defined by formula (2.41). A solution of system (2.123)–(2.126) will be sought in the space $l_2(1)$ [see (2.37)], the known column vectors are assumed to be $f_1, f_2 \in l_2(-1)$. The standard equation system corresponding to (2.123), (2.124), (2.125), and (2.126) is provided by putting $V^{pq} = 0$, $p,q = 1,2$. The nearest task is to derive an analytic solution to the standard equations, the column vectors x and y expressed explicitly via the column vectors f_1 and f_2. After that it will be shown how the infinite system of linear algebraic equations of the second kind, equivalent to system (2.123), (2.124), (2.125), and (2.126), should be constructed.

The basic idea of the explicit solution of the system of standard dual series equations is the conversion to some Riemann–Hilbert vector problem (the conjugation problem in theory of vector analytic functions). Generally speaking, this problem cannot be explicitly solved for arbitrary values of the parameters a and b, which

forces us to restrict the consideration to the case $0 \le ab < 1$ [see (2.124) and (2.126)]. Later on, we will see that this condition is actually satisfied for problems of wave diffraction by a single-periodic grating located on the chiral plane layer interface (Section 2.6).

The interested reader can easily check that system (2.124), (2.125), and (2.126) with $a = b = 0$ is identical to equations (2.33) and (2.34), which makes it possible to use the results from Section 2.2.2 as such.

Proceed to the case $a \neq 0$ and $b \neq 0$. The first thing to do is to verify the unique solvability of the system of standard equations in the space $l_2(1)$ [see (2.124), (2.125), and (2.126) with $V^{pq} = 0$].

Let $f_1 = f_2 = 0$. To prove the unique solvability of the system of standard equations, the existence of the trivial solution $x = 0$ and $y = 0$ will suffice. Assume the contrary, implying that a solution of the standard equations is $x \neq 0$, $y \neq 0$ rather than x, $y = 0$. Introduce the functions

$$F_1(\vartheta) = \sum_{n=-\infty}^{\infty} |n| (ay_n + x_n) \mathrm{e}^{in\vartheta}, \quad F_2(\vartheta) = \sum_{n=-\infty}^{\infty} |n| (bx_n + y_n) \mathrm{e}^{in\vartheta}, \tag{2.127}$$

$$F_3(\vartheta) = \sum_{n=-\infty}^{\infty} x_n \mathrm{e}^{in\vartheta}, \quad F_4(\vartheta) = \sum_{n=-\infty}^{\infty} y_n \mathrm{e}^{in\vartheta}. \tag{2.128}$$

Complying with the previous assumptions about the Fourier series appearing in (2.124), (2.125), and (2.126), these functions obey the equality

$$\int_{-\pi}^{\pi} F_1(\vartheta) F_4^*(\vartheta) \, d\vartheta = 0, \quad \int_{-\pi}^{\pi} F_2(\vartheta) F_3^*(\vartheta) \, d\vartheta = 0. \tag{2.129}$$

As before, the asterisk $*$ indicates complex conjugation. Substituting (2.127) and (2.128) into (2.129) yields

$$\sum_{n=-\infty}^{\infty} |n| \left(ay_n x_n^* + |x_n|^2 \right) = 0, \quad \sum_{n=-\infty}^{\infty} |n| \left(bx_n y_n^* + |y_n|^2 \right) = 0 \tag{2.130}$$

whence

$$b \sum_{n=-\infty}^{\infty} |n| \, |x_n|^2 = a \sum_{n=-\infty}^{\infty} |n| \, |y_n|^2. \tag{2.131}$$

Now it will suffice to address the Cauchy–Bunyakowsky inequality

$$\left| \sum_{n=-\infty}^{\infty} |n| \, x_n y_n \right|^2 \le \sum_{n=-\infty}^{\infty} |n| \, |x_n|^2 \sum_{n=-\infty}^{\infty} |n| \, |y_n|^2,$$

which, in view of (2.131), leads to the inequality $ab \ge 1$ for a and b values.

Thus, the assumption $x \neq 0$ and $y \neq 0$ results in a contradiction, which affirms that the system of standard equations is uniquely solved for $0 \leq ab < 1$.

To construct an analytic solution to these equations, write the standard equations as

$$\sum_{n=-\infty}^{\infty} nx_n \mathrm{e}^{in\vartheta} = 0;\ |\vartheta| < \vartheta_0, \tag{2.132}$$

$$\sum_{n=-\infty}^{\infty} |n|\,(bx_n + y_n)\,\mathrm{e}^{in\vartheta} = \sum_{n=-\infty}^{\infty} f_{1n}\mathrm{e}^{in\vartheta};\ |\vartheta| < \vartheta_0, \tag{2.133}$$

$$\sum_{n=-\infty}^{\infty} ny_n \mathrm{e}^{in\vartheta} = 0;\ |\vartheta| > \vartheta_0, \tag{2.134}$$

$$\sum_{n=-\infty}^{\infty} |n|\,(ay_n + x_n)\,\mathrm{e}^{in\vartheta} = \sum_{n=-\infty}^{\infty} f_{2n}\mathrm{e}^{in\vartheta};\ |\vartheta| > \vartheta_0, \tag{2.135}$$

$$\sum_{n\neq 0} x_n = -x_0,\ \ \sum_{n\neq 0} (-1)^n y_n = -y_0. \tag{2.136}$$

They are evidently equivalent to (2.123), (2.124), (2.125), and (2.126) for $V^{pq} = 0$, $p,q = 1,2$.

Let us show that (2.132), (2.133), (2.134), and (2.135) can be reduced to the Riemann–Hilbert vector problem in the theory of analytic functions [80]. Introduce some piecewise analytic vector functions $\Phi^{\pm}(z)$ as follows:

$$\Phi^{\pm}(z) = \left\{ \begin{matrix} X^{\pm}(z) \\ Y^{\pm}(z) \end{matrix} \right\}, \tag{2.137}$$

with

$$X^{+}(z) = \sum_{n=1}^{\infty} nx_n z^n,\ \ Y^{+}(z) = \sum_{n=1}^{\infty} ny_n z^n, \qquad X^{-}(z) = -\sum_{n=-\infty}^{-1} nx_n z^n.$$
$$Y^{-}(z) = -\sum_{n=-\infty}^{-1} ny_n z^n.$$

The functions $\Phi^{+}(z)$ and $\Phi^{-}(z)$ are clearly analytic, respectively, inside and outside the unit circle. From (2.132), (2.133), (2.134), and (2.135), it follows that the limiting values of these functions on the circle $|z| = 1$ satisfy the conditions

$$\Phi^{+}\left(\mathrm{e}^{i\vartheta}\right) = G_1 \Phi^{-}\left(\mathrm{e}^{i\vartheta}\right) + F_1\left(\mathrm{e}^{i\vartheta}\right);\ |\vartheta| < \vartheta_0, \tag{2.138}$$

$$\Phi^{+}\left(\mathrm{e}^{i\vartheta}\right) = G_2 \Phi^{-}\left(\mathrm{e}^{i\vartheta}\right) + F_2\left(\mathrm{e}^{i\vartheta}\right);\ |\vartheta| > \vartheta_0 \tag{2.139}$$

with G_1, G_2 being quadratic matrices of the appearance

$$G_1 = \begin{Bmatrix} 1 & 0 \\ -2b & -1 \end{Bmatrix}, G_2 = \begin{Bmatrix} -1 & -2a \\ 0 & 1 \end{Bmatrix} \tag{2.140}$$

and with the vector functions

$$F_1\left(\mathrm{e}^{i\vartheta}\right) = \begin{Bmatrix} 0 \\ f_1\left(\mathrm{e}^{i\vartheta}\right) \end{Bmatrix}, F_2\left(\mathrm{e}^{i\vartheta}\right) = \begin{Bmatrix} f_2\left(\mathrm{e}^{i\vartheta}\right) \\ 0 \end{Bmatrix},$$

where

$$f_1\left(\mathrm{e}^{i\vartheta}\right) = \sum_{n=-\infty}^{\infty} f_{1n}\mathrm{e}^{in\vartheta} \text{ and } f_2\left(\mathrm{e}^{i\vartheta}\right) = \sum_{n=-\infty}^{\infty} f_{2n}\mathrm{e}^{in\vartheta}.$$

So, we have arrived at the Riemann–Hilbert vector problem to determine the two vector functions $\Phi^+(z)$ and $\Phi^-(z)$ that are analytic, respectively, inside and outside the circle $|z| < 1$. On the circle, the limiting values of these functions satisfy conditions (2.138) and (2.139). With the restriction $0 < ab < 1$ imposed on the a and b values, the solution to this problem is available in explicit form. Let us derive it on the assumption that the sought vector functions $\Phi^{\pm}(z)$ have an integrable singularity at the discontinuity points of the matrix coefficients G_1 and G_2, that is, at $z = \exp(\pm i\vartheta_0)$.

Introduce the new vector functions

$$\begin{gathered} \widehat{\Phi}^+(z) = \Phi^+(z) - F_2^+(z), \quad \widehat{\Phi}^-(z) = G_2\Phi^-(z) + F_2^-(z); \\ F_2^{\pm}(z) = \begin{Bmatrix} f_2^{\pm}(z) \\ 0 \end{Bmatrix}, \end{gathered} \tag{2.141}$$

where $f_2^+(z) = \sum_{n=0}^{\infty} f_{2n}z^n$ for $|z| \le 1$ and $f_2^-(z) = \sum_{n=-\infty}^{-1} f_{2n}z^n$ for $|z| \ge 1$. With these $\widehat{\Phi}^{\pm}(z)$ functions, relations (2.106) and (2.107) become

$$\widehat{\Phi}^+\left(e^{i\vartheta}\right) = G_1G_2\,\widehat{\Phi}^-\left(\mathrm{e}^{i\vartheta}\right) + \widehat{F}\left(\mathrm{e}^{i\vartheta}\right); \ |\vartheta| < \vartheta_0, \tag{2.142}$$

$$\widehat{\Phi}^+\left(\mathrm{e}^{i\vartheta}\right) = \widehat{\Phi}^-\left(\mathrm{e}^{i\vartheta}\right); \ |\vartheta| > \vartheta_0, \tag{2.143}$$

where

$$\widehat{F}\left(\mathrm{e}^{i\vartheta}\right) = F_1\left(\mathrm{e}^{i\vartheta}\right) - F_2^+\left(\mathrm{e}^{i\vartheta}\right) - G_1G_2F_2^-\left(\mathrm{e}^{i\vartheta}\right).$$

Direct calculations suggest that the square matrix G_1G_2 can be written

$$G_1G_2 = PDP^{-1}, \tag{2.144}$$

with

$$D = \left\{ \begin{matrix} \lambda_+ & 0 \\ 0 & \lambda_- \end{matrix} \right\}; \lambda_\pm = 2ab - 1 \pm i2\sqrt{ab - a^2b^2}$$

and the matrices

$$P = \left\{ \begin{matrix} 1 & -\frac{2a}{1+\lambda_-} \\ -\frac{2b}{1+\lambda_-} & 1 \end{matrix} \right\}, P^{-1} = (1-\lambda_+)^{-1} \left\{ \begin{matrix} 1 & \frac{2a}{1+\lambda_-} \\ \frac{2b}{1+\lambda_-} & 1 \end{matrix} \right\}.$$

In view of representation (2.144), introduce the vector functions $\tilde{\Phi}^{\pm}(z) = P^{-1}\,\widehat{\Phi}^{\pm}(z)$. Then (2.142) and (2.143) take on the appearance

$$\tilde{\Phi}^{+}\left(e^{i\vartheta}\right) = D\tilde{\Phi}^{-}\left(e^{i\vartheta}\right) + \tilde{F}\left(e^{i\vartheta}\right);\ |\vartheta| < \vartheta_0, \tag{2.145}$$

$$\tilde{\Phi}^{+}\left(e^{i\vartheta}\right) = \tilde{\Phi}^{-}\left(e^{i\vartheta}\right);\ |\vartheta| > \vartheta_0, \tag{2.146}$$

where

$$\tilde{F}\left(e^{i\vartheta}\right) = P^{-1}\,\widehat{F}\left(e^{i\vartheta}\right) = P^{-1}F_1\left(e^{i\vartheta}\right) - P^{-1}F_2^{+}\left(e^{i\vartheta}\right) - DP^{-1}F_2^{-}\left(e^{i\vartheta}\right).$$

Thus, by equivalent transformations, we arrived at the Riemann–Hilbert vector problem (2.145) and (2.146), with the conjugation coefficient being the diagonal matrix D. Clearly this problem falls into the two Riemann–Hilbert scalar problems similar to those considered in Section 2.2.3. Namely,

$$\tilde{X}^{+}\left(e^{i\vartheta}\right) = \lambda_+\tilde{X}^{-}\left(e^{i\vartheta}\right) + \tilde{f}_1\left(e^{i\vartheta}\right);\ |\vartheta| < \vartheta_0, \tag{2.147}$$

$$\tilde{X}^{+}\left(e^{i\vartheta}\right) = \tilde{X}^{-}\left(e^{i\vartheta}\right);\ |\vartheta| > \vartheta_0, \tag{2.148}$$

$$\tilde{Y}^{+}\left(e^{i\vartheta}\right) = \lambda_-\tilde{Y}^{-}\left(e^{i\vartheta}\right) + \tilde{f}_2\left(e^{i\vartheta}\right);\ |\vartheta| < \vartheta_0, \tag{2.149}$$

$$\tilde{Y}^{+}\left(e^{i\vartheta}\right) = \tilde{Y}^{-}\left(e^{i\vartheta}\right);\ |\vartheta| > \vartheta_0. \tag{2.150}$$

Here, $\tilde{X}^{\pm}(\exp(i\vartheta))$, $\tilde{Y}^{\pm}(\exp(i\vartheta))$ and $\tilde{f}_1(\exp(i\vartheta)), \tilde{f}_2(\exp(i\vartheta))$ are components of the vector functions $\tilde{\Phi}^{\pm}(\exp(i\vartheta))$ and $\tilde{F}(\exp(i\vartheta))$, respectively.

The solution to problems (2.147), (2.148), (2.149), and (2.150) is [80]

$$\tilde{X}(z) = G_x(z)\left[\frac{1}{2\pi i}\int\limits_{\mathbf{P}} \frac{\tilde{f}_1(\vartheta)\,d\vartheta}{G_x^{+}(\vartheta)(\vartheta - z)} + C_x\right], \tag{2.151}$$

$$\tilde{Y}(z) = G_y(z)\left[\frac{1}{2\pi i}\int\limits_{\mathbf{P}} \frac{\tilde{f}_2(\vartheta)\,d\vartheta}{G_y^{+}(\vartheta)(\vartheta - z)} + C_y\right], \tag{2.152}$$

where $\mathbf{P}$ is the arc connecting $z = \exp(-i\vartheta_0)$ and $z = \exp(i\vartheta_0)$ points through the point $z = 1$ on the circle $|z\hat{o} = 1$, C_x and C_y are arbitrary constants. The functions

$G_{x,y}(z)$ are solutions of the homogeneous Riemann–Hilbert problems ($\tilde{f}_1 = \tilde{f}_2 = 0$) coming from (2.106) upon the substitution $d = d_{\pm} = \ln(-\lambda_{\pm})/2\pi$. The functions $G^{+}{}_{x,y}(\vartheta)$ give the limiting values of $G_{x,y}(z)$ on the arc $\mathbf{P}$ inside the circle, $|z| < 1$. Now let us show how a solution of standard equations (2.132), (2.133), (2.134), (2.135), and (2.136) should be constructed using (2.151) and (2.152).

First of all, take advantage of the relationship between the vector functions $\Phi^{+}(z)$ and $\tilde{\Phi}^{\pm}(z)$

$$\Phi^{+}(z) = P + \tilde{\Phi}(z) + F_2^{+}(z);\ |z| \le 1, \tag{2.153}$$

$$\Phi^{-}(z) = G_2 P \tilde{\Phi}^{-}(z) + G_2 F_2^{-}(z);\ |z| \ge 1. \tag{2.154}$$

Substituting the expressions of quadratic P and G_2 matrices into (2.153) and (2.154) and making some equivalent transformations, one gets the difference $\Phi^{+}(\exp(i\vartheta))$–$\Phi^{-}(\exp(i\vartheta))$ of the vector function limiting values on the unit circle as follows:

$$\begin{cases} X^{+}\left(e^{i\vartheta}\right) - X^{-}\left(e^{i\vartheta}\right) = \tilde{X}^{+}\left(e^{i\vartheta}\right) - \lambda_{+}\tilde{X}^{-}\left(e^{i\vartheta}\right) - \frac{2a}{1+\lambda_{-}}\left(\tilde{Y}^{+}\left(e^{i\vartheta}\right) - \lambda_{-}\tilde{Y}^{-}\left(e^{i\vartheta}\right)\right) \\ \qquad\qquad + f_2^{+}\left(e^{i\vartheta}\right) - f_2^{-}\left(e^{i\vartheta}\right) \\ Y^{+}\left(e^{i\vartheta}\right) - Y^{-}\left(e^{i\vartheta}\right) = \tilde{Y}^{+}\left(e^{i\vartheta}\right) - \tilde{Y}^{-}\left(e^{i\vartheta}\right) - \frac{2b}{1+\lambda_{-}}\left(\tilde{X}^{+}\left(e^{i\vartheta}\right) - \tilde{X}^{-}\left(e^{i\vartheta}\right)\right) \end{cases}. \tag{2.155}$$

Matching the Fourier coefficients in (2.155) yields

$$\begin{cases} x_m = \frac{\delta_m^{+}}{m}\tilde{x}_m - \frac{2a\delta_m^{-}}{(1+\lambda_{-})m}\tilde{y}_m + \frac{f_{2m}}{|m|} \\ y_m = \frac{\tilde{y}_m}{m} - \frac{2b\tilde{x}_m}{(1+\lambda_{-})m} \end{cases};\ m \ne 0, \tag{2.156}$$

$$\tilde{x}_0 = -\frac{f_{20}}{1-\lambda_{+}},\quad \tilde{y}_0 = -\frac{2bf_{20}}{\lambda_{-}-\lambda_{+}}. \tag{2.157}$$

Here $\{\tilde{x}_m\}_{m=-\infty}^{\infty}$ and $\{\tilde{y}_m\}_{m=-\infty}^{\infty}$ are the Fourier coefficients of the functions $\tilde{X}^{+}(\exp(i\vartheta)) - \tilde{X}^{-}(\exp(i\vartheta))$ and $\tilde{Y}^{+}(\exp(i\vartheta)) - \tilde{Y}^{-}(\exp(i\vartheta))$, respectively, and

$$\delta_m^{\pm} = \begin{cases} 1; & m \ge 0 \\ \lambda_{\pm}; & m < 0 \end{cases}.$$

Now, determine the Fourier coefficients $\{\tilde{x}_m\}_{m=-\infty}^{\infty}$ and $\{\tilde{y}_m\}_{m=-\infty}^{\infty}$ from (2.151) and (2.152). For this, it is sufficient to implement the results from Section 2.2.3 [see (2.113), (2.114), (2.115), (2.116), and (2.117)]. Finally,

$$\tilde{x}_m = \sum_{n=-\infty}^{\infty} \tilde{f}_{1n}\,\hat{V}_{m-1}^{n-1}(d_{+},\vartheta_0) + \tilde{x}_0 P_m(d_{+},\vartheta_0), \tag{2.158}$$

$$\tilde{y}_m = \sum_{n=-\infty}^{\infty} \tilde{f}_{2n}\,\hat{V}_{m-1}^{n-1}(d_{-},\vartheta_0) + \tilde{y}_0 P_m(d_{-},\vartheta_0);\ m = \pm 1, \pm 2, \ldots, \tag{2.159}$$

where the values $\widehat{V}_{m-1}^{n-1}(d_-,\vartheta_0)$ come from (2.115) and (2.116), and the functions $P_m(\mathrm{d}_\pm,\vartheta_0)$ are found by formula (2.78) upon the substitution $d = d\pm = \ln(-\lambda_\pm)/2\pi$. The sequences $\left\{\tilde{f}_{1n}\right\}_{n=-\infty}^{\infty}$ and $\left\{\tilde{f}_{2n}\right\}_{n=-\infty}^{\infty}$ in $\{f_{1n}\}_{n=-\infty}^{\infty}$ and $\{f_{2n}\}_{n=-\infty}^{\infty}$ terms are

$$\tilde{f}_{1n} = -\frac{\delta_n^+ f_{2n}}{1-\lambda_+} + \frac{2af_{1n}}{\lambda_- - \lambda_+}, \quad \tilde{f}_{2n} = -\frac{2b\delta_n^- f_{2n}}{\lambda_- - \lambda_+} + \frac{f_{1n}}{1-\lambda_+}. \tag{2.160}$$

Substitute (2.160) and (2.158), (2.149) into (2.156), (2.155) in view of (2.136). Then

$$x_m = \sum_{n=-\infty}^{\infty} W_{mn}^{11} f_{1n} + \sum_{n=-\infty}^{\infty} W_{mn}^{12} f_{2n}, \tag{2.161}$$

$$y_m = \sum_{n=-\infty}^{\infty} W_{mn}^{21} f_{1n} + \sum_{n=-\infty}^{\infty} W_{mn}^{22} f_{2n};\ m = 0, \pm 1, \pm 2,..., \tag{2.162}$$

the coefficients W_{mn}^{pq}, $p,q = 1,2$ are available from the formulas

$$W_{mn}^{11} = \frac{2a}{\lambda_- - \lambda_+} \begin{cases} \frac{1}{m}\left[\delta_m^+ \widehat{V}_{m-1}^{n-1}(d_+,\vartheta_0) - \delta_m^- \widehat{V}_{m-1}^{n-1}(d_-,\vartheta_0)\right]; & m \neq 0 \\ W_{n1}(d_-,\vartheta_0) - W_{n1}(d_+,\vartheta_0); & m = 0 \end{cases},$$

$$W_{mn}^{12} = \begin{cases} \frac{\delta_{mn}}{|m|} - \frac{1}{m}\left[\frac{\delta_m^+\delta_n^+ \widehat{V}_{m-1}^{n-1}(d_+,\vartheta_0)}{1-\lambda_+} + \frac{\delta_m^-\delta_n^- \widehat{V}_{m-1}^{n-1}(d_-,\vartheta_0)}{1-\lambda_-}\right] - \\ \quad -\frac{\delta_{0n}}{m}\left[\frac{\delta_m^+ P_m(d_+,\vartheta_0)}{1-\lambda_+} + \frac{\delta_m^- P_m(d_-,\vartheta_0)}{1-\lambda_-}\right]; \quad m \neq 0 \\ \frac{\delta_n^+ W_{n1}(d_+,\vartheta_0)}{1-\lambda_+} + \frac{\delta_n^- W_{n1}(d_-,\vartheta_0)}{1-\lambda_-} - \frac{1}{|n|};\ m = 0, \quad n \neq 0 \\ \frac{W_{01}(d_+,\vartheta_0)+R_1(d_+,\vartheta_0)}{1-\lambda_+} + \frac{W_{01}(d_-,\vartheta_0)+R_1(d_-,\vartheta_0)}{1-\lambda_-}; \quad m = 0, \quad n = 0 \end{cases}$$

$$W_{mn}^{21} = \begin{cases} \frac{1}{m}\left[\frac{\widehat{V}_{m-1}^{n-1}(d_+,\vartheta_0)\lambda_+}{\lambda_+ - 1} + \frac{\widehat{V}_{m-1}^{n-1}(d_-,\vartheta_0)\lambda_-}{\lambda_- - 1}\right]; & m \neq 0 \\ \frac{W_{n2}(d_+,\vartheta_0)}{\lambda_+ - 1} + \frac{W_{n2}(d_-,\vartheta_0)}{\lambda_- - 1}; & m = 0 \end{cases},$$

$$W_{mn}^{22} = \frac{2b}{\lambda_- \lambda_+}, \begin{cases} \frac{1}{m}\left[\delta_n^+ \widehat{V}_{m-1}^{n-1}(d_+,\vartheta_0) - \delta_n^- \widehat{V}_{m-1}^{n-1}(d_-,\vartheta_0)\right] + \\ \quad + \frac{\delta_0^n}{m}\left[P_m(d_+,\vartheta_0) - P_m(d_-,\vartheta_0)\right]; m \neq 0 \\ \delta_n^- W_{n2}(d_-,\vartheta_0) - \delta_n^+ W_{n2}(d_+,\vartheta_0); \quad m = 0, \quad n \neq 0 \\ W_{02}(d_-,\vartheta_0) - W_{02}(d_+,\vartheta_0) + R_2(d_-,\vartheta_0) - R_2(d_+,\vartheta_0); \\ \quad m = 0, \quad n = 0 \end{cases}.$$

Here $W_{np}(d_\pm,\vartheta_0)$, $R_p(d_\pm,\vartheta_0)$, $p = 1, 2$, represent the series

$$W_{n1}(d_{\pm},\vartheta_0)=\sum_{m\neq 0}\frac{\delta_m^{\pm}\widehat{V}_{m-1}^{n-1}(d_{\pm},\vartheta_0)}{m},\quad W_{n2}(d_{\pm},\vartheta_0)=\sum_{m\neq 0}\frac{(-1)^m V_{m-1}^{n-1}(d_{\pm},\vartheta_0)}{m},$$
$$R_1(d_{\pm},\vartheta_0)=\sum_{m\neq 0}\frac{\delta_m^{\pm}P_m(d_{\pm},\vartheta_0)}{m},\quad R_2(d_{\pm},\vartheta_0)=\sum_{m\neq 0}\frac{(-1)^m P_m(d_{\pm},\vartheta_0)}{m}.$$

Formulas (2.161) and (2.162) provide an explicit solution of the system (2.132), (2.133), (2.134), (2.135), and (2.136) of standard dual series equations. Now this solution will be used to derive the infinite system of linear algebraic equations of the second kind for the unknown column vectors $x=\{x_n\}_{n=-\infty}^{\infty}$, $y=\{y_n\}_{n=-\infty}^{\infty}$, which is equivalent to system (2.91), (2.92), (2.93), and (2.94).

The algebraic scheme of this derivation is as follows. In the first place, we intend to express (2.161) and (2.162) in vector form. Introduce the infinite-dimensional matrices $W^{pq}=\left\{W_{mn}^{pq}\right\}_{m,n=-\infty}^{\infty}$, $p,q=1,2$, and the column vectors $f_p=\left\{f_{pn}\right\}_{n=-\infty}^{\infty}$, $p=1,2$. Then, taking care of the multiplication of a matrix by a column vector, we have expressions (2.161) and (2.162) in the form

$$x=W^{11}f_1+W^{12}f_2, \tag{2.163}$$

$$y=W^{21}f_1+W^{22}f_2. \tag{2.164}$$

Rewrite (2.123), (2.124), (2.125), and (2.126) to get

$$\begin{cases}\displaystyle\sum_{n=-\infty}^{\infty}x_n\mathrm{e}^{in\vartheta}=0; & |\vartheta|<\vartheta_0\\ \displaystyle\sum_{n=-\infty}^{\infty}|n|\,(bx_n+y_n)\,\mathrm{e}^{in\vartheta}=\sum_{n=-\infty}^{+\infty}g_{1n}\mathrm{e}^{in\vartheta}; & |\vartheta|<\vartheta_0\\ \displaystyle\sum_{n=-\infty}^{\infty}y_n\mathrm{e}^{in\vartheta}=0; & |\vartheta|>\vartheta_0\\ \displaystyle\sum_{n=-\infty}^{\infty}|n|\,(ax_n+x_n)\,\mathrm{e}^{in\vartheta}=\sum_{n=-\infty}^{\infty}g_{2n}\mathrm{e}^{in\vartheta}; & |\vartheta|>\vartheta_0\end{cases},$$

where $g_{1n}=f_{1n}-\left(V^{11}x\right)_n-\left(V^{12}y\right)_n$, $g_{2n}=f_{2n}-\left(V^{21}x\right)_n-\left(V^{22}y\right)_n$.

Let us solve these equations as if the column vectors $g_1=\{g_{1n}\}_{n=-\infty}^{\infty}$, $g_2=\{g_{2n}\}_{n=-\infty}^{\infty}$ were known. In view of (2.163) and (2.164),

$$x=W^{11}g_1+W^{12}g_2, \tag{2.165}$$

$$y=W^{21}g_1+W^{22}g_2. \tag{2.166}$$

Now one only needs to replace g_1, g_2 in (2.165) and (2.166) by their expressions in f_1, f_2 and x, y terms. The result is

$$x=-\left(W^{11}V^{11}+W^{12}V^{21}\right)x-\left[\left(W^{11}V^{12}+W^{12}V^{22}\right)y+W^{11}f_1+W^{12}f_2\right], \tag{2.167}$$

$$y = -\left(W^{21}V^{11} + W^{22}V^{21}\right)x - \left[\left(W^{21}V^{12} + W^{22}V^{22}\right)y + W^{21}f_1 + W^{22}f_2\right]. \tag{2.168}$$

Let us show how equation system (2.167) and (2.168) should be transformed to the system of equations of the second kind in the space l_2. Seeking a solution to system (2.123), (2.124), (2.125), and (2.126) in the $l_2(1)$ space makes us use the column vectors

$$\widehat{x} = Tx, \quad \widetilde{y} = Ty, \tag{2.169}$$

with the matrix operator T given by (2.41). One easily finds that $\widehat{x}\,, \widehat{y} \in l_2$.

Introduce the new matrices $\widehat{W}^{pq}$ and the column vectors $\widehat{b}_1$, $\widehat{b}_2$

$$\widehat{W}^{pq} = TW^{pq}T, \quad \widehat{V}^{pq} = -T^{-1}V^{pq}T^{-1}; \quad p,q = 1,2, \tag{2.170}$$

$$\widehat{b}_1 = \widehat{W}^{11}T^{-1}f_1 + \widehat{W}^{12}T^{-1}f_2, \quad \widehat{b}_2 = \widehat{W}^{21}T^{-1}f_1 + \widehat{W}^{22}T^{-1}f_2 \tag{2.171}$$

and substitute (2.169) into (2.167) and (2.168) in view of (2.170) and (2.171). Then

$$\widehat{x} = \left(\widehat{W}^{11}\,\widehat{V}^{11} + \widehat{W}^{12}\,\widehat{V}^{21}\right)\widehat{x} + \left(\widehat{W}^{11}\,\widehat{V}^{12} + \widehat{W}^{12}\,\widehat{V}^{22}\right)\widehat{y} + \widehat{b}_1, \tag{2.172}$$

$$\widehat{y} = \left(\widehat{W}^{21}\,\widehat{V}^{11} + \widehat{W}^{22}\,\widehat{V}^{21}\right)\widehat{x} + \left(\widehat{W}^{21}\,\widehat{V}^{12} + \widehat{W}^{22}\,\widehat{V}^{22}\right)\widehat{y} + \widehat{b}_2. \tag{2.173}$$

Make sure that the matrix operators in (2.172) and (2.173) are compact in l_2. Indeed, the operator $\widehat{V}^{pq}$, $p, q = 1, 2$, is compact by assumption, and the matrix $\widehat{W}^{pq}$ produces the bounded operator in l_2. The latter follows from the analytic estimates of the function $P_n(d_\pm,\vartheta_0)$ as $|n|\to\infty$ [see (2.122)] and formulas (2.116) and (2.117) for $\widehat{V}^{n-1}_{m-1}(d_\pm,\vartheta_0)$. Hence, the matrix operator $\widehat{W}^{\bar{p}\bar{q}}\,\widehat{V}^{pq}$, $p, \bar{p}, q, \bar{q} = 1,2$ is compact as a product of bounded and compact operators [70].

Thus, system (2.172) and (2.173) is an operator equation of the second kind in the space l_2, which guarantees that the solution of this equation can be obtained with any preassigned accuracy by truncation [70]. It means that infinite system (2.172) and (2.173) can be replaced by the finite system for the N unknowns. This method is used in working relevant diffraction problems of single-periodic gratings and yields solid numerical results.

2.3 Inversion of Convolution-Type Matrix Operators in System of Equations in the Mode Matching Technique

The analytic regularization procedure for the inversion of convolution-type matrix operators of infinite system of equations obtained by the mode matching (partial

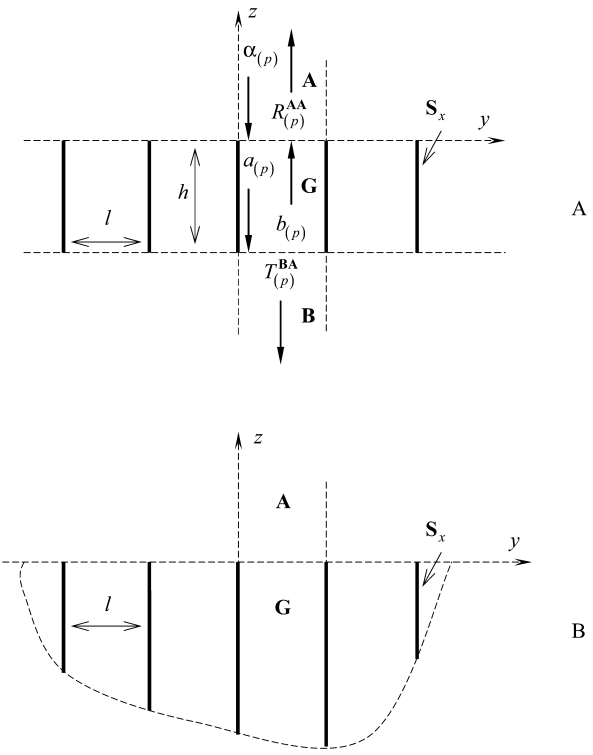

Fig. 2.1 The geometry of gratings: (**a**) Lamellar (or knife) grating and (**b**) grating of perfectly conducting half-planes

domain) method was originally suggested in [22]. Thus, the problem of plane-wave diffraction by a grating made up of vertical metal strips (see Fig. 2.1a) has been solved, and any improvement of that solution does not seem possible. The solution obtained in this way (see Section 2.3.1) is easy to transform to closed-form analytic expressions [16, 18], whether k be small or large or related to the long-wave piece of the resonant range. It can be numerically obtained by the truncation method, with the error decreasing exponentially whatever values the dimensionless parameter kl takes.

The method has been intensively promoted in electrodynamical theory of gratings. Thus, effective solutions to diffraction problems have been built for jalousie-type gratings [16, 17, 97, 98] and echelette gratings [16, 17, 99], lamellar gratings with a sophisticated periodic pattern [17, 100] and echelette gratings with obtuse and acute teeth [17, 101, 102], for dielectric echelettes with one interface metallized [17, 103] and echelettes with two absorbing interfaces [104]. The studies of these structures mainly kept in focus the resonant frequencies and had to rely on computers with limited resources. That is why every algorithmic and computational detail was elaborated very carefully. Such operating characteristics of the method as its actual convergence rate, compliance with the problem conditions,

etc., which were less open to analytic inspection, were examined by means of specially invented procedures during numerical experiments. Great efforts went into the computational realization of the algorithms. In parallel, intensive studies were conducted for their comprehensive mathematical justification [17, 105], including development of a qualitative theory of ill-posed infinite systems of linear algebraic equations resulted from the mode matching method [17, 106–108] and extension of the scope of canonical structures for which the diffraction problem solution is available in explicit analytic form [109]. The new analytic solutions essentially add to the capability of the considered method and extend its possible area of application (see Section 2.3.2).

All these results have been summarized in the books [17, 18]. The first one fully concentrates on approaches, algorithms, and relevant computational schemes. The other one presents the physical results of the theory of wave scattering by diffraction gratings achieved within 1972–1985. The present book is focused on a thorough analysis of various diffraction phenomena. It traces general, common nature scenarios of resonant and nonresonant wave scattering processes and, also, carefully studies some specific situations of both fundamental and applied significance. The main body of the book is composed of authors' original works performed in cooperation with their fellow contributors. It includes analysis of the plane-wave total transition through semitransparent structures and the total reflection from them, threshold effects (Wood's anomalies), "ghosts of grating" phenomena, regimes of the total nonspecular (autocollimation, in particular) wave reflection from nontransparent structures, analysis and synthesis of grating polarization converters for half-plane and semi-sphere scanning, etc.

2.3.1 *Lamellar Gratings: Systems of First-Kind Equations and Analytic Regularization of the Problem*

Let a lamellar grating (see Fig. 2.1a) be illuminated by a plane E-polarized wave $\tilde{U}_p^i(g,k) = \exp\left[i\left(\Phi_p y - \Gamma_p z\right)\right]$, $k > 0$ and let p be an integer. The general solution of boundary value problem (1.26) in domains **A**, **B**, and **G** is

$$\tilde{U}(g,k) = \begin{cases} \tilde{U}_p^i(g,k) + \sum\limits_{n=-\infty}^{\infty} R_{np}^{\mathbf{AA}} \exp\left[i\left(\Phi_n y + \Gamma_n z\right)\right]; & g = \{y,z\} \in \mathbf{A} \\ \sum\limits_{m=1}^{\infty} \left[a_{mp}\exp\left[-i\gamma_m z\right] + b_{mp}\exp\left[i\gamma_m (z+h)\right]\right] \sin\left(\frac{m\pi y}{l}\right); & g \in \mathbf{G} \\ \sum\limits_{n=-\infty}^{\infty} T_{np}^{\mathbf{BA}} \exp\left[i\left(\Phi_n y - \Gamma_n (z+h)\right)\right]; & g \in \mathbf{B} \end{cases} . \tag{2.174}$$

Here, $\tilde{U}(g,k) = \tilde{E}_x(g,k)$, $\gamma_m = \sqrt{k^2 - \left(m\pi/l\right)^2}$, $m = 1,2,\ldots$, are the propagation constants of the H_{0m}-waves in the regular parallel-plate waveguide segment $-h \le z \le 0$ (channel **G**) connecting the reflection and transition zones of the periodic structure, and $\mathrm{Re}\gamma_m \ge 0$, $\mathrm{Im}\gamma_m \ge 0$.

Matching the tangential components $\tilde{E}_x(g,k)$ and $\tilde{H}_y(g,k)$ of the field strength vectors on the partial domain boundaries $z=0$ and $z=-h$ yields the infinite system of linear algebraic equations of the first kind

$$\sum_{n=-\infty}^{\infty}\frac{S_{np}^{\pm}}{\Gamma_n-\gamma_m}=\frac{1}{\Gamma_p+\gamma_m}\mp e^{i\gamma_m h}\left[\sum_{n=-\infty}^{\infty}\frac{S_{np}^{\pm}}{\Gamma_n+\gamma_m}-\frac{1}{\Gamma_p-\gamma_m}\right];\ m=1,2,... \tag{2.175}$$

with the recalculation formula

$$\left(a_{mp}\pm b_{mp}\right)\frac{\gamma_m l^2}{m\pi\left[1-(-1)^m\exp\left(i2\pi\Phi\right)\right]}=\frac{1}{\Gamma_p-\gamma_m}-\sum_{n=-\infty}^{\infty}\frac{S_{np}^{\pm}}{\Gamma_n+\gamma_m};\ m=1,2,... \tag{2.176}$$

Here, $S_{np}^{\pm}=R_{np}^{\mathbf{AA}}\pm T_{np}^{\mathbf{BA}}$.

A part of the solution $\left\{S_{np}^{\pm}\right\}_n$ of problem (2.175) will be extracted that satisfies the system of equations

$$\sum_{n=-\infty}^{\infty}\frac{S_{np}}{\Gamma_n-\gamma_m}=\frac{1}{\Gamma_p+\gamma_m};\ m=1,2,... \tag{2.177}$$

and determines the generalized reflection matrix $\mathbf{R}^{\mathbf{AA}}(\infty)=\left\{\mathbf{S_{np}}\right\}_{\mathbf{n,p}=-\infty}^{\infty}$ of the knife grating for $h\to\infty$. Let the amplitudes S_{np} be determined by the residual calculation technique [42] based on the Mittag-Leffler theorem about the expansion of a meromorphic function into a series of principal parts [36]. Assume that in the plane $\mathbf{C}$ of a complex variable w, there exist functions $f_p(w)$ such that:

- $f_p(w)$ have simple poles at the points $w=\Gamma_n$, $n=0,\pm1,\pm2,\ldots$, and $w=-\Gamma_p$;
- $f_p(\gamma_m)=0$, $m=1,2,\ldots$;
- $\operatorname{Res} f_p(-\Gamma_p)=1$;
- $f_p(w)\to0$ on a regular system of closed contours $\mathbf{C}_{|w|}$ in the plane $\mathbf{C}$ if $|w|\to\infty$.

Under these assumptions,

$$S_{np}=\operatorname{Res} f_p\left(\Gamma_n\right);\ n=0,\pm1,\pm2,... \tag{2.178}$$

Indeed, as for all $m=1,2,\ldots$ [36],

$$\lim_{|w|\to\infty}\frac{1}{2\pi i}\oint_{\mathbf{C}_{|w|}}\left[\frac{f_p(w)}{w-\gamma_m}\right]dw=\sum_{n=-\infty}^{\infty}\frac{\operatorname{Res} f_p\left(\Gamma_n\right)}{\Gamma_n-\gamma_m}+\frac{\operatorname{Res} f_p\left(-\Gamma_p\right)}{-\Gamma_p-\gamma_m}+f_p\left(\gamma_m\right)=0, \tag{2.179}$$

the set $\{S_{np}\}_n$ from (2.178) lends a solution to problem (2.177). The functions $f_p(w)$ possessing all the above-mentioned properties will be expressed as [16, 17]

$$f_p(w) = \mathrm{e}^{i\ln 2(w+\Gamma_p)l/\pi} \frac{(\Gamma_0+\Gamma_p)}{(w+\Gamma_p)(\Gamma_0-w)} \prod_{s=1}^{\infty} \frac{(\gamma_s-w)(\Gamma_s+\Gamma_p)(\Gamma_{-s}+\Gamma_p)}{(\gamma_s+\Gamma_p)(\Gamma_s-w)(\Gamma_{-s}-w)}.$$

For large $|w|$ and $|n|$, one arrives at the following estimations:

$$f_p(w) = O\left[(w+\Gamma_p)^{-1} w^{-1/2}\right] \text{ and } S_{np} = \operatorname{Res} f_p(\Gamma_n) = O\left(n^{-3/2}\right).$$

An examination of the integral

$$\lim_{|w|\to\infty} \frac{1}{2\pi i} \oint_{\mathbf{C}_{|w|}} \left[\frac{f_p(w)}{w+\gamma_m}\right] dw = \sum_{n=-\infty}^{\infty} \frac{\operatorname{Res} f_p(\Gamma_n)}{\Gamma_n+\gamma_m} + \frac{\operatorname{Res} f_p(-\Gamma_p)}{-\Gamma_p+\gamma_m} + f_p(-\gamma_m) = 0,$$

yields

$$\sum_{n=-\infty}^{\infty} \frac{S_{np}}{\Gamma_n+\gamma_m} - \frac{1}{\Gamma_p-\gamma_m} = -f_p(-\gamma_m);\ m = 1,2,... \tag{2.180}$$

Introduce the new unknowns $\bar{\mathbf{S}}^{\pm}_{np} = S^{\pm}_{np} - S_{np}$, $n = 0, \pm 1, \pm 2, \ldots$, and change via (2.177) and (2.180) from problems (2.175) and (2.176) to the problem

$$\sum_{n=-\infty}^{\infty} \frac{\bar{\mathbf{S}}^{\pm}_{np}}{\Gamma_n-\gamma_m} = \mp \mathrm{e}^{i\gamma_m h}\left[\sum_{n=-\infty}^{\infty} \frac{\bar{\mathbf{S}}^{\pm}_{np}}{\Gamma_n+\gamma_m} - f_p(-\gamma_m)\right] = \mathrm{e}^{i\gamma_m h/2}\beta^{\pm}_{mp};\ m = 1,2,..., \tag{2.181}$$

$$\left(a_{mp} \pm b_{mp}\right) \frac{\gamma_m l^2}{m\pi\left[1-(-1)^m \exp(i2\pi\Phi)\right]} = f_p(-\gamma_m) - \sum_{n=-\infty}^{\infty} \frac{\bar{\mathbf{S}}^{\pm}_{np}}{\Gamma_n+\gamma_m} = \pm\beta^{\pm}_m \mathrm{e}^{-i\gamma_m h/2};$$
$$m = 1,2,... \tag{2.182}$$

It has not been possible to identify a pair of infinite-sequence spaces on which the operators of problems (2.175), (2.177), and (2.181) are bounded and have bounded inverses [17, 105, 108]. That is, algorithms for an approximate solution of these infinite systems of linear algebraic equations of the first kind (truncation solution algorithms, for one) withstand justifications [110]. Yet there have been obtained results [17, 42, 106, 107] sufficiently interesting to expect that in some cases an approximate solution of the operator equation of the nature can converge weakly (in coordinate-wise fashion) to the exact solution. Thus, for instance, the values $\bar{\mathbf{S}}^{\pm}_{np}(N)$ found from system (2.181) truncated to the order N ($m = 1,2,\ldots,N$) converge to the

exact $\bar{\mathbf{S}}_{np}^{\pm}$ values for each $n = -M, -M+1,...,N-M-1$ with increasing N. Yet the convergence rate essentially depends on:

- the n value;
- whether a module or a phase of the complex amplitude $\bar{\mathbf{S}}_{np}^{\pm}(N)$ is calculated;
- a choice of the main diagonal of the system constituted by a finite number of equations (a choice of M).

When passing from lamellar gratings to jalousie gratings (see, for example, Fig. 1.3a; $\vartheta \neq 0$), the information provided by the truncated first-kind equation systems corresponding to these asymmetrical structures will be, at best, relatively true only for amplitude modules of several fundamental spatial harmonics.

A rigorous solution of boundary value problems (and, specifically, problems in electromagnetic theory of gratings) proposes algorithms where an approximate problem solution converges to the exact solution in the metric of an appropriate Hilbert space. Thus, for instance, if the solution represented by the amplitude sets $\left\{R_{np}^{\mathbf{AA}}\right\}_n$ and $\left\{T_{np}^{\mathbf{BA}}\right\}_n$, the analysis is most conveniently carried out in the infinite-sequence space $\tilde{l}_2 = \left\{a = \{a_n\}: \ \|a\|_{\tilde{l}_2}^2 = \sum_n |a_n|^2 (1+|n|) < \infty\right\}$. It acts as an energy space in processes relative to the plane-wave scattering by periodic structures [see, for example, relations (1.29)]. And the fulfillment of the conditions $\left\{R_{np}^{\mathbf{AA}}\right\}_n \in \tilde{l}_2$, $\left\{T_{np}^{\mathbf{BA}}\right\}_n \in \tilde{l}_2$ provides the uniqueness of the solution to the (1.26) type of problems for gratings with edges like interface segments where both tangents and normals are undetermined [16, 17, 42].

Return to problem (2.181) to seek its rigorous solution via the analytic inversion of the operator part given by the matrix $A = \left\{(\Gamma_n - \gamma_m)^{-1}\right\}_{m=1,\, n=-\infty}^{\infty}$. Assume the existence of meromorphic functions $\varphi_r(w)$ such that

- $\varphi_r(w)$ have simple poles at points $w = \Gamma_n$, $n = 0,\pm1,\pm2,...$;
- $\varphi_r(\gamma_m) = -\delta_m^r$, $m,r = 1,2,...,$ δ_m^r is the Kronecker delta;
- $\varphi_r(w) \to 0$ on some regular system of closed contours $\mathbf{C}_{|w|}$ in the plane $\mathbf{C}$ if $|w| \to \infty$;
- the series $\sum_r \varphi_r(w)\, e^{i\gamma_r h/2} \beta_{rp}^{\pm}$ converges uniformly within the analyticity domain of the functions $\varphi_r(w)$.

Let us show that by these assumptions, the operator equation (2.181) is equivalent to the following operator equation of the second kind:

$$\bar{\mathbf{S}}_{np}^{\pm} = \sum_{r=1}^{\infty} \operatorname{Res} \varphi_r(\Gamma_n)\, e^{i\gamma_r h/2} \beta_{rp}^{\pm}; \ n = 0, \pm 1, \pm 2, ... \tag{2.183}$$

Indeed, since

$$\lim_{|w|\to\infty}\frac{1}{2\pi i}\oint\limits_{\mathbf{C}_{|w|}}\left[(w-\gamma_m)^{-1}\sum_{r=1}^{\infty}\varphi_r(w)\,\mathrm{e}^{i\gamma_r h/2}\beta_{rp}^{\pm}\right]dw=$$
$$=\sum_{n=-\infty}^{\infty}\left(\sum_{r=1}^{\infty}\mathrm{Res}\;\varphi_r(\Gamma_n)\,\mathrm{e}^{i\gamma_r h/2}\beta_{rp}^{\pm}\right)\frac{1}{(\Gamma_n-\gamma_m)^{-1}}+$$
$$+\sum_{r=1}^{\infty}\varphi_r(\gamma_m)\,\mathrm{e}^{i\gamma_r h/2}\beta_{rp}^{\pm}=0;\;m=1,2,...,$$

each solution of the operator equation (2.183) will be a solution of equation (2.181). Additionally, the regularization on the left (as the previous operation is called) does not lose any solution from the solution set [111]. That is, each solution of equation (2.181) will also simultaneously be a solution of equation (2.183).

The functions $\varphi_r(w)$ that possess all the mentioned properties take the appearance [16, 17]

$$\varphi_r(w)=-\mathrm{e}^{i\ln 2(w-\gamma_r)l/\pi}\frac{(\Gamma_0-\gamma_r)}{(\Gamma_0-w)}\prod_{s=1}^{\infty(r)}\frac{(\gamma_s-w)(\Gamma_s-\gamma_r)(\Gamma_{-s}-\gamma_r)}{(\gamma_s-\gamma_r)(\Gamma_s-w)(\Gamma_{-s}-w)}.$$

Here, the index (r) over the sign of the infinite product indicates that the term $(\gamma_s-w)(\gamma_s-\gamma_r)^{-1}$ corresponding to $s=r$ is discarded. Large $|w|$ and r values satisfy the estimate [17]

$$\varphi_r(w)=O\left[\frac{\gamma_r^{1/2}}{(w-\gamma_r)\,w^{1/2}}\right]. \tag{2.184}$$

From (2.181) and (2.183), in view of the equality

$$\lim_{|w|\to\infty}\frac{1}{2\pi i}\oint\limits_{\mathbf{C}_{|w|}}\left[\frac{\varphi_r(w)}{w+\gamma_m}\right]dw=\sum_{n=-\infty}^{\infty}\frac{\mathrm{Res}\;\varphi_r(\Gamma_n)}{\Gamma_n+\gamma_m}+\varphi_r(-\gamma_m)=0;\;m=1,2,...,$$

one obtains

$$\begin{aligned}\beta_{mp}^{\pm}&=\mp\mathrm{e}^{i\gamma_m h/2}\left[\sum_{n=-\infty}^{\infty}\frac{\bar{\mathbf{S}}_{np}^{\pm}}{\Gamma_n+\gamma_m}-f_p(-\gamma_m)\right]=\\&=\mp\mathrm{e}^{i\gamma_m h/2}\left[\sum_{n=-\infty}^{\infty}\left[\frac{1}{\Gamma_n+\gamma_m}\sum_{r=1}^{\infty}\mathrm{e}^{i\gamma_r h/2}\mathrm{Res}\;\varphi_r(\Gamma_n)\,\beta_r^{\pm}\right]-f_p(-\gamma_m)\right]=\\&=\mp\mathrm{e}^{i\gamma_m h/2}\left[\sum_{r=1}^{\infty}\mathrm{e}^{i\gamma_r h/2}\beta_r^{\pm}\sum_{n=-\infty}^{\infty}\frac{\mathrm{Res}\;\varphi_r(\Gamma_n)}{\Gamma_n+\gamma_m}-f_p(-\gamma_m)\right]=\\&=\pm\mathrm{e}^{i\gamma_m h/2}\left[\sum_{r=1}^{\infty}\mathrm{e}^{i\gamma_r h/2}\beta_r^{\pm}\varphi_r(-\gamma_m)+f_p(-\gamma_m)\right];\;m=1,2,...\end{aligned} \tag{2.185}$$

So, the initial problem has been reduced [see (2.181), (2.182), and (2.185)] to the infinite systems of linear algebraic equations of the second kind

$$\beta_{mp}^{\pm} = \pm e^{i\gamma_m h/2}\left[\sum_{r=1}^{\infty} e^{i\gamma_r h/2}\beta_{rp}^{\pm}\varphi_r(-\gamma_m) + f_p(-\gamma_m)\right]; m = 1,2,... \quad (2.186)$$

(to the operator equations $\left[E + B^{\pm}(k)\right]\beta_{(p)}^{\pm} = b_{(p)}^{\pm}$, where E is the identity matrix, $B^{\pm}(k) = \left\{B_{mr}^{\pm} = \mp e^{i(\gamma_m+\gamma_r)h/2}\varphi_r(-\gamma_m)\right\}_{m,r=1}^{\infty}$, $b_{(p)}^{\pm} = \left\{b_{mp}^{\pm} = \pm f_p(-\gamma_m)e^{i\gamma_m h/2}\right\}_m$, and $\beta_{(p)}^{\pm} = \left\{\beta_{mp}^{\pm}\right\}_m$ are the unknown vectors) with the recalculation formulas

$$R_{np}^{\mathbf{AA}} \pm T_{np}^{\mathbf{BA}} = \sum_{r=1}^{\infty} \operatorname{Res}\varphi_r(\Gamma_n)e^{i\gamma_r h/2}\beta_{rp}^{\pm} + \operatorname{Res} f_p(\Gamma_n); n = 0, \pm 1, \pm 2,..., \quad (2.187)$$

$$\left(a_{mp} \pm b_{mp}\right) = \pm\beta_{mp}^{\pm}\frac{e^{-i\gamma_m h/2}m\pi\left[1 - (-1)^m \exp(i2\pi\Phi)\right]}{\gamma_m l^2}; m = 1,2,... \quad (2.188)$$

The estimates

$$B_{mr}^{\pm} = O\left[e^{-\pi(m+r)h/2l}\frac{r^{1/2}}{(m+r)m^{1/2}}\right], b_{mp}^{\pm} = O\left[e^{-\pi mh/2l}m^{-3/2}\right]; m,r \to \infty \quad (2.189)$$

suggest [70] that the operator equation (2.186) is a Fredholm equation in the sequence space $\tilde{l}_2$. This means that for all $k \notin \Omega_k$ (see Section 1.3.2), bounded inverse operators $\left[E + B^{\pm}(k)\right]^{-1}$ do exist, the unknown vectors $\beta_{(p)}^{\pm} \in \tilde{l}_2$, and infinite systems (2.186) can be solved by the truncation method converging in $\tilde{l}_2$ space norm. The evident equality

$$\beta_{(p)}^{\pm} - \beta_{(p)}^{\pm}(N) = \left(E + B^{\pm}(k)\right)^{-1}\left[\left(B^{\pm}(k) - B^{\pm}(k,N)\right)\beta_{(p)}^{\pm}(N) + \left(b_{(p)}^{\pm} - b_{(p)}^{\pm}(N)\right)\right]$$

and estimates (2.189) suggest that

$$\left\|\beta_{(p)}^{\pm} - \beta_{(p)}^{\pm}(N)\right\|_{\tilde{l}_2} = O\left[e^{-\pi(N+1)h/2l}\right]; N \to \infty,$$

$$R_{np}^{\mathbf{AA}}, T_{np}^{\mathbf{BA}} = O\left(|n|^{-3/2}\right); |n| \to \infty,$$

$$a_{mp}, b_{mp} = O\left(m^{-3/2}\right); m \to \infty.$$

Here, $\beta_{(p)}^{\pm}(N) = \left\{\beta_{mp}^{\pm}(N)\right\}_{m=1}^{N}$ is the solution of the system of equations (2.186) truncated to order N ($\left[E + B^{\pm}(k,N)\right]\beta_{(p)}^{\pm}(N) = b_{(p)}^{\pm}(N)$), $B^{\pm}(k,N) = \left\{B_{mr}^{\pm}\right\}_{m,r=1}^{N}$, and $b_{(p)}^{\pm}(N) = \left\{b_{mp}^{\pm}\right\}_{m=1}^{N}$.

2.3.2 Matrix Scheme of Analytic Regularization Procedure

The algorithmization of the problems in terms of the discussed analytic regularization procedure can be fairly simplified by the application of generalized scattering matrix technique [16, 17, 42, 112]. Let us confirm this statement by two simple examples.

First, assume the availability of the scattering matrices (see Section 1.2.1) $\mathbf{R}^{\mathbf{AA}}(\infty) = \left\{\mathbf{R}^{\mathbf{AA}}_{\mathbf{np}}(\infty)\right\}^{\infty}_{\mathbf{n,p}=-\infty}$, $T^{\mathbf{GA}}(\infty) = \left\{T^{\mathbf{GA}}_{mp}(\infty)\right\}^{\infty}_{m=1,p=-\infty}$, $\mathbf{R}^{\mathbf{GG}}(\infty) = \left\{\mathbf{R}^{\mathbf{GG}}_{\mathbf{ms}}(\infty)\right\}^{\infty}_{\mathbf{m,s=1}}$, and $T^{\mathbf{AG}}(\infty) = \left\{T^{\mathbf{AG}}_{ns}(\infty)\right\}^{\infty}_{n=-\infty,s=1}$ that provide through the relationships

$$A = \mathbf{R}^{\mathbf{AA}}(\infty)\,\alpha + \mathbf{T}^{\mathbf{AG}}(\infty)\,\beta,\ \mathbf{B} = \mathbf{T}^{\mathbf{GA}}(\infty)\,\alpha + \mathbf{R}^{\mathbf{GG}}(\infty)\,\beta;$$
$$A = \{A_n\},\ B = \{B_m\},\ \alpha = \left\{\alpha_p\right\},\ \beta = \{\beta_s\}$$

all the amplitude–frequency characteristics of a grating made up of thin metal half-planes (see Fig. 2.1b) in the field of the E-polarized waves

$$\tilde{U}^i(g,k) = \begin{cases} \sum\limits_{p=-\infty}^{\infty} \alpha_p \exp\left[i\left(\Phi_p y - \Gamma_p z\right)\right]; & g = \{y,z\} \in \mathbf{A}, \quad k > 0 \\ \sum\limits_{s=1}^{\infty} \beta_s \exp\left(i\gamma_s z\right) \sin\left(\frac{s\pi y}{l}\right); & g \in \mathbf{G} \end{cases}. \tag{2.190}$$

Here, $A = \{A_n\}$ and $B = \{B_m\}$ are the amplitudes of the secondary field

$$\tilde{U}^s(g,k) = \begin{cases} \sum\limits_{n=-\infty}^{\infty} A_n \exp\left[i\left(\Phi_n y + \Gamma_n z\right)\right]; & g \in \mathbf{A} \\ \sum\limits_{m=1}^{\infty} B_m \exp\left(-i\gamma_m z\right) \sin\left(\frac{m\pi y}{l}\right); & g \in \mathbf{G} \end{cases}$$

($\tilde{U}(g,k) = \tilde{U}^i(g,k) + \tilde{U}^s(g,k)$) in the grating reflection zone ($\mathbf{A}$) and in the regular parallel-plate waveguide ($\mathbf{G}$).

Now, return to the lamellar grating problem (see Fig. 2.1a) considered in Section 2.3.1. Evidently (see [42, 112]) all amplitudes of waves composing the field (2.174) are related as

$$\begin{cases} R^{\mathbf{AA}}_{(p)} = \mathbf{R}^{\mathbf{AA}}(\infty)\left[\alpha_{(\mathbf{p})}\right] + \mathbf{T}^{\mathbf{AG}}(\infty)\,\mathbf{E}(\mathbf{h})\left[\mathbf{b}_{(\mathbf{p})}\right] \\ a_{(p)} = T^{\mathbf{GA}}(\infty)\left[\alpha_{(p)}\right] + \mathbf{R}^{\mathbf{GG}}(\infty)\,\mathbf{E}(\mathbf{h})\left[\mathbf{b}_{(\mathbf{p})}\right] \\ b_{(p)} = \mathbf{R}^{\mathbf{GG}}(\infty)\,\mathbf{E}(\mathbf{h})\left[\mathbf{a}_{(\mathbf{p})}\right] \\ T^{\mathbf{BA}}_{(p)} = T^{\mathbf{AG}}(\infty)\,E(h)\left[a_{(p)}\right] \end{cases}. \tag{2.191}$$

Here, $R^{\mathbf{AA}}_{(p)} = \left\{R^{\mathbf{AA}}_{np}\right\}_n$, $T^{\mathbf{BA}}_{(p)} = \left\{T^{\mathbf{BA}}_{np}\right\}_n$, $a_{(p)} = \left\{a_{mp}\right\}_m$, $b_{(p)} = \left\{b_{mp}\right\}_m$, $\alpha_{(p)} = \left\{\delta^p_n\right\}_n$, and $E(h) = \left\{\delta^s_m e^{i\gamma_m h}\right\}^{\infty}_{m,s=1}$. Formula (2.191) describes all the stages

of the formation of the response of the periodic structure to the excitation by the plane E-polarized wave $\tilde{U}_p^i(g,k) = \exp\left[i\left(\Phi_p y - \Gamma_p z\right)\right]$ (by signal $\alpha_{(p)}$). Thus, for instance, the first equation of system (2.191) can be interpreted in the following way. The signal $R_{(p)}^{\mathbf{AA}}$ (the waves $\left\{R_{np}^{\mathbf{AA}} \exp\left[i\left(\Phi_n y + \Gamma_n z\right)\right]\right\}_n$) is a sum of two signals. One of them is caused by the reflection of the primary signal $\alpha_{(p)}$ from the aperture $z = 0$ of the half-plane grating. The other is defined by the signal $b_{(p)}$ (by the waves $\left\{b_{mp}\exp\left[i\gamma_m(z+h)\right]\sin\left(m\pi y/l\right)\right\}_m$) that have arisen in the plane $z = -h$, experienced (during the propagation from the plane $z = -h$ to the plane $z = 0$) the action of the regular domain $\mathbf{G}$ (operator $E(h)$), and after that partly penetrated through the aperture $z = 0$ into domain $\mathbf{A}$. From (2.191),

$$R_{(p)}^{\mathbf{AA}} \pm T_{(p)}^{\mathbf{BA}} = \mathbf{R}^{\mathbf{AA}}(\infty)\left[\alpha_{(\mathbf{p})}\right] \pm \mathbf{T}^{\mathbf{AG}}(\infty)\,\mathbf{E}(\mathbf{h})\left[\mathbf{a}_{(\mathbf{p})} \pm \mathbf{b}_{(\mathbf{p})}\right], \tag{2.192}$$

$$a_{(p)} \pm b_{(p)} = T^{\mathbf{GA}}(\infty)\left[\alpha_{(p)}\right] \pm \mathbf{R}^{\mathbf{GG}}(\infty)\,\mathbf{E}(\mathbf{h})\left[\mathbf{a}_{(\mathbf{p})} \pm \mathbf{b}_{(\mathbf{p})}\right]. \tag{2.193}$$

Let us introduce by the relations

$$a_{(p)} \pm b_{(p)} = \pm E\left(-h/2\right) E(\Phi)\left[\beta_{(p)}^{\pm}\right];\; E(\Phi) = \left\{\delta_m^s \frac{m\pi\left[1-(-1)^m\,\mathrm{e}^{i2\pi\Phi}\right]}{\gamma_m l^2}\right\}_{m,s=1}^{\infty} \tag{2.194}$$

[(2.194) is a matrix form of expressions (2.188)] the new unknowns $\beta_{(p)}^{\pm} = \left\{\beta_{mp}^{\pm}\right\}_m$ and pass from (2.192) and (2.193) to the equations

$$R_{(p)}^{\mathbf{AA}} \pm T_{(p)}^{\mathbf{BA}} = \mathbf{R}^{\mathbf{AA}}(\infty)\left[\alpha_{(\mathbf{p})}\right] + \mathbf{T}^{\mathbf{AG}}(\infty)\,\mathbf{E}\left(\mathbf{h}/\mathbf{2}\right)\mathbf{E}(\Phi)\left[\beta_{(\mathbf{p})}^{\pm}\right], \tag{2.195}$$

$$\beta_{(p)}^{\pm} = \pm E\left(h/2\right) E^{-1}(\Phi)\left\{T^{\mathbf{GA}}(\infty)\left[\alpha_{(p)}\right] + \mathbf{R}^{\mathbf{GG}}(\infty)\,\mathbf{E}\left(\mathbf{h}/\mathbf{2}\right)\mathbf{E}(\Phi)\left[\beta_{(\mathbf{p})}^{\pm}\right]\right\}. \tag{2.196}$$

Invoking familiar representations [17] of the operators $R^{\mathbf{AA}}(\infty)$, $T^{\mathbf{GA}}(\infty)$, etc., one finds that equations (2.195) and (2.196) coincide with (2.187) and (2.186). The final result obtained in the matrix scheme formalism becomes the same but takes, at the same time, less analytic efforts.

Such a good rate of convergence as in the previous example is not always the case when the final operator equations obtained via the analytic regularization procedure are solved by the truncation method. The errors in the determination of the field amplitudes are exponentially small only when elementary scatterers in the structure geometry are separated by regular wave propagation regions, such as Floquet channel segments or segments of parallel-plate waveguides. Here those scatterers are called elementary whose diffraction problem solution is available in closed (explicit) form (see, for example [17, 104, 109, 113]). These are

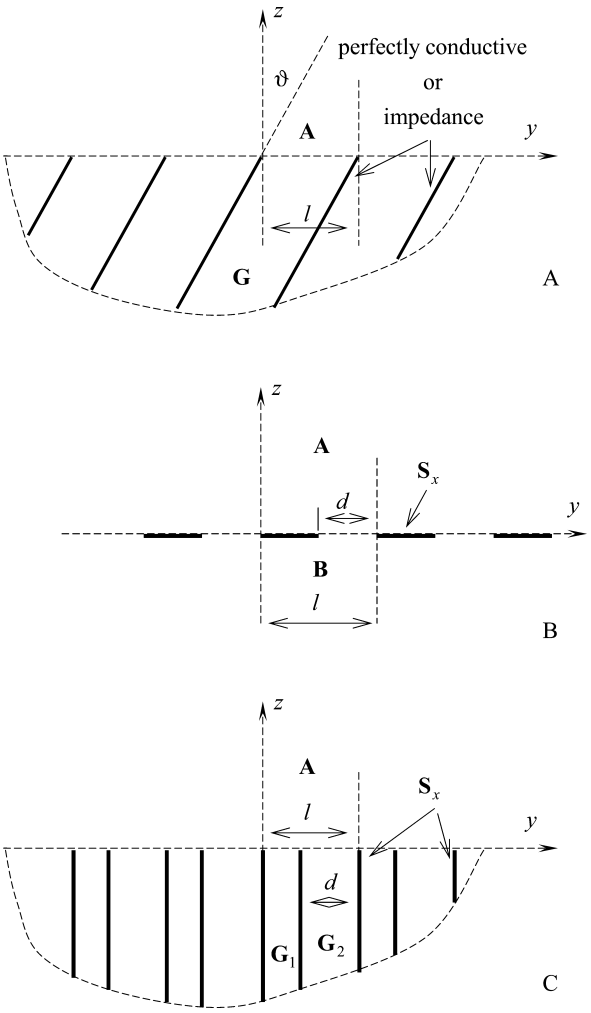

Fig. 2.2 (**a**) Gratings made of vertical and inclined half-planes, (**b**) plane strip gratings, and (**c**) grating with two half-planes in the period

- gratings of vertical or oblique half-planes, both perfectly conducting and absorbing (see Figs. 2.1b and 2.2a);
- planar half-filling strip gratings ($l = 2d$) and gratings with two half-planes per period (see Fig. 2.2b and c) – the half-integer Φ case;
- bifurcation of a parallel-plate waveguide;
- lateral (across Floquet channel or parallel-plate waveguide) interfaces, etc.

The analysis of the final operator equations of the type $[E + B(k)]\beta = b$ in the method gets much more complicated when the elementary inhomogeneities carried by the considered periodic structure cannot be spaced out with a regular wave propagation domain between them. In this case, a simpler, matrix-formalism scheme

of the analytic regularization procedure is more efficient for the following facts. The spectrum and the norm of the operators produced by the generalized scattering matrices of elementary inhomogeneities and defining [by relations like (2.192), (2.193), (2.194), (2.195), and (2.196)] all the qualitative characteristics of the problem $[E + B(k)]\beta = b$ can be evaluated in terms of the energy balance and the reciprocity relations (see Section 1.2.1 and works [17, 42, 105, 108, 114]). By functional analysis techniques [70, 110, 115], this information can be translated into the knowledge needed to prove that the operator equations $[E + B(k)]\beta = b$ are correct and solvable by truncation. It is the route that will be taken to solve the next problem.

Let an echelette grating with perfectly conducting interfaces and a 90° tooth angle (see Fig. 2.3a) be excited by a plane E-polarized wave $\tilde{U}_p^i(g,k) = \exp\left[i\left(\Phi_p y - \Gamma_p z\right)\right]$, with $k > 0$, and p an integer. Imagine the echelette wider wall shifted down along the perfectly conducting half-planes $\{g = \{y,z\}:\ y = z\mathrm{tg}\vartheta + nl;\ n = 0, \pm 1, \pm 2, ...,\ z \le 0\}$. The regular domain obtained in this way is denoted as **G** (see Fig. 2.3b). The general solution of boundary value problem (1.26) for this new structure is

$$\tilde{U}(g,k) = \begin{cases} \tilde{U}_p^i(g,k) + \sum\limits_{n=-\infty}^{\infty} R_{np}^{\mathbf{AA}} \exp\left[i\left(\Phi_n y + \Gamma_n z\right)\right]; & g = \{y,z\} \in \mathbf{A} \\ \sum\limits_{m=1}^{\infty} \left[a_{mp}\exp\left[-i\bar{\gamma}_m \bar{z}\right] + b_{mp}\exp\left[i\bar{\gamma}_m\left(\bar{z} + \bar{h}\right)\right]\right] \sin\left(\frac{m\pi\bar{y}}{l\cos\vartheta}\right); & g \in \mathbf{G} \end{cases} . \tag{2.197}$$

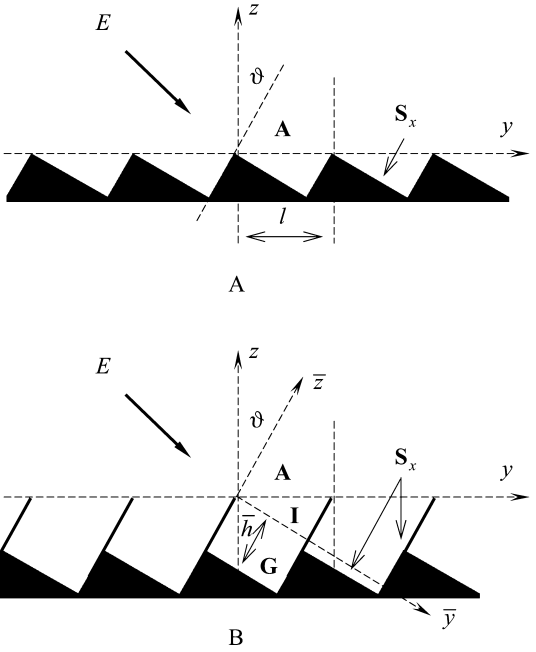

Fig. 2.3 Echelette with *rectangular tooth*: (**a**) original geometry and (**b**) modified geometry

Here, $\bar{\gamma}_m = \sqrt{k^2 - \left(m\pi/l\cos\vartheta\right)^2}$, $m = 1,2,\ldots$, $\mathrm{Re}\bar{\gamma}_m \geq 0$, $\mathrm{Im}\bar{\gamma}_m \geq 0$ are the propagation constants of the H_{0m}-waves in the segment $-\bar{h} \leq \bar{z} \leq 0$ of the regular parallel-plate waveguide (domain **G**). The generalized scattering matrix method relates the amplitudes of the field (2.197) as follows:

$$\begin{cases} R^{\mathbf{AA}}_{(p)} = \mathbf{R}^{\mathbf{AA}}(\mathrm{I})\left[\alpha_{(\mathbf{p})}\right] + \mathbf{T}^{\mathbf{AG}}(\mathrm{I})\,\mathbf{E}\left(\bar{h}\right)\left[\mathbf{b}_{(\mathbf{p})}\right] \\ a_{(p)} = T^{\mathbf{GA}}(\mathrm{I})\left[\alpha_{(p)}\right] + \mathbf{R}^{\mathbf{GG}}(\mathrm{I})\,\mathbf{E}\left(\bar{h}\right)\left[\mathbf{b}_{(\mathbf{p})}\right] \\ b_{(p)} = -E\left(\bar{h}\right)\left[a_{(p)}\right] \end{cases}. \tag{2.198}$$

Here, $E\left(\bar{h}\right) = \left\{\delta^s_m \mathrm{e}^{i\bar{\gamma}_m\bar{h}}\right\}^{\infty}_{m,s=1}$, $R^{\mathbf{AA}}_{(p)} = \left\{R^{\mathbf{AA}}_{np}\right\}_n$, $a_{(p)} = \left\{a_{mp}\right\}_m$, $b_{(p)} = \left\{b_{mp}\right\}_m$, and $\alpha_{(p)} = \left\{\delta^p_n\right\}_n$, $T^{\mathbf{GA}}(\mathrm{I}) = \left\{T^{\mathbf{GA}}_{mp}(\mathrm{I})\right\}^{\infty}_{m=1,p=-\infty}$, $\mathbf{R}^{\mathbf{GG}}(\mathrm{I}) = \left\{\mathbf{R}^{\mathbf{GG}}_{\mathbf{ms}}(\mathrm{I})\right\}^{\infty}_{\mathbf{m,s=1}}$, etc., are the scattering matrices defining all amplitude–frequency characteristics of elementary inhomogeneity **I** (grating of oblique perfectly conducting half-planes). The explicit form of these matrix operators examined by the methods of the complex variable function theory can be found in the books [16, 17] including also the estimations

$$\begin{gathered} R^{\mathbf{AA}}_{np}(\mathrm{I}) = O\left[\frac{p^{1/2}}{(|n|+|p|)n^{1/2}}\right],\ T^{\mathbf{GA}}_{mp}(\mathrm{I}) = O\left[\frac{p^{1/2}}{(m/2\cos\vartheta - |p|)m^{1/2}}\right], \\ R^{\mathbf{GG}}_{ms}(\mathrm{I}) = O\left[\frac{s^{1/2}}{(m+s)m^{1/2}}\right],\ T^{\mathbf{AG}}_{ns}(\mathrm{I}) = O\left[\frac{s^{1/2}}{(s/2\cos\vartheta - |n|)|n|^{1/2}}\right]; \\ |n|,\ |p|, m, s \to \infty. \end{gathered} \tag{2.199}$$

They suggest that for $\bar{h} > 0$ and $k \notin \Omega_k$, the system of equations (2.198) is uniquely solvable in the space $\tilde{l}_2$ and numerically solvable by the truncation method converging in $\tilde{l}_2$ space norm [70, 110]. The error in the determination of the amplitude set $R^{\mathbf{AA}}_{(p)}$ in the metric of this space is equal to $O\left[\mathrm{e}^{-\pi(N+1)h/l\cos\vartheta}\right]$.

Letting $\bar{h} \to 0$ in (2.198) (returning to the initial structure geometry) yields the second-kind operator equation

$$a_{(p)} + \mathbf{R}^{\mathbf{GG}}(\mathrm{I})\left[\mathbf{a}_{(\mathbf{p})}\right] = \mathbf{T}^{\mathbf{GA}}(\mathrm{I})\left[\alpha_{(\mathbf{p})}\right] \tag{2.200}$$

and the recalculation formula

$$R^{\mathbf{AA}}_{(p)} = \mathbf{R}^{\mathbf{AA}}(\mathrm{I})\left[\alpha_{(\mathbf{p})}\right] - \mathbf{T}^{\mathbf{AG}}(\mathrm{I})\left[\mathbf{a}_{(\mathbf{p})}\right]. \tag{2.201}$$

It is essential to show the invertibility of the operator $\left[E + \mathbf{R}^{\mathbf{GG}}(\mathrm{I})\right] : \tilde{l}_2 \to \tilde{l}_2$, or the existence and boundedness of the operator $[E + R^{\mathbf{GG}}(\mathbf{I})]^{-1}$. There are no other ways to guarantee an orthonormalized basis of the $\tilde{l}_2$ space in which the infinite equation system (2.200) can be solved by truncation [110]. However, the operator $R^{\mathbf{GG}}(\mathbf{I})$ is not totally continuous, being a Hilbert-type operator in the $\tilde{l}_2$ space [see [116] and estimations (2.199)], it is only bounded in this space. Also, there

hardly exists a direct way to get the estimate $\left\|\mathbf{R}^{\mathbf{GG}}(\mathrm{I})\right\| < 1$ justifying (the same as the total continuity of the operator $R^{\mathbf{GG}}(\mathbf{I})$) the unique solvability of problem (2.200). The last possibility is to prove that the full spectrum of the operator $R^{\mathbf{GG}}(\mathbf{I})$ is enclosed by the circle $|w|=1$ in the plane $\mathbf{C}$ of complex variable w. This possibility is realized via the energy relationships that are obtained as a result of the complex power theorem applied to the volume of elementary inhomogeneity $\mathbf{I}$ [17, 42, 114].

Thus, it has been shown that for $k\notin\Omega_k$, the spectrum of the operator $R^{\mathbf{GG}}(\mathbf{I})$ is enclosed by the circle $|w|=1$, $w\in\mathbf{C}$. Hence [70, 115], the operator $[E + R^{\mathbf{GG}}(\mathbf{I})]$ is invertible, the sets $a_{(p)}$ and $R^{\mathbf{AA}}_{(p)}$ belong to the space $\tilde{l}_2$ (all scattering operators of the inhomogeneity $\mathbf{I}$ are bounded on the pair of spaces $\tilde{l}_2 \to \tilde{l}_2$ [116]), and a solution of the operator equation (2.200) can be obtained for any parameters l and ϑ by the successive approximation approach:

$$a_{(p)}(M) = \sum_{m=0}^{M} \left(-\mathbf{R}^{\mathbf{GG}}(\mathrm{I})\right)^m T^{\mathbf{GA}}(\mathrm{I})\left[\alpha_{(p)}\right]; M \to \infty.$$

One more consequence of the invertibility of the operator $[E + R^{\mathbf{GG}}(\mathbf{I})]$ refers to the possibility to solve equation (2.200) by the truncation method converging in $\tilde{l}_2$ space norm. Indeed, the use of the evident equality

$$a_{(p)} - a_{(p)}(N) = -\left[E(N) + E(N)\,\mathbf{R}^{\mathbf{GG}}\mathbf{E}(\mathbf{N})\right]^{-1} E(N)\,\mathbf{R}^{\mathbf{GG}}\left[\mathbf{E} - \mathbf{E}(\mathbf{N})\right]\left[\mathbf{a_{(p)}}\right],$$

yields

$$\left\|a_{(p)} - a_{(p)}(N)\right\| \le \mathrm{const}\left\|\left[E - E(N)\right]\left[a_{(p)}\right]\right\|. \tag{2.202}$$

Here, $E(N) = \left\{\delta^s_m\right\}^N_{m,s=1}$ and $a_{(p)}(N)$ is the solution of the truncated system

$$a_{(p)}(N) + E(N)\,\mathbf{R}^{\mathbf{GG}}(\mathrm{I})\,\mathbf{E}(\mathbf{N})\left[\mathbf{a_{(p)}}(\mathbf{N})\right] = \mathbf{E}(\mathbf{N})\,\mathbf{T}^{\mathbf{GA}}(\mathrm{I})\left[\alpha_{(\mathbf{p})}\right].$$

Since for any $a_{(p)} \in \tilde{l}_2$, $\left\|\left[E - E(N)\right]\left[a_{(p)}\right]\right\| \to 0$ as $N\to 0$, then

$$\left\|a_{(p)} - a_{(p)}(N)\right\| \to 0; N \to 0.$$

The scattered field of the grating meets the Meixner condition near the singular points in the structure geometry (near the points where the tangents and the normals to the contour $\mathbf{S}_x$ are not defined). In the considered case of an echelette grating with a 90° tooth angle, this means that $a_{mp} = O\left(m^{-5/3}\right)$, $R^{\mathbf{AA}}_{np} = O\left(|n|^{-5/3}\right)$ for m and $|n|$ large enough [42]. Knowing the rate of decrease of the secondary field amplitude and addressing (2.202), one can estimate the rate of convergence of the truncation method as follows:

$$\left\|a_{(p)} - a_{(p)}(N)\right\| = O\left[(N+1)^{-2/3}\right]; N \to 0.$$

2.4 Electromagnetic Wave Diffraction by Gratings in Presence of a Chiral Isotropic Medium

Chiral composites possessing spatial dispersion have unusual electromagnetic characteristics, such as optical activity and circular dichroism [117, 118]. Certain advances in the technologies used to manufacture chiral materials open up new fields for their application, including effective microwave absorbers, microstrip antenna substrates, chirally filled waveguides, switches, and modulators. In these applications, it is the presence of chiral materials that allow us to vary, and in some cases essentially improve, the characteristics of electrodynamical systems beyond those based on more conventional materials.

Thus, for example, a chiral substrate in place of a dielectric one in a microstrip antenna suppresses the surface wave power [119], and so enhances radiation efficiency, widens the transmission band, and reduces mutual coupling between the antenna elements. Results demonstrating the behavior of chiral materials as substrates and covers for antenna applications are found in [120, 121]. In [120], a chiral substrate is reported to be reducing the pattern size of the patch antenna for a given frequency. The chirality of a microstrip antenna cover makes the antenna more compact, increases gain performances, magnifies the radiation resistance and the antenna efficiency, and also reduces the radar cross-section around the resonance [121]. The analysis carried out in [122] of the scattering by a chiral periodic structure showed that the structure can be used as both a frequency-selective device and a mode-conversion device. Using their polarization properties, chiral materials can be used for filters, polarization converters, and lenses. In view of the circular polarization of chiral medium eigenwaves, a chiral medium couples both linear polarizations of the field, and so gives rise to new and interesting polarization effects.

A chiral inclusion may impart novel properties also in well-known structures. For example, when a linearly polarized wave is normally incident on a perfectly conducting strip grating attached to an isotropic chiral half-space, it is shown in this chapter (see also [123]) that the reflected field contains cross-polarized harmonics; the diffracted field character depends on the direction of the elliptic polarization of the incident wave, and the nature of chiral media losses is responsible for specific features of the diffracted field, which correspond to dichroism.

The phenomenon of nearly total transformation of an elliptically polarized wave into a linearly polarized wave is described herein (also see [124]). It is achieved by reflection from a structure comprising a perfectly conducting ground plate overlaid with a chiral layer and a magnetodielectric layer, and topped off with a perfectly conducting strip grating. This reflecting structure has potential application in various microwave devices. The complete transformation of an obliquely incident linearly polarized wave to a specularly reflected cross-polarized wave may be achieved with this structure [125]; also regimes of essential autocollimation reflection and nearly total nonspecular reflection, with a high-telescopicity factor, have been found [126, 127].

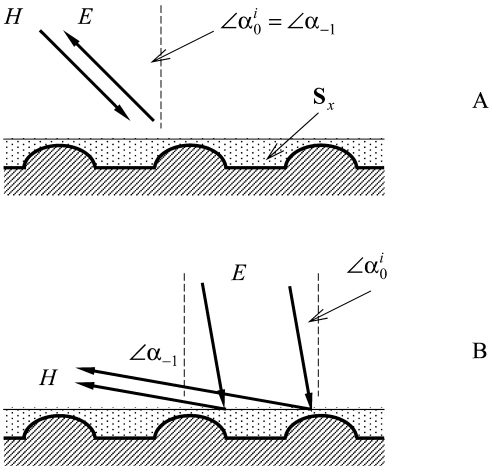

Fig. 2.4 The nonspecular reflection with polarization conversion: (**a**) autocollimation reflection and (**b**) high-telescopicity reflection (telescopicity factor is $r_t = \cos\alpha_0^i / \cos\alpha_{-1}$)

In the autocollimation regime (see Fig. 2.4a), the minus first harmonic of cross-polarization propagates in a direction opposite to the primary incident wave of linear polarization. Thus, in this regime, the structure acts as a frequency-selecting mirror with polarization conversion. The nonspecular reflection regime with a high telescopicity factor (see Fig. 2.4b) is characterized by a quasi-complete conversion of the nearly normally incident wave into the minus first cross-polarized harmonic, which almost skims above the grating surface. In this regime, the energy flux density of the wave is greatly increased and a high-purity polarization transformation is obtained. Thus, the structure can be used as an antenna component.

The determination of those structure parameters, which give the desired reflection regime, faces serious computational difficulties, even ignoring the polarization conversion. While an optimization may be carried out by examining the controlling parameters in a wide band of variation, it must be recognized that the phenomena occurs within narrow limits and often has a resonance nature. The phenomena associated with the polarization transformation are even more narrowly limited and have a striking resonance nature. Therefore an effective and reliable numerical procedure is required.

The presence of a chiral medium complicates the problem mathematically, making it a fully vectorial problem. The analysis of the diffraction in presence of chiral materials has been recently carried out using a variety of numerical methods, such as the finite difference frequency domain formulation [128] used for scattering from arbitrarily shaped chiral objects; the hybrid finite element-boundary integral method [129] applied to scattering of three-dimensional chiral objects above a perfect conducting plane; the T-matrix analysis [130] used to model semicircular channels filled with chiral materials in a conducting plate; etc. Approaches based on these methods are widely used because of their high flexibility when applied to scatterers of different, rather complicated shapes. Although, as a rule, they require high memory and computer resources (in other words, they are computationally expensive), recent developments in computer systems have made the use of such methods

efficient. Actually only one problem, but an essential one, remains. These conventional approaches are based on the numerical solution of a first-kind Fredholm equation which is ill posed, and often displays unpredictable accuracy and possible instability with an increase in the number of iterations. That is why, for example, the authors of [130] stress how carefully their empirical choice of proper truncation number must be followed to get acceptable accuracy in their T-matrix method. The primary concern with these disadvantages is that they most strongly feature in the areas of greatest interest in technical applications, namely, the resonant domain characterized by energetically pronounced effects.

Thus, it is highly desirable to transform this equation into a second-kind Fredholm equation, which provides a stable and fast-converging computational algorithm with the required accuracy of computation. For a certain class of scatterers this transformation can be implemented by the idea of analytic regularization described above (see Section 2.2, and [57]). The use of an analytic regularization [57, 61] allows us to obtain an effective and reliable calculation procedure that overcomes the difficulties mentioned; this procedure solves the optimization problems for obtaining desired characteristics of diffracted field in the resonance regimes.

2.4.1 Field Presentation in Chiral Medium

The unusual electromagnetic characteristics of chiral medium are caused by the essential spatial dispersion which cannot be neglected as in conventional media. The spatial dispersion leads to the results that the field in the chiral medium, i.e., the vectors of electromagnetic induction ($\vec{D}$ and $\vec{B}$), is defined not only by the correspondent strength vectors ($\vec{E}$ and $\vec{H}$), but as well by the rotors of these vectors. The constitutive relations, determining the electromagnetic induction in a homogeneous reciprocal chiral medium for harmonic temporal dependence exp(–*ikt*), are presented in the following form [117]:

$$\vec{D} = \varepsilon_0\,\tilde{\varepsilon}\,\vec{E} + i\gamma\sqrt{\varepsilon_0\mu_0}\vec{H},\ \vec{B} = \mu_0\tilde{\mu}\,\vec{H} - i\gamma\sqrt{\varepsilon_0\mu_0}\vec{E}. \tag{2.203}$$

Here, ε_0 and μ_0 are the electric and magnetic constants, respectively; $\tilde{\varepsilon} = \tilde{\varepsilon}' + i\tilde{\varepsilon}''$ and $\tilde{\mu} = \tilde{\mu}' + i\tilde{\mu}''$ are the relative permittivity and permeability of the chiral medium; and $\gamma = \gamma' + i\gamma''$ is the chirality parameter responsible for the magnetic–electric interaction. We consider an isotropic medium, i.e., $\tilde{\varepsilon}$, $\tilde{\mu}$, and γ are scalars. Due to the composite nature of the artificial chiral medium all its constitutive parameters exhibit frequency dispersion.

In view of the constitutive relations (2.203), we rewrite the system of Maxwell's equations for time-harmonic fields $\vec{E} \equiv \vec{E}\,(g,k) = \left\{\tilde{E}_x, \tilde{E}_y, \tilde{E}_z\right\}$ and $\vec{H} \equiv \vec{H}\,(g,k) = \left\{\tilde{H}_x, \tilde{H}_y, \tilde{H}_z\right\}$, $p = \{x,y,z\}$ in the form

$$\begin{cases} \operatorname{rot}\vec{H} = a_{11}\,\vec{E} + a_{12}\,\vec{H} \\ \operatorname{rot}\vec{E} = a_{21}\,\vec{H} + a_{22}\,\vec{E} \end{cases}, \tag{2.204}$$

where $a_{11} = -ik\eta_0^{-1}\,\tilde{\varepsilon}$, $a_{12} = k\gamma$, $a_{21} = ik\eta_0\,\tilde{\mu}$, $a_{22} = k\gamma$.

The field analysis in an unbounded homogeneous chiral medium is usually based on the introduction of new vectors [131] that allow decoupling of the Maxwell's equations into two independent systems of differential equations of the first order.

Separate the vector of magnetic field strength in (2.204):

$$\begin{cases} \vec{H} = \frac{1}{a_{21}} \left(\mathrm{rot}\vec{E} - a_{22}\vec{E} \right) \\ \mathrm{rotrot}\vec{E} = a_{11}a_{21}\vec{E} - a_{12}a_{22}\vec{E} + a_{12}\,\mathrm{rot}\vec{E} + a_{22}\,\mathrm{rot}\vec{E} \end{cases}.$$

Introducing the operator $M = \mathrm{rotrot} - a_{12}\mathrm{rot} - a_{22}\mathrm{rot} - a_{11}a_{21} + a_{12}a_{22}$, we arrive at the vector Helmholtz's equation

$$M\vec{E} = 0. \tag{2.205}$$

Taking into account $a_{12} = a_{22}$, the operator of the second-order M can be rewritten as

$$M = [\mathrm{rot} - a_{12}]^{\,2} - a_{11}a_{21} = \left[\mathrm{rot} - \left(\sqrt{a_{11}a_{21}} + a_{12}\right)\right]\left[\mathrm{rot} + \left(\sqrt{a_{11}a_{21}} - a_{12}\right)\right]$$

$$= M^{+}M^{-}.$$

Thus, the operator M can be represented as a product of two operators of the first order M^{+} and M^{-}, which commute. Seeking for solution of equation (2.205) in the form of sum $\vec{E} = \vec{E}^{+} + \vec{E}^{-}$, we have

$$M^{+}M^{-}\left(\vec{E}^{+} + \vec{E}^{-}\right) = 0.$$

Since the operators M^{+} and M^{-} commute, this equation is split into the equations $M^{+}\vec{E}^{+} = 0$, $M^{-}\vec{E}^{-} = 0$ or

$$\mathrm{rot}\vec{E}^{+} = -k^{+}\vec{E}^{+}, \qquad \mathrm{rot}\vec{E}^{-} = k^{-}\vec{E}^{-}. \tag{2.206}$$

Here, $k^{\pm} = -\left(\sqrt{a_{11}a_{21}} \pm a_{12}\right) = -k\sqrt{\tilde{\varepsilon}\,\tilde{\mu}}\,(1 \pm \eta)$ and $\eta = \gamma \Big/ \sqrt{\tilde{\varepsilon}\,\tilde{\mu}}$ is the relative chirality parameter.

Thus, the factorization of the vector wave equation (2.205) allowed reducing the problem to the two equations of the first order (2.206). Express the vector of magnetic strength $\vec{H}$ in terms of the vectors $\vec{E}^{\pm}$:

$$\vec{H} = \frac{1}{a_{21}}\left(-\left(k^{+} + a_{22}\right)\vec{E}^{+} + \left(k^{-}a_{22}\right)\vec{E}^{-}\right) = -\frac{i}{\rho}\left(\vec{E}^{+} - \vec{E}^{-}\right) = \vec{H}^{+} + \vec{H}^{-},$$

where $\rho = \sqrt{\mu_0\,\tilde{\mu} \Big/ \varepsilon_0\,\tilde{\varepsilon}}$.

Therefore, the electromagnetic field in the chiral medium is defined by the linear combinations of the so-called wave fields $\vec{E}^{\pm}$. Uncoupled plane waves $\vec{E}^{+}$, $\vec{H}^{+}$ and $\vec{E}^{-}$, $\vec{H}^{-}$ of left- and right-hand circular polarizations with propagation constants k^{+} and k^{-} are shown to be eigenwaves of the unbounded homogeneous chiral medium.

In the case of two-dimensional problems (when, for example, $\partial/\partial x \equiv 0$), we obtain the following field representation in the chiral medium:

$$\begin{aligned} &\vec{E} = \vec{E}^{+} + \vec{E}^{-}, \vec{H} = \vec{H}^{+} + \vec{H}^{-} = -\tfrac{i}{\rho}\left(\vec{E}^{+} - \vec{E}^{-}\right), \\ &\tilde{E}_x^{\pm} = \tilde{U}^{\pm}, \quad \tilde{E}_y^{\pm} = \mp\tfrac{1}{k^{\pm}}\tfrac{\partial \tilde{U}^{\pm}}{\partial z}, \quad \tilde{E}_z^{\pm} = \pm\tfrac{1}{k^{\pm}}\tfrac{\partial \tilde{U}^{\pm}}{\partial y} \end{aligned} \tag{2.207}$$

and

$$\left[\frac{\partial^2}{\partial y^2} + \frac{\partial^2}{\partial z^2}\right]\tilde{U}^{\pm}\left(g, k^{\pm}\right) + \left(k^{\pm}\right)^2 \tilde{U}^{\pm}\left(g, k^{\pm}\right) \equiv \Delta_{y,z}\tilde{U}^{\pm} + \left(k^{\pm}\right)^2 \tilde{U}^{\pm} = 0;\ g = \{y,z\}.$$

Thus, the components $\tilde{E}_x^{\pm}$ are those through which all the other field components can be represented. In the case of a bounded chiral medium, the wave fields $\vec{E}^{\pm}$ are connected to meet the corresponding boundary conditions for total fields $\vec{E}$ and $\vec{H}$. Even for the two-dimensional case, the equations for the sought field show that all the components are coupled, so the problem is a vectorial one.

2.4.2 Formulation of the Problem

At first, let us consider the model problem of electromagnetic wave diffraction from a strip grating placed above (or on) a chiral half-space. The problem geometry is shown in Fig. 2.5a. A periodic grating of infinitely thin and perfectly conducting strips parallel to the x-axis lies in the plane $z = h_1$. The grating period is l, the slot width is d. The interface between the chiral $z < 0$ and nonchiral $z > 0$ media is

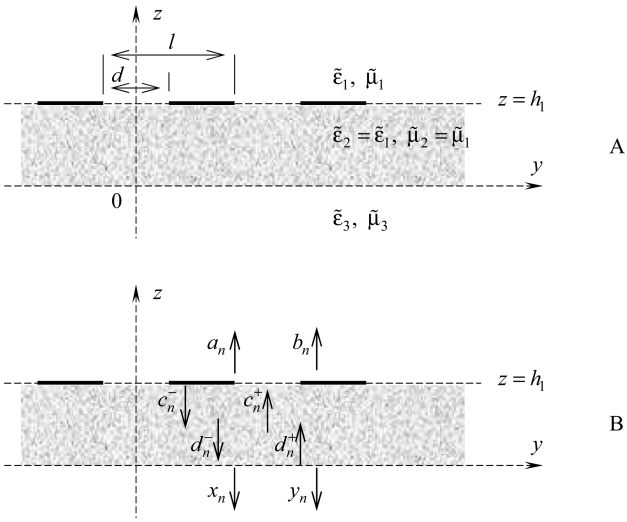

Fig. 2.5 (**a**) The structure profile and (**b**) the secondary field harmonics

given by the plane $z = 0$; $\tilde{\varepsilon}_1$ and $\tilde{\mu}_1$ are the relative permittivity and permeability of the magnetodielectric filling the upper half-space ($z > 0$), and $\tilde{\varepsilon}_3$, $\tilde{\mu}_3$, and $\eta = \gamma \Big/ \sqrt{\tilde{\varepsilon}_3\, \tilde{\mu}_3}$ are the constitutive parameters of the chiral half-space.

A plane electromagnetic wave normally incident on the grating from above is characterized by $\vec{E}^i = \vec{E}_0 \exp(-i(k_1 z + kt))$ and $\vec{H}^i = \vec{H}_0 \exp(-i(k_1 z + kt))$, where $k_1 = k\sqrt{\tilde{\varepsilon}_1\, \tilde{\mu}_1}$ is the wave number of the upper half-space. The diffracted field is to be found.

We will seek the solution in the form of a total field equal to the sum of the incident and secondary fields. Since the incident field is independent of the x-coordinate and the grating is uniform with respect to the x-axis, the desired field is independent of this coordinate. Thus, the problem is the two-dimensional ($\partial/\partial x \equiv 0$) one. Concerning the orientation of the incident wave, the original problem can be reduced to special cases of an E-polarized field where $\vec{E}_0 = \{\tilde{e},0,0\}$ or a H-polarized field where $\vec{H}_0 = \left\{\tilde{h},0,0\right\}$.

For the existence and uniqueness of the solution, it is necessary [45] that the solution obeys the Maxwell equations, the boundary conditions, the radiation condition at infinity, the quasi-periodicity condition, and the condition that the field energy is finite within any bounded volume of space.

2.4.3 The Systems of Dual Series Equations

The geometry of the structure allows us to solve the considered boundary value problem by the method of separation of variables. Assuming that the solution exists, we will seek it in the form of a Fourier series expansion for domains D_j ($j = 1,2,3$), where $D_1{:}h_1 < z$, $D_2{:}0 < z < h_1$, and $D_3{:}z < 0$. Substituting the series into Helmholtz's equation ($\Delta_{yz}\tilde{U}(g) + k_1^2\tilde{U}(g) = 0$ for $z > 0$ and $\Delta_{y,z}\tilde{U}^{\pm}(g) + \left(k^{\pm}\right)^2\tilde{U}^{\pm}(g) = 0$ for $z < 0$), we can represent the field components as follows (see Fig. 2.5b):

$$
\begin{cases}
\tilde{E}_x^1 = \tilde{e}\exp(-ik_1 z) + \sum\limits_{n=-\infty}^{\infty} a_n \exp\left(i\Gamma_n^1 (z - h_1)\right)\, \exp\left(i\,\Phi_n y\right) \\
\tilde{H}_x^1 = \tilde{h}\exp(-ik_1 z) + \sum\limits_{n=-\infty}^{\infty} b_n \exp\left(i\Gamma_n^1 (z - h_1)\right)\, \exp\left(i\,\Phi_n y\right)
\end{cases} ; z > h_1,
$$

$$
\begin{cases}
\tilde{E}_x^2 = \sum\limits_{n=-\infty}^{\infty} \left[c_n^+ \exp\left(i\Gamma_n^2 z\right) + c_n^- \exp\left(-i\Gamma_n^2 (z - h_1)\right)\right] \exp\left(i\,\Phi_n y\right) \\
\tilde{H}_x^2 = \sum\limits_{n=-\infty}^{\infty} \left[d_n^+ \exp\left(i\Gamma_n^2 z\right) + d_n^- \exp\left(-i\Gamma_n^2 (z - h_1)\right)\right] \exp\left(i\,\Phi_n y\right)
\end{cases} ; \quad 0 < z < h_1,
$$

$$
\begin{cases}
\tilde{E}_x^3 = \sum\limits_{n=-\infty}^{\infty} \left[x_n \exp\left(-i\Gamma_n^+ z\right) + y_n \exp\left(-i\Gamma_n^- z\right)\right] \exp\left(i\Gamma_n^1 h_1\right) \exp\left(i\Phi_n y\right) \\
\tilde{H}_x^3 = \frac{-i}{\rho_3} \sum\limits_{n=-\infty}^{\infty} \left[x_n \exp\left(-i\Gamma_n^+ z\right) - y_n \exp\left(-i\Gamma_n^- z\right)\right] \exp\left(i\Gamma_n^1 h_1\right) \exp\left(i\Phi_n y\right)
\end{cases} ; \quad z < 0.
\tag{2.208}
$$

Here, we have denoted the propagation constant of the nth field harmonic by Φ_n in the y-direction and by $\Gamma_n^j; j \neq 3$, $\Gamma_n^{\pm}; j = 3$ in the z-direction for the domain D_j:

$$\Phi_n = \frac{2\pi}{l} n\,, \qquad \Gamma_n^j = \sqrt{k_j^2 - (\Phi_n)^2}, \qquad \Gamma_n^{\pm} = \sqrt{\left(k^{\pm}\right)^2 - (\Phi_n)^2}. \tag{2.209}$$

The root branches with $\mathrm{Im}\left(\Gamma_n^{j,\pm}\right) \geq 0$ are chosen to fit the radiation condition at infinity, $k_j = k\sqrt{\tilde{\varepsilon}_j \tilde{\mu}_j}$, and $\rho_j = \sqrt{\mu_0\,\tilde{\mu}_j / \varepsilon_0\,\tilde{\varepsilon}_j}, j = 1,2,3$.

The obtained field representation (2.208) satisfies the quasi-periodicity condition and corresponds to the Rayleigh expansion of the diffracted field in a superposition of partial harmonics of spatial spectrum. This superposition, which consists of a finite number of plane uniformly propagating waves (for which Γ_n^j, $\Gamma_n^{\pm}$ are real) and an infinite number of slow nonuniform surface waves (with Γ_n^j, $\Gamma_n^{\pm}$ complex), is localized near the inhomogeneity planes $z = h_1, z = 0$. The propagation direction and decay character of these waves are given by (2.209), while the wave amplitudes and phases are determined by the unknown Fourier coefficients: a_n, b_n, $c_n^{\pm}$, $d_n^{\pm}$, and x_n, y_n. It is possible to show that each number n in the series describing the chiral medium field is assigned to a couple of circularly polarized waves with amplitudes x_n, y_n and wave vectors $\vec{k}_n^{\pm} = \left\{0, \Phi_n, -\Gamma_n^{\pm}\right\}$. Note that, complex coefficients a_n, $c_n^{\pm}$ correspond to E-polarization and b_n, $d_n^{\pm}$ to H-polarization. Thus, the problem is to find these coefficients.

Satisfying the boundary condition, that the tangential components of the electric field are equal over the grating period gives

$$\begin{aligned} a_n &= c_n^{+} \exp\left(i\Gamma_n^1 h_1\right) + c_n^{-} - \delta_0^n\,\tilde{e}\,\exp\left(-ik_1 h_1\right) \text{ and} \\ b_n &= d_n^{+} \exp\left(i\Gamma_n^1 h_1\right) - d_n^{-} + \delta_0^n\,\tilde{h}\,\exp\left(-ik_1 h_1\right). \end{aligned} \tag{2.210}$$

Using the obtained relations (2.210) and applying the boundary condition that the magnetic field components are continuous over the grating slot yields the series equation valid on the interval $|y| < d/2$

$$\begin{cases} \sum\limits_{n=-\infty}^{\infty} \Gamma_n^1 c_n^{-} \exp\left(i\Phi_n y\right) = \tilde{e} k_1 \exp\left(-ik_1 h_1\right) \\ \sum\limits_{n=-\infty}^{\infty} d_n^{-} \exp\left(i\Phi_n y\right) = \tilde{h} \exp\left(-ik_1 h_1\right) \end{cases}; \; |y| < d/2.$$

Imposing the boundary condition that the electric field tangential components vanish on the metal strips results in another couple of the series equation valid on the interval $d/2 < |y| < l/2$. Thus, the boundary conditions corresponding to the strip grating at $z = h_1$ allows us to obtain two systems of functional equations

$$\begin{cases} \sum\limits_{n=-\infty}^{\infty} \Gamma_n^1 \, c_n^- \exp\left(i\Phi_n y\right) = \tilde{e} k_1 \exp\left(-ik_1 h_1\right); & |y| < d/2 \\ \sum\limits_{n=-\infty}^{\infty} \left\{c_n^+ \exp\left(i\Gamma_n^1 \, h_1\right) + c_n^-\right\} \exp\left(i\Phi_n y\right) = 0; & d/2 < |y| \le l/2 \end{cases}, \quad (2.211)$$

$$\begin{cases} \sum\limits_{n=-\infty}^{\infty} d_n^- \exp\left(i\Phi_n y\right) = \tilde{h} \exp\left(-ik_1 h_1\right); & |y| < d/2 \\ \sum\limits_{n=-\infty}^{\infty} \Gamma_n^1 \left\{ d_n^+ \exp\left(i\Gamma_n^1 \, h_1\right) - d_n^- \right\} \exp\left(i\Phi_n y\right) = 0; & d/2 < |y| \le l/2 \end{cases}. \quad (2.212)$$

System (2.211) of dual series equations is for E-polarization, and system (2.212) for H-polarization. The continuity of the tangential components of the field at $z = 0$ enables us to determine $c_n^{\pm}$, $d_n^{\pm}$ via the complex amplitudes x_n, y_n of the field in the chiral medium:

$$c_n^+ = \frac{1}{2} \exp\left(i\Gamma_n^1 h_1\right) \left[\left(A_n^{11} - A_n^{12}\right) x_n + \left(A_n^{21} - A_n^{22}\right) y_n\right],$$

$$c_n^- = \frac{1}{2} \left[\left(A_n^{11} + A_n^{12}\right) x_n + \left(A_n^{21} + A_n^{22}\right) y_n\right],$$

$$d_n^+ = -\frac{i}{2\rho_3} \exp\left(i\Gamma_n^1 h_1\right) \left[\left(B_n^{11} - B_n^{12}\right) x_n + \left(B_n^{21} - B_n^{22}\right) y_n\right],$$

$$d_n^- = \frac{i}{2\rho_3} \left[\left(B_n^{11} + B_n^{12}\right) x_n + \left(B_n^{21} + B_n^{22}\right) y_n\right].$$

Here, we have introduced the coefficients

$$A_n^{11} = 1, \quad A_n^{12} = \frac{\tilde{\mu}_1}{\tilde{\mu}_3 \, (1+\eta)} \, \frac{\Gamma_n^+}{\Gamma_n^1}, \quad A_n^{21} = 1, \quad A_n^{22} = \frac{\tilde{\mu}_1}{\tilde{\mu}_3 \, (1-\eta)} \, \frac{\Gamma_n^-}{\Gamma_n^1},$$

$$B_n^{11} = -\frac{\tilde{\varepsilon}_1}{\tilde{\varepsilon}_3 \, (1+\eta)} \, \frac{\Gamma_n^+}{\Gamma_n^1}, \quad B_n^{12} = -1, \quad B_n^{21} = \frac{\tilde{\varepsilon}_1}{\tilde{\varepsilon}_3 \, (1-\eta)} \, \frac{\Gamma_n^-}{\Gamma_n^1}, \; B_n^{22} = 1.$$

Systems (2.211) and (2.212) for the coefficients x_n, y_n take the form

$$\begin{cases} \sum\limits_{n=-\infty}^{\infty} \Gamma_n^1 \left\{x_n \left[A_n^{11} + A_n^{12}\right] + y_n \left[A_n^{21} + A_n^{22}\right]\right\} \exp\left(i\Phi_n y\right) = \\ = 2k_1 \tilde{e} \exp\left(-ik_1 h_1\right); & |y| < d/2 \\ \sum\limits_{n=-\infty}^{\infty} \left\{x_n \left[\Omega_n^+ A_n^{11} + \Omega_n^- A_n^{12}\right] + y_n \left[\Omega_n^+ A_n^{21} + \Omega_n^- A_n^{22}\right]\right\} \exp\left(i\Phi_n y\right) = \\ = 0; & d/2 < |y| \le l/2 \end{cases}, \quad (2.213)$$

$$\begin{cases} \sum\limits_{n=-\infty}^{\infty} \left\{ x_n \left[B_n^{11} + B_n^{12} \right] + y_n \left[B_n^{21} + B_n^{22} \right] \right\} \exp\left(i\Phi_n y \right) = \\ = -2i\rho_3 \tilde{h} \exp\left(-ik_1 h_1 \right); \qquad |y| < d/2 \\ \sum\limits_{n=-\infty}^{\infty} \Gamma_n^1 \left\{ x_n \left[\Omega_n^+ B_n^{11} + \Omega_n^- B_n^{12} \right] + y_n \left[\Omega_n^+ B_n^{21} + \Omega_n^- B_n^{22} \right] \right\} \exp\left(i\Phi_n y \right) = \\ = 0; \qquad d/2 < |y| \le l/2 \end{cases}, \tag{2.214}$$

where $\Omega_n^{\pm} = 1 \pm \exp\left(i2\Gamma_n^1 h_1 \right)$. Systems (2.213) and (2.214) of dual series equations involving exponential functions are equivalent to an operator equation of the first kind in the Hilbert space given by the Meixner condition [132].

The obtained systems are coupled, and describe fields of both linear polarizations. Let, for example, the grating be excited by an E-polarized wave ($\tilde{h} = 0$), then without chirality ($\gamma = 0$), i.e., when lower half-space ($z < 0$) is magnetodielectric, we have $k^+ = k^-$ and $A_n^{11} = A_n^{21}$, $A_n^{12} = A_n^{22}$ and also $B_n^{11} = -B_n^{21}$, $B_n^{12} = -B_n^{22}$. Then systems (2.213) and (2.214) become decoupled, and the homogeneous equations of system (2.214) imply $x_n = y_n$. If so, the H-polarized field disappears, and system (2.213) gives the solution to the scalar diffraction problem in the E-polarization case. The presence of chirality ($\gamma \neq 0$) will give rise to additional field polarization. The appearance of additional polarization is attributed to the fact that the chiral medium eigenwaves represent circularly polarized waves produced by the superposition of E- and H-polarized fields. So despite the two-dimensional problem formulation, the sought field contains components of both polarizations, which are coupled in this problem. Therefore, the vector problem is considered.

2.4.4 An Algebraic System of the Second Kind

In order to separate a series with slow convergence rate, we introduce the new unknown coefficients

$$X_n = x_n \left[B_n^{11} + B_n^{12} \right] + y_n \left[B_n^{21} + B_n^{22} \right] + \delta_0^n 2i\rho_3 \tilde{h} \exp\left(-ik_1 h_1 \right) \text{ and}$$

$$Y_n = x_n \left[\Omega_n^+ A_n^{11} + \Omega_n^- A_n^{12} \right] + y_n \left[\Omega_n^+ A_n^{21} + \Omega_n^- A_n^{22} \right].$$

Now, in the case of $h_1 \neq 0$, i.e., for the grating placed above the chiral half-space, systems (2.213) and (2.214) can be represented in the following form:

$$\begin{cases} \sum\limits_{n=-\infty(n\neq 0)}^{\infty} |n| X_n \exp\left(in\vartheta \right) = F^1\left(\vartheta; X_n, Y_n \right); \qquad |\vartheta| > \vartheta_0 \\ \sum\limits_{n=-\infty}^{\infty} X_n \exp\left(in\vartheta \right) = 0; \qquad |\vartheta| < \vartheta_0 \end{cases}, \tag{2.215}$$

$$\begin{cases} \sum\limits_{n=-\infty}^{\infty} Y_n \exp\left(in\vartheta \right) = 0; \qquad |\vartheta| > \vartheta_0 \\ \sum\limits_{n=-\infty(n\neq 0)}^{\infty} |n| Y_n \exp\left(in\vartheta \right) = F^2\left(\vartheta; X_n, Y_n \right); \qquad |\vartheta| < \vartheta_0 \end{cases}, \tag{2.216}$$

where $\vartheta = 2\pi y/l$ and $\vartheta_0 = \pi d/l$. Then the inequality $|\vartheta| < \vartheta_0$ indicates the grating slot and $\vartheta_0 < |\vartheta|$ refers to the strip. The right-hand sides of the systems $F^{1,2}(\vartheta; X_n, Y_n) = \sum_{n=-\infty}^{\infty} f_n^{1,2}(X_n, Y_n) \exp(in\vartheta)$ are sufficiently smooth functions of ϑ, belonging to the $\mathbf{L}_2[-\pi;\pi]$ space. Their Fourier coefficients are:

$$f_0^1 = i\kappa_1 \left\{ X_0 + \left(x_0 \left[B_0^{11} - B_0^{12} \right] + y_0 \left[B_0^{21} - B_0^{22} \right] \right) \exp(i2k_1 h_1) \right\}$$

$$+2\chi_1 \rho_3 \tilde{h} \exp(-ik_1 h_1),$$

$$f_n^1 = |n| \left\{ \xi_n X_n - (1 - \xi_n) \left(x_n \left[B_n^{11} - B_n^{12} \right] + y_n \left[B_n^{21} - B_n^{22} \right] \right) \exp\left(i2\Gamma_n^1 h_1 \right) \right\},$$

$$f_0^2 = i\kappa_1 \left\{ Y_0 - \left(x_0 \left[A_0^{11} - A_0^{12} \right] + y_0 \left[A_0^{21} - A_0^{22} \right] \right) \exp(i2k_1 h_1) \right\}$$

$$-2i\kappa_1 \tilde{e} \exp(-ik_1 h_1),$$

$$f_n^2 = |n| \left\{ \xi_n Y_n + (1 - \xi_n) \left(x_n \left[A_n^{11} - A_n^{12} \right] + y_n \left[A_n^{21} - A_n^{22} \right] \right) \exp\left(i2\Gamma_n^1 h_1 \right) \right\}.$$

Here, $\xi_n = 1 + i\sqrt{\left(\kappa_1/n\right)^2 - 1}$ is the smallness parameter, $\kappa_1 = l\lambda^{-1}\sqrt{\tilde{\varepsilon}_1 \tilde{\mu}_1}$, and λ is the wavelength in vacuum.

The asymptotic estimates of the coefficients $A_n^{rs} = O(1)$, $B_n^{rs} = O(1)$, $r, s = 1,2$, and the smallness parameter $\xi_n = O(n^{-2})$ show that as $|n| \to \infty$

$$f_n^{1,2} \underset{|n|\to\infty}{=} \frac{\sigma_n^{1,2}}{|n|} + O(|n| \exp(-\sigma\ |n|)),$$

where $\sigma = 4\pi h_1 l^{-1} \left[1 - 0.5 \left(\kappa_1 n^{-1} \right)^2 \right] > 0$, and the sequences $\left\{ \sigma_n^{1,2} \right\}_{n=-\infty}^{\infty}$ belong to l_2 space with weight $(|n| + 1)$. Therefore, the systems' right-hand sides, containing the Fourier expansions of the functions $F^{1,2}$, converge well. The left-hand sides of the systems are the series with slow convergence rate; they correspond to the principal part of the problem operator possessing the singularity. Taking the right-hand sides of (2.215) and (2.216) as known allows us to assume that the obtained functional systems are decoupled. Thus, we have not only extracted the singularity in the left-hand sides of the equations but also managed to decouple the systems in terms of the principal part of the operator.

It should be stressed that such decoupling is possible only for $h_1 \neq 0$, i.e., in the case of the grating placed above the chiral half-space. For $h_1 = 0$, the decoupling of the systems is impossible, and we have to solve the systems jointly. This required the development of an essentially new mathematical approach described above in Section 2.2.4.

For the case $h_1 \neq 0$, systems (2.215) and (2.216) are equivalent to a scalar Riemann–Hilbert boundary value problem (see [45] and Section 2.2.1). Applying this well-known method to the solution of this problem for each system individually yields the following infinite system of linear algebraic equations [133]:

$$\begin{cases} Y_m = \sum\limits_{n=-\infty}^{\infty} V_{mn}(u)\left\{\alpha_n Y_n + \beta_n X_n\right\} + b_m \\ X_m = \sum\limits_{n=-\infty}^{\infty} \tilde{V}_{mn}(\tilde{u})\left\{\tilde{\alpha}_n Y_n + \tilde{\beta}_n X_n\right\} + \tilde{b}_m \end{cases}; \quad m = 0, \pm 1, ... \tag{2.217}$$

The values $V_{mn}(u)$, $\tilde{V}_{mn}(\tilde{u})$, and α_n, β_n, b_m; $\tilde{\alpha}_n$, $\tilde{\beta}_n, \tilde{b}_m$ that appears in system (2.217) have the form

$$u = \cos\delta,\ V_{00} = -\ln\frac{1+u}{2},\ V_{0n} = \frac{1}{n}V_{n-1}^{-1}(u),\ V_{mn} = -\ V_{m-1}^{n-1}(u),$$

$$\tilde{u} = \cos\tilde{\delta},\ \tilde{V}_{00} = -\ln\frac{1+\tilde{u}}{2},\ \tilde{V}_{0n} = \frac{(-1)^n}{n}V_{n-1}^{-1}(\tilde{u}),$$

$$\tilde{V}_{mn} = \frac{(-1)^{m+n}}{m}V_{m-1}^{n-1}(\tilde{u}),\ \alpha_0 = i\kappa_1\frac{R_0^+}{T_0^+},$$

$$\alpha_n = |n|\left\{\xi_n\frac{R_n^+}{T_n^+} + \frac{R_n^-}{T_n^+}\exp\left(i2\Gamma_n^1 h_1\right)\right\},\ \beta_0 = 2i\kappa_1\frac{A_0}{T_0^+}\exp(i2k_1h_1),$$

$$\beta_n = -2|n|(1-\xi_n)\frac{A_n}{T_n^+}\exp\left(i2\Gamma_n^1 h_1\right),\ \tilde{\alpha}_0 = 2i\kappa_1\frac{B_0}{T_0^+}\exp(i2k_1h_1),$$

$$\tilde{\alpha}_n = -2|n|(1-\xi_n)\frac{B_n}{T_n^+}\exp\left(i2\Gamma_n^1 h_1\right),\ \tilde{\beta}_0 = i\kappa_1\frac{C_0}{T_0^+},$$

$$\tilde{\beta}_n = |n|\left\{\xi_n\frac{C_n}{T_n^+} - \frac{T_n^-}{T_n^+}\exp\left(i2\Gamma_n^1 h_1\right)\right\},$$

$$b_m = -2i\kappa_1 V_{m0}(u)\left[\tilde{e}\exp(-ik_1h_1) + 2i\rho_3\tilde{h}\frac{A_0}{T_0^+}\exp(ik_1h_1)\right],$$

$$\tilde{b}_m = 2\rho_3\tilde{h}\kappa_1\tilde{V}_{m0}(\tilde{u})\left[\exp(-ik_1h_1) + \frac{T_0^-}{T_0^+}\exp(ik_1h_1)\right],$$

where the matrix $V_m^n(u)$ is defined in Section 2.2.1, and

$$A_n = A_n^{11}A_n^{22} - A_n^{12}A_n^{21}, \qquad B_n = B_n^{11}B_n^{22} - B_n^{12}B_n^{21},$$

$$C_n = \left[\Omega_n^+A_n^{11} + \Omega_n^-A_n^{12}\right]\left[\Omega_n^+B_n^{21} + \Omega_n^-B_n^{22}\right] - \left[\Omega_n^+A_n^{21} + \Omega_n^-A_n^{22}\right]$$
$$\left[\Omega_n^+B_n^{11} + \Omega_n^-B_n^{12}\right],$$

$$R_n^{\pm} = \left[A_n^{11} \pm A_n^{12}\right]\left[B_n^{21} + B_n^{22}\right] - \left[A_n^{21} \pm A_n^{22}\right]\left[B_n^{11} + B_n^{12}\right],$$

$$T_n^{\pm} = \left[\Omega_n^{+} A_n^{11} + \Omega_n^{-} A_n^{12}\right]\left[B_n^{21} \pm B_n^{22}\right] - \left[\Omega_n^{+} A_n^{21} + \Omega_n^{-} A_n^{22}\right]\left[B_n^{11} \pm B_n^{12}\right].$$

The asymptotic estimates of the coefficients $\alpha_n, \tilde{\beta}_n = 1/|n|$; $\tilde{\alpha}_n, \beta_n = |n| \exp(-\sigma|n|)$ as $|n| \to \infty$, and the behavior of V_m^n for $|m|, |n| \to \infty$, allow us to conclude that (2.217) is a Fredholm-type system of the second kind. This system is the rigorous solution to the formulated vector problem, it finds X_n and Y_n and consequently all the unknowns.

Now we turn to the case when the grating is placed on the chiral half-space, i.e., $h_1 = 0$. We will show herein that the system of equations (2.213) and (2.214) is reducible to the form of the system of equations (2.123), (2.124), (2.125), and (2.126) described in Section 2.2.4. Really, after elementary transformations, equations (2.213) and (2.214) can be represented as

$$\begin{cases} \sum\limits_{n=-\infty}^{\infty} X_n \exp(in\vartheta) = 0; \qquad |\vartheta| < \vartheta_0 \\ \sum\limits_{n=-\infty(n\neq 0)}^{\infty} \Gamma_n^1 \bar{c}_n \left(\bar{b}_n X_n + Y_n\right) \exp(in\vartheta) + k_1 \left(\frac{\rho_1+\rho_3}{\rho_3} Y_0 + 2\tilde{e}\right) = 0; \quad |\vartheta| < \vartheta_0 \end{cases}, \tag{2.218}$$

$$\begin{cases} \sum\limits_{n=-\infty}^{\infty} Y_n \exp(in\vartheta) = 0; \qquad |\vartheta| > \vartheta_0 \\ \sum\limits_{n=-\infty(n\neq 0)}^{\infty} \Gamma_n^1 \bar{d}_n \left(X_n + \bar{a}_n Y_n\right) \exp(in\vartheta) + \frac{k_1\rho_3}{\rho_1+\rho_3}\left(X_0 - i2\rho_1\tilde{h}\right) = 0; \quad |\vartheta| > \vartheta_0 \end{cases}. \tag{2.219}$$

Here, we introduced the coefficients

$$\bar{a}_n = \frac{B_n^{11} + B_n^{21}}{B_n^{21} - B_n^{11}}, \qquad \bar{b}_n = \frac{A_n^{22} - A_n^{12}}{\left(1 + A_n^{12}\right)\left(1 + B_n^{21}\right) + \left(1 + A_n^{22}\right)\left(1 - B_n^{11}\right)},$$

$$\bar{c}_n = \frac{\left(1 + A_n^{12}\right)\left(1 + B_n^{21}\right) + \left(1 + A_n^{22}\right)\left(1 - B_n^{11}\right)}{2 + B_n^{21} - B_n^{11}}, \qquad \bar{d}_n = \frac{B_n^{21} - B_n^{11}}{2 + B_n^{21} - B_n^{11}}. \tag{2.220}$$

Using the explicit expressions for A_n^{pq} and B_n^{pq}, it is possible to obtain the following asymptotic estimates for (2.220) as $|n| \to \infty$:

$$\bar{a}_n = \eta + O\left(n^{-2}\right), \qquad \bar{b}_n = \frac{\tilde{\varepsilon}_3\tilde{\mu}_1\eta}{(\tilde{\varepsilon}_1+\tilde{\varepsilon}_3)(\tilde{\mu}_1+\tilde{\mu}_3)-\tilde{\varepsilon}_3\tilde{\mu}_3\eta^2} + O\left(n^{-2}\right),$$

$$\bar{c}_n = \frac{(\tilde{\varepsilon}_1+\tilde{\varepsilon}_3)(\tilde{\mu}_1+\tilde{\mu}_3)-\tilde{\varepsilon}_3\tilde{\mu}_3\eta^2}{\tilde{\mu}_3\left(\tilde{\varepsilon}_1+\tilde{\varepsilon}_3\left(1-\eta^2\right)\right)} + O\left(n^{-2}\right),$$

$$\bar{d}_n = \frac{\tilde{\varepsilon}_1}{\tilde{\varepsilon}_1+\tilde{\varepsilon}_3\left(1-\eta^2\right)} + O\left(n^{-2}\right). \tag{2.221}$$

Now, taking into account the estimates (2.221) and that $\Gamma_n^1 = |n|\frac{2\pi i}{l}\left[1+O\left(n^{-2}\right)\right]$ as $|n|\to\infty$, we write the system of equations (2.218) and (2.219) in the following form:

$$\begin{cases} \sum\limits_{n=-\infty}^{\infty} X_n \exp(in\vartheta) = 0; \qquad |\vartheta| < \vartheta_0 \\ \sum\limits_{n=-\infty}^{\infty} |n|(bX_n + Y_n)\exp(in\vartheta) + \\ \qquad + \sum\limits_{n=-\infty}^{\infty}\left(V_n^{11}X_n + V_n^{12}Y_n - f_{1n}\right)\exp(in\vartheta); \qquad |\vartheta| < \vartheta_0 \end{cases}, \tag{2.222}$$

$$\begin{cases} \sum\limits_{n=-\infty}^{\infty} Y_n \exp(in\vartheta) = 0; \qquad |\vartheta| > \vartheta_0 \\ \sum\limits_{n=-\infty}^{\infty} |n|(X_n + aY_n)\exp(in\vartheta) + \\ \qquad + \sum\limits_{n=-\infty}^{\infty}\left(V_n^{21}X_n + V_n^{22}Y_n - f_{2n}\right)\exp(in\vartheta); \qquad |\vartheta| > \vartheta_0 \end{cases}. \tag{2.223}$$

Here,

$$a = \eta,\ b = \frac{\tilde{\varepsilon}_3\tilde{\mu}_1\eta}{(\tilde{\varepsilon}_1+\tilde{\varepsilon}_3)(\tilde{\mu}_1+\tilde{\mu}_3)-\tilde{\varepsilon}_3\tilde{\mu}_3\eta^2}. \tag{2.224}$$

The coefficients V_n^{pq} (p,q = 1,2) can be expressed in terms of A_n^{pq}, B_n^{pq}, and Γ_n^1. As $|n|\to\infty$ they satisfy the conditions

$$V_n^{pq} = O\left(|n|^{-1}\right), p,q = 1,2. \tag{2.225}$$

Coefficients f_{1n} and f_{2n} are of the form

$$f_{1n} = -\frac{i\kappa_1\tilde{\mu}_3\left(\tilde{\varepsilon}_1+\tilde{\varepsilon}_3\left(1-\eta^2\right)\right)}{(\tilde{\varepsilon}_1+\tilde{\varepsilon}_3)(\tilde{\mu}_1+\tilde{\mu}_3)-\tilde{\varepsilon}_3\tilde{\mu}_3\eta^2}\tilde{e}\delta_0^n, \tag{2.226}$$

$$f_{2n} = -\frac{2\kappa_1\rho_1\rho_3\left(\tilde{\varepsilon}_1+\tilde{\varepsilon}_3\left(1-\eta^2\right)\right)}{\tilde{\varepsilon}_1(\rho_1+\rho_3)}\tilde{h}\delta_0^n. \tag{2.227}$$

It follows from expressions (2.225), (2.226), and (2.227) that the coefficients of dual series equations (2.222) and (2.223) meet the conditions for applying the analytic regularization method which uses the explicit solution of the vectorial Riemann–Hilbert boundary value problem, described in detail in Section 2.2.4. Namely, the asymptotic estimates (2.225) for the elements V_n^{pq} show that the matrix operators $V^{pq} = \left\{V_n^{pq}\delta_m^n\right\}_{m,\,n=-\infty}^{\infty}$ specify compact operators in l_2 space. From formulas (2.226) and (2.227), it follows that vector columns $f_1 = \{f_{1n}\}_{n=-\infty}^{\infty}$ and $f_2 = \{f_{2n}\}_{n=-\infty}^{\infty}$ belong to the space $l_2(-1)$ (see Section 2.2).

In addition, in the case of real-valued constitutive parameters $\tilde{\varepsilon}_j$, $\tilde{\mu}_j$, and $\eta = \gamma\Big/\sqrt{\tilde{\varepsilon}_3\,\tilde{\mu}_3}$, the coefficients a and b satisfy the inequality $0 \le ab < 1$. Let us prove it. From (2.224) we have

$$ab = \frac{\tilde{\varepsilon}_3\tilde{\mu}_1\eta^2}{(\tilde{\varepsilon}_1+\tilde{\varepsilon}_3)\;(\tilde{\mu}_1+\tilde{\mu}_3)-\tilde{\varepsilon}_3\tilde{\mu}_3\eta^2}. \tag{2.228}$$

It is known [117], that $\eta < 1$, therefore $(\tilde{\varepsilon}_1+\tilde{\varepsilon}_3)\,(\tilde{\mu}_1+\tilde{\mu}_3) - \tilde{\varepsilon}_3\tilde{\mu}_3\eta^2 > 0$. Suppose, that $ab \ge 1$, then from (2.228) we have $\tilde{\varepsilon}_3\,(\tilde{\mu}_1+\tilde{\mu}_3)\,\eta^2 \ge (\tilde{\varepsilon}_1+\tilde{\varepsilon}_3)\,(\tilde{\mu}_1+\tilde{\mu}_3)$ and consequently $\eta \ge \sqrt{1+\left(\tilde{\varepsilon}_1\big/\tilde{\varepsilon}_3\right)}$. Thus, the inequality $0 \le ab < 1$ holds.

Thus, on the basis of the results described in Section (2.2.4.), the system of dual series equations (2.222) and (2.223) is equivalent to the system of linear algebraic equations of the second kind, which has the form as that of (2.172) and (2.173).

2.4.5 Numerical Analysis for Grating and Chiral Half-Space

Introduce the reflection coefficients (a_0^x, a_0^y) and the transmission coefficients (b_0^x, b_0^y) for the x- and y-components of the electric field as follows: $a_0^x = a_0$ and $a_0^y = -\rho_1 b_0$ for $z > h_1$; $b_0^x = \left(x_0 + y_0\right)\exp\left(ik_1h_1\right)$ and $b_0^y = -i\left(x_0 - y_0\right)\exp\left(ik_1h_1\right)$ for $z < 0$. These coefficients determine the field averaged over the grating period. The upper indices x and y relate, respectively, to the field of E-polarization and H-polarization. The incident field polarization is called the principal polarization, and the polarization perpendicular to the principal is called the cross-polarization. Using the boundary conditions, one obtains the following relations:

$$a_0^x + \tilde{e}\exp\left(-ik_1h_1\right) = \Omega b_0^x, \qquad a_0^y + \rho_1\tilde{h}\exp\left(-ik_1h_1\right) = \Omega b_0^y,$$

where

$$\Omega = \frac{1}{2}\left[\left(1-\frac{\rho_1}{\rho_3}\right)\exp\left(ik_1h_1\right) + \left(1+\frac{\rho_1}{\rho_3}\right)\exp\left(-ik_1h_1\right)\right].$$

Note that the coefficients introduced are related by the functional dependence imposed by the boundary conditions.

The distinctive feature of the behavior of reflection coefficients as functions of the frequency parameter $\kappa = l/\lambda$ is the presence of peculiarities analogous to the classical Wood anomalies [45] at the so-called grazing points $\kappa_{1n} = n\Big/\sqrt{\tilde{\varepsilon}_1\tilde{\mu}_1}$ and peculiarities in the vicinity of the points $\kappa_{3n}^{\pm} = n\mathrm{Re}\left(1\Big/\left(\sqrt{\tilde{\varepsilon}_3\tilde{\mu}_3} \pm \gamma\right)\right)$ where $n = 0,\pm1,\ldots$. It is seen from the field representation that the quantities κ_{1n} and $\kappa_{3n}^{\pm}$ determine the frequency parameter values for which the nth harmonic of the nonchiral and chiral half-spaces, respectively, becomes propagating. Figure 2.6a shows the reflection coefficients of the principal-polarized field as a functions of κ. If $\kappa_{31}^{\pm} < \kappa < \kappa_{11}$, then the number of waves propagating in the chiral medium, which is assumed to be optically denser, is greater than that in the nonchiral medium. For small h_1, the surface harmonics decaying with distance from the grating become propagating upon entering the chiral medium and carry away a fraction of the energy. Such an energy redistribution explains the distinctive features of the reflection coefficients of the principal-polarized field in the vicinity of the points $\kappa_{3n}^{\pm}$.

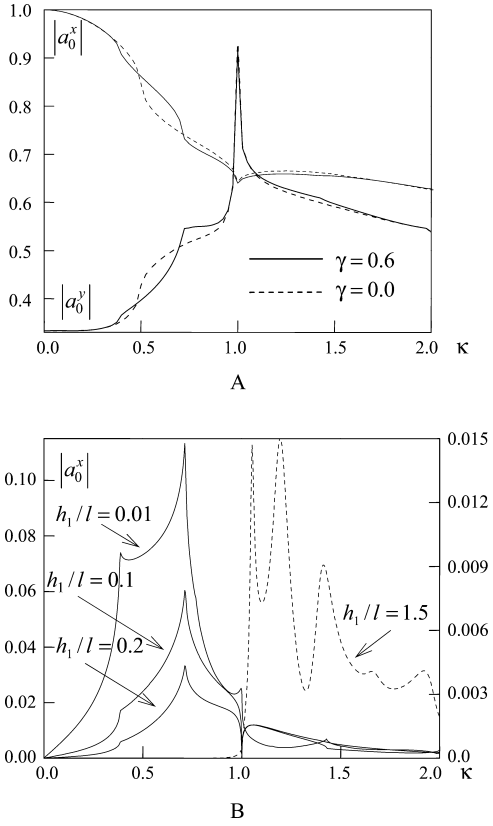

Fig. 2.6 The reflection coefficients versus frequency $\kappa = l/\lambda$ for (**a**) principal polarization field ($h_1/l = 0.05$) and (**b**) cross-polarized field (the *solid* and the *dashed curves* refer to the *left* and *right* vertical axes, respectively; $\gamma = 0.6$): $\tilde{\varepsilon}_1 = 1$, $\tilde{\mu}_1 = 1$, $\tilde{\varepsilon}_3 = 4$, $\tilde{\mu}_3 = 1$, $d/l = 0.5$

The frequency dependences of the reflection coefficients of cross-polarized waves are shown in Fig. 2.6b. The appearance of new propagating circularly polarized waves in the chiral medium at $\kappa_{3n}^{\pm}$ explains the increase in the reflection coefficients of the cross-polarized field at these points. The magnitudes of these coefficients depend on the amount of energy transferred by decaying surface waves to the chiral medium. For small distances, these coefficients decrease with increasing h_1. For $\left|\Gamma_1^1\right| h_1 \gg 1$, the surface field of the grating does not enter the second medium and the zero-order principal-polarized wave propagating normally does not produce the reflection of the cross-polarized field. Hence, the cross-polarized field is absent until the harmonic of the order $n = 1$, propagating at an angle to the z-axis, appears in the upper half-space for $\kappa > \kappa_{11}$.

Now we analyze the frequency dependences of the reflection coefficients in the case where the E- and H-polarized waves are incident simultaneously (see Fig. 2.7). The difference of the phases of the E- and H-polarized waves is $\delta\phi = \arg\left(\rho_1 \tilde{h} \Big/ \tilde{e}\right)$. The superposition of the incident waves will have different polarizations for different values of $\delta\phi$. Let $|\tilde{e}| = 1$ and $\left|\rho_1 \tilde{h}\right| = 1$. In-phase waves yield a linearly polarized wave, whereas for $\delta\phi = \pm\pi/2$, we have waves with right- and left-hand circular polarizations, respectively.

If a wave with right-hand circular polarization is incident, then the peculiarity in the vicinity of κ_{31}^{-} is more pronounced than the one in the vicinity of κ_{31}^{+}. This is explained by the efficient energy transfer in the case when the frequencies and polarizations of the incident wave and the propagating harmonic appearing in the chiral medium in the vicinity of κ_{31}^{-}, having also a right-hand circular polarization, are identical. In the vicinity of κ_{31}^{+}, the incident wave and the corresponding harmonic of the chiral medium interact weakly due to the fact that their field vectors rotate in opposite directions, although they both have circular polarization. For an incident linearly polarized wave, the above-mentioned features in the vicinity of κ_{31}^{+} are equally pronounced.

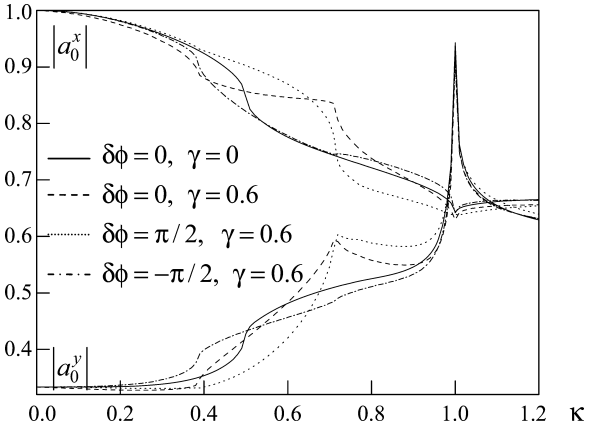

Fig. 2.7 The reflection coefficients versus frequency $\kappa = l/\lambda$ at the simultaneous incidence of E- and H-polarized waves: $\tilde{\varepsilon}_1 = 1$, $\tilde{\mu}_1 = 1$, $\tilde{\varepsilon}_3 = 4$, $\tilde{\mu}_3 = 1$, $d/l = 0.5$, $h_1/l = 0.05$

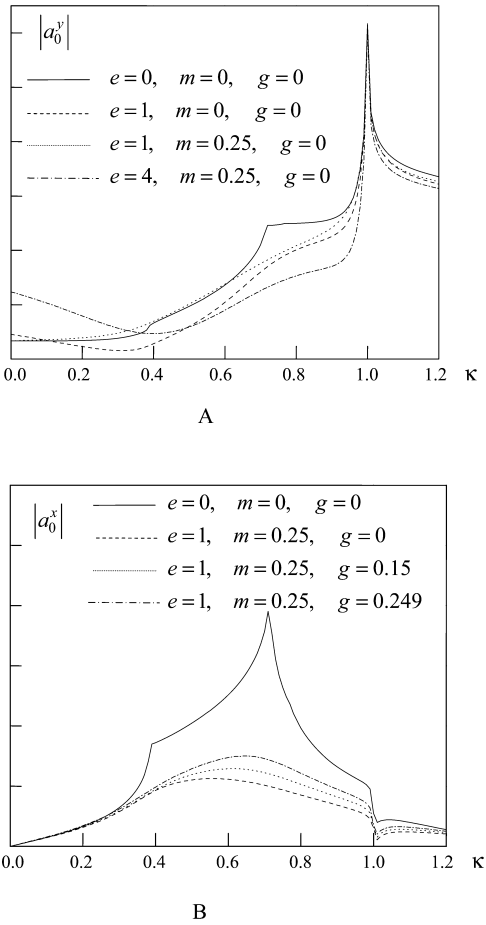

Fig. 2.8 The reflection coefficients versus frequency in the case of (**a**) principal and (**b**) cross-polarizations with damping presence: $\tilde{\varepsilon}_1 = 1$, $\tilde{\mu}_1 = 1$, $\tilde{\varepsilon}_3 = 4 + ie$, $\tilde{\mu}_3 = 1 + im$, $\gamma = 0.6 + ig$, $d/l = 0.5$, $h_1/l = 0.05$

Figure 2.8 shows the frequency dependences of the reflection coefficients in the presence of damping. Presence of losses results in decreasing and smoothing the absolute values of the reflection coefficients. In this case, the effect of losses on the principal-polarized field (Fig. 2.8a) is weaker than that on the cross-polarized field (Fig. 2.8b). The complex-valued chirality parameter stipulates that waves with right- and left-hand circular polarizations propagate with different attenuations since the waves with right- and left-hand circular polarizations have a greater attenuation for $\gamma'' > 0$ and $\gamma'' < 0$, respectively. Therefore, the wave diffraction at the parameter values for which the propagating harmonics are less attenuated is affected by losses to a smaller degree.

Figure 2.9 shows the reflection coefficients as functions of the relative chirality parameter $\eta = \gamma \Big/ \sqrt{\tilde{\varepsilon}_3 \tilde{\mu}_3}$ for $\kappa = \kappa_{31}^{-}(\eta)$ in the case when H-polarized wave is incident. An increase in η leads to an increase in $\kappa_{31}^{-}(\eta)$, and results in the

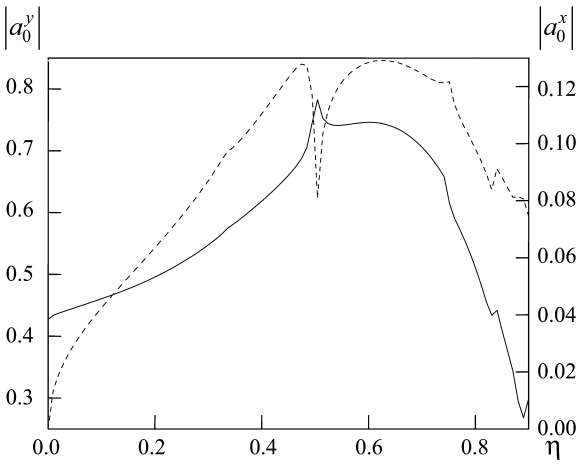

Fig. 2.9 The reflection coefficients as the functions of relative chirality parameter $\eta = \gamma/\sqrt{\tilde{\varepsilon}_3\tilde{\mu}_3}$ for $\kappa = \kappa_{31}^-$: the *solid* and the *dashed curves* refer to the *left* and *right* vertical axes, respectively; $\tilde{\varepsilon}_1 = 1$, $\tilde{\mu}_1 = 1$, $\tilde{\varepsilon}_3 = 4$, $\tilde{\mu}_3 = 1$, $d/l = 0.5$, $h_1/l = 0.05$

transition to the short-wavelength range where the considered reflection coefficient of principal polarization $|a_0^y|$ is generally increasing. The amplitude $|a_0^x|$ of the cross-polarized field caused by the chiral medium is increasing monotonically with increasing η in the single-wave region of the nonchiral half-space ($\kappa < \kappa_{11}$). The reflection coefficients $|a_0^{x,y}|$ exhibit distinctive features at the points of appearance of new propagating harmonics, i.e., under the condition $\kappa_{31}^-(\eta) = \kappa_{1n}$ (see Fig. 2.9).

Figure 2.10 shows the reflection coefficient of the cross-polarized field as function of the grating transparency $\Theta = d/l$ for the case when an *H*-polarized wave is incident. If $\kappa < \kappa_{11}$ and $|\Gamma_1^1| h_1 < 1$, then the excitation of the cross-polarized field is related to the existence of the higher-order spatial harmonics of the grating. In

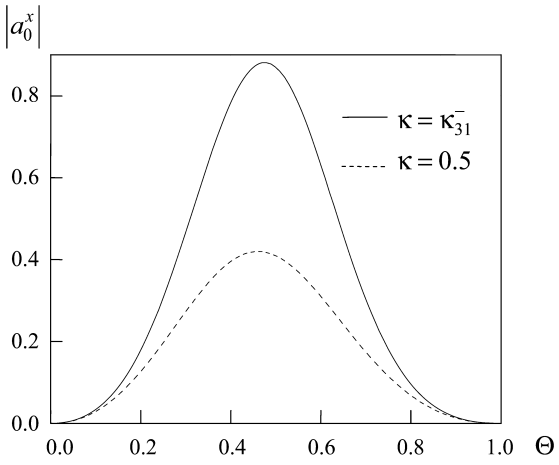

Fig. 2.10 The reflection coefficients versus the grating transparency $\Theta = d/l$ in the cross-polarization case: $\tilde{\varepsilon}_1 = 1$, $\tilde{\mu}_1 = 1$, $\tilde{\varepsilon}_3 = 4$, $\tilde{\mu}_3 = 1$, $\gamma = 0.6$, $h_1/l = 0.05$

this situation, the value of $|a_0^x|$ has a maximum if $\Theta = 0.5$ since this coefficient is mainly determined by the spatial harmonic of order $n = 1$, whose amplitude has a maximum if $\Theta = 0.5$ [45].

2.4.6 Strip Grating with Layered Medium

Consider the diffraction problem for the layered structure composed of a strip grating, a magnetodielectric layer, a chiral layer, and a screen (see Fig. 2.11). Let the grating lie in the plane $z = h_1$, and a perfectly conducting screen is placed in the plane $z = -h_2$. The domains D_1: $h_1 < z$ and D_2: $0 < z < h_1$ are magnetodielectric with relative permittivities $\tilde{\varepsilon}_1$, $\tilde{\varepsilon}_2$ and permeabilities $\tilde{\mu}_1$, $\tilde{\mu}_2$; the domain D_3: $-h_2 < z < 0$ is a chiral layer with the chirality parameter γ and relative permittivity and permeability $\tilde{\varepsilon}_3$, $\tilde{\mu}_3$.

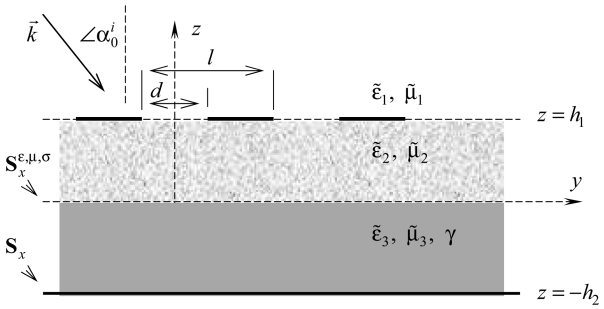

Fig. 2.11 The structure profile and the wave incidence

Suppose, that the monochromatic elliptically polarized plane wave $\vec{E}^i = \vec{E}_0 \exp\left(i\left[\left(\vec{k}\cdot\vec{r}\right) - kt\right]\right)$, $\vec{H}^i = \vec{H}_0 \exp\left(i\left[\left(\vec{k}\cdot\vec{r}\right) - kt\right]\right)$ is obliquely incident on the grating such that

$$\vec{E}_0 = \left\{\tilde{e},\ \rho_1\,\tilde{h}\cos\alpha_0^i\,,\ \rho_1\,\tilde{h}\sin\alpha_0^i\right\} \text{ and } \vec{H}_0 = \left\{\tilde{h},\ -\frac{\tilde{e}}{\rho_1}\ \cos\alpha_0^i,\ -\frac{\tilde{e}}{\rho_1}\ \sin\alpha_0^i\right\}.$$

Here, $\vec{k} = k\sqrt{\tilde{\varepsilon}_1\tilde{\mu}_1}\left\{0, sin\,\alpha_0^i, -cos\,\alpha_0^i\right\}$, α_0^i is the angle between the incident wave vector $\vec{k}$ and the z-axis (see Fig. 2.11); the values $\tilde{e}$, $\tilde{h}$, and ρ_1 have the same meaning as defined above.

As before, we present the diffracted field in the form of a Rayleigh expansion, i.e., an infinite series of the spatial harmonics. In the case of an oblique wave incidence that is under consideration, the propagation constant of the nth harmonic in the y-direction is $\Phi_n = 2\pi l^{-1}\left(n - \kappa\sqrt{\tilde{\varepsilon}_1\tilde{\mu}_1}\sin\alpha_0^i\right)$, and the field components have a form similar to the representation (2.208). For example, in the chiral layer (D_3) the x-components of the field may be represented as:

$$\left\{\begin{matrix}\tilde{E}_x^3\\ \tilde{H}_x^3\, i\rho_3\end{matrix}\right\} = \sum_{n=-\infty}^{\infty}\left[\left(x_n^+\exp\left(i\Gamma_n^+ z\right)+x_n^-\exp\left(-i\Gamma_n^+ z\right)\right)\pm\right. \quad ; \qquad -h_2 < z < 0\,.$$
$$\left.\pm\left(y_n^+\exp\left(i\Gamma_n^- z\right)+y_n^-\exp\left(-i\Gamma_n^- z\right)\right)\right]\exp\left(i\,\Phi_n y\right) \tag{2.229}$$

The boundary conditions at each inhomogeneity planes relates the sought complex amplitudes of the Rayleigh harmonics in all domains of the structure. Also the boundary conditions allow us to obtain two coupled systems of dual series equations to determine the unknown coefficients. The obtained systems being some generalization of systems (2.213) and (2.214) are equivalent to an operator equation of the first kind. It was shown in [123] that these systems can be reduced to

$$\begin{cases}\sum\limits_{n=-\infty\, n\neq 0}^{\infty} X_n\exp\left(in\vartheta\right)+\theta\, X_0=0; & \vartheta_0<|\vartheta|<\pi\\ \sum\limits_{n=-\infty\, n\neq 0}^{\infty}\frac{|n|}{n}X_n\exp\left(in\vartheta\right)+\theta\, X_0=\sum\limits_{n=-\infty}^{\infty} f_n^1\exp\left(in\vartheta\right); & |\vartheta|<\vartheta_0\ ,\\ \sum\limits_{n=-\infty\, n\neq 0}^{\infty}\frac{(-1)^n}{n+\theta}X_n+X_0=0; & \vartheta=\pi\end{cases} \tag{2.230}$$

$$\begin{cases}\sum\limits_{n=-\infty\, n\neq 0}^{\infty} Y_n\exp\left(in\vartheta\right)+\theta\, Y_0=0; & \tilde{\vartheta}_0<|\vartheta|<\pi\\ \sum\limits_{n=-\infty\, n\neq 0}^{\infty}\frac{|n|}{n}Y_n\exp\left(in\vartheta\right)+\theta\, Y_0=\sum\limits_{n=-\infty}^{\infty} f_n^2\exp\left(in\vartheta\right); & |\vartheta|<\tilde{\vartheta}_{00}\ .\\ \sum\limits_{n=-\infty\, n\neq 0}^{\infty}\frac{(-1)^n}{n+\theta}Y_n+Y_0=0; & \vartheta=\pi\end{cases} \tag{2.231}$$

Here, $\tilde{\vartheta}_0=\pi-\vartheta_0$; the value $\theta\in[-0.5;\,0.5)$ is chosen so that $\theta=-m_0+\kappa\,\sin\alpha_0^i$, where m_0 is the nearest integer to $\kappa\,\sin\alpha_0^i$; X_n and Y_n are certain linear combinations of the unknowns x_n^-, y_n^- which are the Fourier coefficients describing the complex amplitudes of the nth order spatial spectrum harmonics in the chiral medium (see (2.229)). The rest of the Fourier coefficients can be expressed in terms of x_n^-, y_n^-; the coefficients $f_n^{1,2}$ are linear combinations of X_n and Y_n.

Using the asymptotic estimates, it is possible to show that

$$f_n^{1,2}\underset{|n|\to\infty}{=}\sigma_n^{1,2}n^{-2}+O\left(\exp\left(-\sigma\,|n|\right)\right),$$

where $\sigma\approx 4\pi\left(h_1/l\right)>0$, and the values $\sigma_n^{1,2}$ satisfy the conditions $\sum\limits_{n=-\infty}^{\infty}\left|\sigma_n^{1,2}\right|^2<\infty$. These representations show that the series in the right-hand sides of (2.230) and (2.231) are uniformly and rapidly convergent series. So for the given problem the singularities, which correspond to the principal part of the operator of

the problem, have been isolated on the left-hand sides of the equations. The obtained functional systems are coupled only through the right-hand sides.

In the form (2.230) and (2.231), the systems are equivalent to the well-known scalar Riemann–Hilbert problem [45]. The method for its solution allows us to obtain the system of linear algebraic equations

$$\begin{cases} \theta X_0 = \sum\limits_{p=-\infty}^{\infty} V_{0p} \left\{ \alpha_p^0 X_p + \beta_p Y_p \right\} + b_0 \\ X_n = \sum\limits_{p=-\infty}^{\infty} V_{np} \left\{ \alpha_p^n X_p + \beta_p Y_p \right\} + b_n \\ \theta Y_0 = \sum\limits_{p=-\infty}^{\infty} \tilde{V}_{0p} \left\{ \tilde{\alpha}_p X_p + \tilde{\beta}_p^0 Y_p \right\} + \tilde{b}_0 \\ Y_n = \sum\limits_{p=-\infty}^{\infty} \tilde{V}_{np} \left\{ \tilde{\alpha}_p X_p + \tilde{\beta}_p^n Y_p \right\} + \tilde{b}_n \end{cases}, \tag{2.232}$$

where the values V_{np}, $\tilde{V}_{np}$; α_p^n, β_p; and $\tilde{\alpha}_p$, $\tilde{\beta}_p^n$ are given in [123]. From the asymptotic estimates of the coefficients α_p^n, $\tilde{\beta}_p^n = O\left(p^{-2}\right)$ and $\tilde{\alpha}_p$, $\beta_p = O\left(exp\ (-\sigma\,|p|)\right)$, and from the behavior of V_{np}, $\tilde{V}_{np}$ as $|n|$, $|p| \to \infty$ it follows that (2.232) is equivalent to a Fredholm system of the second kind. Such a system can be effectively solved by appropriate truncation to meet any preassigned accuracy.

2.4.7 *Electromagnetic Properties of a Strip Grating with Layered Medium in the Resonant Frequency Range*

The diffraction grating changes the incident field into a superposition of spatial spectrum waves. This superposition consists of a finite number of propagating harmonics and an infinite number of surface harmonics decaying in the z-direction. The mth surface harmonic of the jth domain becomes a propagating wave once the frequency parameter κ is such that $\Gamma_m^j(\kappa) = 0$, $j = 1,2$, and $\Gamma_m^{\pm}(\kappa) = 0$ $(j = 3)$. We denote such value of parameter κ by κ_{jm} for $j = 1,2$, and $\kappa_{3m}^{\pm}$ for the chiral domain $(j = 3)$.

Due to the presence of the grating, different harmonics from all domains can interact with each other, and an energy redistribution between harmonics takes place. For certain values of the structure parameters, significant energy redistribution may be achieved, in which the field of one polarization dominates over the field of other polarizations. Such essential energy redistribution is caused by the resonant interaction of harmonics in all domains of the structure.

The far field of the structure is represented as a sum of a finite number of propagating harmonics. Let us introduce the efficiencies in the n-order of the spectrum R_n^x, R_n^y, determining the relative fraction of scattered energy density that is spread from the structure to the upper half-space by propagating harmonics of nth order that has the wave vector $\vec{k}_n^1 = \left\{0, \Phi_n, \Gamma_n^1\right\}$. The superscript x corresponds to the E-polarized field and the superscript y to the H-polarized field.

Our interest is focused on the diffraction properties associated with the conversion of the incident field of principal polarization into the cross-polarized reflected field. Also the phenomenon of nearly total transformation of an elliptically polarized incident wave into a linearly polarized reflected wave is investigated. The efficiency $R_n^{x,y}$ as a function of the frequency parameter κ and the relative thickness of the chiral layer $H_2 = h_2/l$ will be studied numerically in the cases of specular and nonspecular reflections.

2.4.7.1 Specular Reflection

Figure 2.12 presents efficiency $R_0^{x,y}$ in the case of normal incidence of the E-polarized wave. For the upper half-space $h_1 < z$, the single-mode region (when

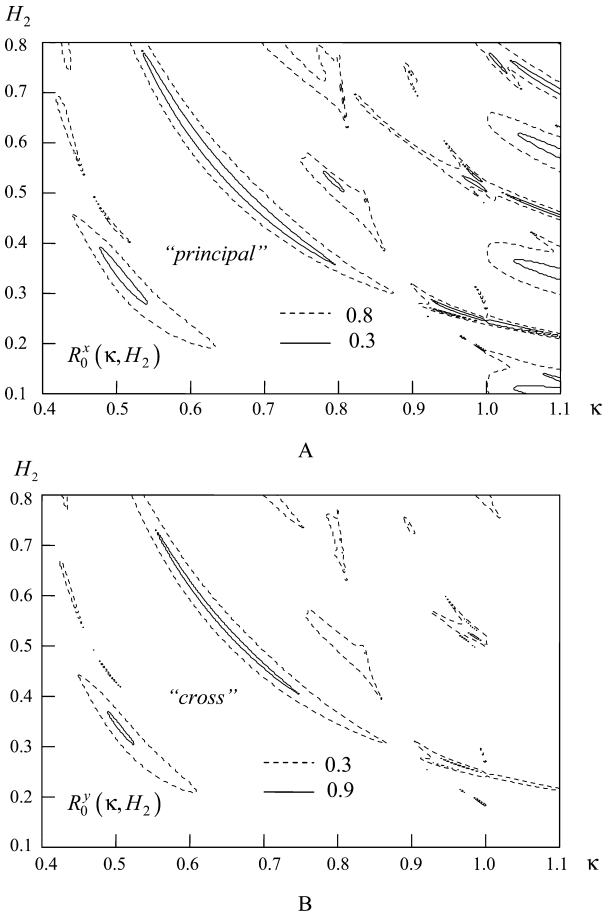

Fig. 2.12 (**a**) The principal and (**b**) cross-polarization efficiency in the normal incidence case: $\tilde{e} = 1.0$, $\tilde{h} = 0$, $\alpha_0^i = 0$, $\tilde{\varepsilon}_1 = 1.0$, $\tilde{\mu}_j = 1.0$, $\tilde{\varepsilon}_2 = \tilde{\varepsilon}_3 = 4.0$, $\eta = 0.3$, $d/l = 0.5$, $h_1/l = 0.03$

$N_1 = 1$) is determined by the condition $-\kappa < \kappa_{11}$, $\kappa_{11}=1$, when $\alpha_0^i = 0$ and $\tilde{\varepsilon}_1 = \tilde{\mu}_1 = 1$. In this region, the minima of efficiency R_0^x of the principal polarization correspond to the maxima of the efficiency R_0^y of the cross-polarization, and the equality $R_0^x + R_0^y = \tilde{e}^2 + \left(\rho_1 \tilde{h}\right)^2$ holds. In the parameter region of existence of the higher propagating harmonics of the first medium, i.e., when $\kappa \geq \kappa_{11}$, this picture is changed because of the energy redistribution between the higher harmonics. The vicinities of frequencies $\kappa_{3n}^{\pm}$ are characterized by effective polarization conversion, which is most pronounced in the interval $\kappa \in [0; \kappa_{11}]$.

In the case of the oblique incidence ($\alpha_0^i \neq 0$) of the *E*-polarized wave, the cross-polarization efficiency R_0^y is presented in Fig. 2.13. A linearly polarized wave normally incident on a chiral medium produces the left- and right-hand circularly

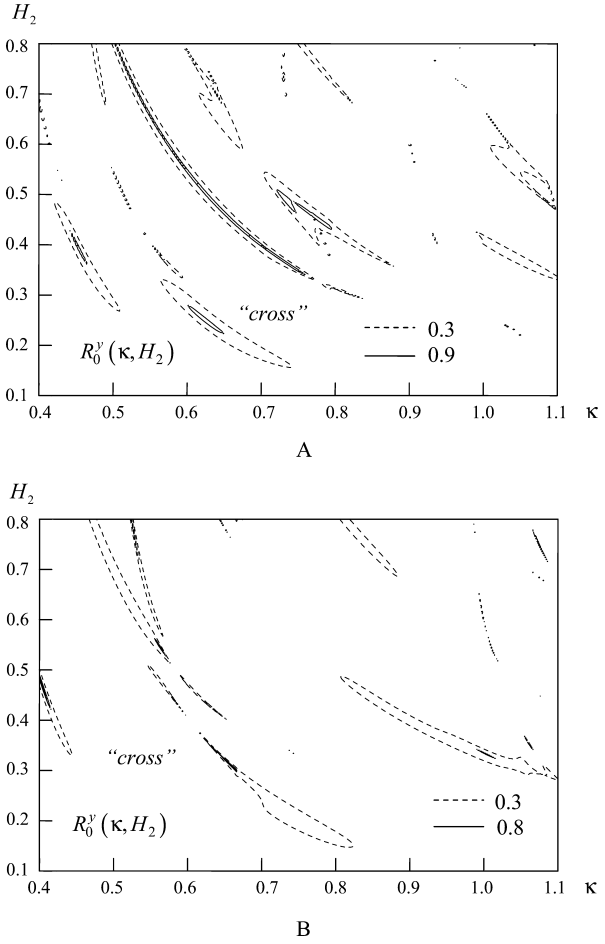

Fig. 2.13 The cross-polarization efficiency in the oblique incidence case: $\tilde{e} = 1.0$, $\tilde{h} = 0$, $\tilde{\varepsilon}_1 = 1.0$, $\tilde{\mu}_j = 1.0$, $\tilde{\varepsilon}_2 = \tilde{\varepsilon}_3 = 4.0$, $\eta = 0.3$, $d/l = 0.5$, $h_1/l = 0.03$, (**a**) $\alpha_0^i = 15°$ and (**b**) $\alpha_0^i = 30°$

polarized waves in it. For normal incidence, they propagate in the same direction as the incident wave, and their superposition would be a linear-polarized wave, with the rotation of polarization plane as the propagation proceeds inside the chiral medium. In the case of oblique incidence, the circularly polarized waves propagate in the different directions, and their superposition is not a linearly polarized wave. In the case of normal incidence, the nth and $(-n)$th harmonics appear at the same frequency. But they do not behave like that in the case of the oblique incidence. As α_0^i increases, the points of appearance of the higher harmonics move away from $\kappa_{jn} = \kappa_{j(-n)}$, $j = 1,2$, and $\kappa_{3n}^{\pm} = \kappa_{3(-n)}^{\pm}$: to the left for the positive harmonics and to the right for the negative. The phase velocities of the plus and minus nth harmonics are different when $\alpha_0^i \neq 0$. Hence the resonances split, and their number is doubled. The splitting is most evident at small angles. Since at the oblique incidence, the higher harmonics of the chiral medium appear before those at $\alpha_0^i = 0$; the polarization conversion region extends along κ to the left (to the low frequency region) as α_0^i grows. The most broadband conversion is observed at $\alpha_0^i = 0$. The efficiency in the zeroth order of spectrum for the cross-polarization is the same, whether an E- or H-polarized wave is incident.

The performed numerical analysis [125] shows that the incident linearly polarized wave can be nearly completely converted into the specularly reflected wave of cross-polarization almost at any incident angle α_0^i.

The combination of the nth propagating harmonics of E- and H-polarization generally gives an elliptically polarized wave. Now our concern will be with the diffraction features associated with the change of the incident elliptically polarized wave into a specularly reflected zero-order harmonic of linear (E- or H-) polarization. The value $\Delta R_0 = R_0^x - R_0^y$ as a function of the structure parameters will be considered. Let the energy density of the incident elliptically polarized wave, which is proportional to $\tilde{e}^2 + \left(\rho_1 \tilde{h}\right)^2$, equal 100%. Thus, when $\Delta R_0 = 100\%$, the total transformation from an incident elliptically polarized wave into a specularly reflected zero-order harmonic of linear E-polarization with the energy density 100% occurs. Similarly, $\Delta R_0 = -100\%$ means a total transformation into an H-polarized wave with the density 100%. Thus, the value ΔR_0 measures the efficiency of elliptical to linear polarization transformation.

The complex amplitudes $\tilde{e}$, $\tilde{h}$ define a character of elliptical polarization of incident wave. For example, if $|\tilde{e}| = \left|\rho_1 \tilde{h}\right|$ and $\delta\phi = \arg\left(\rho_1 \tilde{h} \Big/ \tilde{e}\right) = \pm\pi/2$, the resultant is a right-handed or left-handed circularly polarized incident wave; when $\tilde{e} = 0$ or $\tilde{h} = 0$, then the incident wave, respectively, has linear H- or E-polarization.

The value ΔR_0 as a function of κ and $H_2 = h_2/l$ for the different relations of the E- and H-polarized field components in three incident wave of elliptical polarization is presented in Fig. 2.14. The domains of high-purity polarization transformation, in which $|\Delta R_0| > 90\%$, may be identified for different polarizations in the incident wave [124]. The domains of transformation into E- and H-polarized specularly reflected waves are situated close to each other, and their extent depends on the content of E- and H-polarized field components in the incident wave. These domains

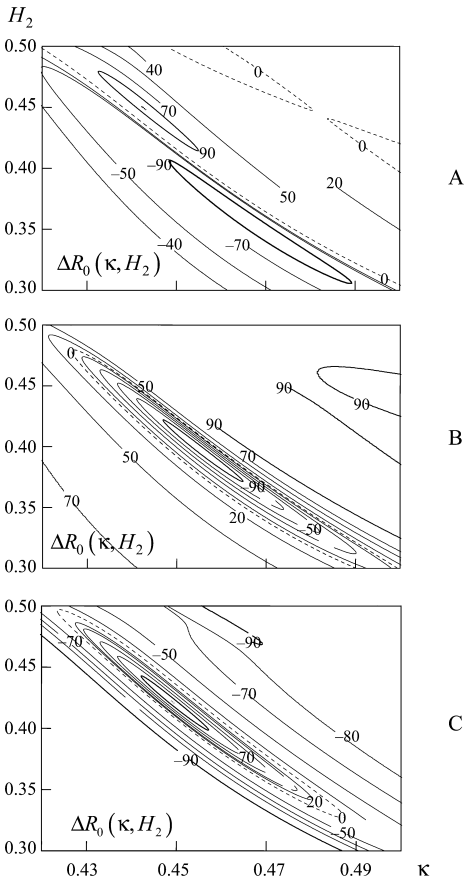

Fig. 2.14 The polarization transformation efficiency ΔR_0 versus κ and H_2 for different polarizations of the incident wave: $\tilde{\varepsilon}_1 = 1.0$, $\tilde{\mu}_j = 1.0$, $\tilde{\varepsilon}_2 = \tilde{\varepsilon}_3 = 4.0$, $\eta = 0.3$, $d/l = 0.5$, $h_1/l = 0.015$, $\alpha_0^i = 15°$, $\delta\phi = -\pi/2$; (**a**) $|\tilde{e}| = \left|\rho_1 \tilde{h}\right|$; (**b**) $|\tilde{e}| = 4\left|\rho_1 \tilde{h}\right|$; and (**c**) $4|\tilde{e}| = \left|\rho_1 \tilde{h}\right|$

as a whole are rather wide and their location depends on the elliptical polarization parameters of the incident wave.

When the efficiency of elliptical to linear polarization transformation does not take extreme values ($\Delta R_0 \neq \pm 100\%$, i.e., the scattered field has both *E*- and *H*-polarized components), a wave of some elliptical polarization is specularly reflected from the structure. Its elliptical polarization may be described by the Stokes parameters [134]. These parameters for the reflected elliptically polarized wave of zero order may be expressed in terms of ΔR_0 and the phase difference ΔF_0 between the zero-order harmonics of *E*- and *H*-polarizations.

The efficiency of the polarization transformation for different incident wave angles is illustrated in Fig. 2.15. Nearly total polarization transformation ($|\Delta R_0| > 97\%$) is seen to take place in a wide range $\left(\Delta\alpha_0^i \approx 20°\right)$ of incident wave angles. Considering the values of ΔR_0 and ΔF_0, one can analyze how the reflected field polarization depends on frequency.

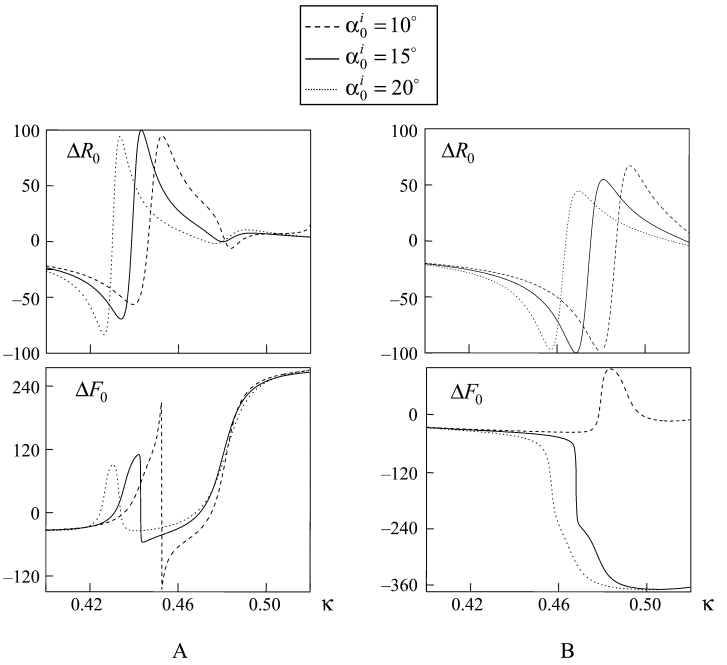

Fig. 2.15 The polarization transformation efficiency ΔR_0 and the phase difference ΔF_0 versus κ for different incident angles: $\tilde{\varepsilon}_1 = 1.0$, $\tilde{\mu}_j = 1.0$, $\tilde{\varepsilon}_2 = \tilde{\varepsilon}_3 = 4.0$, $\eta = 0.3$, $d/l = 0.5$, $h_1/l = 0.015$, $|\tilde{e}| = \left|\rho_1 \tilde{h}\right|$, $\delta\phi = -\pi/2$; (**a**) $H_2 = 0.448$; and (**b**) $H_2 = 0.354$

The dependence of the transformation of the elliptical to linear polarization on geometrical and constitutive parameters of the considered structure was studied. It was found that the polarization transformation might be effectively controlled by an appropriate choice of the structure parameters. For instance, a small decrease of the magnetodielectric layer thickness increases the polarization transformation bandwidth, and a change of the grating slot width allows frequency tuning.

2.4.7.2 Nonspecular Reflection

The information about the direction of the wave vector $\vec{k}_n^1$ allows us to define a difference between the angles of the primary wave arrival and the secondary nth harmonic departure. Given the angle difference, we can specify the κ to α_0^i relationship. In particular, from the condition $\vec{k}_n^1 = -\vec{k}$, we derive the relation

$$\alpha_0^i = -arc\,sin\left(n/2\kappa_1\right),$$

which defines the autocollimation reflection regime of the nth spatial harmonic. In the regime, the nth wave of the upper half-space propagates in the direction opposite

to the primary wave, that is, $\alpha_0^i = \alpha_n$, where α_n is the nth harmonic angle of propagation. An energy concentration in this nth wave may be achieved by optimizing the structure parameters.

Denote by N_j the number of the propagating waves in jth domain harmonics with different propagation constants. The scattering regime can be characterized by the vector $N(\kappa) = \{N_1, N_2, N_3\}$.

Further on, nonspecular reflection accompanied by polarization conversion will be traced [127] as applied to the minus fist propagating harmonic with the wave vector $\vec{k}_{-1}^{1} = \left\{0, \Phi_{-1}, \Gamma_{-1}^{1}\right\}$.

For an incident H-polarized wave, the cross-polarization efficiency R_{-1}^{x} in the autocollimation regime is illustrated in Figs. 2.4a and 2.16. As seen, within $1.283 < \kappa < 1.289$ (which matches $22°56' > \alpha_{-1} > 22°50'$) and $0.760 < H_2 < 0.767$, there exists a zone where the efficiency for cross-polarization exceeds 0.9. The R_{-1}^{x} maximum reaches 0.933, it is found to be at $\kappa = 1.285$ ($\alpha_{-1} = 22°54'$) and $H_2 = 0.765$. This effect takes place in the frequency zone specified by $N(\kappa) = \{2,6,9\}$. A similar regime can be also observed for the E-polarized wave incidence. The autocollimation regime with no polarization conversion may have both explicit and implicit resonance character. But the autocollimation regime with the polarization conversion has sharp resonances.

The excitation of the structure at $\alpha_0^i = 87°$ when the incident H-polarized wave nearly skims the structure is illustrated in Figs. 2.4b and 2.17a. In this regime, one observes a quasi-complete conversion of the incident, nearly surface-parallel wave into the $n = -1$ cross-polarized harmonic propagating at $\alpha_{-1} = 8°12'$. The telescopicity coefficient ($r_t = \cos\alpha_{-1} / \cos\alpha_0^i$) amounts to 18.925. The maxima of R_{-1}^{x} is 0.99 at $\kappa = 0.876$ and $H_2 = 0.313$. The zone of this effect at a level of $R_{-1}^{x} > 0.9$

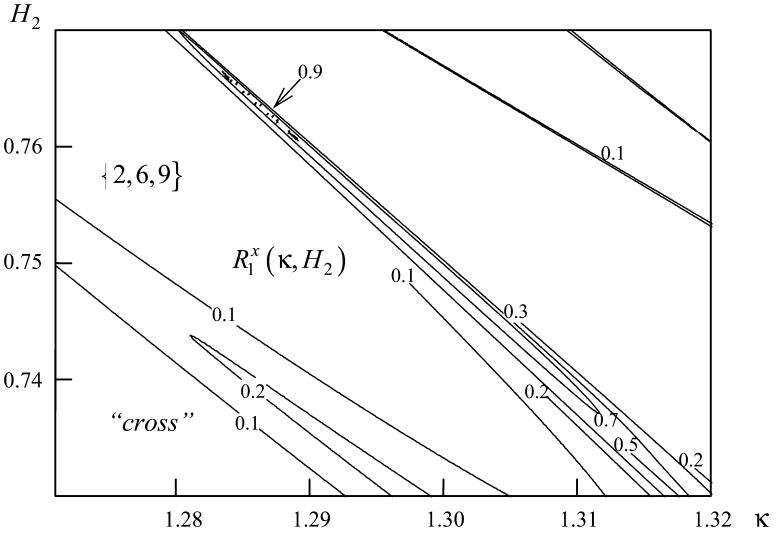

Fig. 2.16 The cross-polarization efficiency in the autocollimation regime: $\tilde{e} = 0$, $\rho_1 \tilde{h} = 1.0$, $\alpha_0^i = -\arcsin(1\ 2\kappa)$, $\tilde{\varepsilon}_1 = 1.0$, $\tilde{\mu}_j = 1.0$, $\tilde{\varepsilon}_2 = \tilde{\varepsilon}_3 = 4.0$, $\eta = 0.3$, $d/l = 0.448$, $h_1/l = 0.015$

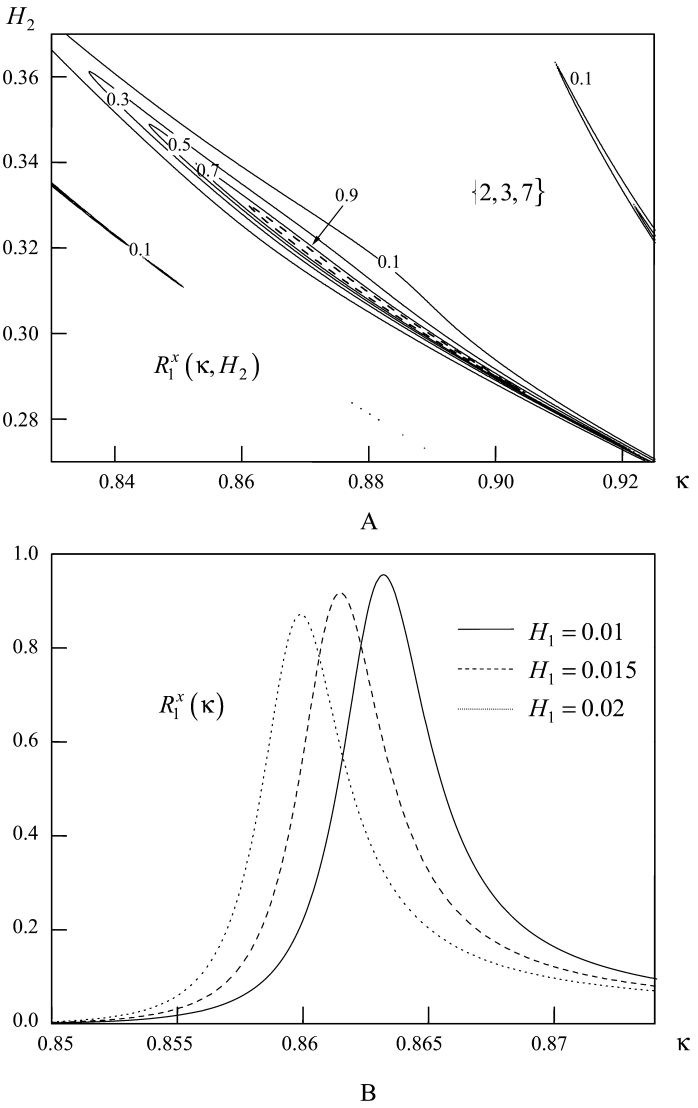

Fig. 2.17 The cross-polarization efficiency in enhanced-telescopicity regime: $\tilde{e} = 0$, $\rho_1 \tilde{h} = 1.0$, $\alpha_0^i = 87°$, $\tilde{\varepsilon}_1 = 1.0$, $\tilde{\mu}_j = 1.0$, $\tilde{\varepsilon}_2 = \tilde{\varepsilon}_3 = 4.0$, $\eta = 0.3$, $d/l = 0.9$, (**a**) $H_1 = h_1/l = 0.015$, and (**b**) $H_2 = 0.313$

with the telescopicity coefficient r_t from 18.827 to 19.009 lies within $0.853 < \kappa < 0.904$ and $0.287 < H_2 < 0.340$. In this case, the number of the harmonics propagating in the media is {2,3,7}. For the *E*-polarized wave incidence, the telescopicity regime has not been found.

The broadband property of the regimes of polarization transformation is effectively controlled by the distance h_1 ($H_1 = h_1/l$) between the grating and the chiral layer (see, for example, Fig. 2.17b). The value of this distance defines the electromagnetic coupling between the grating and the chiral layer via the higher harmonics. As h_1 increases, the higher surface harmonics of the grating cannot reach the chiral layer. Only when h_1 is small, such that $\left|\Gamma_1^2 h_1\right| \ll 1$, the higher harmonics localized near the grating are able to participate in the energy transport and redistribution actions essential for the discussed processes. In this case, the magnetodielectric layer thickness is too small ($h_1 \ll \lambda$) to have any valuable effect on the location of the considered regimes in the plane κ, H_2. As h_1 increases, the grating to chiral layer coupling weakens, the quality of the resonance effects goes up, and the zones of existence of the effects shrink. Thus, the broadband property of the regime can be effectively controlled by small h_1 variations.

The phenomenon of polarization transformation is caused by the presence of the chiral medium. The discussed structure can be considered as an open resonator where the grating and the screen act as the mirrors and the chiral and dielectric layers are the resonator fillings. On the one hand, being a periodical inhomogeneity, the grating converts the incident wave into a superposition of an infinite number of spatial harmonics and thus excites higher order oscillations in the resonator layers. On the other hand, the grating makes different oscillations interact with each other and so establishes electromagnetic coupling between different Floquet harmonics both inside and outside the resonator.

Due to the circular polarization of a chiral medium eigenwaves, the *E*- and *H*-polarized waves are coupled in the chiral layer, and that makes possible the polarization transformation. At a given frequency and with a suitable choice of the structure parameters, the wave interference redistributes the energy between the propagating harmonics so that the discussed regimes of polarization transformation occur. Effective polarization transformation occurs when the number of the harmonics propagating in the "resonator layers" is more than in free space. This phenomenon is of resonance character, and it is a response to the oscillatory excitations which are close to the structure eigenmodes that are described in [135].

2.5 Resonant Scattering of Electromagnetic Waves by Gratings and Interfaces Between Anisotropic Media and Metamaterials

This section is concerned with the boundary value diffraction problem of a strip grating located on different media interfaces: anisotropic dielectric, ferrite, metamaterial, etc. The solution strategy begins with the partial domain (sewing) method to reduce the initial boundary value problem in terms of Helmholtz (Maxwell's) equations to dual series equations. Owing to the regularization theory of dual series equations outlined in Section 2.2, we arrive at an infinite system of linear algebraic equations of the second kind solvable by truncation to any accuracy desired.

Examples illustrating the computation of various physical characteristics (transition and reflection coefficients, eigenfrequencies, diffraction fields, etc.) are given. For more details about the processes of the electromagnetic wave interaction with a strip grating located on a medium interface, we refer to the original papers [18, 136–148].

2.5.1 Resonant Wave Scattering by a Strip Grating Loaded with a Metamaterial Layer

The knowledge of characteristic features of wave processes in metamaterial-loaded open structures (open resonators and waveguides, diffraction gratings, etc.) will lend us fresh opportunities in forming new physical principles of electromagnetic wave generation, amplification, and channeling. A very important stage is explorations into resonance phenomena occurring when monochromatic electromagnetic waves interact with single-periodic metamaterial-loaded structures. The present section is concerned with resonant effects arising during the electromagnetic wave scattering by a strip grating backed by a metamaterial layer such that its effective permittivity depends on the excitation wave frequency. It is shown that in the frequency region where the real part of the metamaterial effective permittivity takes on negative values, the open structure of this kind has an infinite number of complex eigenfrequencies with a finite accumulation point. These frequencies match eigenoscillations whose amplitudes decay exponentially with time. When the frequency of the monochromatic linearly polarized incident wave coincides with the real part of one of the eigenfrequencies of the structure, effects of nearly total reflection and transition of the wave energy arise.

The process of monochromatic plane-wave interaction with a strip grating located on a metamaterial surface will be modeled in terms of the following boundary value problem:

Let the layer $-h < z < 0$ (Fig. 2.18) be filled with some isotropic metamaterial whose effective permittivity depends on frequency as follows

$$\tilde{\varepsilon}(\omega) = 1 - \frac{\omega_p^2}{\omega(\omega + i\nu)}, \tag{2.233}$$

where $\omega = kc$ is the circular frequency, $k = 2\pi/\lambda$, c and λ are the velocity of light and wavelength in a vacuum, ω_p is the characteristic frequency established by the parameters of the metamaterial constituents, and $\nu \geq 0$ is the frequency responsible for the losses. The permeability is $\mu = 1$. The metamaterial boundary ($z = 0$) supports an x-infinite and x-homogeneous perfectly conducting strip grating with d-wide grooves and a period l (see Fig. 2.18). We assume that the excitation wave and the diffraction field are also x-independent. The time dependence is $\exp(-ikt)$. From the half-space $z > 0$ and along the z-axis, an H-polarized unit-amplitude plane electromagnetic wave

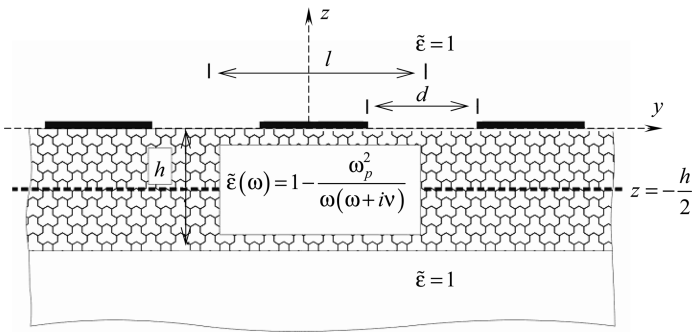

Fig. 2.18 The problem geometry

$$\tilde{H}_x^i = \mathrm{e}^{-ikz}, \qquad \tilde{E}_y^i = \mathrm{e}^{-ikz}, \qquad \tilde{E}_x^i = \tilde{E}_z^i = \tilde{H}_y^i = \tilde{H}_z^i = 0$$

is incident.

The diffraction field $\left\{\vec{E}^s, \vec{H}^s\right\}$ satisfies the homogeneous system of Maxwell's equations and satisfies the Meixner condition, radiation condition at infinity ($z \to \pm\infty$), periodicity condition, boundary condition on perfectly conducting grating strips, and the conjugation condition on the metamaterial surface. Under these assumptions, the diffraction field $\left\{\vec{E}^s, \vec{H}^s\right\}$ is governed by the unique nonzero component $\tilde{H}_x^s$ of the magnetic field as follows:

$$\tilde{E}_y^s = -\frac{1}{ik\tilde{\varepsilon}} \frac{\partial \tilde{H}_x^s}{\partial z}, \qquad \tilde{E}_z^s = \frac{1}{ik\tilde{\varepsilon}} \frac{\partial \tilde{H}_x^s}{\partial y}.$$

The other components of the field $\left\{\vec{E}^s, \vec{H}^s\right\}$ vanish, suggesting that the diffraction field is H-polarized.

Introduce the function $\tilde{U}(g,k)$, $g = \{y, z\}$, coinciding with the magnetic component of the total field $\tilde{H}_x^i + \tilde{H}_x^s$. As follows from Maxwell's equations, everywhere but on the grating strips and the metamaterial surface this function satisfies the Helmholtz equation

$$\Delta_{y,z}\tilde{U}(g,k) + k^2(z)\,\tilde{U}(g,k) = 0; \qquad k^2(z) = \begin{cases} k^2; & z > 0 \quad \text{and} \quad z < -h \\ k^2\tilde{\varepsilon}; & -h < z < 0 \end{cases}. \tag{2.234}$$

In addition, the $\tilde{U}(g,k)$ function is periodic with period l along the y-axis and meets the radiation condition in the half-spaces $z > 0$ and $z < -h$. The functions $\tilde{U}(g,k)$ and $(k(z))^{-2}\,\partial\tilde{U}(g,k)/\partial z$ are required to be continuous across the grating slots $\left\{g\colon\ z = 0,\ \left|2\pi y l^{-1} + n\right| > \pi\left(1 - dl^{-1}\right);\ \ n = 0, \pm 1, \pm 2, \ldots.\right\}$ and across the interface between the metamaterial and the free space at $z = -h$. On the grating strips $\left\{g\colon\ z = 0,\ \left|2\pi y l^{-1} + n\right| < \pi\left(1 - dl^{-1}\right);\ \ n = 0, \pm 1, \pm 2, \ldots.\right\}$, they satisfy the boundary conditions

$$\left.\frac{\partial \tilde{U}(g,k)}{\partial z}\right|_{z=0+0}=0, \qquad \left.\frac{\partial \tilde{U}(g,k)}{\partial z}\right|_{z=0-0}=0. \tag{2.235}$$

On this basis, the sought function $\tilde{U}(g,k)$ can be expressed via its Fourier series in the Y-variable in the three domains: the half-spaces $\mathbf{A}$ ($z>0$) and $\mathbf{B}$ ($z<-h$) and the layer $-h<z<0$, taking the appearance

$$\tilde{U}(g,k)=\begin{cases} \mathrm{e}^{-ikz}+\sum\limits_{n=-\infty}^{\infty} R_{n0}^{\mathbf{AA}}\mathrm{e}^{i(\Phi_n y+\Gamma_{1n}z)}; & z>0 \\ \sum\limits_{n=-\infty}^{\infty} \mathrm{e}^{i\Phi_n y}\left(C_{1n}\mathrm{e}^{i\Gamma_{2n}(z+h)}+C_{2n}\mathrm{e}^{-i\Gamma_{2n}z}\right); & -h<z<0 \\ \sum\limits_{n=-\infty}^{\infty} T_{n0}^{\mathbf{BA}}\mathrm{e}^{i(\Phi_n y-\Gamma_{1n}(z+h))}; & z<-h \end{cases}. \tag{2.236}$$

Here $\Gamma_{1n}=\sqrt{k^2-\Phi_n^2}$, $\Gamma_{2n}=\sqrt{k^2\tilde{\varepsilon}-\Phi_n^2}$, $\Phi_n=2\pi n/l$. The root branches are chosen via the radiation condition (cf. Section 1.1.4) to have $k\mathrm{Re}\Gamma_{1n}\geq 0$, $\mathrm{Im}\Gamma_{1n}\geq 0$. Notice that any branch of the root Γ_{2n} can be adopted. For definiteness sake, let $k\mathrm{Re}\Gamma_{2n}\geq 0$, $\mathrm{Im}\Gamma_{2n}\geq 0$.

Now we will reduce the boundary value diffraction problem to dual series equations for the unknown coefficients $\left\{R_{n0}^{\mathbf{AA}}\right\}_{n=-\infty}^{\infty}$ of the $\tilde{U}(g,k)$ expansion into the Fourier series in the half-space $z>0$ [see (2.236)]. Indeed, using (2.236) and applying the conjugation conditions on the metamaterial boundaries yields the relationships between the coefficients $\left\{C_{pn}\right\}_{n=-\infty}^{\infty}$, $p=1,2$, $\left\{T_{n0}^{\mathbf{BA}}\right\}_{n=-\infty}^{\infty}$, and $\left\{R_{n0}^{\mathbf{AA}}\right\}_{n=-\infty}^{\infty}$ in the form

$$T_{n0}^{\mathbf{BA}}=\frac{2\tilde{\varepsilon}\Gamma_{1n}\exp(i\Gamma_{2n}h)}{\Gamma_n}\left(R_{n0}^{\mathbf{AA}}-\delta_0^n\right). \tag{2.237}$$

$$C_{1n}=\frac{\tilde{\varepsilon}\Gamma_{1n}(\Gamma_{2n}-\tilde{\varepsilon}\Gamma_{1n})}{\Gamma_{2n}\Gamma_n}\left(R_{n0}^{\mathbf{AA}}-\delta_0^n\right) \tag{2.238}$$

$$C_{2n}=\frac{\tilde{\varepsilon}\Gamma_{1n}(\Gamma_{2n}+\tilde{\varepsilon}\Gamma_{1n})}{\Gamma_{2n}\Gamma_n}\left(R_{n0}^{\mathbf{AA}}-\delta_0^n\right) \tag{2.239}$$

Here, $\Gamma_n=\exp(i2\Gamma_{2n}h)(\Gamma_{2n}-\tilde{\varepsilon}\Gamma_{1n})-\Gamma_{2n}-\tilde{\varepsilon}\Gamma_{1n}$ and δ_m^n is the Kronecker delta.

Satisfying the strip and slot boundary conditions yields

$$1+\sum_{n=-\infty}^{\infty} R_{n0}^{\mathbf{AA}}\mathrm{e}^{i\Phi_n y}=\sum_{n=-\infty}^{+\infty}\left(C_{1n}\mathrm{e}^{i2\Gamma_{2n}h}+C_{2n}\right)\mathrm{e}^{i\Phi_n y}; \qquad |y|>\frac{l-d}{2}, \tag{2.240}$$

$$k-\sum_{n=-\infty}^{\infty} R_{n0}^{\mathbf{AA}}\Gamma_{1n}\mathrm{e}^{i\Phi_n y}=0; \qquad |y|<\frac{l-d}{2}. \tag{2.241}$$

Having denoted $\vartheta = 2\pi y/l$ and $\vartheta_0 = \pi(1–d/l)$ and substituting (2.238) and (2.239) into (2.240), we finally obtain

$$1 + d_0 + \sum_{n=-\infty}^{\infty} R_{n0}^{\mathbf{AA}} (1 - d_n) \, \mathrm{e}^{in\vartheta} = 0; \qquad |\vartheta| > \vartheta_0, \tag{2.242}$$

$$k - \sum_{n=-\infty}^{\infty} R_{n0}^{\mathbf{AA}} \Gamma_{1n} \mathrm{e}^{in\vartheta} = 0; \qquad |\vartheta| < \vartheta_0, \tag{2.243}$$

where

$$d_n = \frac{\tilde{\varepsilon}\Gamma_{1n}\left[\exp\left(i2\Gamma_{2n}h\right)\left(\Gamma_{2n} - \tilde{\varepsilon}\Gamma_{1n}\right) + \Gamma_{2n} + \tilde{\varepsilon}\Gamma_{1n}\right]}{\Gamma_{2n}\left[\exp\left(i2\Gamma_{2n}h\right)\left(\Gamma_{2n} - \tilde{\varepsilon}\Gamma_{1n}\right) - \Gamma_{2n} - \tilde{\varepsilon}\Gamma_{1n}\right]}. \tag{2.244}$$

Let us demonstrate that equations (2.242) and (2.243) are dual series equations of the same type as equations (2.36) and (2.37) in Section 2.2.2. Represent the coefficients Γ_{1n} and d_n from (2.242) and (2.243) in the form

$$\Gamma_{1n} = i\frac{2\pi}{l} |n| \left(1 + \delta_{1n}\right); \qquad n \neq 0, \tag{2.245}$$

$$d_n = -\tilde{\varepsilon} + \delta_{2n}. \tag{2.246}$$

It is easily seen that as $n \to \pm\infty$, the coefficients δ_{1n} and δ_{2n} are

$$\delta_{1n} = O\left(n^{-2}\right), \qquad \delta_{2n} = O\left(n^{-2}\right). \tag{2.247}$$

Indeed, from (2.245),

$$\delta_{1n} = \frac{l\Gamma_{1n}}{i2\pi\,|n|} - 1 = \sqrt{1 - \frac{\kappa^2}{n^2}} - 1 = -\frac{\kappa^2}{n^2\left(\sqrt{1 - \frac{\kappa^2}{n^2}} + 1\right)} = O\left(n^{-2}\right).$$

Here, $\kappa = lk/2\pi = l/\lambda$. Substitute (2.245) and (2.246) into (2.242) and (2.243). Finally,

$$\sum_{n=-\infty}^{\infty} R_{n0}^{\mathbf{AA}} \mathrm{e}^{in\vartheta} - \sum_{n=-\infty}^{\infty} R_{n0}^{\mathbf{AA}} \frac{\delta_{2n}}{1 + \tilde{\varepsilon}} \mathrm{e}^{in\vartheta} + \frac{1 + d_0}{1 + \tilde{\varepsilon}} = 0; \qquad |\vartheta| > \vartheta_0, \tag{2.248}$$

$$\sum_{n=-\infty}^{\infty} |n| \, R_{n0}^{\mathbf{AA}} \mathrm{e}^{in\vartheta} + \sum_{n=-\infty}^{\infty} R_{n0}^{\mathbf{AA}} \, |n| \, \delta_{1n} \mathrm{e}^{in\vartheta} + i\kappa\left(1 - R_{00}^{\mathbf{AA}}\right) = 0; \qquad |\vartheta| < \vartheta_0. \tag{2.249}$$

To make it clear that equations (2.247) and (2.248) are similar to equations (2.36) and (2.37) in Section 2.2.2, introduce the matrix operators $V = \{V_{mn}\}_{m,n=-\infty}^{\infty}$ and $U = \{U_{mn}\}_{m,n=-\infty}^{\infty}$ by the formulas

$$V_{mn} = |n|\,\delta_{1n}\delta_m^n, \qquad U_{mn} = -\frac{\delta_{2n}}{1+\varepsilon}\delta_m^n, \tag{2.250}$$

and the column vectors $f = \{f_n\}_{n=-\infty}^{\infty}$ and $g = \{g_n\}_{n=-\infty}^{\infty}$; $f_n = -i\kappa\delta_0^n$, $g_n = -\frac{1+d_0}{1+\tilde{\varepsilon}}\delta_0^n$. With these notations, equations (2.248) and (2.249) are written as

$$aR_{00}^{\mathbf{AA}} + \sum_{n=-\infty}^{\infty} R_{n0}^{\mathbf{AA}}\,|n|\,e^{in\vartheta} + \sum_{n=-\infty}^{\infty}\left[(VR)_n - f_n\right]e^{in\vartheta} = 0; \qquad |\vartheta| < \vartheta_0, \tag{2.251}$$

$$\sum_{n=-\infty}^{\infty} R_{n0}^{\mathbf{AA}} e^{in\vartheta} + \sum_{n=-\infty}^{\infty}\left[(UR)_n - g_n\right]e^{in\vartheta} = 0; \qquad |\vartheta| > \vartheta_0, \tag{2.252}$$

where $a = -i\kappa$ and $R = \left\{R_{n0}^{\mathbf{AA}}\right\}_{n=-\infty}^{\infty}$.

Asymptotical formulas (2.247) suggest that the matrix operators $T^{-1}VT^{-1}$ and TUT^{-1} are compact in the space l_2, and the column vectors f and g are such that $g \in l_2(1), f \in l_2(-1)$ (see definitions for matrix T and space $l_2(\eta)$ in Section 2.2).

Hence the dual series equations (2.251) and (2.252) allow the analytic regularization procedure outlined in Section 2.2.2. The application of this procedure provides the infinite system of linear algebraic equations

$$(1+\tilde{\varepsilon})\,R_{m0}^{\mathbf{AA}} + \sum_{n=-\infty}^{\infty} H_{mn}R_{n0}^{\mathbf{AA}} = b_m; \qquad m = 0, \pm 1, ... \tag{2.253}$$

The matrix $H = \{H_{mn}\}_{m,n=-\infty}^{\infty}$ of this system and its right-hand side $b = \{b_m\}_{m=-\infty}^{\infty}$ are given by the expressions

$$b_m = (1+\tilde{\varepsilon})\begin{cases} \dfrac{1+d_0}{d_0-1} + \dfrac{i\kappa W_0\,(1+\tilde{\varepsilon})}{1-d_0}; & m = 0 \\ -\dfrac{i\kappa V_{m-1}^{-1}}{m}; & m \neq 0 \end{cases}, \tag{2.254}$$

$$H_{mn} = \begin{cases} \dfrac{i\kappa W_0\,(1+\tilde{\varepsilon})^2}{1-d_0}; & m = n = 0 \\ \dfrac{\delta_n\,|n|\,(1+\tilde{\varepsilon})}{(d_0-1)\,n}V_{n-1}^{-1}; & m = 0, \quad n \neq 0 \\ -\dfrac{i\kappa}{m}V_{m-1}^{-1}; & m \neq 0, \quad n = 0 \\ \dfrac{|n|\,\delta_n}{m}V_{m-1}^{n-1}; & m, n \neq 0, \quad m \neq n \\ d_m + \tilde{\varepsilon} + \dfrac{|m|\,\delta_m}{m}V_{m-1}^{m-1}; & m = n, \quad m \neq 0 \end{cases}, \tag{2.255}$$

where $\delta_n = -\delta_{2n} - \delta_{1n}(1+\tilde{\varepsilon})$, and the coefficients W_0, V_{m-1}^{n-1} are calculated in Section 2.2. From the asymptotic formula (2.247), $\delta_n = O(n^{-2})$ as $n \to \pm\infty$. Hence,

based on the results from Section 2.2.2, one finds that the matrix operator H of system (2.253) is compact in the l_2 space.

Thus, with $R = \left\{R_{n0}^{\mathbf{AA}}\right\}_{n=-\infty}^{\infty}$ coming from system (2.253) and using formulas (2.236), (2.237), (2.238), and (2.239), the initial diffraction problem has been solved. Here an important point should be mentioned. For a lossless metamaterial layer ($\nu = 0$), the solution of the initial diffraction problem readily comes from (2.253) for all excitation wave frequencies but $\omega = \omega_p/\sqrt{2}$, which is equivalent to $\tilde{\varepsilon} = -1$. In some sense, this frequency is especial. As $\omega \to \omega_p/\sqrt{2}$, the matrix operator $\left[(\tilde{\varepsilon}+1)E + H\right]$ of system (2.253) becomes compact, having, consequently, no bounded inverse and thus forbidding a direct application of the truncation method to system (2.253). By a solution is meant the limit to which the solution $\left\{R_{n0}^{\mathbf{AA}}\right\}_{n=-\infty}^{\infty}$ of system (2.253) proceeds as the metamaterial becomes lossless, $\nu \to 0$.

Now turn to the spectral problem describing peculiar features of the analytic continuation of the diffraction field to the complex frequency domain. The mathematical formulation of the spectral problem differs from the statement of the diffraction problem. In the first place, the former is independent of the excitation wave. Second, the function $\tilde{U}(g,k)$ in (2.236) forms accounting for the radiation condition is analytically continued from the real-valued frequency domain to the corresponding infinite-sheeted Riemannian surface (see, for instance, Section 1.3). So, the spectral problem of the grating backed by the metamaterial layer with the effective permittivity in (2.233) form is a problem about eigenfrequencies and eigenoscillations bearing an l-periodic dependence on the grating spatial coordinate y. The sought spectral parameter is the wave number k (or normalized frequency $\varkappa = l/\lambda = kl/2\pi$) belonging to the Riemannian surface $\mathbf{K}$ (or $\mathbf{K}_\varkappa$). From this point on, the metamaterial is assumed lossless ($\nu = 0$), its effective permittivity is

$$\varepsilon(\omega) = 1 - \frac{\omega_p^2}{\omega^2},$$

and the spectral parameter $\varkappa$ belongs to the first – physical – sheet of the Riemannian surface $\mathbf{K}_\varkappa$ (see Section 1.3).

The discussed spectral problem is equivalent to equation (2.253) with $b = 0$ (the excitation wave is absent), the matrix elements in the (2.254) form are considered as a function of the spectral parameter $\varkappa$ varying on the physical sheet of the surface $\mathbf{K}_\varkappa$. The problem of the kind means finding the characteristic numbers and the eigenvectors of the operator-function $E + B(\varkappa)$, where $B(\varkappa) = (1+\tilde{\varepsilon})^{-1}H(\varkappa)$. The results from Section 1.3 let us establish that the matrix operator $B(\varkappa)$ is a finite-meromorphic kernel operator-function of the complex variable $\varkappa$ on the physical sheet of the Riemannian surface excepting the points $\varkappa = 0$ and $\varkappa = \pm\varkappa_p/\sqrt{2}$ ($\varkappa_p = \omega_p l/2\pi c$) and, also, the branch points $\varkappa_n^{\pm}$:$\Gamma_{1n}(\varkappa_n^{\pm}) = 0$; $n = \pm 1, \pm 2, \ldots$. The poles of the operator-function $E + B(\varkappa)$ coincide with the point $\varkappa = 0$ and the roots of the equations

$$\exp(i2\Gamma_{2n}h)(\Gamma_{2n} - \varepsilon\Gamma_{1n}) - \Gamma_{2n} - \tilde{\varepsilon}\Gamma_{1n} = 0; \qquad n = 1,2,\ldots. \tag{2.256}$$

Then the characteristic numbers and, hence, the eigenfrequencies are roots of the equation

$$\det\left[E + B\left(\kappa\right)\right] = 0, \tag{2.257}$$

where det[...] is the infinite determinant of the operator $E + B(\kappa)$. Evidently the function det[E+$B(\kappa)$] is meromorphic in any bounded domain not carrying the points $\kappa = 0$, $\kappa = \pm\kappa_p/\sqrt{2}$ and the branch points $\kappa = \kappa_n^{\pm}$. Hence the set of the roots of equation (2.257) is nothing more than a denumerable set on the physical sheet of the surface $\mathbf{K}_\kappa$ with probable accumulation points coinciding with either $\kappa = 0$, $\kappa = \pm\kappa_p/\sqrt{2}$, or the poles coming from (2.256).

Consider some qualitative properties of the root set of equation (2.257). Suppose that the grating strips are sufficiently small, $1 - d/l \ll 1$ (at $d/l = 1$ the grating disappears). Represent the operator-function $B(\kappa)$ as a sum of two operator-functions so that $B(\kappa) = B_1(\kappa)$+$B_2(\kappa)$, where $B_1(\kappa) = \left\{\delta_m^n \gamma_m\right\}_{m,n=-\infty}^{\infty}$, $\gamma_0 = 0$, $\gamma_m = \frac{d_m + \tilde{\varepsilon}}{1+\tilde{\varepsilon}}$ for $m \neq 0$. Estimating the values of W_0, V_{m-1}^{n-1} when $d/l \to 1$ (see, e.g., [45]) one finds that the operator-function $B_2(\kappa)$ obeys the condition

$$\|B_2(\kappa)\| < \text{const}\ \sin\left[\pi\left(1 - \frac{d}{l}\right)\right], \tag{2.258}$$

where $\|...\|$ is the norm of the operator-function $B_2(\kappa)$ in l_2. Hence as $d/l \to 1$, the norm of $B_2(\kappa)$ tends to zero in any bounded domain of κ values except for $\kappa = 0$, $\kappa = \pm\kappa_p/\sqrt{2}$ the branch points, and the poles. It is easy to check that the characteristic numbers of the operator-function $E + B_1(\kappa)$ match the roots of the equations

$$\exp\left(i\Gamma_{2n}h\right)\left(\Gamma_{2n} - \tilde{\varepsilon}\Gamma_{1n}\right) \pm \left(\Gamma_{2n} + \tilde{\varepsilon}\Gamma_{1n}\right) = 0; \qquad n = 1,2,... \tag{2.259}$$

Next it can be shown that the κ domain where $\mathrm{Re}(\tilde{\varepsilon}) < 0$ allows real-valued roots of equation (2.259). Figure 2.19 plots results from (2.259) computed for different $n = 1,2,....$ (squares for the plus and circles for the minus). As $n \to \infty$, these roots asymptotically tend to $\kappa = \kappa_p/\sqrt{2}$ (Fig. 2.19, dotted line), indicating that $\kappa = \kappa_p/\sqrt{2}$ is the accumulation point. It is notable that equation (2.259) suggests some metamaterial characteristic frequency $\tilde{\kappa}_p = x_0 l/2\pi h$, where $x_0 \approx 1.325$ satisfies the equation

$$x\mathrm{e}^{-0.5\sqrt{x^2+4}} + 2 - \sqrt{x^2+4} = 0.$$

For $\kappa_p \leq \tilde{\kappa}_p$, some finite number of the roots of equation (2.259) exceed $\kappa_p/\sqrt{2}$ (Fig. 2.19) and for $\kappa_p > \tilde{\kappa}_p$, no one is over $\kappa_p/\sqrt{2}$ (Fig. 2.19b).

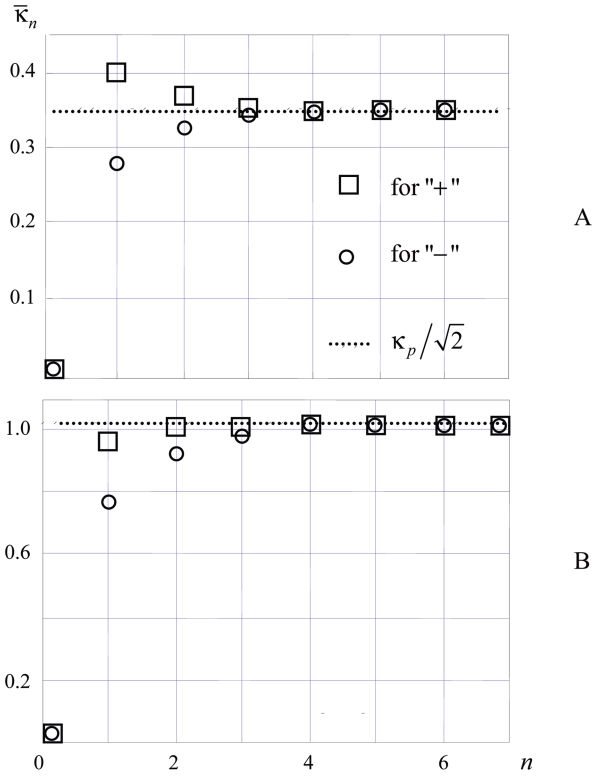

Fig. 2.19 The roots $\bar{\kappa}_n$ of equation (2.259) for different n values: $h/l = (2\pi)^{-1}$, (**a**) $\kappa_p = 0.5$, and (**b**) $\kappa_p = 1.45$

Now let $1–d/l$ be a small number and $\bar{\kappa}_0$ be a characteristic number of the operator-function $E + B_1(\kappa)$, i.e., $\det[E + B_1(\bar{\kappa}_0)] = 0$. Evidently there is a circle with the point $\bar{\kappa}_0$ as center and a radius so small that the operator-function $[E + B_1(\kappa)]^{-1}$ is bounded on the circumference line. Then from (2.257) it follows that if $1–d/l$ is small enough, the inequality

$$\left\| [E + B_1(\kappa)]^{-1} B_2(\kappa) \right\| < 1$$

is true on the circumference line. Through the operator generalization provided by the Rouche theorem [15], one finds that the mentioned circle carries a characteristic number of the operator-function $E + B_1(\kappa) + B_2(\kappa)$, suggesting, at least phenomenologically, that the characteristic numbers of the operator-function $E + B(\kappa)$ and, hence, the characteristic numbers of the examined electrodynamical structure (a grating loaded with a metamaterial layer) have the accumulation point $\kappa = \kappa_p/\sqrt{2}$.

The eigenfrequency computation for $0 < d/l \leq 1$ follows the algebraic scheme outlined below. Let a finite-dimensional matrix operator-function $B_N(\kappa)$ represent

the $N \times N$ truncation of the matrix $B(\kappa)$. In view of the compactness of $B(\kappa)$ for any $\delta > 0$ as small as desired and in any bounded domain of κ (excluding $\kappa = 0, \pm\kappa_p/\sqrt{2}$ and the branch points $\kappa = \kappa_n^{\pm}$), a natural number N exists such that

$$\|B(\kappa) - B_N(\kappa)\| < \delta. \tag{2.260}$$

The eigenfrequencies of the finite-dimensional operator-function $E + B_N(\kappa)$ can be sought as roots of the determinant-function $\det[E + B_N(\kappa)]$. By virtue of (2.260), each solution $\bar{\kappa}_m$ of spectral problem (2.257) is approximated to any desired accuracy by the solution $\bar{\kappa}_m^N$ of the equation $\det[E + B_N(\kappa)] = 0$ provided that N is large enough. Using the compactness property of the operator-function $B(\kappa)$, one easily verifies [11] that the procedure described right above is computationally stable as N rises.

To analyze the solution of the spectral problem (2.257), the domain $\mathrm{Re}(\kappa) > 0$ of the spectral parameter will suffice. From formulas (2.238), we have

$$\det[I - B(\kappa)] = \left(\det\left[E - B(-\kappa^*)\right]\right)^*,$$

where the $*$ indicates complex conjugation. Therefore, if $\bar{\kappa}$ is an eigenfrequency with $\mathrm{Re}(\kappa) > 0$, then $-\bar{\kappa}^*$ is an eigenfrequency with $\mathrm{Re}(\kappa) < 0$ (for details, refer to Section 1.3). From the considered structure symmetry with respect to the plane $y = 0$ (see Fig. 2.18) it follows that there are two classes of eigenoscillations: even and odd with respect to y variable. Besides, when the metal strips of the grating disappear, leaving the metamaterial layer alone, the structure acquires an additional symmetry about the plane $z = -h/2$, thus giving rise to two more solution types: even and odd in the coordinate z about the plane $z = -h/2$. They correspond to the characteristic equations (2.259) with the minus and the plus signs, respectively.

Figures 2.20 and 2.21 illustrate the dependence of the real and imaginary parts of the first three eigenfrequencies $\bar{\kappa}$ on the geometrical parameter d/l (grating slot normalized width). These were obtained by the numerical solution of equation (2.257), with specially designed algorithms and programs. The eigenfrequencies of the oscillations which in the limiting case $d/l = 1$ are symmetric about the plane $z = -h/2$ [minus in equation (2.259)] are shown in Fig. 2.20. The eigenfrequencies of the oscillations asymmetric about the plane $z = -h/2$ [plus in (2.259)] are shown in Fig. 2.21. The solid line plots the eigenfrequencies of oscillations symmetric with respect to the plane $y = 0$, the dashed line is for asymmetric oscillations. Notice that the imaginary parts of the eigenfrequencies of oscillations asymmetric about the plane $y = 0$ practically vanish and are not visible in Figs. 2.20b and 2.21b. The dotted curves in Figs. 2.20a and 2.21a correspond to $\kappa_p/\sqrt{2}$. As seen from Figs. 2.20 and 2.21, for $d/l = 1$ (i.e., the grating is absent), the imaginary parts of eigenfrequencies vanish (the metamaterial layer is lossless, $\nu = 0$).

The real parts of the eigenfrequency oscillations symmetric and asymmetric with respect to the plane $z = -h/2$ for prescribed $\kappa_p = 0.5 < \tilde{\kappa}_p$ are, as shown above, located on different sides of the point $\kappa = \kappa_p/\sqrt{2}$ and match at $d/l = 1$, the corresponding $\bar{\kappa}_n$ values presented in Fig. 2.19a. In Fig. 2.22, one observes the equal

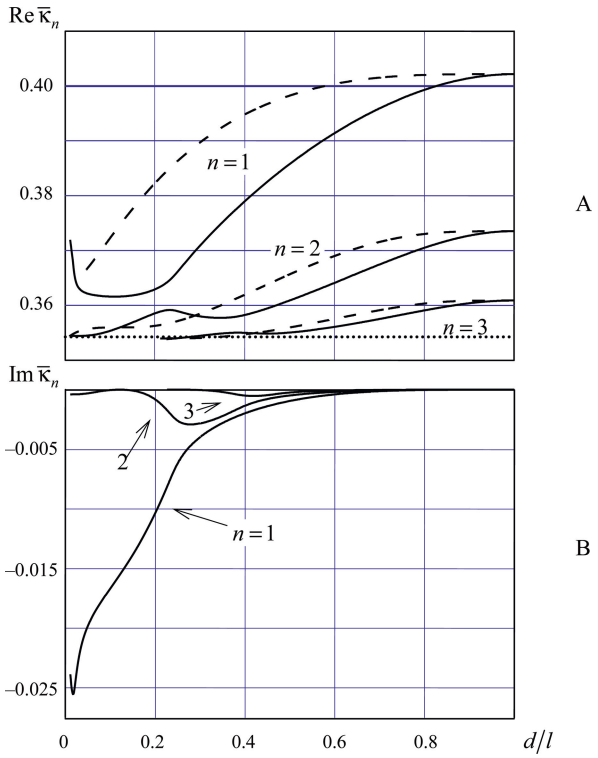

Fig. 2.20 The eigenfrequencies $\bar{\kappa}_n$ versus d/l for oscillations cophasal about $z = -h/2$: (**a**) Real and (**b**) imaginary parts; $\kappa_p = 0.5$, $h/l = (2\pi)^{-1}$

module $\left|\tilde{H}_x\right| = \text{const}$ and the equal phase $\arg\left(\tilde{H}_x\right) = \text{const}$ lines of the unique nonzero component $\tilde{H}_x(y,z)$ of the magnetic field for some eigenoscillations of the grating backed by the metamaterial layer. The oscillation with the eigenfrequency $\bar{\kappa} = 0.36565 - i10^{-12}$ in Fig. 2.22a is asymmetric about the plane $y = 0$ and in phase at $d/l = 1$ with respect to the plane $z = -h/2$ (the same oscillation phase on both interfacial sides of the metamaterial). The oscillation with the eigenfrequency $\bar{\kappa} = 0.35173 - i7.079 \cdot 10^{-5}$ in Fig. 2.22b is symmetric about the plane $y = 0$ and opposite in phase with respect to the plane $z = -h/2$ at $d/l = 1$ validating the above-made division of the examined structure eigenoscillations into classes of symmetry.

Interestingly also that as $d/l \to 1$ (the grating changes into a perfectly conducting plane), the real parts of some eigenfrequencies tend to the poles of the operator-function $E+B(\kappa)$, which are the roots of equation (2.256), the imaginary parts vanishing. This numerical result resists analytic justification because the d/l dependence of the matrix elements [see (2.255)] of the operator-function $H(\kappa)$ and, hence, of $B(\kappa) = (1 + \tilde{\varepsilon})^{-1}H(\kappa)$ is singular at $d/l = 0$.

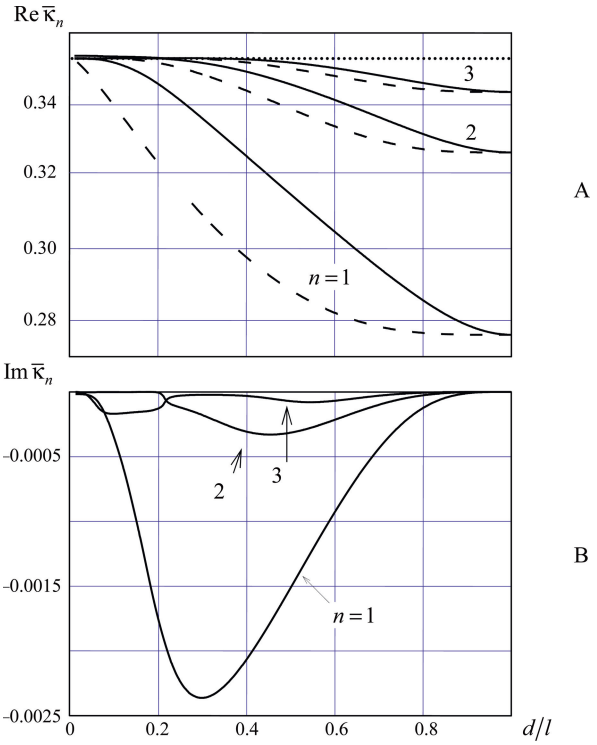

Fig. 2.21 The eigenfrequencies $\bar{\kappa}_n$ versus d/l for oscillations antiphasal about $z = -h/2$: (**a**) Real and (**b**) imaginary parts; $\kappa_p = 0.5$, $h/l = (2\pi)^{-1}$

Next we consider the eigenfrequency behavior as the metamaterial characteristic frequency varies. As the characteristic frequency $\kappa_p \to 0$, the eigenfrequencies of all oscillation types tend to zero (see Fig. 2.23). This is attributed to the fact that the grating has no eigenfrequencies in free space (at $\kappa_p = 0$, the effective permittivity of our metamaterial is $\tilde{\varepsilon} = 1$) [10]. The increase $\kappa_p \to \infty$ leads to different results for eigenfrequencies of different oscillation types. Thus, the real parts of eigenfrequencies corresponding to oscillations opposite in phase with respect to the plane $z = -h/2$ asymptotically tend to the branch point $\kappa_{\pm 1}^{+} = 1$ (see Fig. 2.23a). They asymptotically tend to the line $\mathrm{Re}\bar{\kappa} = \kappa_p/\sqrt{2}$ for oscillations in phase with respect to the plane $z = -h/2$. In this case, for both oscillation types, the imaginary parts of the eigenfrequency tend to zero as $\kappa_p \to \infty$ (see Fig. 2.23b). For other values of the metamaterial layer normalized thickness and the grating slot width, the indicated eigenfrequency behavior persists.

Examine the eigenfrequency behavior as the normalized thickness h/l of the metamaterial layer changes, whereas the grating slot width $d/l = 0.5$ and the characteristic frequency κ_p=0.5 are fixed. Begin with the case $d/l \approx 1$, where the roots of equations (2.259) approximate the real parts of the eigenfrequency rather well.

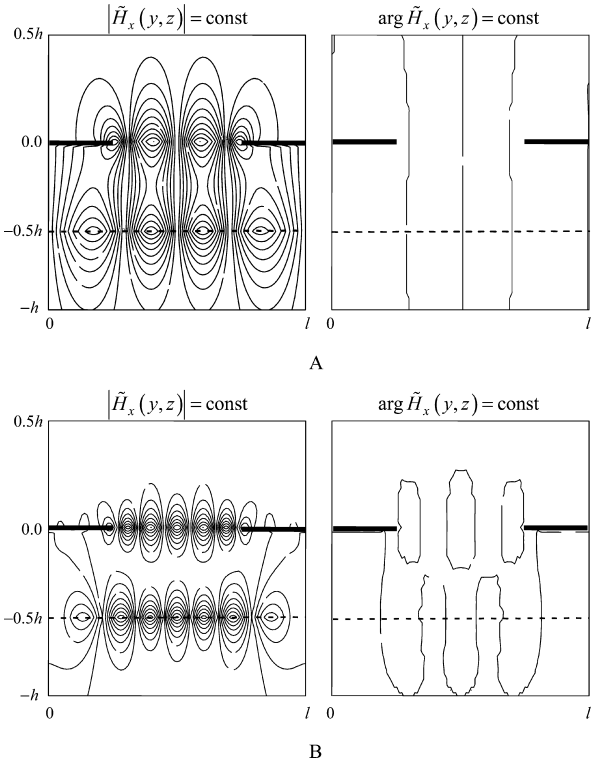

Fig. 2.22 The structure of some eigenoscillation types for (**a**) $\bar{\kappa} = 0.36565 - i10^{-12}$; and (**b**) $\bar{\kappa} = 0.35173 - i7.079 \cdot 10^{-5}$: $\kappa_p = 0.5$, $h/l = (2\pi)^{-1}$, $d/l = 0.5$

At a sufficiently small layer thickness $\bar{h} = 2\pi h/l \ll 1$ and for $\kappa_p < 1$, we arrive at the following eigenfrequency approximations:

$$\bar{\kappa}_{n+} \approx \kappa_p \sqrt{\frac{n\bar{h}}{2}}, \qquad \bar{\kappa}_{n-} \approx \kappa_p \left(1 - \frac{n^2 \bar{h}}{2\sqrt{n^2 - \kappa_p^2}}\right). \tag{2.261}$$

Here, κ_n^+ and κ_n^- are the roots of equations (2.259) for the minus and plus signs, respectively. As seen, $\bar{\kappa}_{n+} \to 0$ and $\bar{\kappa}_{n-} \to \kappa_p$ as $\bar{h} \to 0$. It has been shown numerically that this eigenfrequency behavior is also typical for $d/l \neq 1$ (see Fig. 2.24a). When the real parts of eigenfrequencies $\bar{\kappa}$ satisfy $\mathrm{Re}\bar{\kappa} > \kappa_p/\sqrt{2}$, they asymptotically tend to κ_p as the layer becomes thin and to $\bar{\kappa} = \kappa_p/\sqrt{2}$ as it becomes thick. It was already mentioned that the eigenfrequency accumulation point is $\kappa = \kappa_p/\sqrt{2}$. If for the indicated κ_p and d/l values, the eigenfrequencies are such that $\mathrm{Re}\bar{\kappa} < \kappa_p/\sqrt{2}$, they tend to zero as $h/l \to 0$ and approach the relevant eigenfrequencies of the grating

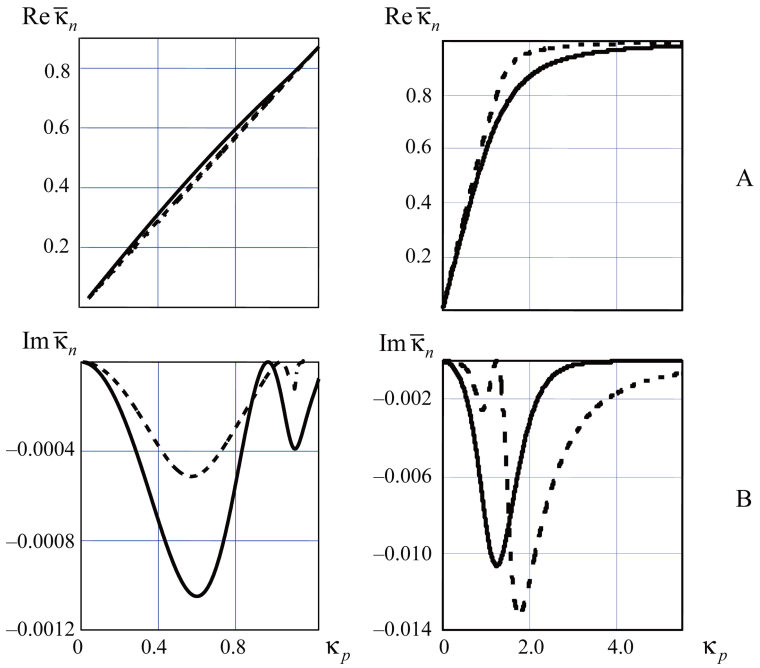

Fig. 2.23 The eigenfrequencies $\bar{\kappa}_n$ versus κ_p: (**a**) Real and (**b**) imaginary parts; $h/l = (2\pi)^{-1}$, $d/l = 0.5$

backed by a metamaterial half-space as $h/l \to \infty$ [145]. When $h/l \to 0$, the imaginary parts typically tend to zero for both oscillation types $\mathrm{Re}\bar{\kappa} > \kappa_p/\sqrt{2}$ and $\mathrm{Re}\bar{\kappa} < \kappa_p/\sqrt{2}$ (Fig. 2.24b). As the layer thickness grows, the imaginary parts of eigenfrequencies such that $\mathrm{Re}\bar{\kappa} < \kappa_p/\sqrt{2}$ approach those of the grating backed by a metamaterial half-space [145]. For other values of the characteristic frequency κ_p and the grating slot width, this dependence of the structure eigenfrequency on the metamaterial layer thickness still remains.

We proceed to a description of the solution of the diffraction of a plane H-polarized wave by a strip grating placed on a metamaterial layer surface. We consider the case that the normalized frequency κ of the excitation wave is less than κ_p. First of all, we mention again that the real part of the metamaterial permittivity in this frequency region is negative, $\mathrm{Re}\tilde{\varepsilon} < 0$. Second, it is a region that contains real parts of the eigenfrequencies of the spectral problem. Assume that $\kappa_p/\sqrt{2} \leq 1$, which is actually realized by a proper choice of the grating period. Then from (2.236) it follows that the diffraction field in the reflection (**A**) and the transition (**B**) zones is a superposition of the traveling zeroth harmonic and an infinitely large number of surface harmonics exponentially decaying away from the grating along the z-axis ($z \to \pm\infty$). Hence the diffraction field away from the grating is solely governed by the zeroth traveling harmonic characterized by the amplitude $R_{00}^{\mathbf{AA}}$ (reflection coefficient) in the reflection zone ($z > 0$) and the amplitude $T_{00}^{\mathbf{BA}}$

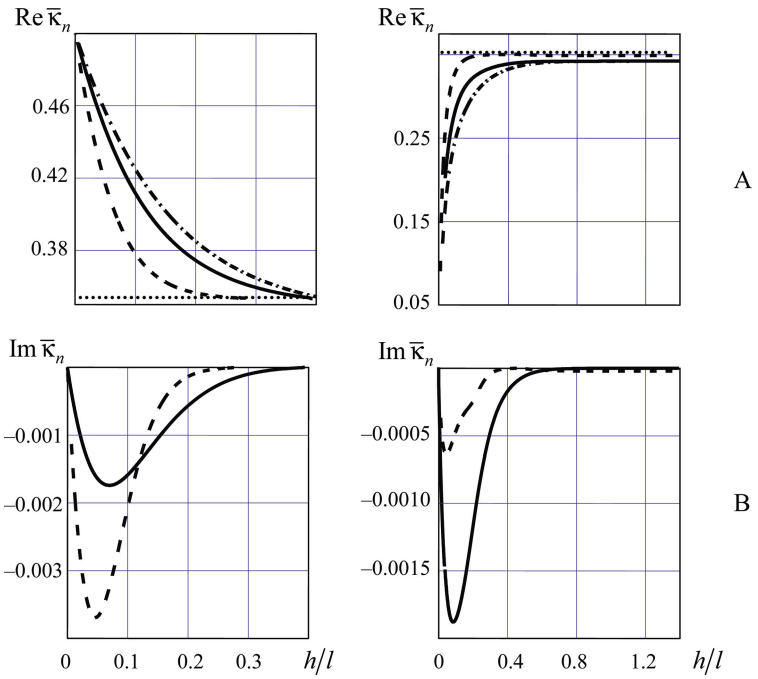

Fig. 2.24 The eigenfrequencies $\bar{\kappa}_n$ versus h/l: (**a**) Real and (**b**) imaginary parts; $d/l = 0.5$, $\kappa_p = 0.5$. The *dotted curves* in (**a**) correspond to $\kappa_p/\sqrt{2}$

(transition coefficient) in the transition zone ($z < -h$). In the case of plane electromagnetic wave incidence, Fig.2.25a plots the transition coefficient module versus frequency for: a metamaterial layer and a grating with $\kappa_p = 0.5$, $v = 10^{-5}$, $d/l = 0.5$, $h/l = 1/(2\pi)$ (solid line), a metamaterial layer single with $\kappa_p = 0.5$, $v = 10^{-5}$, $d/l = 0.5$, $h/l = 1/(2\pi)$ (dashed line), and a grating in a vacuum with $\kappa_p = 0$, $d/l = 0.5$ (dotted line).

It is seen that neither the grating nor the metamaterial layer exhibits resonance properties in the indicated domain $0.3 \le \kappa \le 0.41$ of the normalized frequency parameter. The incident plane-wave energy is practically completely transmitted with $\left|T_{00}^{\mathbf{BA}}\right| > 0.9$. But the incorporation of the grating with the metamaterial layer makes a clearly resonant structure in the indicated κ region, and a discrete set of κ values exists when this construction either almost completely reflects the excitation field energy, $\left|T_{00}^{\mathbf{BA}}\right| \approx 0$ or practically completely transmits it, $\left|T_{00}^{\mathbf{BA}}\right| \approx 1$. A comparison of these κ values with the real parts of the eigenfrequencies at corresponding problem parameters (Figs. 2.20a and 2.21a) indicates that the resonances of the transmission coefficient module keep pace with the excitation of structure eigenoscillations. The excitation fields at some resonance κ values are illustrated in Fig. 2.25b and c. Figure 2.22 demonstrates that the oscillation structure at the resonances of the transmission coefficient $\left|T_{00}^{\mathbf{BA}}\right|$ resembles the eigenoscillation field of

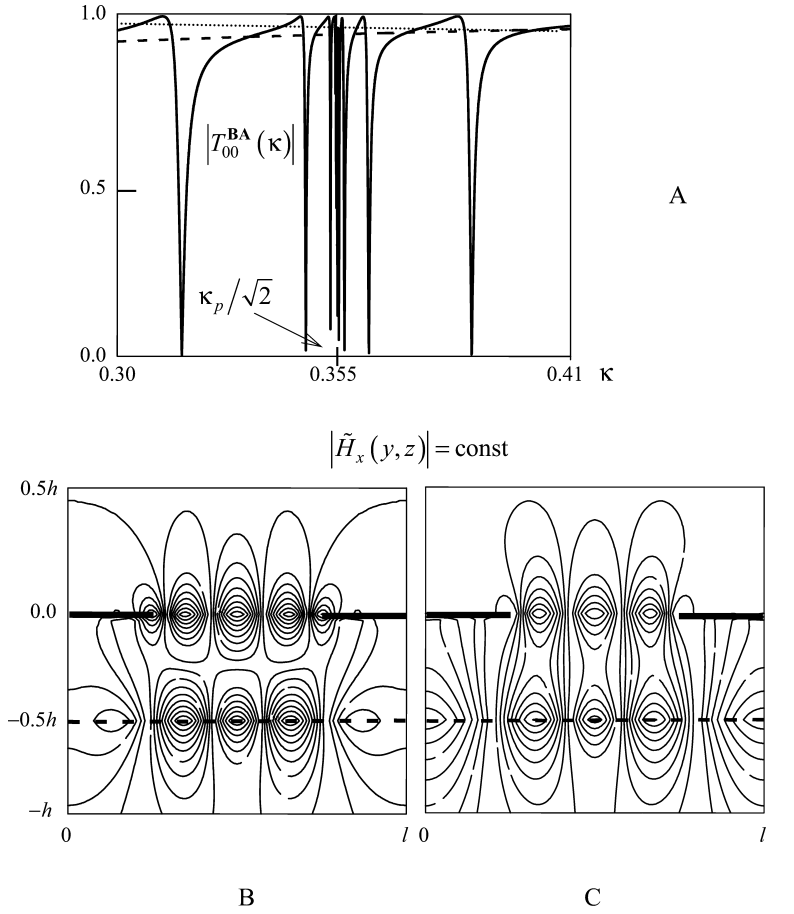

Fig. 2.25 (**a**) The transition coefficient module $\left|T_{00}^{\mathbf{BA}}\right|$ versus normalized frequency $\kappa = l/\lambda$. (**b** and **c**) The excitation field structure at resonance frequencies: $\kappa_p = 0.5$, $v = 10^{-5}$, $d/l = 0.5$, $h/l = (2\pi)^{-1}$, (**b**) $\kappa = 0.34576$; and (**c**) $\kappa = 0.36106$

an open electrodynamical structure – a strip grating backed by a metamaterial layer. Owing to the fact that the excitation field is symmetric about the $y = 0$ plane, only eigenoscillations symmetric about the plane $y = 0$ are excited.

2.5.2 The Plane-Wave Diffraction from a Strip Grating with Anisotropic Medium

In this section, the analytic regularization method (see Section 2.2.3) will be discussed as applied to the monochromatic plane-wave diffraction from a perfectly

conducting strip grating located on the boundary of an anisotropic dielectric half-space. The sewing (partial domain) method is adopted to reduce this problem to the dual series equations of (2.91) and (2.92) type (see Section 2.2.3). The regularization procedure turns them into an infinite system of linear algebraic equations of the second kind in the space l_2, which can be solved effectively.

Let us formulate the diffraction problem. A plane wave is incident along the z-axis on an infinite grating composed of infinitely thin perfectly conducting strips as that in Fig. 2.26. The incident field is assumed to be H-polarized in the x-direction. If so, the magnetic field of the incident wave has only the $\tilde{H}_x^i = \exp(-ikz)$ component. The electric field components lie in the plane x=const. The time dependence is $\exp(-ikt)$. Also, it is assumed that the grating is located in the plane $z = 0$ and extends infinitely along the x-axis. The half-space $z < 0$ is filled with a homogeneous anisotropic medium whose permeability is $\mu = 1$ and whose permittivity is given by the second-rank tensor

$$\tilde{\varepsilon} = \begin{pmatrix} \varepsilon_3 & 0 & 0 \\ 0 & \varepsilon_1 & -i\varepsilon_2 \\ 0 & i\varepsilon_2 & \varepsilon_1 \end{pmatrix}. \tag{2.262}$$

It is required to find the diffraction field $\{\vec{E}^s, \vec{H}^s\}$ governed by a homogeneous system of Maxwell's equations and meeting the radiation condition at infinity $z \to \pm\infty$, the Meixner condition, the periodicity condition, the boundary conditions on the grating perfectly conducting strips, and the field conjugation condition on the anisotropic half-space boundary. The incident wave is x-independent. So, in view of the uniqueness theorem for the solution and the infinity and the homogeneity of the grating in the x-direction, the diffraction field is also x-independent, suggesting us a two-dimensional problem, $\partial/\partial x \equiv 0$.

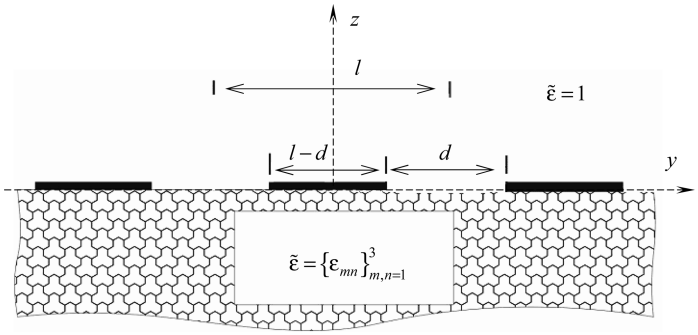

Fig. 2.26 The problem geometry

Using (2.262) and considering the listed assumptions, one easily verifies that the diffraction field components $\{\vec{E}^s, \vec{H}^s\}$ are expressed via the unique nonzero component $\tilde{H}_x^s$ of the magnetic field as follows:

$$\tilde{E}_y^s = \frac{1}{ik\varepsilon_\perp}\left(i\frac{\varepsilon_2}{\varepsilon_1}\frac{\partial \tilde{H}_x^s}{\partial y} - \frac{\partial \tilde{H}_x^s}{\partial z}\right), \qquad \tilde{E}_z^s = \frac{1}{ik\varepsilon_\perp}\left(\frac{\partial \tilde{H}_x^s}{\partial y} + i\frac{\varepsilon_2}{\varepsilon_1}\frac{\partial \tilde{H}_x^s}{\partial z}\right), \qquad (2.263)$$

where $\varepsilon_\perp = \left(\varepsilon_1^2 - \varepsilon_2^2\right)\varepsilon_1^{-1}$ is the effective permittivity of the anisotropic half-space. For the half-space $z > 0$, put $\varepsilon_1 = 1$, $\varepsilon_2 = 0$. From (2.263) it follows that the diffraction field is H-polarized.

For the sake of convenience, introduce the function $\tilde{U}(g,k)$

$$\tilde{U}(g,k) = \begin{cases} \tilde{H}_x^i + \tilde{H}_x^s; & z > 0 \\ \tilde{H}_x^s; & z < 0 \end{cases}. \qquad (2.264)$$

By the Maxwell's equations, everywhere but at the anisotropic half-space boundary this function satisfies the Helmholtz equation

$$\Delta_{y,z}\tilde{U}(g,k) + k^2(z)\,\tilde{U}(g,k) = 0;\ g = \{y,z\},\ k^2(z) = k^2\begin{cases} 1; & z > 0 \\ \varepsilon_\perp; & z < 0 \end{cases}. \qquad (2.265)$$

Rewrite the boundary condition on the grating strips and the conjugation condition on the anisotropic half-space boundary in terms of the function $\tilde{U}(g,k)$. On the perfectly conducting grating strips the tangential electric field component $\tilde{E}_y$ has to vanish, giving

$$\left.\frac{\partial \tilde{U}(g,k)}{\partial z}\right|_{z=0+0} = 0, \qquad \left.\left(\frac{\partial \tilde{U}(g,k)}{\partial y} + i\frac{\varepsilon_2}{\varepsilon_1}\frac{\partial \tilde{U}(g,k)}{\partial z}\right)\right|_{z=0-0} = 0 \qquad (2.266)$$

for $|2\pi y/l + n| < \pi(1 - d/l);\ n = 0, \pm 1, \pm 2, ...$

As the tangential components $\tilde{H}_x$ and $\tilde{E}_y$ are continuous across the grating slots, the relationships (2.263) yield

$$\begin{array}{c} \left.\frac{\tilde{U}(g,k)}{\partial z}\right|_{z=0+0} = \frac{1}{\varepsilon_\perp}\left.\left(\frac{\partial \tilde{U}(g,k)}{\partial z} - i\frac{\varepsilon_2}{\varepsilon_1}\frac{\partial \tilde{U}(g,k)}{\partial y}\right)\right|_{z=0-0}, \\ \left.\tilde{U}(g,k)\right|_{z=0+0} = \left.\tilde{U}(g,k)\right|_{z=0-0} \end{array} \qquad (2.267)$$

for $|2\pi y/l + n| > \pi(1 - d/l);\quad n = 0, \pm 1, \pm 2, ...$ Here, l and d are, respectively, the period and the width of the grating slots (see Fig. 2.2b).

Take the Fourier series expansion of the function $\tilde{U}(g,k)$ in the variable y for the half-spaces $z > 0$ (domain **A**) and $z < 0$ (domain **B**). Considering that $\tilde{U}(g,k)$ must satisfy equation (2.265) and implying the radiation condition, we have

$$\tilde{U}(g,k) = \begin{cases} e^{-ikz} + \sum\limits_{n=-\infty}^{\infty} R_{n0}^{\mathbf{AA}} e^{i(\Phi_n y + \Gamma_{1n} z)}; & z > 0 \\ \sum\limits_{n=-\infty}^{\infty} T_{n0}^{\mathbf{BA}} e^{i(\Phi_n y - \Gamma_{2n} z)}; & z < 0 \end{cases}. \qquad (2.268)$$

Here, $\left\{R_{n0}^{\mathbf{AA}}\right\}_{n=-\infty}^{\infty}$ and $\left\{T_{n0}^{\mathbf{BA}}\right\}_{n=-\infty}^{\infty}$ are the sought unknown coefficients and $\Gamma_{1n} = \sqrt{k^2 - \Phi_n^2}$, $\Gamma_{2n} = \sqrt{k^2\varepsilon_\perp - \Phi_n^2}$. The choice of the root branches Γ_{1n} and Γ_{2n} is governed by the radiation condition (see Section 2.5.1): $k\mathrm{Re}\Gamma_{pn} \geq 0$, $\mathrm{Im}\Gamma_{pn} \geq 0$, $p = 1,2$, $n = 0, \pm 1, \pm 2, \ldots$

So, we have arrived at the problem of finding the coefficients $\left\{R_{n0}^{\mathbf{AA}}\right\}_{n=-\infty}^{\infty}$ and $\left\{T_{n0}^{\mathbf{BA}}\right\}_{n=-\infty}^{\infty}$ in the Fourier series expansion of the function $\tilde{U}(g,k)$. Use boundary conditions (2.266) and (2.267) and derive the equations these coefficients satisfy.

Substitute (2.268) into (2.266) and (2.267) to arrive at the dual series equations

$$\sum_{n=-\infty}^{\infty} T_{n0}^{\mathbf{BA}} \left(in\frac{2\pi\varepsilon_2}{l\varepsilon_1} + \Gamma_{2n} \right) \mathrm{e}^{in\vartheta} = 0; \qquad |\vartheta| < \vartheta_0, \tag{2.269}$$

$$\sum_{n=-\infty}^{\infty} \left(R_{n0}^{\mathbf{AA}} - T_{n0}^{\mathbf{BA}_n} + \delta_0^n \right) \mathrm{e}^{in\vartheta} = 0; \qquad |\vartheta| > \vartheta_0, \tag{2.270}$$

where $\vartheta = (2\pi y)/l$, $\vartheta_0 = \pi(1 - d/l)$.

From (2.266) and (2.267), one easily finds that the coefficients $\left\{R_{n0}^{\mathbf{AA}}\right\}_{n=-\infty}^{\infty}$ and $\left\{T_{n0}^{\mathbf{BA}}\right\}_{n=-\infty}^{\infty}$ are related as

$$R_{n0}^{\mathbf{AA}} = \delta_0^n - \frac{in\frac{2\pi\varepsilon_2}{l\varepsilon_1} + \Gamma_{2n}}{\varepsilon_\perp \Gamma_{1n}} T_{n0}^{\mathbf{BA}}; \qquad n = 0, \pm 1, \pm 2, \ldots \tag{2.271}$$

Introduce the new unknowns $x = \{x_n\}_{n=-\infty}^{\infty}$ by the formula

$$x_n = R_{n0}^{\mathbf{AA}} - T_{n0}^{\mathbf{BA}} + \delta_0^n; \qquad n = 0, \pm 1, \pm 2, \ldots \tag{2.272}$$

Use (2.271) and bring equations (2.269) and (2.270) to the form

$$\sum_{n=-\infty}^{\infty} x_n \gamma_n \mathrm{e}^{in\vartheta} - \frac{2\kappa}{1 + \sqrt{\varepsilon_\perp}} = 0; \qquad |\vartheta| < \vartheta_0, \tag{2.273}$$

$$\sum_{n=-\infty}^{\infty} x_n \mathrm{e}^{in\vartheta} = 0; \qquad |\vartheta| > \vartheta_0. \tag{2.274}$$

Here, as before, $\kappa = kl/2\pi = l/\lambda$ and

$$\gamma_n = \frac{\Gamma_{1n}\left(in\frac{\varepsilon_2}{\varepsilon_1} + \frac{l}{2\pi}\Gamma_{2n} \right)}{\varepsilon_\perp \Gamma_{1n} + \Gamma_{2n} + in\frac{2\pi\varepsilon_2}{l\varepsilon_1}}. \tag{2.275}$$

Let us show that equations (2.273) and (2.274) can be expressed in the form of equations (2.91) and (2.92) (see Section 2.2.3). First of all, notice that Γ_{1n} and Γ_{2n} obey the following asymptotical formulas as $n \to \pm\infty$ [see (2.245) and (2.247)]:

$$\Gamma_{1n} = i\frac{2\pi}{l}\,|n|\,(1+\delta_{1n})\,, \tag{2.276}$$

$$\Gamma_{2n} = i\frac{2\pi}{l}\,|n|\,(1+\delta_{2n})\,, \tag{2.277}$$

where $\delta_{pn} = O\left(n^{-2}\right)$; $p = 1, 2$. Using (2.276) and (2.277) one finds that the coefficient γ_n from (2.275) can be written as

$$\gamma_n = i\,|n| \begin{cases} C^+\left[1+O\left(n^{-2}\right)\right]; & n\to+\infty \\ C^-\left[1+O\left(n^{-2}\right)\right]; & n\to-\infty \end{cases}, \tag{2.278}$$

where $C^+ = (1+\varepsilon_1-\varepsilon_2)^{-1}$, $C^- = (1+\varepsilon_1-\varepsilon_2)^{-1}$. Now substitute (2.278) into (2.273). After some elementary manipulations, one obtains

$$ax_0 + \sum_{\substack{n=1 \\ |\vartheta|<\vartheta_0}}^{\infty} nx_n e^{in\vartheta} - b\sum_{n=-\infty}^{-1} nx_n e^{in\vartheta} + \sum_{n=-\infty}^{\infty} |n|\,\delta_n x_n e^{in\vartheta} + \frac{i2\kappa(1+\varepsilon_1-\varepsilon_2)}{1+\sqrt{\varepsilon_\perp}} = 0; \tag{2.279}$$

$$\sum_{n=-\infty}^{\infty} x_n e^{in\vartheta} = 0; \qquad |\vartheta| > \vartheta_0. \tag{2.280}$$

Here,

$$a = -\frac{i\kappa\,(1+\varepsilon_1-\varepsilon_2)}{1+\sqrt{\varepsilon_\perp}}; \tag{2.281}$$

$$b = \frac{1+\varepsilon_1-\varepsilon_2}{1+\varepsilon_1+\varepsilon_2}, \tag{2.282}$$

$$\delta_n = \begin{cases} \dfrac{\gamma_n}{i\,|n|\,C^+} - 1; & n>0 \\ \dfrac{\gamma_n}{i\,|n|\,C^+} - \dfrac{C^-}{C^+}; & n<0 \end{cases}. \tag{2.283}$$

From (2.278) it follows that $\delta_n = O(n^{-2})$ as $n\to\pm\infty$. Introduce the matrix operator $V = \{V_{mn}\}_{m,n=-\infty}^{\infty}$ and the column vector $f = \{f_n\}_{n=-\infty}^{\infty}$ by the formulas

$$V_{mn} = |n|\,\delta_n\delta_m^n, \qquad f_n = -\frac{i2\kappa\,(1+\varepsilon_1-\varepsilon_2)}{1+\sqrt{\varepsilon_\perp}}\delta_0^n. \tag{2.284}$$

Substituting (2.284) into (2.279) yields

$$ax_0 + \sum_{n=1}^{\infty} nx_n e^{in\vartheta} - b\sum_{n=-\infty}^{-1} nx_n e^{in\vartheta} + \sum_{n=-\infty}^{\infty}\left[(Vx)_n - f_n\right]e^{in\vartheta} = 0; \qquad |\vartheta|<\vartheta_0, \tag{2.285}$$

$$\sum_{n=-\infty}^{\infty} x_n e^{in\vartheta} = 0; \qquad |\vartheta| > \vartheta_0. \tag{2.286}$$

One easily checks that equations (2.284) and (2.285) match (2.91) and (2.92) with $U = 0$ and $g = 0$. Now it will suffice to verify that the matrix operator $\widehat{V} = \widehat{T}^{-1} V \widehat{T}^{-1} = \left\{\widehat{V}_{mn}\right\}_{m,n=-\infty}^{\infty}$ is compact on the space l_2, where the operator $\widehat{T}$ is given by (2.95). From (2.284) and (2.91), it follows that the matrix elements of the operator $\widehat{V}$ have the appearance

$$\widehat{V}_{mn} = |n|^{1-\eta}\, \delta_n \delta_m^n; \quad n \neq 0 \qquad \text{and} \qquad \widehat{V}_{00} = 0, \tag{2.287}$$

where $\eta = 1 + \arg b/\pi$, $-\pi \leq \arg b < \pi$.

As soon as $\delta_n = O(n^{-2})$, then $\widehat{V}_{nn} \to 0$ for $n \to \pm\infty$, suggesting that the operator $\widehat{V}$ is compact on the l_2 [70].

So, the analytic regularization method outlined in Section 2.2.3 is acceptable for the dual series equations (2.285) and (2.286). As a result, they are equivalent to the infinite system of linear algebraic equations of the second kind on the space l_2 and can be written in the form

$$\left(E + \widehat{H}\right) \widehat{x} = \widehat{b}\,, \tag{2.288}$$

where the operator $\widehat{H} = -a\,\widehat{P} + \widehat{W}\,\widehat{V}$ is compact on the l_2, $\widehat{b} = \widehat{W}\,\widehat{f}$, $\widehat{x} = \widehat{T}\,x$, $\widehat{f} = \widehat{T}^{-1} f$, and the matrix elements of the operators $\widehat{P}$ and $\widehat{W}$ are available from (2.115), (2.117), and (2.121). System (2.288) can be solved with any preassigned accuracy by truncation [144].

Owing to the discussed technique, we have obtained a vast collection of numerical results. Some of them are published in references [144, 145].

Let us analyze some results coming from the numerical solution of equation (2.282). For an anisotropic dielectric medium, we will take a cold electron plasma confined in a constant magnetic field $\vec{H}_0 = \{H_0,0,0\}$ aligned with the x-axis ($\vec{H}_0$ is parallel to the grating edges). Then the components of the permittivity tensor are

$$\varepsilon_1 = 1 - \frac{\omega_p^2\,(\omega + i\nu)}{\omega\left[(\omega + i\nu)^2 - \omega_c^2\right]}, \qquad \varepsilon_2 = -\frac{\omega_p^2 \omega_c}{\omega\left[(\omega + i\nu)^2 - \omega_c^2\right]}, \; \varepsilon_3 = 1 - \frac{\omega_p^2}{\omega\,(\omega + i\nu)}. \tag{2.289}$$

Here ω_p is the plasma frequency, $\omega_c = eH_0/mc$ is the electron cyclotron frequency, ν is the effective collision frequency of electrons, with e and m being, respectively, the electron charge and mass, and c is the speed of light in vacuum.

In the subsequent discussion it will be convenient to use the dimensionless parameters $\kappa = l\omega/2\pi c = l/\lambda$, $\kappa_p = \omega_p l/2\pi c$, $\kappa_c = \omega_p l/2\pi c$ (we recall that l is the grating period).

The computations mainly refer to the excitation frequency band $0 < \kappa < 3$. In this case, as follows from (2.268), the field in the half-space $z > 0$ is a superposition of the incident field and the diffraction field consisting of an infinite series of spatial harmonics of the form $\tilde{U}_n^s(g,k) = R_{n0}^{\mathbf{AA}} \exp\left[i(\Phi_n y + \Gamma_{1n} z)\right]$, $n = 0,\pm1,\pm2,\ldots$. A finite number of harmonics whose numbers satisfy the condition $|n| < \kappa$ are plane H-polarized waves outgoing away from the grating. When $\kappa < 1$, only one wave $\tilde{U}_0^s(g,k) = R_{00}^{\mathbf{AA}} \exp(ikz)$ goes out from the grating. An infinite number of harmonics with numbers $|n| \geq 1$ are surface waves decaying exponentially as $z \to \pm\infty$ and traveling along the grating with phase velocities whose absolute values are less than the speed of light. Hence far away from the grating (the half-space $z > 0$), the diffraction field is governed only by the principal spatial harmonic $\tilde{U}_0^s(g,k)$. The principal harmonic amplitude $R_{00}^{\mathbf{AA}}$ normalized to the incident wave amplitude is a complex coefficient representing the reflection of the field from the grating lying on the boundary of the anisotropic half-space ($z > 0$).

Consider the behavior of the reflection coefficient depending on the excitation wave frequency, grating parameters, and the characteristic frequencies κ_p, κ_c of the anisotropic half-space. For definiteness sake, suppose that $\kappa_p < 1$ and $\kappa_c < 1$ (this is always possible via a reasonable choice of the grating period). The calculations from the numerical solution of (2.288) reveal the frequency range $\alpha_- < \kappa < \kappa_c$; $\alpha_\pm = 0.5\left(\sqrt{\kappa_c^2 + 2\kappa_p^2} \pm \kappa_c\right)$ where even if grating slots are very narrow, the electromagnetic field almost completely transmitted to the anisotropic medium (the reflection coefficient module is $\left|R_{00}^{\mathbf{AA}}\right| \leq 0.3$). Typical dependences of the reflection coefficient module are given in Fig. 2.27a and b, showing a pronounced negative peak of the reflection coefficient amplitude. Thus, at the excitation wavelength more than 10^3 times as large as the grating slot width, the reflection coefficient module is $\left|R_{00}^{\mathbf{AA}}\right| \approx 0.3$. Compare it with the module of the reflection coefficient of a grating free from the anisotropic medium ($\kappa_p = \kappa_c = 0$; dashed line).

As is known [45], a metal strip grating is practically transparent to plane H-polarized waves in the long-wavelength part ($\kappa \ll 1$) of spectrum. The reflection coefficient grows fast as κ increases ($\kappa \to 1$) (see Fig. 2.27a). With the anisotropic half-space present, there is a range of variation of κ ($\kappa < 1$) when even for very narrow slots ($\lambda/d \sim 10^3$), the reflection coefficient module can be substantially less than that of a grating in free space. Also, it is interesting that the characteristic frequency κ_c can effectively control the reflection coefficient (see Fig. 2.27b).

Consider now the behavior of the reflection coefficient in the resonance range $\kappa \approx 1$ (the excitation field wavelength is comparable with the grating period). In this case the well-known resonances (Wood's anomalies) [45] coexist with the resonances caused by the anisotropic medium. In support of this, see Fig. 2.27c for $\left|R_{00}^{\mathbf{AA}}\right|$ curves corresponding to various characteristic frequencies κ_p of the anisotropic medium. The first resonance, $\kappa \approx 1$ (the excitation field wavelength equals the grating period) does not depend on κ_p (Wood's anomaly). The second occurs at

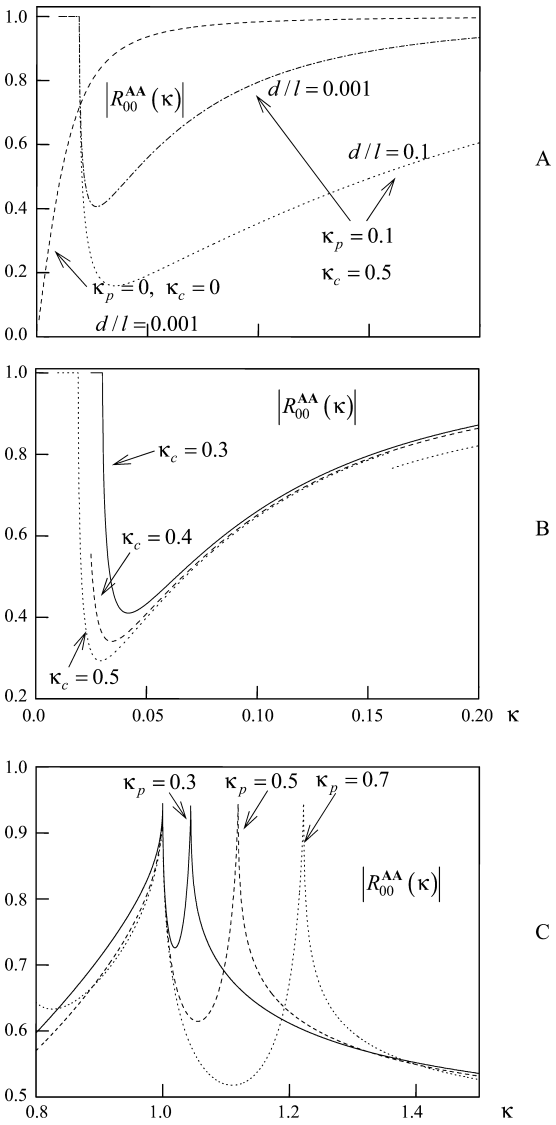

Fig. 2.27 (**a**) The reflection coefficients $\left|R_{00}^{AA}\right|$ versus frequency $\kappa = l/\lambda$ for different structure parameters: (**b**) $\kappa_p = 0.1$, $d/l = 0.01$; (**c**) $\kappa_c = 0.1$, $d/l = 0.5$

$\kappa \approx 1/\sqrt{\varepsilon_\perp}$, where $\varepsilon_\perp = \left(\varepsilon_1^2 - \varepsilon_2^2\right)/\varepsilon_1$ is the effective permittivity of the anisotropic half-space. And it disappears when $\kappa_p \to 0$ and $\kappa_c \to 0$. Attention is drawn to the fact that as κ_p (the plasma frequency) increases, the frequency at which this resonance is possible moves toward the short-wavelength end. This behavior of the reflection coefficient can be used for the determination of the physical characteristics (such as κ_p) of an anisotropic medium. Indeed, knowing the grating geometrical parameters (d and l), the cyclotron frequency κ_c and the frequency κ_{res} at which the reflection

coefficient module is at a maximum, one finds the plasma frequency

$$\omega_p = \frac{2\pi c}{l}\sqrt{\frac{2\kappa_{res}^2 - 1 + \sqrt{1 + 4\kappa_c^2\left(\kappa_{res}^2 - 1\right)}}{2}},$$

and, consequently, the cold electron plasma density from $\kappa_{res}\sqrt{\varepsilon_\perp} \approx 1$.

Now, examine the features of the reflection coefficient behavior with the anisotropic lossy medium [see (2.289), $\nu \neq 0$]. Figure 2.28 shows characteristic dependences of the module of the reflection coefficient in frequency bands where the real part of the effective permittivity takes on positive values. By numerical calculations it was found that these frequency bands carry particular frequencies $\kappa = \alpha_\pm$ in whose vicinities the reflection coefficient can exhibit resonances, and these are due to the surface waves existing on the anisotropic half-space boundary (with the grating absent). At the frequency $\kappa = \alpha_\pm$, the phase velocities of these surface waves become zero. The resonances are most pronounced when the grating slots are

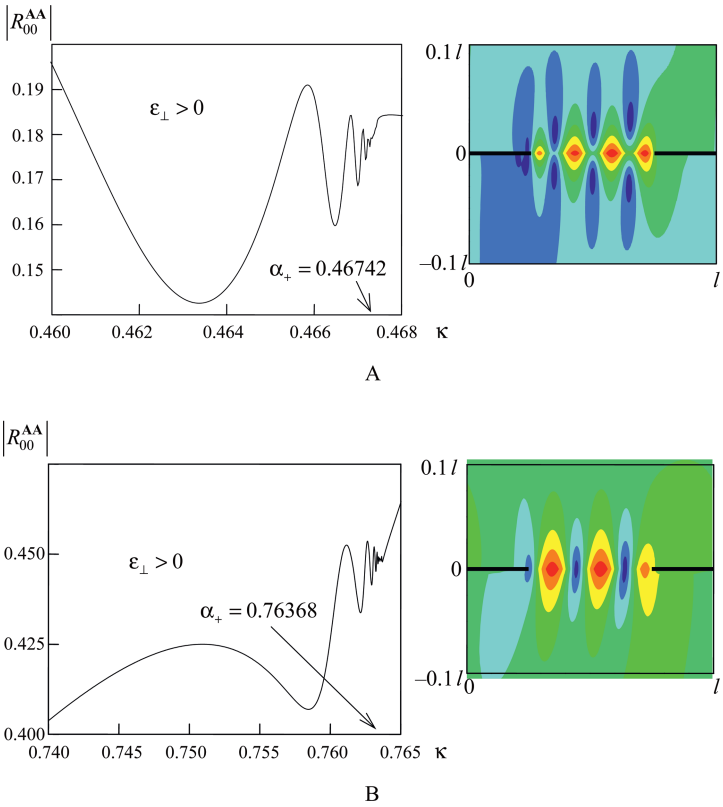

Fig. 2.28 The reflection coefficient module versus frequency and the field structure at resonance frequencies: (**a**) $\kappa_p = 0.5$, $\kappa_c = 0.2$; and (**b**) $\kappa_p = 0.5$, $\kappa_c = 0.6$

sufficiently wide ($d/l \geq 0.5$). Figure 2.28 shows the $\tilde{H}_x$ component distribution at some resonance frequencies, $d/l = 0.5$. As seen, the field is concentrated near the grating slots.

Another resonance type is due to the surface wave supported by the interface between the perfectly conducting metal and an anisotropic half-space. The frequency at which the phase velocity of this wave vanishes matches the cyclotron frequency κ_c. In its vicinity, the reflection coefficient can be resonant (Fig. 2.29). In this frequency region, the real part of the effective permittivity takes on negative values. Therefore with losses absent ($\nu = 0$), the reflection coefficient module equals unity ($\left|R_{00}^{\mathbf{AA}}\right| = 1$). The situation changes completely when the anisotropic half-space is lossy. Namely, the reflection coefficient module as a function of frequency demonstrates clear negative peaks (see Fig. 2.29a) which are most pronounced when the grating slots are sufficiently narrow ($d/l \leq 0.1$). For the field structure at some

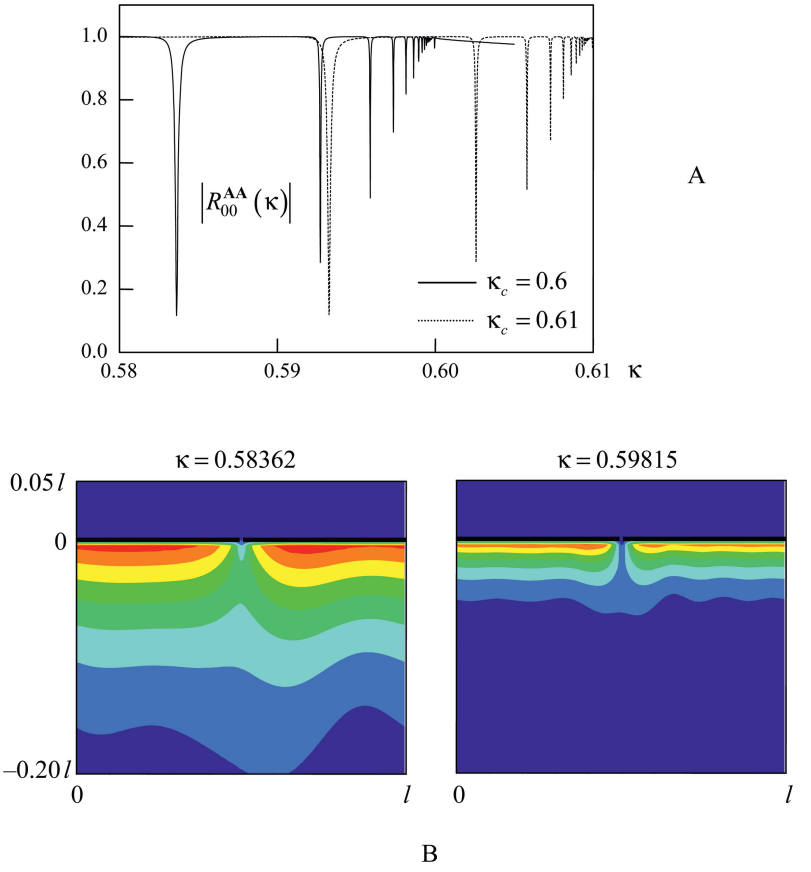

Fig. 2.29 (**a**) The reflection coefficient module versus frequency for $d/l = 0.01$, $\kappa_p = 0.5$, $\kappa_c = 0.6$, and $\kappa_c = 0.61$; and (**b**) the field structure at some resonance frequencies

frequencies corresponding to minima of the amplitude of the reflection coefficient, see Fig. 2.29b. The resonance field is concentrated in the anisotropic medium near the grating metal strips.

At this point, our presentation of numerical results obtained with the aid of the analytic regularization method has come to an end, in the present context. We hopefully appreciate that the cited results provide at least a partial answer to the long-standing question of what is the practical use of all these analytic regularization procedures with their sometimes complicated transformations and bulky constructions.

2.6 Diffraction of Quasi-Periodic Waves by Obstacles with Cylindrical Periodical Wavy Surfaces

The purpose of this section is the demonstration of the simplest initial technique of the analytic regularization method. That is why the subject of our consideration herein is mathematical modeling of simple, but key problems of electromagnetic wave diffraction by obstacles with infinite and smooth one-dimensional periodical wavy surfaces (see Fig. 2.30). We study these problems in the system of nondimensional time and spatial coordinates $\bar{y} = 2\pi y/l$, $\bar{z} = 2\pi z/l$, $\bar{t} = 2\pi t/l$, according to which the period of gratings is equal to 2π.

Such a cylindrical surface $\bar{\mathbf{S}}$ is supposed to be 2π-periodical with respect to the space variable $\bar{y}$ and homogeneous in the longitudinal $\bar{x}$-direction. The cross-section $\bar{\mathbf{S}}_x$ of $\bar{\mathbf{S}}$ by the plane $\bar{x} = \text{const}$ can be described as the set of contours:

$$\bar{\mathbf{S}}_x = \bigcup_{j=-\infty}^{\infty} \bar{\mathbf{S}}_{x,j} \in \mathbf{C}^{\infty};\ \bar{\mathbf{S}}_{x,j} = \left\{\bar{g}_j = \{\bar{y} + 2\pi j, \bar{z}\} :\ \bar{g} = \{\bar{y}, \bar{z}\} \in \bar{\mathbf{S}}_{x,0};\ 0 \le \bar{y} \le 2\pi\right\}. \tag{2.290}$$

We assume that contour $\bar{\mathbf{S}}_x$ is nonself-crossing and (just for simplicity) infinitely smooth. Contour $\bar{\mathbf{S}}_{x,0}$ is supposed to be of finite length.

Corresponding parameterizations of contours $\bar{\mathbf{S}}_x$ and $\bar{\mathbf{S}}_{x,0}$ play an essential role in our future explanation. Necessary constructions and assumptions can be summarized as follows:

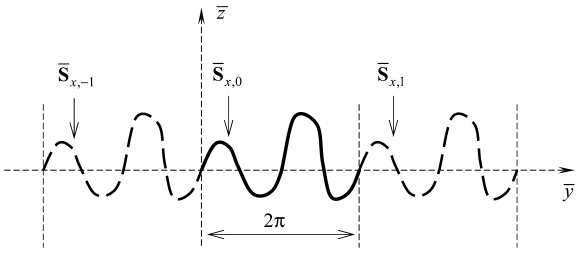

Fig. 2.30 Perfectly conducting metallic 2π-periodic grating of arbitrary profile

- The vector function

$$\eta^0(\vartheta) \equiv \{\bar{y}(\vartheta), \bar{z}(\vartheta)\}; \vartheta \in [-\pi;\pi] \tag{2.291}$$

is assumed to be given as a smooth parameterization of the contour $\bar{\mathbf{S}}_{x,0}$. It means that $\bar{y}(\vartheta)$ and $\bar{z}(\vartheta)$ are such functions that for every $\vartheta \in [-\pi;\pi]$ they give corresponding to this ϑ point $\bar{g} = \{\bar{y}, \bar{z}\} = \{\bar{y}(\vartheta), \bar{z}(\vartheta)\} \in \bar{\mathbf{S}}_{x,0}$ with the property that function $l(\vartheta) \equiv \left\{\left[d\bar{z}(\vartheta)/d\vartheta\right]^2 + \left[d\bar{y}(\vartheta)/d\vartheta\right]^2\right\}^{1/2}$ is finite and strongly positive (one-to-one mapping condition):

$$0 < l(\vartheta) < \infty. \tag{2.292}$$

- The parameterization $\eta^j(\vartheta) \equiv \left\{\bar{y}_j(\vartheta), \bar{z}_j(\vartheta)\right\}$, $j = 0, \pm 1, \pm 2, \ldots$, for every contour $\bar{\mathbf{S}}_{x,j}$ is constructed according to (2.290) and (2.291):

$$\bar{y}_j(\vartheta) = \bar{y}(\vartheta - 2\pi j), \bar{z}_j(\vartheta) = \bar{z}(\vartheta - 2\pi j); \vartheta \in \left[-\pi + 2\pi j; \pi + 2\pi j\right]. \tag{2.293}$$

- The parameterization $\eta(\vartheta)$ of the contour $\bar{\mathbf{S}}_x$ is

$$\eta(\vartheta) \equiv \eta^j(\vartheta); \vartheta \in \left[-\pi + 2\pi j; \pi + 2\pi j\right], \bar{y}(\vartheta + 2\pi) = \bar{y}(\vartheta) + 2\pi, \quad \bar{z}(\vartheta + 2\pi) = \bar{z}(\vartheta), \tag{2.294}$$

and, due to the construction,

$$\eta: (-\infty;\infty) \leftrightarrow \bar{\mathbf{S}}_x \tag{2.295}$$

is a one-to-one mapping of $(-\infty;\infty)$ to $\bar{\mathbf{S}}_x$.
- The parameterization $\eta(\vartheta)$ thus obtained is infinitely smooth:

$$\eta(\vartheta) \in \mathbf{C}^\infty(-\infty;\infty). \tag{2.296}$$

We will say that the function $f(\vartheta)$ is a 2π-quasi-periodical one (with respect to variable ϑ) if the function satisfies the condition

$$f(\vartheta + 2\pi) = e^{i2\pi\Phi} f(\vartheta) \tag{2.297}$$

for each ϑ in the domain of the function definition. Parameter Φ is introduced in Section 1.1.3 and it is known as the parameter of quasi-periodicity. According to (2.291), Φ in (2.297) can be always chosen (by means of adding or extraction of an integer number) satisfying the inequalities that we assume to be valid below:

$$-1/2 < \Phi \leq 1/2. \tag{2.298}$$

For concreteness, we assume also that the surface $\bar{\mathbf{S}} = \bar{\mathbf{S}}_x \times [-\infty < x < \infty]$ is excited by an electromagnetic plane wave

$$\tilde{U}_p^i(\bar{g},\kappa) = \exp\left[i\left(\bar{\Phi}_p\bar{y} - \bar{\Gamma}_p\bar{z}\right)\right];\ \bar{g}\in\mathbf{R}^2 \tag{2.299}$$

(p is integer), which is 2π-quasi-periodical with respect to $\bar{y}$, does not depend on $\bar{x}$, and comes from the upper half-space. Here [see also (1.22)], $\bar{\Phi}_n = \Phi + n$, $\bar{\Gamma}_n = \sqrt{\kappa^2 - \bar{\Phi}_n^2}$, $\mathrm{Re}\bar{\Gamma}_n\mathrm{Re}\kappa \geq 0$, and $\mathrm{Im}\bar{\Gamma}_n \geq 0$. As well, $\tilde{U}_p^i(\bar{g},\kappa)$ can be, in principal, any 2π-quasi-periodical in respect to $\bar{y}$, not depending on $\bar{x}$, and smooth in some vicinity $\mathbf{V}$ of $\bar{\mathbf{S}}$ function.

The incident field, the obstacle's material parameters, and the geometrical structure do not depend on the space variable $\bar{x}$, then, evidently, the scattered field $\tilde{U}^s(\bar{g},\kappa)$ does not depend on $\bar{x}$ either. Consequently, the electromagnetic fields can be expressed by means of two scalar functions $\tilde{E}_x$ (E-polarization) and $\tilde{H}_x$ (H-polarization) satisfying homogeneous Helmholtz equations. Thus, the problems under consideration are scalar and two-dimensional ones.

There are three typical kinds of boundary conditions on the surface $\bar{\mathbf{S}}$, namely, Dirichlet, Neumann, and transmission ones. When $\bar{\mathbf{S}}$ is the surface of a perfectly conducting screen, we have Dirichlet or Neumann boundary value problems (BVPs) for E- or H-polarization, respectively. For the case when the surface separates two media with different material parameters (it will be the surface $\bar{\mathbf{S}}^{\varepsilon,\mu,\sigma}$), we arrive at transmission problems (for both polarizations).

In this section, we restrict ourselves at rather brief consideration of the Dirichlet and Neumann problems only. There is a big similarity in construction of analytic regularization method for the other BVPs mentioned above. Also, it is necessary to have much more room for going into all details even for a Dirichlet BVP only. That is why we recommend our reader to look at the publications [10, 11, 57, 58, 63, 64, 149, 150], where similar and more complicated problems are investigated.

In Section 2.6.1, we consider a Dirichlet BVP. Section 2.6.2 is devoted to reducing the BVP to a standard integral equation of the first kind. Differential and singular properties of the transformed integral equation kernel are the subject of the analysis in Section 2.6.3. In Section 2.6.4, we discuss the splitting of the integral equation kernel and the requirements for the result of the splitting. In Section 2.6.5, we reduce the integral equation to an infinite system of the first kind. In Section 2.6.6, we use the splitting constructed for obtaining the algebraic system of the second kind, which forms functional equations of the type $(E + H)\ x = b$, x, $b\in l_2$ with identity operator E and compact operator H in the space l_2 of square-summable sequences. Section 2.6.7 outlines the difference in application of the analytic regularization method for the Neumann BVP in comparison with the Dirichlet one. Here we obtain similar result: the Neumann BVP is reduced to the algebraic system of the second kind, which is qualitatively the same as one mentioned above for the Dirichlet BVP.

As it is well known, solving such an algebraic system of the second kind by means of the reduction method is numerically stable process that gives principal possibility to obtain the solution with any predetermined accuracy (in contrast to many popular, but unstable methods like the family of Galerkin and the other direct methods).

2.6.1 The Dirichlet Diffraction Problem

The initial version of the algorithm explained herein can be found in publication [149]. Similar problem, but for semitransparent grating, is the subject of publication [150].

Let the above-mentioned $\bar{\mathbf{S}}$ be a surface of a perfectly conducting screen, which is illuminated by an E-polarized wave with given 2π-quasi-periodical component $\tilde{E}_x^i(\bar{g},\kappa) = \tilde{U}_p^i(\bar{g},\kappa)$ [see formula (2.299) and the next paragraph].

We pose the Dirichlet BVP in the same way as it is explained in Chapter 1 – see (1.20) and (1.22). Nevertheless, some details of the boundary conditions and their exact mathematical sense must be added. We use the problem posing in the classical sense similar to [9]. That is why we assume that unknown and seeking for 2π-quasi-periodical function $\tilde{U}^s(\bar{g},\kappa)$, $\bar{g} \in \mathbf{R}^2$, i.e., scattering field, belongs to the following functional class:

$$\tilde{U}^s(\bar{g},\kappa) \in \mathbf{C}^2\left(\mathbf{R}^2 \backslash \bar{\mathbf{S}}_x\right) \cap \mathbf{C}^{1,\alpha}\left(\overline{\mathbf{R}^{2(+)}}\right) \cap \mathbf{C}^{1,\alpha}\left(\overline{\mathbf{R}^{2(-)}}\right). \tag{2.300}$$

Here, $\mathbf{R}^{2(\pm)}$ are open parts of $\mathbf{R}^2$ placed over and under the contour $\bar{\mathbf{S}}_x$ correspondingly, and $\overline{\mathbf{R}^{2(\pm)}}$ are their closures. This description (2.300) of the class of functions means, in particular, the existence of the following limits, uniform on $\mathbf{S}$:

$$\tilde{U}^{s(\pm)}(\bar{g},\kappa) = \lim_{h\to+0} \tilde{U}^s\left(\bar{g} \pm h\vec{n}_{\bar{g}},\kappa\right);\ \bar{g} \in \bar{\mathbf{S}}_x, \tag{2.301}$$

$$\frac{\partial \tilde{U}^{s(\pm)}(\bar{g},\kappa)}{\partial \vec{n}_{\bar{g}}} = \lim_{h\to+0} \frac{\partial \tilde{U}^{s(\pm)}\left(\bar{g} \pm h\vec{n}_{\bar{g}},\kappa\right)}{\partial \vec{n}_{\bar{g}}};\ \bar{g} \in \bar{\mathbf{S}}_x, \tag{2.302}$$

where $\vec{n}_{\bar{g}}$ is unit outward (directed from $\mathbf{R}^{2(+)}$ to $\mathbf{R}^{2(-)}$) normal to $\bar{\mathbf{S}}_x$ in point $\bar{g} \in \bar{\mathbf{S}}_x$, and, in general, the $(\pm)$ limits are not equal, but can be equal, of course [as this takes place, for example, in condition (2.303)].

We assume also that Dirichlet boundary condition is satisfied, which corresponds to E-polarized wave diffraction by a perfectly conductive cylindrical wavy surface $\bar{\mathbf{S}}_x$:

$$\tilde{U}^{s(\pm)}(\bar{g},\kappa) + \tilde{U}_p^i(\bar{g},\kappa) = 0;\ \bar{g} \in \bar{\mathbf{S}}_x. \tag{2.303}$$

As follows from (1.24), the canonic Green function $\tilde{G}_0(\bar{g},\bar{g}_0,\kappa,\Phi)$ becomes infinite for $\bar{\Gamma}_n = 0$ (that corresponds to branch points of the BVP operator). That is why we will assume below that κ and Φ are chosen in such a way that $\bar{\Gamma}_n \neq 0$.

2.6.2 Reduction of the Dirichlet BVP to the Integral Equations

It can be proved by standard technique of Green's formulas that the scattered field $\tilde{U}^s(\bar{g},\kappa)$ has the following representation:

$$\tilde{U}^s(\bar{g}_1,\kappa) = \int\limits_{\bar{\mathbf{S}}_{x,0}} \tilde{G}_0(\bar{g}_1,\bar{g}_2,\kappa,\Phi)\, M_D(\bar{g}_2)\, dl_{\bar{g}_2};\ \bar{g}_1 \in \mathbf{R}^2 \backslash \bar{\mathbf{S}}_x. \tag{2.304}$$

Here,

$$M_D(\bar{g}) = \frac{\partial \tilde{U}^{s(+)}(\bar{g},\kappa)}{\partial \vec{n}_{\bar{g}}} - \frac{\partial \tilde{U}^{s(-)}(\bar{g},\kappa)}{\partial \vec{n}_{\bar{g}}};\ \bar{g} \in \bar{\mathbf{S}}_x, \tag{2.305}$$

and $M_D(\bar{g})$ is quasi-periodic function satisfying the integral identity

$$\int\limits_{\bar{\mathbf{S}}_{x,0}} \tilde{G}_0(\bar{g}_1,\bar{g}_2,\kappa,\Phi)\, M_D(\bar{g}_2)\, dl_{\bar{g}_2} = -\tilde{U}^i_p(\bar{g}_1,\kappa);\ \bar{g}_1 \in \bar{\mathbf{S}}_{x,0}. \tag{2.306}$$

$\tilde{G}_0(\bar{g}_1,\bar{g}_2,\kappa,\Phi)$ is the canonic Green's function (1.24) of free space for Helmholtz equation and for 1-D periodical structures, but written with respect to nondimensional normalized spatial coordinates $\bar{g} = \{\bar{y},\bar{z}\}$ and points $\bar{g}_j$, $j = 1, 2$. Here, $\kappa = l/\lambda$, where l is the realistic grating period and λ is the wavelength of the incident wave. This function has view (1.24), but value l in factor $-i/2l$ before the symbol of the sum must be changed by $-i/4\pi$, because the grating period in respect to normalized value $\bar{y}$ is equal to 2π (value l in (1.24) has nothing common with function $l(\vartheta)$ in (2.292) that should not be a cause of any confusion, because nowhere below in this section notation l is used as the grating period, but only function $l = l(\vartheta)$ may appear in formulas).

It is noteworthy that series (1.24) is absolutely useless for numerical calculation of $\tilde{G}_0(\bar{g}_1,\bar{g}_2,\kappa,\Phi)$ in domain $|\bar{z}_1 - \bar{z}_2| \ll 1$, because of the series' slow convergence. In a number of papers their authors used extraction of the main asymptotic part of the common term of the series in the form ρ^n/n, where $|\rho| \le 1$. Thus, the series need not any acceleration, if $|\rho| \ll 1$, i.e., $|\bar{z}_1 - \bar{z}_2| \gg 1$. In the same time, series $\sum \rho^n/n$ can be summarized analytically and the sum is an elementary function, which has analytic singularity proportional to $\ln(1-\rho)$. The series similar to $\sum \rho^n/n$ can be extracted term by term from the right-hand side of (1.24) and the result is series of the kind $\sum p_n^{(1)}$, where $p_n^{(1)}$ are some numbers possessing property $p_n^{(1)} = O\left(\rho^n/n^2\right)$. Only the last series needs numerical calculation after that. This is essential progress, because the last series is at least absolutely convergence. Nevertheless, its convergence is still too slow for to be called the summation efficient. The above-explained extraction can be continued with terms ρ^n/n^m, $m = 2,3,4,\ldots$, but, unfortunately, the series $\sum \rho^n/n^m$ are not representable by elementary functions for $m \ge 2$. Perhaps, this fact prevented the mentioned above authors from such extraction and based on it acceleration of series (1.24) convergence.

Nevertheless, we managed (see [11]) to obtain for any fixed $m = 2,3,4,\ldots$ the representation of the kind $\tilde{G}_0(\bar{g}_1,\bar{g}_2,\kappa,\Phi) = S_m + \sum p_n^{(m)}$, where S_m and $p_n^{(m)}$ are expressed by means of elementary functions of $\bar{g}_1$, $\bar{g}_2$, κ and Φ, and $p_n^{(m)} = O(\rho^n/n^m)$. Actually, we even found the relevant recurrent algorithm, which avoids

the necessity of knowing and direct calculation of (rather bulky for big m) analytic expressions of S_m. As well, the number m of the extracted terms, as it is explained above, is regulated dependently on value $|\bar{z}_1 - \bar{z}_2|$: it is maximal for $|\bar{z}_1 - \bar{z}_2| = 0$ (i.e., when $|\rho| = 1$), and any extraction is not necessary for $|\bar{z}_1 - \bar{z}_2| \gg 1$. Thus, the problem of fast calculation of $\tilde{G}_0(\bar{g}_1, \bar{g}_2, \kappa, \Phi)$ (and its derivatives of any finite order) is completely solved.

From modified as above-mentioned formula (1.24) and from (2.305) and (2.304), it follows immediately that $\tilde{G}_0(\bar{g}_1, \bar{g}_2, \kappa, \Phi)$ and $M_D(\bar{g}_1)$ are 2π-quasi-periodic function with respect to $\bar{g}_1$ – in the sense of (2.297) – and $\tilde{G}_0(\bar{g}_1, \bar{g}_2, \kappa, \Phi)$ is 2π-quasi-periodic function in the same sense, but with the negated (i.e., $-\Phi$) parameter of quasi-periodicity:

$$M_D(\bar{y} + 2\pi, \bar{z}) = \mathrm{e}^{i2\pi\Phi} M_D(\bar{y}, \bar{z}) \,;\, \bar{g} = \{\bar{y}, \bar{z}\} \in \bar{\mathbf{S}}_x, \tag{2.307}$$

$$\tilde{G}_0(\bar{y}_1 + 2\pi j, \bar{z}_1, \bar{y}_2 + 2\pi s, \bar{z}_2, \kappa, \Phi) = e^{i2\pi(j-s)\Phi} \tilde{G}_0(\bar{y}_1, \bar{z}_1, \bar{y}_2, \bar{z}_2, \kappa, \Phi)$$
$$\{\bar{y}_1, \bar{z}_1\}, \ \{\bar{y}_2, \bar{z}_2\} \in \mathbf{R}^2, \tag{2.308}$$

In accordance with the standard approach, we will consider (2.306) from now as the integral equation for the unknown function $M_D(\bar{y}, \bar{z})$. It can be proved that if this function has been found, then one can obtain the scattered field in every point by means of the integral representation (2.304).

Using the parameterization $\eta(\vartheta) \equiv \{\bar{y}(\vartheta), \bar{z}(\vartheta)\}$ of contour $\bar{\mathbf{S}}_x$, one can easily reduce the integral equation (2.306) on contour $\bar{\mathbf{S}}_{x,0}$ to an ordinary integral equation on interval $[-\pi;\pi]$ by means of the substitutions

$$\bar{y}_1 = \bar{y}(\tau), \ \bar{z}_1 = \bar{z}(\tau) \,;\, \tau \in [-\pi;\pi], \tag{2.309}$$

$$\bar{y}_2 = \bar{y}(\vartheta), \ \bar{z}_2 = \bar{z}(\vartheta) \,;\, \vartheta \in [-\pi;\pi] \tag{2.310}$$

and direct definition of new functions

$$\mu^0(\tau) = M_D(\bar{y}(\tau), \bar{z}(\tau)) \,;\, \tau \in [-\pi;\pi], \tag{2.311}$$

$$G^0(\vartheta,\tau) = l(\tau) \tilde{G}_0(\bar{y}(\vartheta), \bar{z}(\vartheta), \bar{y}(\tau), \bar{z}(\tau), \kappa, \Phi) \,;\, \vartheta,\tau \in [-\pi;\pi], \tag{2.312}$$

where the fixed parameters κ and Φ are omitted for the sake of brevity. Such a direct way has the following drawback. Due to formulas (2.307) and (2.308), these new functions $\mu^0(\tau)$ and $G^0(\vartheta,\tau)$ are 2π-quasi-periodical ones and are not 2π-periodical, in general. We are going to use Fourier series of these functions. Unfortunately, Fourier coefficients of a function $\mu^0(\tau)$, defined in the way (2.311), tend to zero very slowly (due to the nonperiodicity of the function), and, which is the most important, the same holds for the function $G^0(\vartheta,\tau)$ that brings a very strong limitation on the efficiency of any algorithm thus constructed. Moreover, the behavior

of Fourier coefficients of function $G^0(\vartheta,\tau)$ does not allow us to obtain anyhow an algebraic system of the second kind, which is our final goal.

That is why, we define other – just 2π-periodic – functions:

$$\tilde{\mu}(\tau) = e^{-i\Phi\tau} M_D(\bar{y}(\tau), \bar{z}(\tau)), \tag{2.313}$$

$$\tilde{G}(\vartheta,\tau) = e^{i\Phi(\tau-\vartheta)} \tilde{G}_0(\bar{y}(\vartheta), \bar{z}(\vartheta), \bar{y}(\tau), \bar{z}(\tau), \kappa, \Phi), \tag{2.314}$$

$$\tilde{f}(\vartheta) = -e^{-i\Phi\vartheta} \tilde{U}_p^i(\bar{y}(\vartheta), \bar{z}(\vartheta), \kappa). \tag{2.315}$$

Using formulas (2.313), (2.314), and (2.315) one can rewrite equation (2.306) after some obvious transformations into the following integral equation of the first kind for the unknown function $\tilde{\mu}(\tau)$:

$$\int_{-\pi}^{\pi} \tilde{\mu}(\tau)\, \tilde{G}(\vartheta,\tau)\, l(\tau)\, d\tau = \tilde{f}(\vartheta);\ \vartheta \in [-\pi;\pi]. \tag{2.316}$$

One can consider the function $\tilde{\mu}(\tau)$ on the interval $(-\infty;\infty)$ as the result of its 2π-periodic continuation from $[-\pi;\pi]$. As it follows from formulas (2.314), (2.315), (2.312), (2.308), and (2.315), functions $\tilde{G}(\vartheta,\tau)$, $\tilde{\mu}(\tau)$, and $\tilde{f}(\vartheta)$ are 2π-periodical ones for $\vartheta,\tau\in(-\infty;\infty)$.

2.6.3 Investigation of the Differential Properties of the Integral Equation Kernel

Before any attempt to solve the integral equation (2.316) and a choice of a proper method for such a purpose, it is necessary to investigate the differential and singular properties of the kernel $\tilde{G}(\vartheta,\tau)\, l(\tau)$.

First of all, $\tilde{G}(\vartheta,\tau)$ is an infinitely smooth function for $0 < |\vartheta-\tau| < 2\pi$, because $\tilde{G}_0(\bar{y}_1, \bar{z}_1, \bar{y}_2, \bar{z}_2, \kappa, \Phi)$ is infinitely smooth for $\{\bar{y}_1,\bar{z}_1\} \neq \{\bar{y}_2,\bar{z}_2\}$ as a solution of the homogeneous Helmholtz equation. An explanation of the differential properties of $\tilde{G}(\vartheta,\tau)$ for small $|\vartheta-\tau|$ and $|2\pi - |\vartheta - \tau||$ requires the formulation of a few definitions as follows.

The function $\psi(\vartheta)$, $\vartheta\in[-\pi;\pi]$ belongs to class $\mathbf{C}_Q^m(\mathbf{R}^1)$, if it is m times continuously differentiable after its 2π-periodic continuation on $(-\infty;\infty)$ (in particular, $\psi^{(k)}(-\pi+0) = \psi^{(k)}(\pi-0)$, $k = 0,1,\ldots,m$).

The function $\psi(\vartheta,\tau)$, $\vartheta,\tau\in[-\pi;\pi]$ belongs to class $\mathbf{C}_Q^m(\mathbf{R}^2)$, if all its partial and mixed derivatives of orders $k = 0,1,\ldots,m$ exist and are continuous after the function 2π-periodic continuation with respect to both variables on $(-\infty,\infty) \times (-\infty,\infty)$.

The function $\psi(\vartheta)$, $\vartheta\in[-\pi;\pi]$ belongs to the Hölder-like 2π-periodical class $\mathbf{C}_Q^{m,\alpha}(\mathbf{R}^1)$, if $\psi \in \mathbf{C}_Q^m(\mathbf{R}^1)$ and such fixed constants $\alpha\in(0;1)$ and $C > 0$ exist that

$$\left|\psi^{(m)}(\vartheta_1)-\psi^{(m)}(\vartheta_2)\right|\le C\left|2\sin\frac{\vartheta_1-\vartheta_2}{2}\right|^{\alpha};\ \vartheta_1,\ \vartheta_2\in[-\pi;\pi], \tag{2.317}$$

where $\psi^{(m)}(\vartheta)$ is the derivative of order m of function $\psi(\vartheta)$.

The function $\psi(\vartheta,\tau)$, $\vartheta,\tau\in[-\pi;\pi]$ belongs to the Hölder-like 2π-periodical class $\mathbf{C}_Q^{m,\alpha}\left(\mathbf{R}^2\right)$, if $\psi\in\mathbf{C}_Q^m\left(\mathbf{R}^2\right)$ and such fixed constants $\alpha\in(0;1)$ and $C>0$ exist that

$$\left|\frac{\partial^m\left[\psi(\vartheta_1,\tau_1)-\psi(\vartheta_2,\tau_2)\right]}{\partial^{m_1}\vartheta\,\partial^{m_2}\tau}\right|\le C\left|2\sin\frac{\vartheta_1-\tau_1}{2}\right|^{\alpha}\left|2\sin\frac{\vartheta_2-\tau_2}{2}\right|^{\alpha}, \tag{2.318}$$

for any $m_1\ge 0$ and $m_2\ge 0$ that $m=m_1+m_2$.

The corresponding classes $\mathbf{C}_Q^{\infty}\left(\mathbf{R}^1\right)$ and $\mathbf{C}_Q^{\infty}\left(\mathbf{R}^2\right)$ are defined in standard way:

$$\mathbf{C}_Q^{\infty}\left(\mathbf{R}^1\right)=\bigcap_{m=0}^{\infty}\mathbf{C}_Q^m\left(\mathbf{R}^1\right)\ \text{and}\ \mathbf{C}_Q^{\infty}\left(\mathbf{R}^2\right)=\bigcap_{m=0}^{\infty}\mathbf{C}_Q^m\left(\mathbf{R}^2\right). \tag{2.319}$$

For any $p=0,1,2,\ldots$, we introduce 2π-periodical functions:

$$\widehat{\Phi}_{2p}(\tau)=-(-1)^p(2p)!\sum_{n=1}^{\infty}\frac{\cos n\tau}{n^{2p+1}}, \tag{2.320}$$

$$\widehat{\Phi}_{2p+1}(\tau)=-(-1)^p(2p+1)!\sum_{n=1}^{\infty}\frac{\sin n\tau}{n^{2p+2}}. \tag{2.321}$$

In particular,

$$\widehat{\Phi}_0(\tau)=\ln\left|2\sin\frac{\tau}{2}\right|. \tag{2.322}$$

The functions $\widehat{\Phi}_m(\tau)$ possess the properties

$$\widehat{\Phi}_m(\tau)\in\mathbf{C}_Q^{m-1}\left(\mathbf{R}^1\right);\ m\ge 1;\ \widehat{\Phi}_m(\tau)-\left(2\sin\frac{\tau}{2}\right)^m\ln\left|2\sin\frac{\tau}{2}\right|\in\mathbf{C}_Q^{m+1}\left(\mathbf{R}^1\right), \tag{2.323}$$

$$\frac{d}{d\tau}\widehat{\Phi}_m(\tau)=m\,\widehat{\Phi}_{m-1}(\tau). \tag{2.324}$$

Thus, functions $\widehat{\Phi}_m(\tau)$, $m=0,1,2,\ldots$, form a sequence of functions, where each next function is more smooth than the preceding one.

It can be shown that for any fixed finite number $N=2,3,4,\ldots$ the following singular expansion of the function $\tilde{G}(\vartheta,\tau)$ is valid:

$$\tilde{G}(\vartheta,\tau)-\frac{1}{2\pi}\sum_{n=1}^{N}A_n(\vartheta)\,\widehat{\Phi}_n(\delta)\in\mathbf{C}_Q^N\left(\mathbf{R}^2\right). \tag{2.325}$$

Here, $\delta = \tau - \vartheta$ and $A_n(\vartheta)$ are some infinitely smooth functions:

$$A_n(\vartheta) \in \mathbf{C}^{\infty}(-\infty;\infty). \tag{2.326}$$

After some calculation one can obtain the analytic form of the first few functions $A_n(\vartheta)$. In particular,

$$A_0(\vartheta) \equiv 1, A_1(\vartheta) = i\Phi = \text{const}, A_2(\vartheta) = -\frac{\Phi^2}{2} - \frac{\kappa^2 l^2(\vartheta)}{4}. \tag{2.327}$$

This singular expansion completely describes the singular properties of $\tilde{G}(\vartheta,\tau)$. In particular, from it follows that $\tilde{G}(\vartheta,\tau)$ has singularities in points $\{\vartheta,\tau\}$ where $\vartheta - \tau = 0$ or $\vartheta - \tau = \pm 2\pi$ and in these points only.

Having constructed the singular expansion as above, we can try to derive the analytic regularization method similar to the construction in Section 2.12.1, because the principal singularities of the kernels are similar. This idea encounters an obstacle in the form of the function $l(\tau)$ appearing as a factor in the integral equation kernel. The simplest remedy for this is the introduction of a new unknown function $\tilde{\mu}_{\gamma}(\tau)$ by the relation $\tilde{\mu}(\tau) = \tilde{\mu}_{\gamma}(\tau)[l(\tau)]^{\gamma-1}$ for any number γ, and multiplication of both sides of integral equation (2.316) by $[l(\vartheta)]^{-\gamma}$. This leads to a similar integral equation with unknown function $\tilde{\mu}_{\gamma}(\tau)$, but with a new kernel of the form $[l(\tau)]^{\gamma}[l(\vartheta)]^{-\gamma}\tilde{G}(\vartheta,\tau)$. According to (2.325), (2.327), and (2.322), the principal singularity of this kernel is $(1/2\pi)\ln\left|2\sin(\vartheta-\tau)/2\right|$, and the same algorithm as the one in Section 2.1 (given for the example in that section) for the analytic regularization method construction is applicable, in principle. Nevertheless, a much better algorithm can be constructed. Indeed, as we see, $A_1(\vartheta) \neq 0$. That is why application of the mentioned algorithm has a strong limitation on the rate of decay of the Fourier coefficients of the kernel. Thus, if it is possible to include the subordinate singularity $(1/2\pi)A_1(\vartheta)\widehat{\Phi}_1(\delta)$ into the principal one (extracted from the kernel – see below), then a much more efficient algorithm can be constructed. The coefficient $A_1(\vartheta)$ in (2.325) is constant, and for such a singularity its necessary inclusion can be achieved easily – see below. At the same time, for any $\gamma \neq 0$, the corresponding term $(1/2\pi)A_1(\vartheta)\widehat{\Phi}_1(\delta)$ of the singular expansion of kernel $[l(\tau)]^{\gamma}[l(\vartheta)]^{-\gamma}\tilde{G}(\vartheta,\tau)$ will include functions $l(\vartheta)$ and $dl(\vartheta)/d\vartheta$ that are not constants in general. That is why, it is necessary to take $\gamma = 0$ and to introduce the new unknown function

$$\tilde{\mu}_0(\tau) = l(\tau)\tilde{\mu}(\tau), \tag{2.328}$$

and consider it as a solution of integral equation

$$\int_{-\pi}^{\pi} \tilde{G}(\vartheta,\tau)\tilde{\mu}_0(\tau)\,d\tau = \tilde{f}(\vartheta);\ \vartheta \in [-\pi;\pi], \tag{2.329}$$

with $\tilde{\mu}_0$ and $\tilde{f}$ belonging to the relevant sets:

$$\tilde{\mu}_0 \in \mathbf{H}^{-1/2} \cap \mathbf{C}_Q^{0,\alpha}\left(\mathbf{R}^1\right), \tilde{f} \in \mathbf{H}^{1/2} \cap \mathbf{C}_Q^{1,\alpha}\left(\mathbf{R}^1\right). \tag{2.330}$$

The sets $\mathbf{H}^{-1/2} \cap \mathbf{C}_Q^{0,\alpha}\left(\mathbf{R}^1\right)$ and $\mathbf{H}^{1/2} \cap \mathbf{C}_Q^{1,\alpha}\left(\mathbf{R}^1\right)$ are defined in the same manner as sets $\mathbf{H}^{-1/2} \cap \mathbf{C}^{0,\alpha}[-\pi;\pi]$ and $\mathbf{H}^{1/2} \cap \mathbf{C}^{1,\alpha}[-\pi;\pi]$ in Section 2.1, with the only difference that here we directly request the 2π-periodicity of $\tilde{\mu}_0$ and $\tilde{f}$ functions. As it follows from the below, instead of $\mathbf{H}^{-1/2} \cap \mathbf{C}_Q^{0,\alpha}\left(\mathbf{R}^1\right)$ and $\mathbf{H}^{1/2} \cap \mathbf{C}_Q^{1,\alpha}\left(\mathbf{R}^1\right)$ in (2.330) we can, as well, use corresponding Sobolev spaces $\mathbf{H}^{-1/2}$ and $\mathbf{H}^{1/2}$ of 2π-periodical functions for the integral equation (2.329) posing, and this change does not influence anyhow the algorithm of the equation solving. Nevertheless, we will use posing (2.330) for simplicity and convenience of our reader.

2.6.4 Additive Splitting of the Integral Equation Kernel into a Sum of Main Singular Part and Some More Smooth Function

The kernel $\tilde{G}(\vartheta,\tau)$ can be additively splitted now into a sum of the principal singularity and a relatively smooth part as follows:

$$\tilde{G}(\vartheta,\tau) = \frac{1}{2\pi}\left\{\left[\left(-\frac{1}{2} + \ln\left|2\sin\frac{\vartheta-\tau}{2}\right|\right) + i\Phi\,\widehat{\Phi}_1(\tau-\vartheta)\right] + K_0(\vartheta,\tau)\right\}. \tag{2.331}$$

The expression in round brackets is the main singularity, the next term in square brackets is the subordinate singularity, and the next term in figure brackets is the relatively smooth part of the kernel.

Formally, we can now construct the analytic regularization method for equation (2.329) with its kernel splitting (2.331), and the construction is simple because double Fourier series for both principal and subordinated extracted singularities have diagonal form (see Section 2.1 and below). Nevertheless, something more should be done for calculation efficiency. Namely, the function $\widehat{\Phi}_1(\tau-\vartheta)$ is known to be nonrepresentable in elementary functions. That is why, its calculation requires some extra effort, which is not necessary if we can construct another function having equivalent singular behavior, but representable itself by means of elementary functions, and with its Fourier coefficients also representable by means of elementary functions.

To this end, let us consider the simplest function $\Psi(\vartheta)$ of the necessary kind:

$$\Psi_1(\vartheta) = -\sum_{n=2}^{\infty}\Psi_n \sin n\vartheta = i\frac{1}{2}\sum_{n=-\infty}^{\infty}\Psi_n \mathrm{sign}(n)\,\mathrm{e}^{in\vartheta};\ \vartheta \in [-2\pi;2\pi], \tag{2.332}$$

$$\Psi_n = \begin{cases} 0; & |n| \le 1 \\ \left(n^2-1\right)^{-1}; & |n| \ge 2 \end{cases}, \ \mathrm{sign}(n) = \begin{cases} 1; & n > 0 \\ 0; & n = 0 \\ -1; & n < 0 \end{cases}. \tag{2.333}$$

The Fourier coefficients $(i/2)\Psi_n \mathrm{sign}(n)$ of function $\Psi_1(\vartheta)$ are expressed by means of elementary functions already. As well, the function $\Psi_1(\vartheta)$ itself can easily be expressed by means of elementary functions (we leave this calculation to the reader). It is evident that $\Psi_1, \ \widehat{\Phi}_1 \in \mathbf{C}_Q^{0,\alpha}\left(\mathbf{R}^1\right)$, but $\Psi_1 - \widehat{\Phi}_1 \in \mathbf{C}_Q^{2,\alpha}\left(\mathbf{R}^1\right)$, and substitution of $\Psi_1(\vartheta)$ instead of $\widehat{\Phi}_1(\tau - \vartheta)$ in the singular expansion (2.325) does not influence the next term of the expansion, but changes only the term $n = 3$.

Let us make a splitting of the kernel $\tilde{G}(\vartheta,\tau)$ similar to (2.331), but now with $-\Psi_1(\vartheta - \tau) = \Psi_1(\tau - \vartheta)$ instead of $\widehat{\Phi}_1(\tau - \vartheta)$:

$$\tilde{G}(\vartheta,\tau) = \frac{1}{2\pi}\left\{\left[\left(-\frac{1}{2} + \ln\left|2\sin\frac{\vartheta-\tau}{2}\right|\right) - i\Phi\Psi_1(\vartheta-\tau)\right] + K_D(\vartheta,\tau)\right\}. \tag{2.334}$$

One can consider formula (2.334) as definition of the function $K_D(\vartheta,\tau)$. From singular expansion (2.325) and formulas (2.332) and (2.334) it immediately follows that:

$$K_D(\vartheta,\tau) \in \mathbf{C}^1\left((-\infty;\infty)\times(-\infty;\infty)\right), \tag{2.335}$$

$$\frac{\partial^2 K_D(\vartheta,\tau)}{\partial\vartheta\partial\tau}, \ \frac{\partial^2 K_D(\vartheta,\tau)}{\partial\vartheta^2}, \ \frac{\partial^2 K_D(\vartheta,\tau)}{\partial\tau^2} \ \in \ \mathbf{L}_2\left([-\pi;\pi]\times[-\pi;\pi]\right). \tag{2.336}$$

Using formula (2.334), one can reduce integral equation (2.329) to the view:

$$\begin{gathered}\frac{1}{2\pi}\int_{-\pi}^{\pi}\tilde{\mu}_0(\tau)\left\{\ln\left|2\sin\tfrac{\vartheta-\tau}{2}\right| - i\Phi\Psi_1(\vartheta-\tau) + K_D(\vartheta,\tau)\right\}d\tau = \tilde{f}(\vartheta); \\ \vartheta\in[-\pi;\pi].\end{gathered} \tag{2.337}$$

2.6.5 Reduction of the Integral Equation to an Infinite System of Linear Algebraic Equations of the First Kind

Now one can make Fourier transform of all functions in formula (2.337). According to formulas (2.334) and (2.335), function $K(\vartheta,\tau)$ can be expanded into its double Fourier series and is representable by this series:

$$K_D(\vartheta,\tau) = \sum_{s=-\infty}^{\infty}\sum_{j=-\infty}^{\infty} K_{sj}^D e^{i(s\vartheta+j\tau)}; \ \vartheta, \ \tau\in[-\pi;\pi]. \tag{2.338}$$

The following identity can be proved:

$$-\frac{1}{2} + \ln\left|2\sin\frac{\vartheta-\tau}{2}\right| \ = \ -\frac{1}{2}\sum_{n=-\infty}^{\infty}\frac{e^{in(\vartheta-\tau)}}{\tau_n^2}; \ \tau_n = \max\left(1,|n|^{1/2}\right). \tag{2.339}$$

The unknown and given functions $\mu(\vartheta)$ and $f(\vartheta)$, respectively, are representable by their Fourier series:

$$\tilde{\mu}_0(\tau) = \sum_{n=-\infty}^{\infty} \mu_n \exp(in\vartheta);\ \vartheta \in [-\pi;\pi], \tag{2.340}$$

$$-2\tilde{f}(\vartheta) = \sum_{n=-\infty}^{\infty} f_n \exp(in\vartheta);\ \vartheta \in [-\pi;\pi]. \tag{2.341}$$

We define infinite vector columns μ^D and f^D of Fourier coefficients of unknown and given functions and of the infinite matrix W^D, which is formed by Fourier coefficients of function $K(\vartheta,\tau)$, as follows:

$$\mu^D = \{\mu_n\}_{n=-\infty}^{\infty}, f^D = \{f_n\}_{n=-\infty}^{\infty}, W^D = \left\{w_{sn}^D\right\}_{s,n=-\infty}^{\infty}, w_{sn}^D = -2K_{s,-n}^D. \tag{2.342}$$

Substituting series (2.338), (2.339), (2.340), and (2.341) into equation (2.437) and using the orthogonality properties of the system of functions $\{\exp(is\tau)\}_{s=-\infty}^{\infty}$ on $[-\pi;\pi]$, one obtains after simple manipulation the following series equation:

$$\sum_{n=-\infty}^{\infty} \mu_n \left(\tau_n^D\right)^{-2} e^{in\vartheta} + \sum_{n=-\infty}^{\infty} \left(W^D\mu^D\right)_n e^{in\vartheta} = \sum_{n=-\infty}^{\infty} f_n e^{in\vartheta};\ \vartheta \in [-\pi;\pi]. \tag{2.343}$$

Here,

$$\tau_n^D = \tau_n (1 - \Phi n\psi_n)^{-1/2};\ \tau_n^D = |n|^{1/2}\left[1 + O\left(n^{-1}\right)\right] \text{ for } n \to \infty, \tag{2.344}$$

and $(W^D\mu^D)_n$ is the nth component of the infinite vector column $W^D\mu^D$. According to (2.298), $|\Phi| \leq 1/2$. From here and definitions (2.332) and (2.339) of ψ_n and τ_n, respectively, one can conclude that $\tau_n > 0$ and $1-\Phi n\psi_n > 0$. Consequently, the values $\tau_n^D > 0$ are correctly definite for every $n = 0,\pm1,\pm2,\ldots$.

Taking into account the equality of Fourier coefficients of left- and right-hand sides in equation (2.343), one obtains the following infinite set of linear algebraic equations:

$$\mu_s \left(\tau_s^D\right)^{-2} + \left(W^D\mu^D\right)_s = f_s;\ s = 0, \pm 1, \pm 2,\ldots \tag{2.345}$$

The system of linear algebraic equations (2.349) is evidently one of the first kind [see (2.344)]. Our next purpose is to transform it to an equation of the second kind in the space l_2 of square-summable sequences.

2.6.6 Construction of an Infinite System of Linear Algebraic Equations of the Second Kind

Let us define new unknown and known coefficients

$$\widehat{\mu}_s = \mu_s/\tau_s^D,\ \widehat{f}_s = \tau_s^D f_s, \tag{2.346}$$

$$\widehat{w}_{s,n}^D = \tau_s^D \tau_n^D w_{sn}^D = -2\tau_s^D \tau_n^D 2K_{s,-n}^D, \tag{2.347}$$

and corresponding vector columns $\widehat{\mu}$ and $\widehat{f}$ and matrix operator $\widehat{W}$:

$$\widehat{\mu} = \left\{\widehat{\mu}_n\right\}_{n=-\infty}^{\infty},\ \widehat{f} = \left\{\widehat{f}_n\right\}_{n=-\infty}^{\infty};\ \widehat{W}^D = \left\{\widehat{w}_{sn}^D\right\}_{s,n=-\infty}^{\infty}. \tag{2.348}$$

Multiplying every equation (2.345) by τ_s^D and using the new coefficients $\widehat{\mu}_s$ and $\widehat{f}_s$, one obtains after a simple transformation the new algebraic system of the kind

$$\widehat{\mu}_s + \left(\widehat{W}^D \widehat{\mu}\right)_s = \widehat{f}_s;\ s = 0, \pm 1, \pm 2, ..., \tag{2.349}$$

which can be rewritten in the operator form

$$\left[E + \widehat{W}^D\right]\widehat{\mu} = \widehat{f};\ \widehat{\mu},\ \widehat{f} \in l_2. \tag{2.350}$$

It follows (see [11]) from (2.335) and (2.336) that $\widehat{W}$ is a compact operator in l_2 and even more: the coefficients of the matrix operator $\widehat{W}$ satisfy the inequality

$$\sum_{s=-\infty}^{\infty} \sum_{n=-\infty}^{\infty} (1 + |s|)(1 + |n|) \left|\widehat{w}_{sn}^D\right|^2 < \infty. \tag{2.351}$$

Thus, the Dirichlet BVP considered is reduced to the infinite algebraic system (2.350), which forms a functional equation of the second kind in the space l_2 with the compact in l_2 operator $\widehat{W}^D$.

2.6.7 The Neumann Diffraction Problem

The Neumann BVP posing is the same as the one for the Dirichlet BVP, but with the replacement of the Dirichlet boundary condition (2.305) by the Neumann one:

$$\frac{\partial \tilde{U}^{s(\pm)}(\bar{g}, \kappa)}{\partial \vec{n}_{\bar{g}}} + \frac{\partial \tilde{U}_p^i(\bar{g}, \kappa)}{\partial \vec{n}_{\bar{g}}} = 0;\ \bar{g} \in \bar{\mathbf{S}}_x. \tag{2.352}$$

By means of standard technique of Green's formulas, one obtains that the scattering field $\tilde{U}^{s(\pm)}(\bar{g},\kappa)$ has the following representation:

$$\tilde{U}^{s(\pm)}(\bar{g}_1,\kappa)=\int\limits_{\mathbf{S}_{x,0}}\frac{\partial\tilde{G}_0(\bar{g}_1,\bar{g}_2,\kappa,\Phi)}{\partial\vec{n}_{\bar{g}_2}}M_N(\bar{g}_2)\,dl_{\bar{g}_2}=0;\ \bar{g}_1\in\mathbf{R}^2\backslash\bar{\mathbf{S}}_x, \tag{2.353}$$

$$M_N(\bar{g})=\tilde{U}^{s(-)}(\bar{g},\kappa)-\tilde{U}^{s(+)}(\bar{g},\kappa);\ \bar{g}\in\bar{\mathbf{S}}_x. \tag{2.354}$$

The contour $\bar{\mathbf{S}}_x$ is assumed to be smooth. Consequently, there are such a number $H>0$ and an open vicinity $\mathbf{V}_H$ of $\bar{\mathbf{S}}_x$ such that $\bar{\mathbf{S}}_x\subset\mathbf{V}_H$ and for any point $\bar{g}_h\in\mathbf{V}_H$ the point $\bar{g}\in\bar{\mathbf{S}}_x$ (which is known as the projection of $\bar{g}_h$ onto $\bar{\mathbf{S}}_x$) and the number h with $|h|<H$ exist that $\bar{g}_h$ has the unique representation of the kind

$$\bar{g}_h=\bar{g}+h\vec{n}_{\bar{g}};\quad \bar{g}\in\bar{\mathbf{S}}_x. \tag{2.355}$$

Here, $\vec{n}_{\bar{g}}$ is unit outward (oriented from $\mathbf{R}^{2(+)}$ to $\mathbf{R}^{2(-)}$) normal to $\bar{\mathbf{S}}_x$ in the point $\bar{g}\in\bar{\mathbf{S}}_x$. Thus, any point $\bar{g}_h\in\mathbf{V}_H$ has view (2.355) with $\vec{n}_{\bar{g}}$ uniquely defined by $\bar{g}$. That is why, derivative $\partial\big/\partial\vec{n}_{\bar{g}}$ is correctly defined in $\mathbf{V}_H$.

Applying this derivative to both sides of (2.353), one obtains that

$$\begin{aligned}&\tfrac{\partial\tilde{U}^{s(\pm)}(\bar{g}_h,\kappa)}{\partial\vec{n}_{\bar{g}}}=\tfrac{\partial}{\partial\vec{n}_{\bar{g}}}\int\limits_{\mathbf{S}_{x,0}}\tfrac{\partial\tilde{G}_0(\bar{g}_h,\bar{g}_2,\kappa,\Phi)}{\partial\vec{n}_{\bar{g}_2}}M_N(\bar{g}_2)\,dl_{\bar{g}_2};\\ &\bar{g}_h\in\left(\mathbf{V}_H\backslash\bar{\mathbf{S}}_x\right).\end{aligned} \tag{2.356}$$

According to (2.302), there exist uniform on $\bar{\mathbf{S}}_x$ limits $\lim\limits_{h\to\pm0}\partial\tilde{U}^{s(\pm)}(\bar{g}_h,\kappa)\big/\partial\vec{n}_{\bar{g}}$. Consequently, substitution of (2.356) for $h\to\pm0$ into boundary conditions (2.352) brings the identity

$$\lim_{h\to\pm0}\frac{\partial}{\partial\vec{n}_{\bar{g}}}\int\limits_{\mathbf{S}_{x,0}}\frac{\partial\tilde{G}_0(\bar{g}_h,\bar{g}_2,\kappa,\Phi)}{\partial\vec{n}_{\bar{g}_2}}M_N(\bar{g}_2)\,dl_{\bar{g}_2}=-\frac{\partial\tilde{U}^i_p(\bar{g},\kappa)}{\partial\vec{n}_{\bar{g}}};\ \bar{g}\in\bar{\mathbf{S}}_x. \tag{2.357}$$

Using parameterization $\eta(\vartheta)\equiv\{\bar{y}(\vartheta),\bar{z}(\vartheta)\}$ of the contour $\bar{\mathbf{S}}_x$ [see (2.291), (2.292), (2.293), (2.294), and (2.295)] and being based on the analogy to the treatment made above for the Dirichlet problem, one can define the following functions:

$$\tilde{D}_h(\bar{g},\bar{g}_2)=\frac{\partial^2\tilde{G}_0\left(\bar{g}+h\vec{n}_{\bar{g}},\bar{g}_2,\kappa,\Phi\right)}{\partial\vec{n}_{\bar{g}}\partial\vec{n}_{\bar{g}_2}};\ \bar{g},\ \bar{g}_2\in\bar{\mathbf{S}}_{x,0}, \tag{2.358}$$

$$D_h(\vartheta,\tau)=e^{i\Phi(\tau-\vartheta)}\tilde{D}_h(\bar{g},\bar{g}_2)\Big|_{\bar{g}=\eta(\vartheta),\ \bar{g}_2=\eta(\tau)}, \tag{2.359}$$

$$\nu(\tau)=e^{-i\Phi\tau}M_N(\eta(\tau)), \tag{2.360}$$

$$\tilde{g}\,(\vartheta) = -\mathrm{e}^{-i\Phi\vartheta}\,\frac{\partial \tilde{U}_p^i\,(\bar{g},\kappa)}{\partial \vec{n}_{\bar{g}}}\bigg|_{\bar{g}=\eta(\vartheta)}. \tag{2.361}$$

Functions $D_h(\vartheta,\tau)$, $\nu(\tau)$, and $\tilde{g}\,(\vartheta)$ are periodical ones, as this evidently follows from their definitions.

Using formulas (2.359), (2.360), and (2.361), one can rewrite identity (2.357) in parameterized form:

$$\lim_{h\to\pm 0}\int_{-\pi}^{\pi} D_h\,(\vartheta,\tau)\,\nu\,(\tau)\,l\,(\tau)\,d\tau = \tilde{g}\,(\vartheta)\,;\ \vartheta\in[-\pi;\pi]\,. \tag{2.362}$$

Identity (2.362) is not suitable for further analysis and transformation, because it involves limits $h\to\pm 0$. Direct substitution of $h=0$ in (2.362) is illegal even because the integral in (2.362) is divergent for $h=0$. Thus, the problem of analytic "calculation" of these limits, i.e., of their expression in terms of some elementary operations arises. It is clear that function $D_0(\vartheta,\tau)$ (i.e., $D_h(\vartheta,\tau)$ for $h=0$) must somehow appear in any result of such limit "calculation." That is why we need an investigation of the differential and singular properties of $D_0(\vartheta,\tau)$.

First of all, $D_0(\vartheta,\tau)$ is evidently smooth function everywhere on $[-\pi;\pi]\times[-\pi;\pi]$, but with exception of the points $\{\vartheta,\tau\}$ under relations $\vartheta=\tau$ or $|\vartheta-\tau|=2\pi$. Detailed investigation results into the singular expansion

$$\begin{aligned} D_0\,(\vartheta,\tau) \;-\; \tfrac{1}{2\pi l(\vartheta)l(\tau)}\,\Bigg\{ \tfrac{1}{4\sin^2\frac{\vartheta-\tau}{2}} \;+\; i\Phi\,\tfrac{1}{2}\mathrm{ctg}\,\tfrac{\tau-\vartheta}{2} \;+ \\ +\sum_{m=0}^{M} B_m\,(\vartheta)\,\widehat{\Phi}\,(\tau-\vartheta)\Bigg\} \;\in\; C_Q^M\left(\mathbf{R}^2\right), \end{aligned} \tag{2.363}$$

which is valid for any fixed $M=0,\pm1,\pm2,\ldots$, and where $B_m(\vartheta)$ are some functions of the kind $B_m\in C_Q^{\infty}\left(\mathbf{R}^1\right)$. In particular,

$$B_0\,(\vartheta) = \frac{[\kappa l\,(\vartheta)]^2}{2},\; B_1\,(\vartheta) \;=\; \frac{1}{4}\frac{d\,[\kappa l\,(\vartheta)]^2}{d\vartheta} \;+\; i\Phi\frac{[\kappa l\,(\vartheta)]^2}{2}. \tag{2.364}$$

Taking into account formulas (2.320) and (2.322), one obtains after elementary calculations that

$$\frac{1}{4\sin^2\frac{\vartheta-\tau}{2}} = \frac{d^2}{d\vartheta^2}\ln\left|2\sin\frac{\vartheta-\tau}{2}\right|, \tag{2.365}$$

$$\frac{d^2}{d\vartheta^2}\ln\left|2\sin\frac{\vartheta-\tau}{2}\right| \approx \frac{1}{2}\sum_{n=-\infty}^{\infty}|n|\mathrm{e}^{in(\vartheta-\tau)}; \tag{2.366}$$

$$\frac{1}{2}\mathrm{ctg}\frac{\vartheta-\tau}{2} = -\frac{1}{2}\mathrm{ctg}\frac{\tau-\vartheta}{2} = -\frac{d}{d\vartheta}\ln\left|2\sin\frac{\vartheta-\tau}{2}\right|, \tag{2.367}$$

$$-\frac{d}{d\vartheta}\ln\left|2\sin\frac{\vartheta-\tau}{2}\right| \;\approx\; i\frac{1}{2}\sum_{n=-\infty}^{\infty}\operatorname{sign}(n)\,e^{in(\vartheta-\tau)}. \tag{2.368}$$

The series (2.366) and (2.368) are formal ones, because they are divergent. Nevertheless, the sense of the Fourier series of corresponding 2π-periodical generalized functions (distributions) can be given to them, and most right-hand sided expressions in (2.365) and (2.367) have sense of the regularization of these generalized functions. Without going into such far from the main topic details, we note only herein that these series are really useful for better understanding of the features of $D_0(\vartheta,\tau)$ as the kernel of the differential integral equation that we will consider below.

One can conclude from (2.363) that $D_0(\vartheta,\tau)$ has nonintegrable singularity of the type $(\tau–\vartheta)^2$, and consequently, the exchange of the order of limiting operation and integration in (2.362) is indeed illegal.

It follows from (2.360), (2.354), and (2.300) that $\nu(\vartheta)\in C_Q^{1,\alpha}\left(\mathbf{R}^1\right)$. As the result of rather bulky and nontrivial calculation, based on the relevant singular expansion of the function similar to $D_h(\vartheta,\tau)$, $h\geq 0$, but generated by nonperiodical Green's function $(-i/4)\,H_0^{(1)}(\kappa|g-g_0|)$, and under the same assumption for $\nu(\vartheta)$, the limit of the type (2.362) has been calculated – see [11] and the references therein. The similar, in some respect, calculation of the limits (2.362) results into the relation of the kind:

$$\begin{aligned}\lim_{h\to\pm 0}\int_{-\pi}^{\pi} D_h(\vartheta,\tau)\,\nu(\tau)\,d\tau \;&=\; \tfrac{1}{2\pi l(\vartheta)}\left\{\left[\tfrac{1}{2}\int_{-\pi}^{\pi}\nu(\tau)\,d\tau+\right.\right.\\ &\left.\left.+\left(\tfrac{d^2}{d\vartheta^2}-i\Phi\tfrac{d}{d\vartheta}\right)\int_{-\pi}^{\pi}\ln\left|2\sin\tfrac{\vartheta-\tau}{2}\right|\nu(\tau)\,d\tau\right]+\int_{-\pi}^{\pi}K_N(\vartheta,\tau)\,\nu(\tau)\,d\tau\right\};\\ &\vartheta\in[-\pi;\pi].\end{aligned} \tag{2.369}$$

Here, function $K_N(\vartheta,\tau)$, $\vartheta,\tau\in[-\pi;\pi]$, is defined by the following equality:

$$D_0(\vartheta,\tau) \;=\; \frac{1}{2\pi l(\vartheta)\,l(\tau)}\left\{\frac{1}{2}+\frac{1}{4\sin^2\frac{\vartheta-\tau}{2}}+i\Phi\frac{1}{2}\operatorname{ctg}\frac{\tau-\vartheta}{2}+K_N(\vartheta,\tau)\right\}. \tag{2.370}$$

Substitution of (2.369) into (2.362) and multiplying the result by $l(\vartheta)$ bring the identity:

$$\begin{aligned}&\tfrac{1}{2\pi}\left\{\left[\tfrac{1}{2}\int_{-\pi}^{\pi}\nu(\tau)d\tau+\left(\tfrac{d^2}{d\vartheta^2}-i\Phi\tfrac{d}{d\vartheta}\right)\int_{-\pi}^{\pi}\ln\left|2\sin\tfrac{\vartheta-\tau}{2}\right|\nu(\tau)d\tau\right]+\right.\\ &\left.+\int_{-\pi}^{\pi}K_N(\vartheta,\tau)\,\nu(\tau)\,d\tau\right\}=l(\vartheta)\,g(\vartheta);\;\vartheta\in[-\pi;\pi].\end{aligned} \tag{2.371}$$

In accordance with standard approach, we will consider identity (2.371) from now as the differential–integral equation to unknown function $\nu(\tau)$ under assumptions:

$$\nu(\tau) \in \mathbf{H}^{1/2} \cap \mathbf{C}_Q^{1,\alpha}\left(\mathbf{R}^1\right), l(\vartheta)\, g(\vartheta) \in \mathbf{H}^{-1/2} \cap \mathbf{C}_Q^{0,\alpha}\left(\mathbf{R}^1\right). \tag{2.372}$$

It can be proved that if the equation is solved and function $\nu(\vartheta)$ is found, then one can obtain the scattered field by means of the integral representation (2.353), where function $M_N(\bar{g})$ is given by inversion of formulas (2.360), namely, $M_N(\bar{g}) = \left[e^{i\Phi\tau}\nu(\tau)\right]\big|_{\tau=\eta^{-1}(\bar{g})}$ – function $\eta(\tau)$ is constructed above as an invertible one.

As one can see, domains of definition and image of the differential operator in (2.371) are exchanged in comparison with the same domains, but for integral operator generated by the Dirichlet BVP – see (2.330) for comparison. This exchange is in the proper agreement with physical and mathematical senses of functions $\nu(\tau)$ and $\mu(\tau)$ correspondingly – see (2.305) and (2.354) also. It is possible to say that operators of equations (2.329) and (2.371) have somewhat opposite qualities: the kernel of the first one is too smooth, but the kernel of the second is too singular for making the operators boundedly invertible in space $\mathbf{L}_2[-\pi,\pi]$.

The structure of the differential–integral equation in (2.371) is in some respects similar to one of (2.337). Namely, the expression in square brackets in (2.371) is the singularity extracted from the operator and, as well as in (2.337), it involves the first two principal singularities as corresponding derivatives of logarithmic singularity (the very first integral in (2.371) is extracted for the only convenience to have the extracted singularity to be formally invertible).

The rest of the necessary transforms is almost the same as for the Dirichlet problem. Namely, let us expand $\nu(\vartheta)$, $l(\vartheta)\,\tilde{g}(\vartheta)$, and $K_N(\vartheta,\tau)$ into their Fourier series:

$$\nu(\vartheta) = \sum_{n=-\infty}^{\infty} \nu_n e^{in\vartheta},\ l(\vartheta)\,\tilde{g}(\vartheta) = \sum_{n=-\infty}^{\infty} g_n e^{in\vartheta}, \tag{2.373}$$

$$K_N(\vartheta,\tau) = \sum_{s=-\infty}^{\infty}\sum_{n=-\infty}^{\infty} K_{sn}^N e^{i(s\vartheta+n\tau)}. \tag{2.374}$$

Substituting these series into (2.371), making term by term integration, and term by term differentiation, when necessary (all these operations can be mathematically justified – see [11]), one arrives into the series equation similar to (2.343), from which (2.345) follows. Exactly in the same manner, one derives from the series equation just obtained an algebraic equation similar to (2.345), but of the kind:

$$\left(\tau_s^N\right)^2 \nu_s + \sum_{n=-\infty}^{\infty} w_{sn}^N \nu_n = g_s;\ s = 0, \pm 1, \pm 2... \tag{2.375}$$

Here,

$$\tau_s^N = \tau_s \left[1 - \Phi \operatorname{sign}(n)/\tau_n^2\right]^{1/2} = \begin{cases} 1; \, n = 0 \\ \tau_n \left[1 - \Phi/n\right]^{1/2}; \quad n = \pm 1, \pm 2, \ldots \end{cases}, \tag{2.376}$$

$$w_{sn}^N = 2K_{s,-n}^N. \tag{2.377}$$

Values $\tau_s^N > 0$ for any $s = 0, \pm 1, \pm 2, \ldots$, due to the same reason as $\tau_s^D > 0$ (see the previous section), and $\tau_n^N = O(|n|)$ for $n \to \pm\infty$. The last means evidently that equation (2.375) is one of the first kind in space l_2, where its matrix operator is unbounded.

The analytic regularization of equation (2.375) is trivial now. Indeed, let us define vector columns

$$\widehat{v} = \left\{\widehat{v}_n\right\}_{n=-\infty}^{\infty}; \; \widehat{v}_n = \tau_n^N v_n, \; \widehat{g} = \left\{\widehat{g}_s\right\}_{s=-\infty}^{\infty}; \; \widehat{g}_s = g_s/\tau_s^N \tag{2.378}$$

and matrix operator

$$\widehat{W}^N = \left\{\widehat{w}_{sn}\right\}_{s,n=-\infty}^{\infty}; \; \widehat{w}_{sn} = \left(\tau_s^N \tau_n^N\right)^{-1} w_{sn}^N, \tag{2.379}$$

and divide each equation (2.375) by τ_s^N. As the result, we obtain an algebraic equation in l_2 of the kind

$$\left[E + \widehat{W}^N\right] \widehat{v} = \widehat{g}; \; \widehat{v}, \; \widehat{g} \in l_2. \tag{2.380}$$

It can be shown that

$$\sum_{s=-\infty}^{\infty} \sum_{n=-\infty}^{\infty} (1 + |s|)(1 + |n|) \left|w_{sn}^N\right|^2 < \infty. \tag{2.381}$$

It is noteworthy that matrix operator for $\widehat{W}^N$ satisfies exactly the same inequality (2.381) as matrix operator $\widehat{W}^D$ does – see (2.351).

Thus, the Neumann BVP considered is reduced to the infinite algebraic system (2.380), which forms functional equation of the second kind in space l_2 with compact in l_2 operator $\widehat{W}^N$.

We wish to emphasize again that more complicated transmission BVP can be solved in similar way.

http://www.springer.com/978-1-4419-1199-5

Modern Theory of Gratings
Resonant Scattering: Analysis Techniques and Phenomena
(Eds.)Y.K. Sirenko; S. Ström
2010, XVI, 386 p. 120 illus., 43 in color., Hardcover
ISBN: 978-1-4419-1199-5